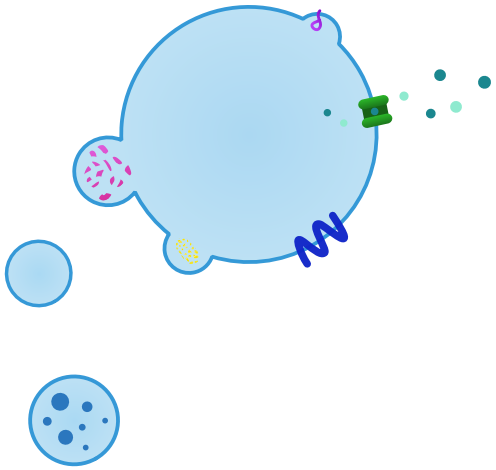


Molecular and Functional Studies on Niemann-Pick Type C Disease

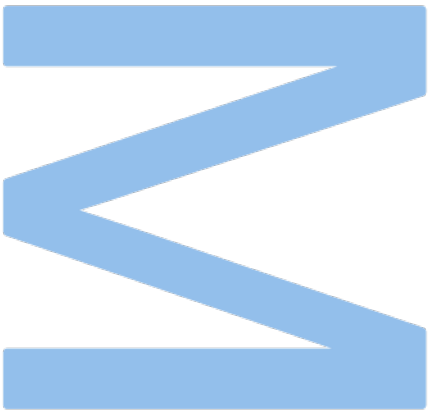
Hugo Daniel Sousa David
Cell and Molecular Biology
Department of Biology
2023

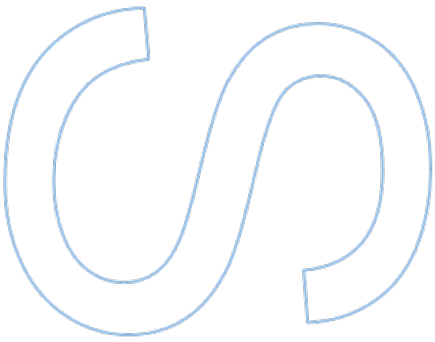
Supervisor
Marisa Encarnação, Auxiliary Researcher, INSA

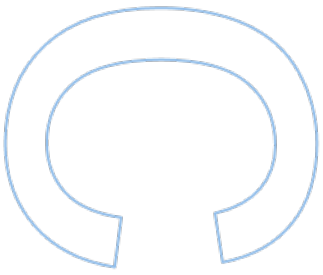
Co-supervisor
Sandra Alves, Auxiliary Researcher, INSA


Instituto_Nacional de Saúde
Doutor Ricardo Jorge


U.PORTO
FACULDADE DE CIÊNCIAS
UNIVERSIDADE DO PORTO







“It’s kind of fun to do the impossible.”

Acknowledgements

First and foremost, I would like to express my immense gratitude to my supervisor, Marisa, for giving me the chance to delve into a new subject, to broaden my horizons, and to mature as a scientist. For not being a mere supervisor, but a true mentor, who was always approachable, cheerful and optimistic. For always believing in me and pushing me forward, leading me to develop new skills and deepen my knowledge.

I am also deeply thankful to my co-supervisor, Sandra, for allowing me to integrate her research team at the National Institute of Health Dr. Ricardo Jorge, for all her kind helpfulness, openness and guidance.

To all my colleagues (and now friends) at the “TZero”, for taking me under their wing, making me feel at home from day one. For the daily walks in Santa Catarina, the weekly desserts at *Lavoratta* and the monthly celebrations at the office. For all the laughter, fun and good humour, which made coming to the lab everyday an absolute joy. It was truly a pleasure to work amongst you.

To all the friends I made along my academic journey through the University of Porto, but especially Diana, my gym (and gossip) buddy who kept me company in many train rides for the past 7 years, and Tita, my lab partner from day one who shared so much more than a lab bench.

To the “MLovers”, for being the silliest, most awesome group of friends a guy could ask for and for all the 10 PM get-togethers, randomly deep or simply casual conversations, and joyful moments we shared.

To Ricky, for all our past memories and future adventures, weeknight dinners and weekend getaways, countless game nights and plentiful beach days, warm *natinhas* and warmer hugs. But, most importantly, for always being there each step of the way, cheering me on and making me smile, encouraging me to live life to the fullest every single day.

To my parents, who encouraged my passion for knowledge, for showing me all there is to discover in this world. But, above all, for always giving me the freedom to fly, while being my ever-present safety net.

Last, but certainly not least, my biggest thank you is to my grandparents, my endless source of love and support. For indulging every single one of my makeshift experiments and wild ideas, ever since I was a child. And for being my inspiration to strive to make the world a better place. As always, I dedicate this to you.

Resumo

A Niemann-Pick tipo C (NPC) é uma doença lisossomal de sobrecarga rara, progressiva e neurodegenerativa, provocada por variantes patogénicas nos genes *NPC1* ou *NPC2* – que codificam proteínas envolvidas no exporte lisossomal de colesterol não-esterificado. Este lípido é acumulado, juntamente com outros, no interior de lisossomas, espoletando uma cascata de eventos celulares e moleculares que culminam na grave sintomatologia neuro-visceral associada a esta doença.

Apesar de ter sido descrita pela primeira vez há cerca de 100 anos, vários aspetos da NPC permanecem enigmáticos, nomeadamente a elevada variabilidade fenotípica observada até em doentes pertencentes à mesma família. Dos vários fatores que podem influenciar a manifestação fenotípica desta doença, nós abordamos dois: o alelo complexo p.Ala1035Val + p.Ile858Val no gene *NPC1* – para o qual ainda não foram publicados estudos funcionais – e o perfil de expressão de microRNAs (miRNAs) – um ramo virtualmente inexplorado na investigação sobre NPC.

Não existe cura para a NPC, e a única terapia aprovada para a qual há um efeito modificador de doença comprovado – miglustat – não está disponível nem é eficaz para todos os doentes afetados por esta doença. Vários moduladores da proteostase estão atualmente em testes clínicos para a NPC, mas os esforços de desenvolvimento de fármacos têm encontrado complicações com modelos animais de doença, que podem não ser apropriados para avaliar as vias de tráfego e degradação da proteína NPC1.

Tendo em consideração todas estas dificuldades, criámos modelos de doença *in vitro* para a NPC específicos para cada variante, ao transduzir de forma estável células *NPC1*$^{-/-}$ ARPE-19 com diversos vetores que codificam diferentes variantes de NPC1 marcada com fluorescência. Utilizando estas novas linhas celulares que estabelecemos, a par de fibroblastos de pele derivados de doentes, investigámos o posicionamento lisossomal, os percursos de tráfego e as vias de degradação evocadas por duas das variantes *NPC1* mais prevalentes – a p.Ile1061Thr e a p.Ala1035Val (com e sem o polimorfismo p.Ile858Val em *cis*). Os nossos resultados corroboram a retenção da p.Ile1061Thr-NPC1 previamente descrita, e sugerem um padrão de retenção semelhante, se não mais grave, para a variante p.Ala1035Val, posicionando-a como uma candidata para a qual abordagens baseadas em moduladores da proteostase podem ser opções terapêuticas promissoras.

Dados de sequenciação de RNA de nova geração em fibroblastos da pele de doentes NPC revelaram várias espécies de miRNA desreguladas. Selecionámos dois miRNAs diferencialmente expressos para validar através de reação de polimerase em cadeia em tempo real quantitativa (qRT-PCR), o miR-143-3p e o miR-199a-3p, que poderão estar relacionados com a acumulação lipídica e defeitos na autofagia e no tráfego intracelular na NPC. Apesar dos dados obtidos para fibroblastos da pele se terem revelado inconclusivos, a validação por qRT-PCR em amostras de soro revelou expressão aumentada em 19.50 vezes para o miR-143-3p, e em 15.79 vezes para o miR-199a-3p, em circulação no soro de doentes com NPC. Os nossos resultados relativos a estes dois miRNAs diferencialmente expressos propõem-nos como potenciais e promissores biomarcadores para a NPC, que poderão representar opções de diagnóstico minimamente intrusivas, específicas e eficazes, ou até mesmo ferramentas para acompanhar a progressão da doença e avaliar respostas a terapia.

De forma global, estes estudos integrais contribuíram para aprofundar o conhecimento científico acerca dos mecanismos fisiopatológicos envolvidos na NPC. Em suma, criámos um novo modelo celular para estudar os mecanismos celulares envolvidos nas vias de tráfego e degradação de diferentes variantes em *NPC1*, que poderão até vir a ser úteis para ensaios de *screening* de fármacos em larga-escala; traçámos o perfil de expressão de miRNAs de doentes NPC; e propusemos novos biomarcadores putativos para esta doença.

Palavras-chave: doenças lisossomais de sobrecarga, Niemann-Pick tipo C, variantes patogénicas, processamento proteico, modelos de doença, microRNAs, biomarcadores.

Abstract

Niemann-Pick type C (NPC) is a rare, progressive and neurodegenerative lysosomal storage disorder, caused by pathogenic variants in either the *NPC1* or *NPC2* genes – which encode proteins involved in the lysosomal export of unesterified cholesterol. This and other lipids accumulate inside lysosomes, triggering a cascade of other cellular and molecular events, culminating in the severe neuro-visceral symptomatology associated with this disorder.

Despite first being described around 100 years ago, many aspects of NPC disease are still quite enigmatic, namely the vast phenotypic variability observed even in patients within the same family. Out of the various factors that may the influence the phenotypic manifestation of this disease, we addressed two: the p.Ala1035Val + p.Ile858Val complex allele in *NPC1* – for which no functional studies have been published – and the microRNA (miRNA) expression profile – a virtually uncharted scope of research in NPC.

There is no cure for NPC, and the only approved therapy for which there is a proven disease-modifying benefit – miglustat – is neither broadly available nor effective for all patients affected by this disorder. Several proteostasis modulators are currently undergoing laboratory and clinical trials for NPC, but drug development efforts have met complications with animal models of disease, which may not be appropriate to assess the trafficking and degradation routes of the NPC1 protein.

Taking all of those difficulties into account, we created variant-specific *in vitro* models of NPC disease, by stably transducing *NPC1*$^{-/-}$ ARPE-19 cell lines with several constructs encoding different fluorescently-tagged variants of NPC1. Using these newly established cell lines, alongside patient-derived primary skin fibroblasts, we investigated the lysosomal positioning, trafficking routes and degradation pathways elicited by two of the most common *NPC1* variants – p.Ile1061Thr and p.Ala1035Val (both with and without the p.Ile858Val polymorphism in *cis*). Our results corroborate the previously described retention of p.Ile1061Thr-NPC1, and suggest a similar, if not worse, retention pattern for the p.Ala1035Val variant, posing it as a candidate for which proteostasis modulator-based approaches might be promising therapeutic options.

Next-generation small RNA sequencing approaches in NPC dermal fibroblasts revealed several dysregulated miRNA species. We selected two differentially expressed miRNAs to validate using quantitative real-time polymerase chain reaction (qRT-PCR), miR-143-3p and miR-199a-3p, which may be related to lipid accumulation, autophagy

and intracellular trafficking impairment in NPC disease. While data obtained from skin fibroblasts appeared inconclusive, qRT-PCR validation in serum revealed a 19.50-fold overexpression of miR-143-3p, and 15.79-fold upregulation of miR-199a-3p in circulation within the serum of NPC patients. Our figures regarding these two differentially expressed miRNAs pose them as encouraging potential biomarkers for NPC, which may represent a minimally-intrusive, specific, time- and cost-effective diagnostic option, or even a way to track disease progression and response to therapy.

Overall, these comprehensive studies contributed to further the knowledge concerning the pathophysiological mechanisms engaged in NPC. In summary, we created a new cell model to study the cellular mechanisms involved in the protein trafficking and degradation pathways of different *NPC1* variants, which could even be useful for large-scale drug screenings; we plotted the miRNA expression profile of NPC patients; and we proposed two circulating miRNAs as novel putative biomarkers of this disease.

Keywords: lysosomal storage disorders, Niemann-Pick type C, pathogenic variants, protein processing, disease models, microRNAs, biomarkers.

Table of Contents

List of Tables xi

List of Figures xiii

List of Abbreviations xv

1. Introduction 1

1.1. Lysosomes 3

1.2. Lysosomal Storage Diseases 4

1.3. Niemann-Pick type C 8

1.4. NPC1 Protein 10

1.5. Disease-causing variants 11

1.6. NPC Pathogenesis 13

1.7. Models to study NPC 14

1.8. NPC Diagnosis 15

1.9. MicroRNAs 16

1.10. Aims 18

2. Materials & Methods 21

2.1. Materials 23

2.1.1. Patient and control-derived samples 23

2.1.2. Cell lines 24

2.1.3. Plasmids 24

2.1.4. Equipment 25

2.1.5. Consumables 26

2.1.6. Reagents 27

2.1.7. Kits.. 28

2.1.8. Antibodies 28

2.1.9. Enzymes 29

2.1.10. Primers 29

2.1.11. Software 30

2.2. Methods 30
2.2.1. Cell culture 30
2.2.1.1. Culture conditions 30
2.2.1.2. Subculturing cells 31
2.2.1.3. Counting cells 31
2.2.1.4. Pelleting cells 31
2.2.1.5. Cryopreserving cells 31
2.2.1.6. Reviving cells 32
2.2.1.7. Mycoplasma testing 32
2.2.2. Protein analysis 32
2.2.2.1. Protein extraction 32
2.2.2.2. Protein quantification 32
2.2.2.3. Deglycosylation assay 33
2.2.2.4. SDS-PAGE 34
2.2.2.5. Western blot 34
2.2.3. Generation of stably transduced *NPC1*$^{-/-}$ ARPE-19 cells and functional analysis of different *NPC1* variants 35
2.2.3.1. Transformation of competent *E. coli* cells 35
2.2.3.2. Glycerol stock preparation 36
2.2.3.3. Plasmid purification 36
2.2.3.4. Site-directed mutagenesis 37
2.2.3.5. Sequencing PCR 38
2.2.3.6. Whole plasmid sequencing 39
2.2.3.7. Diagnostic restriction digest 39
2.2.3.8. Cell viability assay 40
2.2.3.9. Transient transfection of HEK293T cells and γ-retroviral collection 40
2.2.3.10. Retroviral transduction of *NPC1*$^{-/-}$ ARPE-19 cells 41
2.2.3.11. Bafilomycin A_1 Assay 42
2.2.3.12. Filipin staining 42

2.2.3.13. Immunofluorescence assays 43
2.2.3.14. Lysosome clustering scoring 43
2.2.3.15. Colocalization quantification 44
2.2.4. RNA-based studies on NPC patients' fibroblasts and sera 44
2.2.4.1. Blood serum separation 44
2.2.4.2. RNA extraction 44
2.2.4.3. RNA quantification 45
2.2.4.4. cDNA synthesis 45
2.2.4.5. Disease-causing variant confirmation 46
2.2.4.6. Next-generation RNA sequencing 46
2.2.4.7. Quantitative real-time polymerase chain reaction 47
2.2.5. Bioinformatic data treatment 48
2.2.5.1. Image processing 48
2.2.5.2. Statistical analysis 48
3. Results & Discussion 49
3.1. Establishment of stably transduced *NPC1*$^{-/-}$ ARPE-19 cell lines 53
3.1.1. γ-retroviral plasmid identity was confirmed by diagnostic restriction digest. 54
3.1.2. Site-directed mutagenesis of the pBABE-puro+NPC1-mNeonGreen constructs was validated by Sanger and whole plasmid sequencing 56
3.1.3. Puromycin selection concentration was determined through cell viability assays…. 58
3.1.4. NPC1-mNeonGreen expression was visualized using fluorescence microscopy 59
3.1.5. Characteristic free-cholesterol accumulation was observed through filipin staining…. 60
3.2. Altered lysosome biogenesis and positioning 62
3.2.1. Decreased lysosomal turnover 62
3.2.2. Lysosomal clustering 62
3.3. Anomalous NPC1 trafficking and degradation 65
3.3.1. NPC1 variants are retained and likely degraded in the ER 65

3.3.2. NPC1 variants trigger different degradation pathways 69
3.4. Differentially expressed miRNAs in NPC 70
3.4.1. Disease-causing variants in *NPC1* were confirmed by dye-terminator sequencing 71
3.4.2. NPC patients display different miRNA expression patterns 72
3.4.3. Differentially expressed miRNA hits were validated in patient cells and sera…… 74
4. Conclusions & Future Perspectives 79
References 85
Outputs 105
Attachments 111
Attachment 1 113
Attachment 2 129
Attachment 3 147
Attachment 4 151
Attachment 5 155
Attachment 6 159
Attachment 7 163
Attachment 8 167
Attachment 9 171
Attachment 10 175

List of Tables

Table 1 – Lysosomal storage diseases, respective affected genes, defective proteins and accumulated substrates / products. 5

Table 2 – Summary of the molecular, biochemical and clinical characteristics of the patients from which primary skin fibroblasts were obtained. 23

Table 3 – Demographic data regarding the control and patient populations from which peripheral blood was collected. 24

Table 4 – Information about the plasmids used in this project. 24

Table 5 – Information about the equipment used in this project. 25

Table 6 – Information about the consumables used in this project. 26

Table 7 – Information about the reagents used in this project. 27

Table 8 – Information about the kits used in this project. 28

Table 9 – Information about the antibodies used in this project. 28

Table 10 – Information about the enzymes used in this project. 29

Table 11 – Information about the oligonucleotide primer sequences used for site-directed mutagenesis. 29

Table 12 – Information about the oligonucleotide primer sequences used for sequencing PCRs. 30

Table 13 – Information about the software used in this project. 30

Table 14 – Preparation of the reaction tubes for the deglycosylation assay. 33

Table 15 – Cycling conditions for the site-directed mutagenesis PCR. 38

Table 16 – Cycling conditions for the sequencing PCR. 39

Table 17 – Preparation of the reaction tubes for the diagnostic restriction digestion. .. 39

Table 18 – Plasmid ratios for the transient transfection. 41

Table 19 – Preparation of the cDNA MasterMix. 46

Table 20 – Cycling conditions for the cDNA synthesis. 46

Table 21 – Preparation of the qRT-PCR mix. 47

Table 22 – Cycling conditions for the qRT-PCR. 48

Table 23 – Differentially expressed cellular miRNAs in NPC patients vs. controls. 72

List of Figures

Figure 1 – Major functions of the lysosome 3

Figure 2 – Clinical forms of Niemann-Pick type C disease 9

Figure 3 – NPC1 protein topology 10

Figure 4 – miRNA biogenesis 17

Figure 5 – Scheme of the western blot “transfer sandwich”. 34

Figure 6 – Scheme of the puromycin serial dilutions for the cell viability assay 40

Figure 7 – Schematic view of the different methodologies used to develop a new, variant-specific disease model for NPC and to study lysosomal positioning and NPC1 protein trafficking and degradation routes. 52

Figure 8 – Schematic view of the different methodologies employed to survey the miRNA expression profile of NPC patients and to explore new putative disease biomarkers for NPC. 53

Figure 9 – Enzymatic restrictions of pCMV-VSV-G and pUMVC 54

Figure 10 – Diagnostic restriction digest of pCMV-VSV-G and pUMVC 55

Figure 11 – pBABE-puro+NPC1-mNeonGreen annotated plasmid structure 56

Figure 12 – DNA Sanger sequencing electropherograms 57

Figure 13 – Multiple sequence alignment of the different pBABE-puro+NPC1-mNeonGreen constructs (after site-directed mutagenesis) 58

Figure 14 – Puromycin kill curve 59

Figure 15 – NPC1-mNeonGreen expression in non-transduced and transduced *NPC1*$^{-/-}$ ARPE-19 cells 60

Figure 16 – Filipin staining in transduced c.3591+1G>A fibroblasts 61

Figure 17 – LAMP1 quantification 62

Figure 18 – Perinuclear lysosome clustering in transduced *NPC1*$^{-/-}$ ARPE-19 cells 63

Figure 19 – Scoring of lysosome clustering in transduced *NPC1*$^{-/-}$ ARPE-19 cells 64

Figure 20 – PGNase F- and Endo H-mediated cleavage of simple and complex glycoproteins. 65

Figure 21 – Endo H-sensitivity quantification. 66

Figure 22 – LAMP1 and NPC1-mNeonGreen colocalization in transduced *NPC1*$^{-/-}$ ARPE-19 cells 67

Figure 23 – Cross colocalization of LAMP1 with NPC1-mNeonGreen in transduced *NPC1*$^{-/-}$ ARPE-19 cells 68

Figure 24 – Bafilomycin A_1 recovery quantification 70

Figure 25 – DNA dye-terminator Sanger sequencing electropherograms 71

Figure 26 – Cluster analysis of differentially expressed miRNAs 73

Figure 27 – Histogram of target gene candidates 74

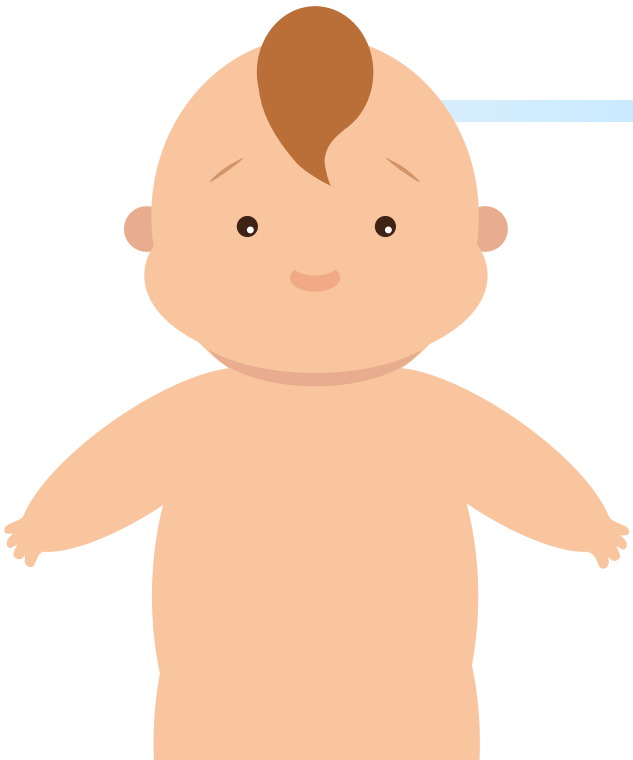
Figure 28 – Expression levels of miR-143-3p and miR-199a-3p in fibroblasts 75

Figure 29 – Expression levels of miR-143-3p and miR-199a-3p in serum 75

List of Abbreviations

AmpR	Ampicillin resistance
ARPE-19	Arising human retinal pigment epithelium
Baf	Bafilomycin A_1
BP	Biological processes
BSA	Bovine serum albumine
BSL-3	Biosafety level 3
CC	Cellular components
cDNA	complementary DNA
CHUdSA	Centro Hospitalar Universitário de Santo António
CNS	Central nervous system
CRL	Cysteine-rich loop
CTRL	Control
DMEM	Dulbecco's modified Eagle medium
EDTA	Ethylenediaminetetraacetic acid
EE	Early-endosome
Endo H	Endoglycosidase H
ER	Endoplasmic reticulum
ER-phagy	Endoplasmic reticulum autophagy
ERAD	Endoplasmic reticulum-associated degradation
ERQC	Endoplasmic reticulum quality control
FBS	Fetal bovine serum
GA	Golgi apparatus
GO	Gene ontology
GSD	Glycogen storage disease
HCV	Hepatitis C virus
HDFa	Human dermal fibroblast, adult
HEK293T	Human embryonic kidney 293 T
HIV	Human immunodeficiency virus
KEGG	Kyoto Encyclopedia of Genes and Genomes
LAMP1	Lysosomal associated membrane protein 1
LAMP2	Lysosomal associated membrane protein 2
LDL	Low-density lipoprotein
LE	Late-endosome
LE/Lys	Late-endosome / lysosome
LIMP2	Lysosomal integral membrane protein 2
LSD	Lysosomal storage disease
LTR	Long terminal repeat
M6PR	Manoose-6-phosphate receptor
MF	Molecular functions
miRNA	microRNA
MPS	Mucopolysaccharidosis

mRNA	messenger RNA
mTORC1	Mammalian target of rapamycin complex 1
MuLV	Murine leukemia retrovirus
NGS	Next-generation sequencing
NMD	Nonsense mediated decay
NPC	Niemann-Pick type C
NPC1	NPC cholesterol transporter protein 1
NPC2	NPC cholesterol transporter protein 2
NT	Non-transduced
NTD	N-terminal domain
PBS	Phosphate buffered saline
PCR	Polymerase chain reaction
PNGase F	Peptide-*N*-glycosidase F
pri-miRNA	Primary microRNA
PuroR	Puromycin resistance
qRT-PCR	Quantitative real-time polymerase chain reaction
RIN	RNA integrity number
RISC	RNA-induced silencing complex
RNA Pol II	RNA polymerase II
RNA-Seq	RNA-sequencing
rRNA	ribosomal RNA
SARS-CoV-2	Severe acute respiratory syndrome coronavirus 2
SDS	Sodium dodecyl sulfate
SDS-PAGE	Sodium dodecyl sulfate - polyacrylamide gel electrophoresis
SMPD1	Sphingomyelin phosphodiesterase 1
snoRNA	small nucleolar RNA
SNP	Single nucleotide polymorphism
snRNA	small nuclear RNA
sRNA	small RNA
sRNA-Seq	small RNA-sequencing
SSD	Sterol-sensing domain
TE	Trisaminomethane-ethylenediaminetetraacetic acid
TFEB	Transcription factor EB
TGN	*trans*-Golgi network
TGS	Tris / Glycine / Sodium dodecyl sulfate
TM	Transmembrane
TPM	Transcripts per million
tRNA	transfer RNA
VCM	Viral collection medium
Veh	Vehicle
VRM	Virus-rich medium
VSGP	Vertical supranuclear gaze palsy
WT	Wild type



Introduction

1.1. Lysosomes

In the 1950s, Christian de Duve's research team, corroborated by Alex B. Novikoff's observations, first identified and hypothesized "a special class of granules", envisioned as "[sacs], consisting of fluid enclosed in a semi-permeable membrane" which contained acid phosphatase, as well as a number of other hydrolases [1–4]. They proposed the designation "lysosomes", underlining their richness in hydrolytic enzymes [5]. And thus began the decades-long vision of lysosomes as catabolic stations of the cell.

We now know lysosomes as dynamic, ubiquitous, membrane-enclosed, cytoplasmic organelles implicated not just in the degradation and turnover of a plethora of cellular components [6], but also in several other cellular processes, including metabolic signaling, gene regulation, immunity, tumorigenesis, nutrient sensing, secretion, plasma membrane repair, lipid transport, cholesterol, calcium and metal ion homeostasis [7–10].

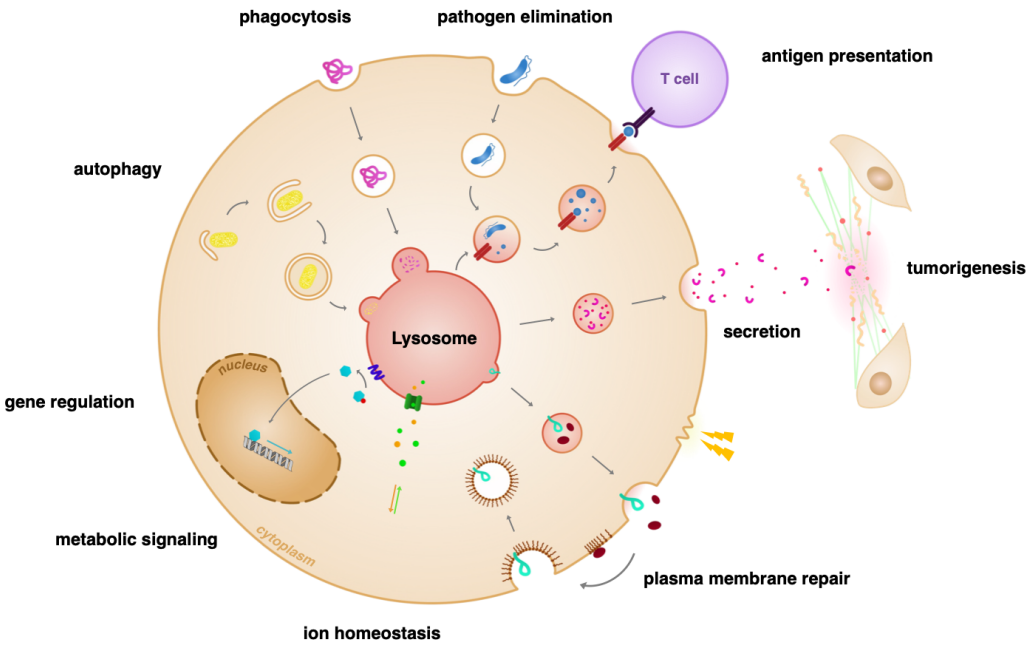


Figure 1 – Major functions of the lysosome. Human lysosomes are involved in a surfeit of cellular functions, including autophagy, phagocytosis, pathogen elimination, antigen presentation, secretion, tumorigenesis, plasma membrane repair, ion homeostasis, metabolic signaling and gene regulation, among others.

The two most vital classes of proteins for lysosome function are soluble lysosomal hydrolases (i.e. acid hydrolases) and integral lysosomal membrane proteins. The first group is involved in bulk degradation, pro-protein processing, antigen processing, extracellular matrix degradation and apoptotic initiation, while the latter is tasked with lysosomal luminal acidification, membrane protection, substrate import, export of degradation products to the cytoplasm, and participation in the formation of membrane

contact sites and fusion with other organelles [8,11]. Many of these proteins interact with other, non-lysosomal, counterparts, to fulfil their function.

Lysosome biogenesis implies integration of the endocytic and biosynthetic pathways. The plasma membrane internalizes cargo into endocytic vesicles, that are mainly delivered to early-endosomes (EEs), which mature over time, through a gradual molecular, structural and functional remodeling into late-endosomes (LEs), and ultimately lysosomes [8]. Throughout this process, there is an acidification of the lumen, an accumulation of Ca^{2+} and other ions, and a direct or indirect delivery of lysosomal proteins, essential events for normal lysosomal function [12].

Soluble lysosomal hydrolases are first synthetized and *N*-glycosylated in the endoplasmic reticulum (ER). During transport through the Golgi apparatus (GA), some mannose residues in most of those *N*-linked oligosaccharides are phosphorylated and recognized by the mannose-6-phosphate receptor (M6PR) in the *trans*-Golgi network (TGN), triggering their enclosure in clathrin-coated vesicles which are then delivered to EEs [13]. A small fraction of lysosomal hydrolases is trafficked through M6PR-independent pathways – most of which still remain unexplored to date, except for the transport of β-glucocerebrosidase [14–16].

The delivery of lysosomal membrane proteins follows different routes. After synthesis in the ER, maturation in the GA, and sorting in the TGN, some of those proteins are directly delivered to endosomes, while others are first delivered to the plasma membrane through the default secretory pathway, before reaching EEs through the endocytic pathway [17,18].

Despite their small size (0.1 – 1.2 μm) [19], lysosomes play an integral role in eukaryotic cells, and their dysfunction has been associated with a number of disorders affecting different organs and systems, notably the central nervous system (CNS) [20].

1.2. Lysosomal Storage Diseases

In the decades following the discovery of lysosomes, the study of these organelles unveiled the biochemical defects underlying many previously described clinical manifestations, bringing forth a new group of disorders categorized as lysosomal storage diseases (LSDs).

LSDs represent over 70 different, rare and recessively inherited monogenic disorders [21], caused by pathogenic variants in genes encoding proteins directly (or even

marginally) involved in lysosomal function and homeostasis [22]. While individually rare, they are collectively estimated to affect 1 in every 5 000 live births worldwide [21], and 1 in every 4 000 live births in Portugal [23].

Clinical manifestations of LSDs are wide-ranging, comprising visceral, ocular, auditive, respiratory, cardiovascular, hematological, skeletal and neurological involvements [24]. The first symptoms can arise as soon as early infancy – usually ensuing the premature death of patients – or as late as adulthood, depending on the affected systems and the severity of the phenotype [25]. This broad scope of clinical manifestations, alongside the rarity of these disorders, often lead to belated diagnoses, hampering more effective treatment options [21].

At the cellular scale, most LSDs are characterized by the intracellular accumulation of undegraded lysosomal substrates, with each disorder displaying a specific set of stored metabolites, depending on the primary genetic defect (Table 1) [26]. Historically, the clinical manifestations of LSDs have been regarded as direct consequences of this abnormal storage, but recent advances are beginning to clarify the pathogenic cascade of events that contribute to LSD pathophysiology [6]. These secondary effects of aberrant substrate accumulation include anomalous membrane composition, aberrant intracellular vesicular trafficking and fusion, autophagy impairment, calcium homeostasis perturbation, mitochondrial dysfunction and oxidative stress, as well as the dysregulation of several signaling pathways and the activation of inflammatory mechanisms [27].

Table 1 – Lysosomal storage diseases, respective affected genes, defective proteins and accumulated substrates / products. Adapted from Platt *et al* (2018) [21].

Disease	Affected gene	Defective protein	Accumulated substrates / products
Sphingolipidoses			
Fabry disease	*GLA*	α-Galactosidase A	Globotriasylceramide
Farber lipogranulomatosis	*ASAH1*	Acid ceramidase	Ceramide
Gaucher disease	*GBA*	β-Glucocerebrosidase	Glucocerebrosidase, glucosylsphingosine
GM1 gangliosidosis	*GLB1*	β-Galactosidase	GM1 ganglioside, keratan sulfate, oligosaccharides
GM2 gangliosidosis (Tay-Sachs disease)	*HEXA*	β-Hexosaminidase A	GM2 ganglioside, glycophospholipids, oligosaccharides
GM2 gangliosidosis (Sandhoff disease)	*HEXB*	β-Hexosaminidase B	GM2 ganglioside, GA2 glycolipid, oligosaccharides
GM2 gangliosidosis (GM2 activator deficiency)	*GM2A*	GM2 ganglioside activator	GM2 ganglioside, glycophospholipids
Globoid cell leukodystrophy (Krabbe disease)	*GALC*	Galactosylceramidase	Galactosylceramide, psychosine

Metachromatic leukodystrophy	*ARSA*	Arylsulfatase A	Sulfatides
	PSAP	Prosaposin	
Niemann-Pick disease types A and B	*SMPD1*	Sphingomyelin phosphodiesterase 1	Sphingomyelin
Mucopolysaccharidoses (MPSs)			
MPS I (Hurler, Hurler-Scheie or Scheie syndrome)	*IDUA*	α-L-Iduronidase	Dermatan sulfate, heparan sulfate
MPS II (Hunter syndrome)	*IDS*	Iduronate 2-sulfatase	Dermatan sulfate, heparan sulfate
MPS IIIA (Sanfilippo syndrome A)	*SGSH*	*N*-Sulfoglucosamine sulfohydrolase	Heparan sulfate
MPS IIIB (Sanfilippo syndrome B)	*NAGLU*	*N*-Acetyl-α--glucosaminidase	
MPS IIIC (Sanfilippo syndrome C)	*HGSNAT*	Heparan-α--glucosaminide-*N*--acetyltransferase	
MPS IIID (Sanfilippo syndrome D)	*GNS*	*N*-Acetylglucosamine-6--sulfatase	
MPS IVA (Morquio syndrome A)	*GALNS*	*N*-Acetylgalactosamine--6-sulfatase	Keratan sulfate, chondroitin-6-sulfate
MPS IVB (Morquio syndrome B)	*GLB1*	β-Galactosidase	Keratan sulfate
MPS VI (Maroteaux-Lamy syndrome)	*ARSB*	Arylsulfatase B	Dermatan sulfate
MPS VII (Sly disease)	*GUSB*	β-Glucuronidase	Dermatan sulfate, heparan sulfate, chondroitin-6-sulfate
MPS IX	*HYAL1*	Hyaluronidase 1	Hyaluronan
Glycogen storage diseases (GSDs)			
GSD II (Pompe disease)	*GAA*	Lysosomal α-glucosidase	Glycogen
α-Mannosidosis	*MAN2B1*	Lysosomal α-mannosidase	Mannose-rich oligosaccharides
β-Mannosidosis	*MANBA*	β-Glucosidase	Man(β1<4)-*N*--acetylglucosamine
Fucosidosis	*FUCA1*	α-L-Fucosidase	Fucose-rich oligosaccharides, glycoproteins, glycolipids
Aspartylglucosaminuria	*AGA*	Aspartoglucosaminidase	Arpartylglucosamine
Schindler disease (Kanzaki disease)	*NAGA*	α-*N*-Acetylgalactosaminidase	Sialylated or asialo glycopeptides, glycosphingolipids
Sialidosis type I (cherry-red spot myoclonus syndrome)	*NEU1*	Neuraminidase-1	Sialylated oligosaccharides, glycopeptides
Sialidosis type II (mucolipidosis I)			Sialylated oligosaccharides, glycopeptides, LAMP1, amyloid precursor protein
Galactosialidosis	*CTSA*	Protective protein cathepsin A, β-Galactosidase, Neuraminidase-1	Sialylated oligosaccharides, glycopeptides, LAMP2, bioactive peptides
Lipid storage diseases			
Acid lipase deficiency (Wolman disease)	*LIPA*	Lysosomal acid lipase / Cholesteryl ester hydrolase	Cholesteryl esters, triglycerides, other lipids

Post-translational modification defects			
Multiple sulfatase deficiency	*SUMF1*	Formylglycine--generating enzyme	Sulfatides
Mucolipidosis II α/β (I-cell disease)	*GNPTAB*	*N*-Acetylglucosamine-1--phosphotransferase subunits α/β	Oligosaccharides, glucosaminoglycans, glycosphingolipids
Mucolipidosis III α/β (pseudo-Hurler polydystrophy)			
Mucolipidosis III γ (variant pseudo-Hurler polydystrophy)	*GNPTG*	*N*-Acetylglucosamine-1--phosphotransferase subunit γ	
Integral membrane protein disorders			
Cystinosis	*CTNS*	Cystinosin	Cystine
Danon disease	*LAMP2*	Lysosome-associated protein 2 (LAMP2)	Cytoplasmic debris, glycogen
Action myoclonus-renal failure syndrome	*SCARB2*	Lysosomal integral membrane protein 2	*Unknown*
Sialic acid storage disease (Salla disease)	*SLC17A5*	Sialin	Sialic acid
Niemann-Pick disease type C	*NPC1*	NPC intracellular cholesterol transporter 1	Cholesterol, sphingolipids
	NPC2	NPC intracellular cholesterol transporter 2	
Mucolipidosis IV	*MCOLN1*	Mucolipin 1	Lipids, mucopolysaccharides
Neuronal ceroid lipofuscinoses			
CLN1 (Haltia-Santavuori disease)	*PPT1*	Palmitoyl-protein thioesterase 1	Lipidated thioesters, saposins A and D
CLN2 (Jansky-Bielschowsky disease)	*TPP1*	Tripeptidyl peptidase 1	Mitochondrial ATP synthase subunit c
CLN3 (Batten-Spielmeyer--Sjogren disease)	*CLN3*	Battenin	
CLN4 (Parry disease, Kufs types A and B)	*DNAJC5*	Cysteine string protein	
CLN5 (Finnish variant)	*CLN5*	Ceroid-lipofuscinosis neuronal protein 5	
CLN6 (Lake-Cavanagh or Indian variant)	*CLN6*	Transmembrane ER protein	
CLN7 (Turkish variant)	*MFSD8*	Major facilitator superfamily domain containing 8	
CLN8 (Northern epilepsy)	*CLN8*	Protein CLN8	
CLN9	*CLN9*	Protein CLN9	*Unknown*
CLN10	*CTSD*	Cathepsin D	Saposins A and D
CLN11	*GRN*	Granulin	*Unknown*
CLN12 (Kufor-Rakeb syndrome)	*ATP13A2*	Cation-transporting ATPase 13A2	Inorganic cations
CLN13	*CTSF*	Cathepsin F	*Unknown*
CLN14	*KCTD7*	Potassium channel tetramerization domain containing 7	*Unknown*

1.3. Niemann-Pick type C

Amongst this vast and varied group of disorders, Niemann-Pick disease was first described by Albert Niemann in 1914 [28], and its anatomic depiction was further outlined by Ludwig Pick in the following decade [29]. Its large clinical variability and the "cumulative affliction" that it encompassed within hospitals led Allan C. Crocker, in 1961, to propose the sorting of these patients into four groups: Niemann-Pick types A, B, C and D [30], which have since been extensively studied and characterized.

Types A and B of Niemann-Pick disease are now known to be caused by defective sphingomyelinase activity, due to mutations in the sphingomyelin phosphodiesterase 1 (*SMPD1*) gene, which render the resulting enzyme either totally or partially dysfunctional, respectively. Patients with these two subtypes differ clinically in the extent of neurodegeneration, symptomatology and life expectancy [31–33].

Niemann-Pick type C (NPC, ORPHA:646) disease is a slowly progressive LSD, caused by pathogenic variants in the *NPC1* (in 95% of cases) or *NPC2* (in the remaining 5 %) genes [34], which encode proteins responsible for the lysosomal export of unesterified cholesterol. The direct effect is the intracellular accumulation of cholesterol, sphingosine and other lipids [35] – hallmarks of this disease – which, in turn, trigger a cascade of other cellular and molecular events, ultimately resulting in the severe neuro-visceral symptomatology associated with NPC [6].

The D type of Niemann-Pick disease has since become obsolete, seeing as this subgroup of patients was found to be merely a cluster of NPC individuals that all originated from Nova Scotia, Canada, who shared a specific founder mutation in the *NPC1* gene [36].

Clinical presentations of NPC patients sway between a swiftly progressing neonatal form to an adult-onset chronic condition. The most common symptoms include (hepato)splenomegaly, jaundice, cognitive impairment, vertical supranuclear gaze palsy (VSGP), ataxia, dystonia, dysarthria, dysphagia, seizures, progressive dementia and other psychiatric signs [37].

Even though this disorder may be described as somewhat of a continuum of symptomatic evolution [38,39], the most broadly accepted classification groups patients considering the age of onset of their first neurological signs (Figure 2) [40]. Ascites and hydrops fetalis are common perinatal presentations of NPC, emphasizing the underlying organomegaly [41]. Cases where the first neurologic symptoms become apparent before patients reach 2 years of age are categorized as "early-infantile", with

hepatosplenomegaly and liver problems becoming nearly invariable manifestations of disease [42]. The “late-infantile” form of NPC (between 2 and 6-years-old) often exacerbates (hepato)splenomegaly, and the first neurologic symptoms usually include gelastic cataplexy, ataxia, seizures and impediments in speech and fine motor skills [43]. Patients neurologically diagnosed between 6 and 15-years-old represent the “juvenile” form of disease, where, besides the almost ever-present hepatosplenomegaly, VSGP becomes apparent, and attention deficits and motor impairments aggravate [43]. The “adult” form of disease often includes psychiatric as well as neurologic complications, such as severe ataxia, dysarthria, dysphagia, dystonia, dementia and psychosis, which present after the age of 15 [44].

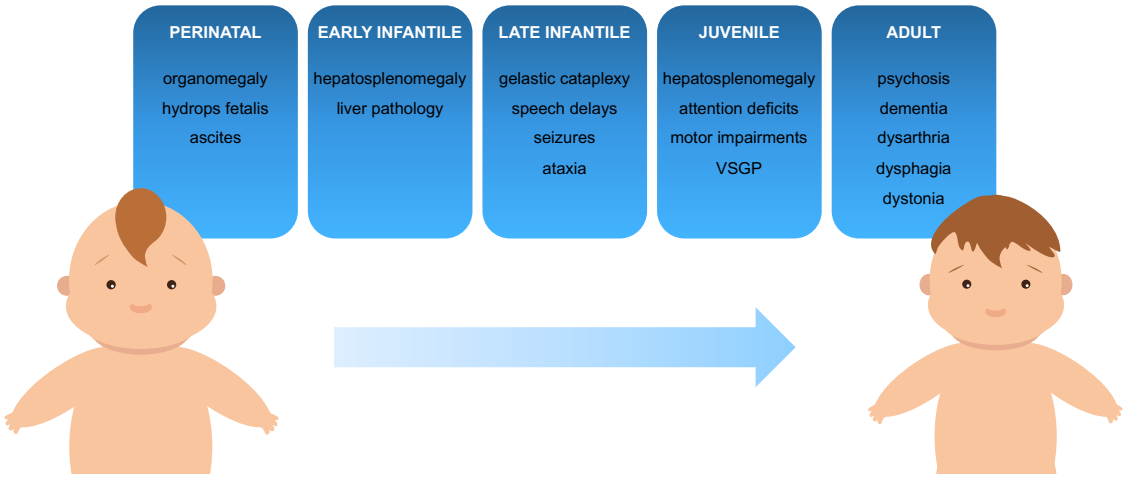


Figure 2 – Clinical forms of Niemann-Pick type C disease. Scheme representing the main symptoms associated with the different subtypes of NPC, evolving from a rapidly progressing neonatal form to an adult-onset chronic condition.

There is no cure for NPC. And despite the different possible therapies undergoing clinical trials, as of today, there is only one substrate reduction therapy approved within the European Union for the treatment of neurological symptoms of NPC patients – – miglustat [45]. The active substance in this medicine – *N*-butyldeoxynojirimycin – acts by inhibiting the synthesis of glycosphingolipids [46], deterring their lysosomal accumulation in the CNS, thereby decelerating neurological damage and dysfunction [47]. Miglustat was initially approved for the treatment of type-1 Gaucher disease, but has since seen its approval extended for NPC patients with neurological manifestations [48].

1.4. NPC1 Protein

The *NPC1* gene spans 55 kb on the reverse strand of human chromosome 18, more specifically at the 18q11.2 *locus* [49]. Its cDNA sequence comprises 25 exons, and it predicts a 1278 amino acid protein, with a molecular weight of about 142 kDa [50]. However, the isolated protein was found to actually be closer to 170 - 190 kDa [51]. This is because NPC1 is co-translationally *N*-glycosylated and folded in the ER, before being transported to the Golgi where it undergoes processing to a mature complex glycosylated protein, which ultimately localizes to late endosomes / lysosomes (LE/Lys) [52].

Topologically, the NPC1 protein has 13 transmembrane (TM) domains, connected by 4 small and 3 large luminally-protruding loops – which are heavily glycosylated, probably to shield them from the abundant endosomal and lysosomal proteases – and various smaller cytoplasmic loops, culminating in a C-terminal cytoplasmic tail (Figure 3) [53]. The protein's N-terminal domain (NTD) is known to bind cholesterol with nanomolar affinity, being hypothesized as the docking place of arriving cholesterol molecules [54–56]. The region between TM domains 3 to 7 displays robust homology with known sterol-sensing domains (SSDs) of several other cholesterol-responding membrane proteins [50], and is thus generally accepted as NPC1's putative SSD [57]. Greer *et al.* first noticed that most disease-causing variants in NPC1 cluster in a luminal cysteine-rich loop (CRL) that appears to be conserved in *NPC1*-related sequences from different organisms, hinting that the integrity of this specific region may be particularly critical for normal protein function [58].

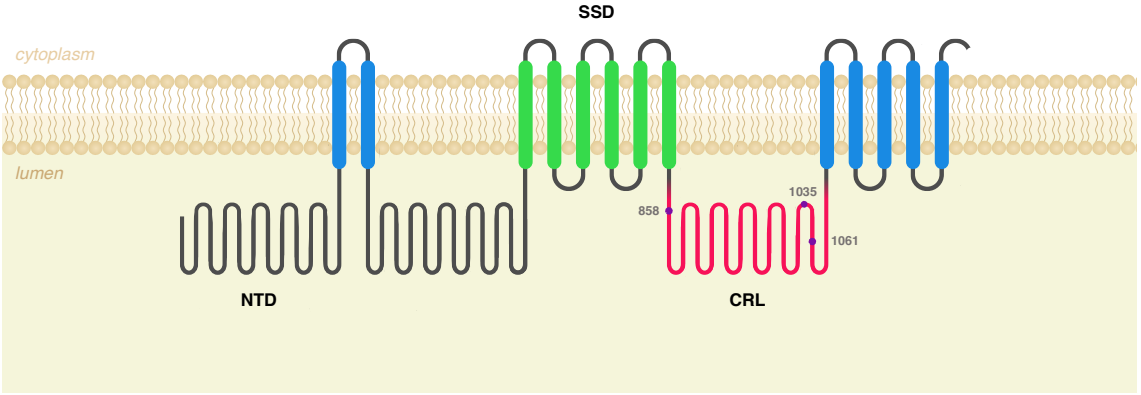


Figure 3 – NPC1 protein topology. The human NPC1 protein has 13 transmembrane domains (blue and green), connected by 4 small and 3 large loops that protrude into the lysosomal lumen, and 5 cytoplasmic loops, culminating in a C-terminal cytoplasmic domain. Cholesterol is delivered to the protein through its N-terminal domain (NTD), which hands the molecules over to its putative sterol-sensing domain (SSD, in green). Most disease-causing mutations in NCP1 are clustered within the protein's cysteine-rich loop (CRL, in pink), which is thought to be particularly critical for normal protein function. The three variants under study in this thesis (in purple) all localize to the CRL.

Once in LE/Lys, it is thought that NPC1's main task is the transport of unesterified cholesterol across the lysosomal membrane. Cholesterol travels across the organism mostly in the form of esters, packaged into the core of low-density lipoproteins (LDLs). Once these molecules are endocytosed, they are transported to the LE/Lys compartment, where lysosomal acid lipase liberates cholesterol from its ester form. Free cholesterol then binds to the soluble lysosomal protein NPC2, which mediates its transfer to the NTD of transmembrane NPC1. Cholesterol is then handed over from the NTD to the putative SSD. Once cholesterol is bound to its SSD, it is thought that NPC1 undergoes a series of still elusive conformational changes, allowing the cholesterol molecule to be integrated into the lysosomal lipid bilayer, making it accessible to the rest of the cell [59–61].

Other proteins, namely the lysosomal associated membrane protein 2 (LAMP2) and the lysosomal integral membrane protein 2 (LIMP2) have also been hypothesized to play some part in the transport of free cholesterol across the lysosomal membrane, even though knowledge about the underlying mechanisms is still in its infancy [62,63].

Novel functions of the NPC1 protein are constantly being discovered, such as its newly uncovered part in the modulation of STING trafficking and immune signaling [64], a possible involvement in specific membrane cargo trafficking [65], or its critical role during infection by several pathogens, including numerous pathogenic *Mycobacterium* species (namely *M. tuberculosis*, *M. bovis*, *M. abscessus*, *M. avium*) [66], the severe acute respiratory syndrome coronavirus 2 (SARS-CoV-2) [67], the Zika, Dengue, and various other flaviviruses [68–70], the Ebola and Marburg filoviruses [71,72], the Chikungunya virus [73], as well as the hepatitis C (HCV) virus [74] and the human immunodeficiency virus (HIV) [75].

1.5. Disease-causing variants

Over 660 disease-causing variants have been identified in the *NPC1* gene and deposited in the Human Gene Mutation Database [76].

The rarest are nonsense and frameshift mutations, which can produce a premature stop codon or a nonsense codon in the messenger RNA (mRNA) transcript, often resulting in degradation of the aberrant mRNA molecules through nonsense mediated decay (NMD) [77,78]. Some variants in *NPC1* can affect the splicing of the resulting mRNA molecule. Such splicing variants can occur either in intronic or exonic regions (even without changing the encoded codon [79]), and they are usually situated in splicing

regulatory sequences [80]. Even when NMD is not recruited, such mutations typically lead to truncated, incomplete or nonfunctional versions of the protein [81].

Most missense pathogenic variants – which account for over half of all disease--causing variants in *NPC1* – lead to conformational modifications that result in the disruption of NPC1 trafficking [82], through mechanisms that still remain somewhat obscure for many of them. These misfolded proteins often trigger the ER quality control (ERQC) machinery, leading to their (partial or complete) retention and degradation either by the proteasome – through MARCH6-dependent ER-associated degradation (ERAD) – or in the lysosome – following selective ER autophagy (ER-phagy) – or even concurrently by both of these pathways [82–84].

In patients of Western European descent, the most frequently reported variant is p.Ile1061Thr, which also happens to be the most widely studied in NPC literature [85]. Mounting evidence has revealed p.Ala1035Val as the most common variant in Portugal and Latin America, and the second most prevalent variant worldwide [86–88]. Both of these variants are located within the protein's CRL, but they present different phenotypes. Growing (unpublished) data from our collaborators, Isaura Ribeiro and Dulce Quelhas, has revealed that all of the analyzed Portuguese p.Ala1035Val alleles are in *cis* with a single nucleotide polymorphism (SNP) on the 858 position (p.Ile858Val), which may contribute to the severity of the phenotype observed in NPC patients with this variant (early infantile form when present in homozygosity).

Studies conducted on the p.Ile1061Thr variant have discovered the resulting mutant protein to be functional, if it could bypass the ERQC triage and reach its ultimate destination: the lysosome [89]. This finding poses protein folding and trafficking as promising targets for NPC therapeutic approaches. In fact, this idea has been explored before for other LSDs (namely Gaucher disease, α-mannosidosis and mucopolysaccharidosis type IIIA) [90–92], and has also been shown to ameliorate cholesterol and sphingolipid accumulation in NPC patient fibroblasts [93], highlighting the importance of studying the trafficking routes and degradation pathways of NPC1 variants.

A recent phase 2/3 trial disclosed somewhat encouraging results for the safety and efficacy of arimoclomol – a novel drug aimed at the treatment of NPC patients following a similar tactic. This small, orally-available molecule is able to cross the blood-brain barrier and stimulate the heat-shock response through the production of heat-shock proteins (molecular chaperones), thus preventing mutant NPC1 protein misfolding, stabilizing lysosomal homeostasis and evading cell death under lysosomal stress [94].

Even despite upholding the safety of this new drug and its alleged 65 % reduction in annual disease progression in NPC patients, the authors withdrew their application for marketing authorization from the European Medicines Agency following the latter's concerns regarding arimoclomol efficacy in improving NPC-related symptoms [95].

1.6. NPC Pathogenesis

Lysosomes are now regarded as dynamic organelles that move inside the cell, fusing with a plethora of targets and undergoing continuous regeneration [96]. For longer distances, lysosomes move bidirectionally between the center and the periphery of cells across the microtubule network, while, for shorter trips, they travel along actin microfilament arrangements [97].

Pathogenic variants in the cholesterol transporter proteins NPC1 or NPC2 lead to an impaired efflux of LDL-derived cholesterol from the LE/Lys compartment, which accumulates within this organelle, alongside other lipids such as sphingosine [35]. The exacerbated lipid accumulation slows down the endocytic pathway by keeping dynein – a motor protein that moves organelles away from the periphery and towards the center of the cell – tethered to the lysosomes, immobilizing these organelles away not just from incoming early-endosomal vesicles but also from the ER [98]. Under normal circumstances, the ER is thought to replenish the endolysosomal calcium stores, which are deliberately released during vesicle fusion events [99–101]. As a result of this mispositioning, NPC cells exhibit diminished Ca^{2+} stocks, and obstructed endolysosomal activity [102–104]. The aberrant accumulation of sphingosine, in specific, is thought to trigger an insufficient lysosomal Ca^{2+} release from the LE/Ly compartment during fusion with endolysosomal vesicles, resulting in less transcription factor EB (TFEB) translocation to the nucleus, where it would act to centrally regulate lysosome biogenesis and autophagic flux [105–107].

With the development of high-throughput next-generation sequencing technologies, genome- and transcriptome-wide analyses may uncover additional mechanisms associated with disease pathogenesis, new biomarker candidates, and even potential therapeutic targets [108–110].

1.7. Models to study NPC

Nowadays, biomedical research on human diseases relies almost entirely on experimental models, which can range from single-celled organisms to non-human primates. Each model can be more or less useful for a specific project, according to its underlying scientific query. In general, an ideal experimental model should mimic the crucial pathological changes and / or systematic symptoms associated with the disorder, and it should allow for the extrapolation of results to the target organism [111].

When studying a human disease, one may be tempted to think of mammalian models as the ideal experimental prototypes. Nonetheless, history has shown that extrapolability is not proportional to evolutionary kinship. Even though we've seen a rising number of mouse models for NPC disease in the last few years [111], new evidence shows that mice are not an appropriate model system to study disease mechanisms like mutant NPC1 protein trafficking and degradation, nor therapeutic strategies that target such pathways [112].

In the 1960s, Donald S. Fredrickson's research team isolated and successfully cultured primary fibroblasts from NPC patients' skin biopsies [113]. Their groundbreaking work initiated a decades-long series of studies based on these primary cell cultures. To this day, patient-derived fibroblasts retain their status as the predominant *in vitro* model for NPC research [111]. This preference can be justified by their readily-available source (skin biopsies), their ease of maintenance and established use as diagnostic tools for NPC.

However useful for some studies, primary fibroblast cultures may become senescent after repeated subculturing and cannot enlighten researchers about the effects of NPC1 dysfunction in highly-specialized cell types, such as neurons. Primary cultures of neurons are very hard to come by, and not feasible for most research purposes [114]. So, as of late, there has been a growing number of studies using embryonic or induced stem cells, which can be differentiated *in vitro* into virtually any cell type [115]. These models have contributed to the exploration and assessment of new therapeutic approaches. The major issue with stem-cell derived models of NPC is the fact that results obtained in different labs are still far from comparable, because of the unstandardized reprogramming and differentiation protocols used across the scientific community [116].

Cell lines are mostly suitable for the discovery of basic molecular functions and pathways involving NPC1 (and its dysfunction), in addition to providing a comparable model to investigate disease-relevant gene variants and their significance [56,117–119].

ARPE-19 is an easily transfected, spontaneously arising human retinal pigment epithelium cell line [120], that has recently been used to study other LSDs and even the role of the NPC1 protein in cholesterol transport [121,122]. In 2019, a PhD candidate at the Telethon Institute of Genetics and Medicine and the University of Oxford generated *NPC1*$^{-/-}$ ARPE-19 cells, using CRISPR/Cas9 technology, and characterized them as exhibiting the classical spectrum of pathological cellular phenotypes of NPC, with ample accumulation of free-cholesterol, sphingosine, and glycosphingolipids, as well as enlarged size and altered morphology and positioning of the LE/Lys compartment [123].

These genetically engineered cells are therefore a promising new model to study NPC disease and, by transfecting / transducing them with *NPC1* constructs harboring different pathogenic mutations, assess their effect *in vitro*, as well as to perform large-scale drug screenings to identify existing drugs that may serve as possible therapies for NPC. Such studies are indispensable to direct any future treatment strategies, as is the timely and effective diagnosis of these NPC patients.

1.8. NPC Diagnosis

The disease is estimated to affect around 1 in every 90 000 live births, even though this incidence rate is likely to be underestimated, due to the amount of belated and misdiagnoses of NPC [124].

Its non-specific and heterogeneous presentations (which can lead to numerous misdiagnoses), alongside the rarity of this disorder (which can make medical professionals unexperienced or unfamiliar with the condition), make it so that several NPC patients go through many appointments and various medical specialties before obtaining a correct diagnosis, which can take decades – this is called the diagnostic odyssey [125].

As this disease is inherited in an autosomal recessive manner, a definitive diagnosis is established for a proband with suggestive findings, by identifying biallelic pathogenic variants (through molecular genetic testing) in either *NPC1* or *NPC2*.

The problem is defining said suggestive findings amidst such a diverse assortment of phenotypes [126]. As of yet, there is no general consensus on clinical diagnostic criteria for NPC. Typical clinical findings should take into account the age on onset, with the most evident symptoms usually shifting from visceral signs at an early age, to neurological and psychiatric manifestations, as patients grow older [34].

Expert panels recommend that, upon reasonable clinical suspicion of NPC, patients should undergo an initial screening, to determine whether they should proceed to genetic confirmation [127]. The filipin staining test – which allows for the visualization of unesterified cholesterol that accumulates within the LE/Lys compartment – was endorsed until recently as the gold standard screening assay for NPC [128,129]. In the last decade, significant advances have prompted the development of sensitive, non-invasive, time- and cost-effective biomarkers, that no longer require a skin biopsy (as opposed to the filipin test). The most prominent examples of these new putative biomarkers include oxysterol species such as cholestane-3β,5α,6β-triol [130] or 7-ketocholesterol [131,132], *N*-palmitoyl-*O*-phosphocholineserine (previously named lyso-sphingomyelin-509) [133,134] and 3β,5α,6β-trihydroxycholanoyl-glycine [135,136]. The issue remains that no single one of these biomarkers is specific for NPC [137], leading researchers to look for other possibilities, among which microRNAs (miRNAs) emerge as particularly promising [138].

1.9. MicroRNAs

In humans, RNA polymerase II operates the transcription of (mainly non-coding) DNA into a long, mono or polycistronic primary transcript named primary microRNA (pri-miRNA), which forms hairpin structures up to thousands of nucleotides in length. These molecules are cleaved by Drosha – a ribonuclease III enzyme – forming pre-miRNA, which is then exported from the nucleus through exportin-5. Once in the cytoplasm, the Dicer ribonuclease III enzyme cleaves these strands into 20-22 nucleotide miRNA double helixes (miR-5p and miR-3p). The guide strand is separated from the passenger strand by helicase and loaded onto the RNA-induced silencing complex (RISC), acting as a template for RISC to recognize a complementary region in the 3' untranslated region of mRNA molecules. If the targeted mRNA region displays extensive complementarity to the miRNA molecule, it will be cleaved by RISC; if, however, this complementarity is only partial, RISC will remain bound to the target mRNA, thereby blocking its binding to ribosomes. In either case, the action of RISC will repress the expression of the target mRNA (Figure 4) [139].

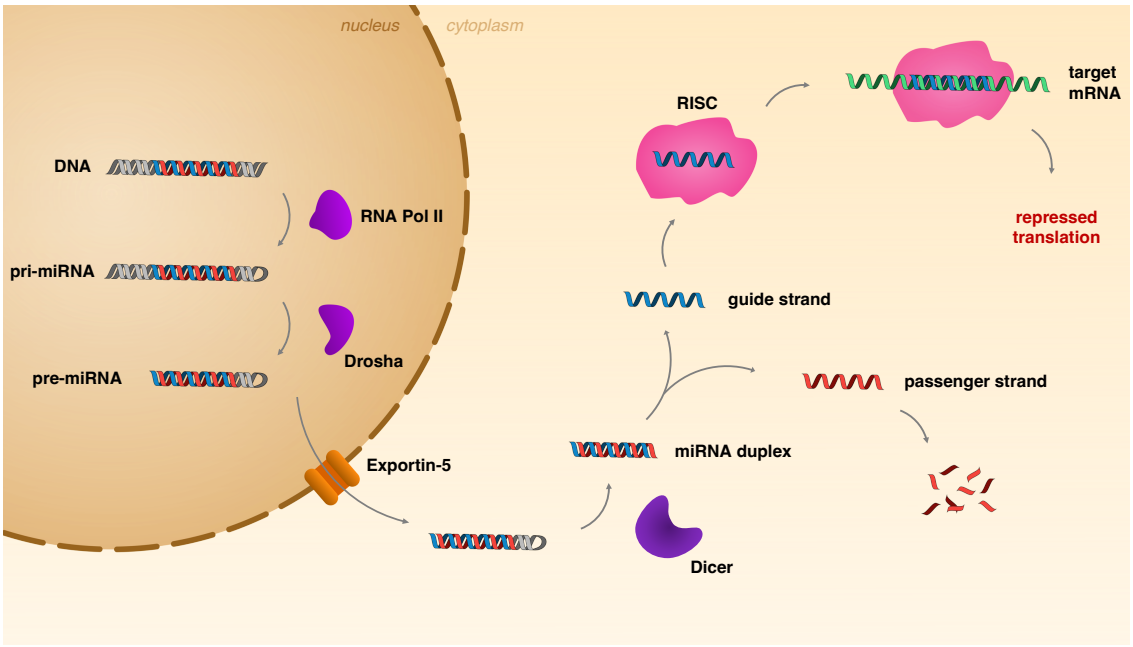


Figure 4 – miRNA biogenesis. RNA polymerase II (RNA Pol II) transcribes primary microRNA (pri-miRNA) from mostly non-coding DNA. This molecule is then cleaved by Drosha, forming pre-miRNA, which is exported through exportin-5 from the nucleus to the cytoplasm, where its hairpin structure is cleaved by Dicer into 20-22 nucleotide miRNA double helixes. The guide strand (blue) is separated from the passenger strand (red) and loaded onto the RNA-induced silencing complex (RISC), acting as a template for RISC to locate and bind a complementary region in the 3' untranslated region of target mRNA molecules (green), thus repressing their expression.

By fine-tuning the expression of several mRNA molecules, miRNAs are vital regulators of cellular development, differentiation and homeostasis. Hence, it is not surprising that their dysregulation has been associated with an escalating number of diseases, from cardiovascular problems to neurological disorders [140]. So far, we could only find two studies regarding miRNAs in NPC disease. In 2010, a Finnish research team characterized the miRNA profile of NPC skin fibroblasts using a low-density array, and found 3 upregulated and 38 downregulated miRNA species [141]. More recently, in 2019, researchers from Chicago indicated miR-155 as a potential indicator of liver and spleen pathology in NPC, reporting this miRNA as upregulated in the liver and downregulated in spleen tissue of *NPC1*$^{-/-}$ mice [142].

miRNAs are detected in circulation within various bodily fluids, including plasma, serum, urine, cerebrospinal fluid, saliva, tears, semen and even breast milk [143]. It remains uncertain whether these molecules are actively exported into circulation or if they simply end up there following cellular degradation [144]. No matter the case, shifts in circulating miRNA levels have been related to diseases and other physiological circumstances. Their inclusion within extracellular vesicles, binding to proteins and association with high--density lipoproteins, allow them to resist circulating ribonucleases, extended storage, freeze-thaw and extreme pH levels, making miRNAs quite stable in blood serum [145].

This stability, alongside the development of swift, high-throughput detection techniques such as RNA-sequencing (RNA-Seq), whose results can be validated through reliable, accurate and sensitive quantification methods, like quantitative real-time polymerase chain reaction (qRT-PCR), bestow serum miRNAs with a great potential as novel biomarkers of disease [146].

In fact, a shift towards miRNAs is taking place in the quest for new disease biomarkers in LSDs [147]. Besides the two aforementioned studies on miRNAs in NPC, their expression has been evaluated in other LSDs, namely Gaucher, Pompe and Fabry diseases. In 2014, a screening of 875 miRNAs was performed using Gaucher disease fibroblasts, identifying miRNAs involved in the regulation of glucocerebrosidase activity in this disorder [148]. A different paper from the same year reported 14 differentially expressed miRNAs that modulate inflammatory response in a murine model of Gaucher disease [149]. In 2019, two independent studies used either small RNA sequencing or miRNA PCR panels to screen for differentially expressed miRNAs in Pompe disease, and both teams validated their results using qRT-PCR, finding several dysregulated circulating miRNAs in the serum of Pompe disease patients [150,151], in a similar fashion to what had been accomplished in 2018 for Fabry disease [152]. Despite the limited number of studies in this field, miRNAs seem to be gaining momentum as possible biomarkers for the diagnosis and assessment of the response to therapies in various LSDs.

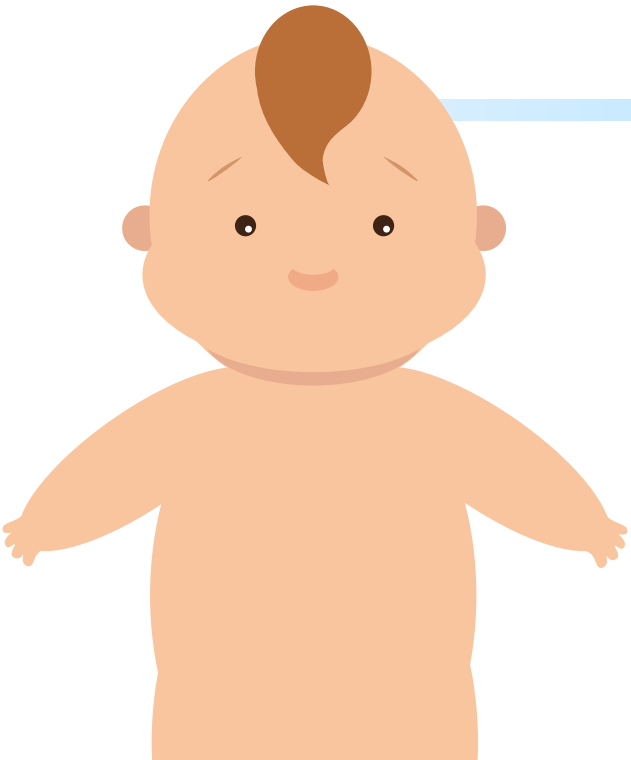
1.10. Aims

The p.Ala1035Val variant in the *NPC1* gene seems to be associated with a severe disease phenotype, but no functional or mechanistic studies have been reported so far. To the best of our knowledge, all NPC alleles harboring the p.Ala1035Val also carry the p.Ile858Val SNP in *cis*. Recent data suggests that the NPC1 protein is extremely sensitive to genetic perturbation, leading us to hypothesize that the additive effect of this frequent polymorphism may impact p.Ala1035Val-NPC1's structure even further, perhaps hindering its interaction with other important proteins on the lysosomal membrane, which could explain the even harsher phenotype observed in these patients, when compared with those carrying the p.Ile1061Thr variant.

The first aim of this project was to survey, study and compare the trafficking and degradation routes of the most widely studied NPC1 variant, p.Ile1061Thr, as well as the most prevalent variant in Portuguese and Latin American NPC patients, p.Ala1035Val, with and without the p.Ile858Val SNP. Since there were no suitable cell models for this

analysis, we aimed to develop cell lines stably expressing the native and differently mutated variants of the protein, through γ-retroviral transduction of NPC1 constructs with a fluorescent tag, allowing us to circumvent the lack of appropriate antibodies for immunofluorescence. This will be an important step towards the elucidation of the cellular and molecular pathophysiology of NPC disease, imperative for steering future therapies.

Therapeutic efficacy often relies on a correct and prompt diagnosis, particularly in irreversibly neurodegenerative diseases, such as NPC, for which there are still no specific biomarkers, and where diagnoses are often belated and thwarted by the vast phenotypic variability. This is why, as a second aim, we undertook the task of tracing and comparing the miRNA profile of NPC patients with that of healthy controls, and validating the most differentially expressed miRNA hits in blood serum, in hopes of finding reliable, minimally-invasive and specific biomarker candidates for this disorder.



Materials & Methods

2.1. Materials

2.1.1. Patient and control-derived samples

Two different types of samples were used for this project: primary skin fibroblasts and peripheral blood. These biological samples were collected in compliance with the Declaration of Helsinki, after dully informing the donor (or a legal guardian) who provided their consent to partake in this study, which was approved by the Ethics Committee of all the participating institutions.

Primary skin fibroblasts from NPC patients with the p.Val505Gly/Val562=, p.Ile1061Thr/p.Ile1061Thr, p.Ala1035Val/p.Ala1035Val and p.Ala1035Val/c.1554--1009G>C *NPC1* genotypes (Table 2) were obtained from two Portuguese reference centres of rare inherited metabolic disorders – *Centro Hospitalar Universitário de Santo António* (CHUdSA) and *Centro Hospitalar Universitário de São João*. The biochemical and molecular diagnoses of patients NPC_1, NPC_2 and NPC_4 was carried out at the Biochemical Genetics Unit of the *Centro de Genética Médica Dr. Jacinto Magalhães*, CHUdSA, and the NPC_3 patient was diagnosed at our lab.

Table 2 – Summary of the molecular, biochemical and clinical characteristics of the patients from which primary skin fibroblasts were obtained.

Patient	Clinical subtype	Pathogenic variant		Reference
		coding DNA	Protein	
NPC_1	Early infantile	c.3104C>T	p.Ala1035Val	[86]
		c.3104C>T	p.Ala1035Val	
NPC_2	Early infantile	c.3104C>T	p.Ala1035Val	[86]
		c.3104C>T	p.Ala1035Val	
NPC_3	Juvenile	c.1514T>G	p.Val505Gly	[153]
		c.1686G>A	p.Val562=	[154]
NPC_4	Late infantile	c.3104C>T	p.Ala1035Val	[86]
		c.1554-1009G>A	-	[155]

Primary skin fibroblasts from another NPC patient, homozygous for the c.3591+1G>A splicing variant in *NPC1* were also obtained from the two previously mentioned reference centres of rare hereditary metabolic disorders, to test the transduction and filipin staining protocols [86]. These cells effectively produce no detectable NPC1 protein, mimicking cells where *NPC1* has been artificially knocked-out.

Peripheral blood samples were collected from 3 healthy controls and 4 NPC patients from the same two reference centres, with biochemical and molecular diagnosis of NPC, but for whom the genotype was not provided (Table 3).

Table 3 – Demographic data regarding the control and patient populations from which peripheral blood was collected.

Group	Age (mean ± SD)	Sex (male / female)
Control	38 ± 9	0 / 3
Patient	32 ± 12	3 /1

2.1.2. Cell lines

Three primary human dermal fibroblast cell lines were used as controls in several trials. Two of them were anonymized cell lines already available at the laboratory, and the last was a Human Dermal Fibroblast, adult (HDFa) cell line commercially acquired from Innoprot (*P10856*).

For the production of γ-retroviral particles carrying the different *NPC1* constructs, a Human Embryonic Kidney 293 T (HEK293T) cell line was used, which was a kind gift from John Neidhardt, at the Carl von Ossietzky University of Oldenburg.

ARPE-19 and *NPC1*$^{-/-}$ ARPE-19 cells were kindly gifted through Andrea Ballabio's group at the Telethon Institute of Genetics and Medicine, for functional studies with the different *NPC1* variants.

2.1.3. Plasmids

The three plasmids used for this study (Table 4) were obtained through Addgene, being kindly gifted by either Kartik Chandran, from the Albert Einstein College of Medicine, or Bob Weinberg, from the Massachusetts Institute of Technology.

Table 4 – Information about the plasmids used in this project.

Plasmid	Type	Size	Bacterial Antibiotic Resistance	Gifted by
pBABE-puro+NPC1-mNeonGreen	transfer	9.7 kb	Ampicillin (100 µg/mL)	Kartik Chandran
pCMV-VSV-G	envelope	6.5 kb	Ampicillin (100 µg/mL)	Bob Weinberg
pUMVC	packaging	9.3 kb	Kanamycin (50 µg/mL)	Bob Weinberg

2.1.4. Equipment

All of the laboratory equipment used for this project is listed in Table 5.

Table 5 – Information about the equipment used in this project.

Equipment	Model	Source
Counting chamber	Neubauer improved	Marienfeld Superior™
DNA Analyzer	ABI 3130XL	Applied Biosystems™
DNA fragment analysis system	2100 Bioanalyzer	Agilent Technologies
Dry heating block	ThermoMixer® Comfort	eppendorf®
Electrophoresis system	Compact Multi-Wide	Biometra
Fluorescence microscope	DM 4000 B	Leica
Gel imaging system	GelDoc™ XR	Bio-Rad
Freezing container	Mr. Frosty™	Thermo Scientific™
Imaging system	ChemiDoc™ XRS+	Bio-Rad
Incubator shaker	KS 4000i control	IKA
Inverted microscope	DM IL	Leica
Magnetic hot-plate stirrer	Advanced VMS-C7	VWR®
Microcentrifuge	MiniStar silverline	VWR®
Microplate reader	SpectraMax® iD3	Molecular Devices
Mili-Q purification system	Millipore RiOS™ 5	MERCK
PAGE system	Mini-PROTEAN® Tetra	Bio-Rad
Pipet filler	S1	Thermo Scientific™
Plate reader	VICTOR® Nivo™	PerkinElmer
Power supply	PowerPac™ Basic	Bio-Rad
Precision balance	CBS series	COBOS
Real-time thermocycler	CFX96™	Bio-Rad
Refrigerated centrifuge	KR-20000T	KUBOTA
Refrigerated centrifuge	3K30	Sigma Laborzentrifugen
Refrigerated microcentrifuge	5415 R	eppendorf®
Refrigerated shaker incubator	Innova™ 4230	New Brunswick™
Repetitive pipette	Multipette® plus	eppendorf®
Sequencing system	NextSeq 2000	illumina®
Shaker	Rotamax 120	Heidolph
Spectrophotometer	NanoDrop™ 1000	Thermo Scientific™
Thermocycler	TProfessional Basic	Biometra
Vortex mixer	VV3	VWR®
Water bath	Aqualine AL18	LAUDA

2.1.5. Consumables

The consumables used in this project are listed in Table 6.

Table 6 – Information about the consumables used in this project.

Consumable	Source
0.2 mL Multiply®-Pro PCR tubes	SARSTEDT
1.5 mL RNase-free microfuge tubes	invitrogen™
10 Combitips® plus dispenser tips	eppendorf®
10 mL CLEARline® serological pipettes	Biosigma
10 µL pipette filter tips	SARSTEDT
1000 µL pipette filter tips	SARSTEDT
12-well OrPlate tissue culture plates	Orange Scientific
13 mL round-bottom tubes	SARSTEDT
15 mL conical centrifuge tubes	SARSTEDT
2 mL CLEARline® serological pipettes	Biosigma
20 µL pipette filter tips	SARSTEDT
200 µL pipette filter tips	SARSTEDT
24 x 50 mm, 1.5 thickness cover glasses	VWR®
25 cm^2 vented cap, tissue culture flasks	VWR®
25 mL CLEARline® serological pipettes	Biosigma
5 mL CLEARline® serological pipettes	Biosigma
50 mL conical centrifuge tubes	SARSTEDT
6-well OrPlate tissue culture plates	Orange Scientific
75 cm^2 vented cap, tissue culture flasks	VWR®
8-well, Lab-Tek II chamber slides	nunc™
9 mL CAT serum clot activator tubes	VACUETTE®
96-well microtest plate	SARSTEDT
CryoTube™ vials	Thermo Scientific™
Disposable Pasteur pipettes	VWR®
Glass Pasteur pipettes	Normax
Hard-shell 96-well PCR plates	Bio-Rad
KIMTECH precision wipes	Kimberly-Clark®
Microseal® 'B' seals	Bio-Rad
Mini-PROTEAN® Stain-free 4 – 15 % gels	Bio-Rad
Nunclon™ Delta-treated 96-well plates	nunc™
parafilm® laboratory film	BEMIS®
PROTRAN® nitrocellulose membrane	Whatman®

2.1.6. Reagents

General chemicals and other reagents used in this study are listed in Table 7.

Table 7 – Information about the reagents used in this project.

Reagent	Source
2-Propanol (isopropanol), for analysis	EMSURE®
Acetic acid (glacial)	EMSURE®
alamarBlue®	invitrogen™
Albumine from bovine serum	Sigma-Aldrich®
Ampicilin (sodium salt)	NZYtech
Bafilomycin A1	Enzo
BioWhittaker™ 10X PBS (without Ca^{2+} and Mg^{2+})	Lonza
Chloroform, for analysis	EMSURE®
Dimethyl sulfoxide (DMSO)	Sigma-Aldrich®
DMEM (1X) + GlutaMAX™-I + D-Glucose (1g/L) + Pyruvate	gibco™
DMEM/F-12 (1:1) + L-Glutamine	gibco™
Ethanol, absolute, for analysis	EMSURE®
Ethidium Bromide solution (10 mg/mL)	Sigma-Aldrich®
EverBrite™ mounting medium with DAPI	Biotium
Fetal Bovine Serum, Qualified	gibco™
Filipin complex, from *Streptomyces filipinensis*	Sigma-Aldrich®
FuGENE® HD Transfection Reagent	Promega
Glycine, Electran® molecular biology grade	VWR®
HEPES (1 M) buffer solution	gibco™
Kanamycin solution from *Streptomyces kanamyceticus*	Sigma-Aldrich®
LB-Agar powder	Panreac Applichem
LB-Medium powder	Panreac Applichem
Methanol, for analysis	EMSURE®
NuPAGE™ LDS sample buffer (4X)	invitrogen™
NuPAGE™ sample reducing agent (10X)	invitrogen™
NZY Broth powder	Fisher BioReagents™
NZYSpeedy qPCR Green MasterMix (2X)	NZYtech
PageRuler™ Plus prestained protein ladder	Thermo Scientific™
Ponceau S powder	Sigma-Aldrich®
ProLong™ Diamond antifade mountant	invitrogen™
Protease Inhibitor cocktail	Sigma-Aldrich®
Puromycin Dihydrochloride (10 mg/mL)	gibco™
SeaKem® GTG® Agarose	Lonza
Sodium Dodecyl Sulfate	Fisher BioReagents™
Terrific Broth, for microbiology	MERCK

TrackIt™ 1kb Plus DNA ladder	invitrogen™
TriTrack DNA Loading Dye (6X)	Thermo Scientific™
TE buffer, for laboratory research	invitrogen™
Tris/Glycine/SDS Buffer (10X)	Bio-Rad
Trypsin-EDTA, 0.05 %	gibco™
Tween® 20, molecular biology grade	VWR®
Water, for molecular biology, sterile, filtered	Sigma-Aldrich®

2.1.7. Kits

The commercially acquired kits used in this study are listed in Table 8.

Table 8 – Information about the kits used in this project.

Kit	Company
Clarity™ Western ECL Substrate	Bio-Rad
illustra™ ExoProStar™ 1-Step	Cytiva
miRNeasy® Serum/Plasma Kit	QIAGEN
Monarch® Plasmid MiniPrep Kit	New England BioLabs®
QIAfilter Plasmid Maxi Kit	QIAGEN
QuikChange Lightning Site-Directed Mutagenesis Kit	Agilent Technologies
Ready-To-Go™ You-Prime First-Strand Beads	Cytiva
RNA 6000 Pico Kit	Agilent Technologies
TaqMan™ MicroRNA Assays	Applied Biosystems™
TruSeq® small RNA Library Prep Kit	illumina®

2.1.8. Antibodies

The primary, secondary and conjugate antibodies used for western blots and immunofluorescence assays are all listed in Table 9.

Table 9 – Information about the antibodies used in this project.

Antibody	Dilution	Host species	Company
α-Actin	WB | 1:5000	mouse	Santa Cruz Biotechnology
α-LAMP1	WB | 1:500	mouse	Santa Cruz Biotechnology
	IF | 1:200		
α-rabbit IgG-HRP	WB | 1:40000	mouse	Santa Cruz Biotechnology
α-mouse IgG-HRP	WB | 1:40000	goat	Santa Cruz Biotechnology
Alexa Fluor™ 594 α-mouse	IF | 1:500	goat	Invitrogen
α-NPC1	WB | 1:5000	rabbit	Abcam

2.1.9. Enzymes

Several enzymes were used throughout this project. Table 10 lists the ones not included in commercial kits.

Table 10 – Information about the enzymes used in this project.

Enzyme	Company
BamHI	New England BioLabs®
DraI	
EcoNI	
Endo H	
NcoI	
NdeI	
NotI	
PNGase F	
XhoI	

2.1.10. Primers

Oligonucleotide primers were synthesized by Invitrogen. The ones used for site-directed mutagenesis (Table 11) were purified through high-performance liquid chromatography (HPLC), while those used for sequencing PCRs (Table 12) were purified by the desalting method.

Table 11 – Information about the oligonucleotide primer sequences used for site-directed mutagenesis.

Designation	Oligonucleotide sequence (5' → 3')	Tm (ºC)
p.Ala1035Val_F	GCACCAGGGTCGGAGTCACGTACTTCATGAC	62
p.Ala1035Val_R	GTCATGAAGTACGTGACTCCGACCCTGGTGC	62
p.Ile858Val_F	TCGCAGTCCTGAACAAAGTAGATGTTGGATTGGATCAG	60
p.Ile858Val_R	CTGATCCAATCCAACATCTACTTTGTTCAGGACTGCGA	60
p.Ile1061Thr_F	ACGCTCTGAAGAAAGCCCGACTTACGGCCAGTAATGTCAC	65
p.Ile1061Thr_R	GTGACATTACTGGCCGTAAGTCGGGCTTTCTTCAGAGCGT	65

Table 12 – Information about the oligonucleotide primer sequences used for sequencing PCRs.

Designation	Oligonucleotide sequence (5' → 3')	Tm (ºC)
NPC1_Ex21-24_F	GTCGGAGCCACGTACTTCAT	60
NPC1_Ex21-24_R	GACCATGGCCAAATACATCC	60
NPC1_Ex16-21_F	CTGTCATTCAGCATCGCAGT	60
NPC1_Ex16-21_R	GGCTTTCTTCAGAGCGTCAA	60
NPC1_Ex13-17_F	TCGAAGGTCTCACTAGGCATC	60
NPC1_Ex13-17_R	CTGGCATCGAAAGAGACTGA	60

2.1.11. Software

Table 13 lists all the software used in this study.

Table 13 – Information about the software used in this project.

Software	Version	Developer
ImageJ2	2.3.0	Open source
Image Lab	6.1	Bio-Rad
Microsoft Office	16.75	Microsoft
SnapGene Viewer	6.2.1	SnapGene
SPSS Statistics	29.0.0.0	IBM
MEGA	11.0.10	Pennsylvania State University

2.2. Methods

2.2.1. Cell culture

2.2.1.1. Culture conditions

Human cell cultures were grown on tissue-culture treated 25 cm^2 and 75 cm^2 polystyrene flasks or 6- and 12-well plates. They were incubated at 37 ºC, and 5 % CO_2. HDFa, HEK293T and control- and patient-derived fibroblasts were all cultured in DMEM, supplemented with 10 % FBS, 1 g/L D-Glucose, with pyruvate and GlutaMAX™. ARPE-19 and *NPC1*$^{-/-}$ ARPE-19 cells were cultured using DMEM/F-12 (1:1), supplemented with 10 % FBS and 2.5 mM L-glutamine.

2.2.1.2. Subculturing cells

Once cells reached around 80 % confluency, they were passaged to new flasks or plates. After removing the growth medium, adherent cells were washed with 1X PBS, and incubated with 0.05 % Trypsin-EDTA for 5 min, at 37 ºC, and 5 % CO_2. The reaction was inhibited by resuspension in at least 2 volumes of new culture medium. For the ARPE-19 and *NPC1*$^{-/-}$ ARPE-19 an additional step was taken before passaging the resuspended cells to new flasks / plates, which consisted in centrifuging the cells for 10 min, at 125 x g, discarding the supernatant and resuspending the cells in fresh culture medium. Cells were then seeded into new flasks or plates, and re-incubated at 37 ºC, and 5 % CO_2.

2.2.1.3. Counting cells

When cell quantification and viability needed to be assessed, an aliquot of suspended cells was collected during the subculture procedure – before seeding them in the new flask or plate – and mixed with an equal volume of 0.4 % Trypan Blue stain. 10 µL of the mix were then pipetted into each side of the improved Neubauer chamber, and the unstained (viable) cells were counted and averaged per square, multiplied by the dilution factor (2) and by 10^4, in order to obtain the number of viable cells per mL.

2.2.1.4. Pelleting cells

Cell pellets were obtained by washing adherent cell cultures with 1X PBS and incubating them with 0.05% Trypsin-EDTA for 5 min, at 37 ºC, and 5 % CO_2, before resuspending them in at least 2 volumes of new culture medium and centrifuging them for 5 min, at 1000 x g. The supernatant was discarded, and the centrifugation step was repeated twice, but at 4 ºC, and using ice-cold 1X PBS to resuspend the cells before spinning. Cell pellets were stored at -80 ºC.

2.2.1.5. Cryopreserving cells

For long-term storage, cells were stored in liquid nitrogen. After trypsinization, cell cultures were resuspended in freezing medium – either DMEM or DMEM/F-12, containing 20 % FBS and 10 % DMSO. The resuspension was transferred to cryovials and placed inside an isopropanol-filled freezing container, in order to achieve a

-1 °C / min cooling rate (optimal for cell preservation), and left overnight at -80 ºC. The cryovials were then transferred to a liquid nitrogen (-196 ºC) container.

2.2.1.6. Reviving cells

Cells stored in liquid nitrogen were recovered by thawing the cryovials in a 37 ºC water-bath, until close to 80 % of the cell solution had thawed. The contents of the vial were then slowly added to 9 mL of pre-warmed culture medium, inside a 15 mL Falcon tube, which was then centrifuged for 5 min, at 1000 x g, and room-temperature. The DMSO-containing supernatant was discarded, and the cells resuspended in the appropriate culture medium, before being seeded in a tissue-culture treated flask or plate, and incubated at 37 ºC, and 5 % CO_2.

2.2.1.7. Mycoplasma testing

All the cell cultures were tested for mycoplasma, by growing them for at least 2 weeks without antibiotics and collecting two 1 mL samples of growth medium, which was then subject to polymerase chain reaction (PCR) analysis, performed at the Research and Development Unit of the National Institute of Health Dr. Ricardo Jorge, in Lisbon.

2.2.2. Protein analysis

2.2.2.1. Protein extraction

Frozen cell pellets were thawed on ice and resuspended in an appropriate amount of RIPA buffer (25 mM Tris, pH = 7.6, 150 mM NaCl, 1 % nonidet P40, 1 % sodium deoxycholate and 0.1 % SDS) with 0.01 % Protease Inhibitor cocktail. The suspensions were kept on ice for 1 h, resuspending every 15 min, before being centrifuged for 5 min, at 3000 x g, and 4 ºC. The supernatant was collected into a new 1.5 mL Eppendorf tube and stored at -20 ºC until further use.

2.2.2.2. Protein quantification

Total protein quantification was carried out following the Pierce™ BCA Protein Assay Kit, from Thermo Scientific™.

Standard dilutions of Bovine Serum Albumin (BSA) were prepared according to the manufacturer's instructions. 10 µL of sample or BSA standard were pipetted into the wells of a 96-well microplate (in duplicates), and 200 µL of Working Reagent were added to each well. The plate was sealed with adhesive film, placed in a plate shaker of 30 s, and incubated for 30 min, at 37 ºC. After cooling the plate down to room temperature, the adhesive film seal was removed, and absorbance was measured at 562 nm, using a VICTOR® Nivo™ multimode plate reader. After subtracting the average Abs_{562} blank value from all the other standards and samples, a standard curve was prepared by plotting the blank-corrected Abs_{562} measurement of each BSA standard vs. its concentration. Linear regression analysis showed a very strong correlation with $R^2 \geq 0.99$. The standard curve was then used to the determine the total protein concentration for each sample tested.

2.2.2.3. Deglycosylation assay

In order to evaluate and compare the glycosylation status of wildtype and mutant NPC1 protein variants, protein extracts were incubated with either the Peptide-*N*--Glycosidase F (PNGase F) or the Endoglycosidase H (Endo H) enzymes, both from New England BioLabs®, following the protocol described by Schultz *et al.* (2022) [112].

For each sample, three 1.5 mL Eppendorf tubes were prepared, containing 20 µg of protein, 1 µL of 10X Glycoprotein Denaturing Buffer, and MiliQ water up to 10 µL. The tubes were heated to 37 ºC for 15 min, and quickly cooled by incubating them on ice, for 20 s. After a short spin-down, the reactions were prepared according to Table 14.

Table 14 – Preparation of the reaction tubes for the deglycosylation assay.

Tube	MiliQ water	Buffer		NP-40 (10%)	Enzyme	
Non-treated	8 µL	2 µL	Glycobuffer 3 (10X)	-	-	-
Endo H	6 µL	2 µL	Glycobuffer 3 (10X)	-	2 µL	Endo H
PNGase F	6 µL	3 µL	Glycobuffer 2 (10X)	2 µL	1 µL	PNGase F

The reactions were then incubated for 3 h, at 37 ºC. Following the incubation period, 7 µL were removed from each reaction tube, making a final volume of 13 µL, to which 5 µL of 4X NuPAGE™ LDS Sample Buffer and 2 µL of 10X NuPAGE™ Sample Reducing Agent were added. The tubes were incubated for 10 min, at 70 ºC, and kept at -20 ºC until further use.

2.2.2.4. SDS-PAGE

For samples that were not denatured before, 13 µg of protein were mixed with 5 µL of 4X NuPAGE™ LDS Sample Buffer, 2 µL of 10X NuPAGE™ Sample Reducing Agent and MiliQ water up to a final volume of 20 µL, and the mix was heated to 70 ºC, for 10 min, before performing the Sodium Dodecyl Sulphate – Polyacrylamide Gel Electrophoresis (SDS-PAGE).

After assembling the Bio-Rad Mini-PROTEAN® Tetra System, using gels and a buffer dam (when appropriate), 1X Tris/Glycine/SDS (TGS) Buffer was used to fill the upper and lower buffer chambers. Then, 10 µL of protein ladder were loaded onto the first well of each gel, and 20 µL of denatured sample mix were loaded onto the remaining wells. A constant voltage of 200 V was set on the power source, and the electrophoresis ran for 40 - 45 min.

2.2.2.5. Western blot

Following SDS-PAGE, the stratified proteins were transferred from the gel to a nitrocellulose membrane. A “transfer sandwich” was assembled in ice-cold Transfer Buffer, according to the scheme in Figure 5, and held together by a plastic cassette. The cassette was then placed inside the Bio-Rad Mini-PROTEAN® Tetra System, which was filled to the top line with more ice-cold Transfer Buffer, and the transfer took 45 min, at a constant amperage of 300 mA.

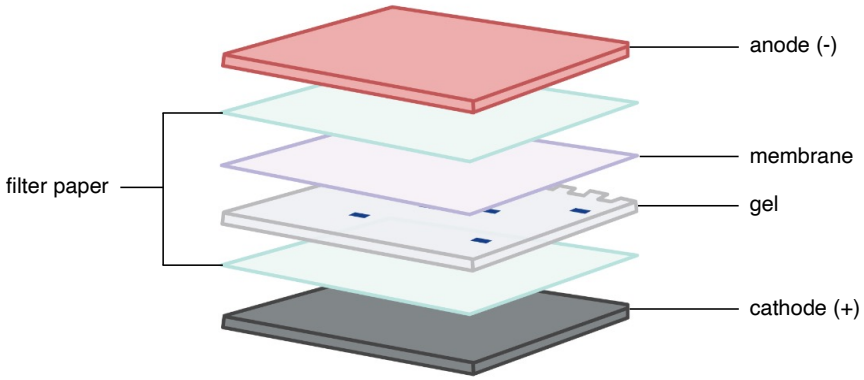


Figure 5 – Scheme of the western blot “transfer sandwich”.

At this point, the Ponceau S staining was performed on the nitrocellulose membrane, by incubating it with Ponceau S solution [0.1 % (w/V) Ponceau S in 5 % (V/V) acetic acid] for 5 min, before washing the membrane 3 times with Wash Buffer (0.1 % Tween-20® in 1X PBS) and proceeding with the blot.

The membrane was then incubated with Blocking Solution [5 % (w/V) BSA in Wash Buffer] for 1 h, at room temperature, on a shaker. Then, the blocked membrane was cut into two sections, around the 70 kDa molecular weight marker. Each section was then incubated overnight with its respective primary antibodies, at 4 ºC, in a wet chamber, on a shaker. The lower half of the membrane, corresponding to proteins with lower molecular weight, was incubated with α-Actin antibody, the loading control used in this study, while the upper section, containing the heavier proteins was incubated with either α-LAMP1 or α-NPC1 antibody, according to the goal of each experiment.

After being washed 3 times for 10 min with Wash Buffer, both membrane sections were incubated for 40 min with the respective secondary antibody. The lower section, containing the now antibody-bound Actin protein, was incubated with goat α-mouse IgG--HRP antibody, and the upper section, containing the LAMP1 or NPC1 antibody-bound proteins, was incubated with the same goat α-mouse IgG-HRP for LAMP1 labelling or mouse α-rabbit IgG-HRP antibody for NPC1.

The sections were then washed again 3 times using Wash Buffer, before being incubated with ECL solution for 5 min, protected from the light, draining the excess solution and capturing the image on a ChemiDoc™ XRS+ imaging system.

2.2.3. Generation of stably transduced *NPC1*$^{-/-}$ ARPE-19 cells and functional analysis of different *NPC1* variants

2.2.3.1. Transformation of competent *E. coli* cells

Upon receiving the pBABE-puro+NPC1-mNeonGreen plasmid diluted in Nuclease--free water, we needed to multiply it, for which we followed the New England BioLabs® High Efficiency Transformation Protocol using NEB® 10-β Competent *E. coli*, according to the company's instructions, except for growth temperature, which was changed to 30 ºC (instead of the recommended 37 ºC), pursuant to the plasmid author's advice.

A tube of 10-β *E. coli* cells was thawed on ice until every ice crystal had disappeared, at which point a volume corresponding to 100 ng of plasmid DNA was added to each tube, carefully flicking to mix. The mixture was chilled on ice for 30 min, swiftly heat shocked for 30 s, in a 42 ºC water-bath, and left on ice for 5 min, to rest. After this incubation, 950 µL of room-temperature NEB® 10-β/Stable Outgrowth Medium were added to the mix, which was then incubated for 1 h, at 30 ºC, and 300 rpm shaking. Next,

the tubes were flicked to mix the cells, and 10-fold serial dilutions of the cell suspension were spread onto several selection plates (LB-Agar containing 100 µg/mL Ampicillin), which were incubated for 36 h, at 30 ºC, and 300 rpm shaking.

2.2.3.2. Glycerol stock preparation

Single colonies were picked from the selection plates and inoculated in 5 mL LB Medium, containing the appropriate antibiotic, and grown overnight, at 30 ºC, with 300 rpm shaking. For long-term storage, glycerol stock cryovials were prepared by mixing 500 µL bacterial culture with 500 µL of 50 % glycerol, being stored at -80 ºC until further use.

2.2.3.3. Plasmid purification

For initial preparations, the New England BioLabs® Monarch® Plasmid DNA Miniprep Kit was used, according to the manufacturer's directions and recommendations. Transformed and selected bacterial cultures were grown in antibiotic-containing LB medium, at 30 ºC, and 300 rpm shaking, to < Abs_{600}. 1.5 mL of bacterial culture was then transferred to a 1.5 mL Eppendorf tube, centrifuged for 30 s, at 16 000 x g. The supernatant was discarded, and the pellet resuspended in 200 µL Plasmid Resuspension Buffer, by pipetting up and down. 200 µL Plasmid Lysis Buffer was added and the tube was immediately inverted 5-6 times, until the solution turned clear and viscous. 1 min later, 400 µL Plasmid Neutralization Buffer was added, and the tube gently inverted until a precipitate formed. Following a 2 min incubation, at room temperature, the tube was centrifuged for 5 min, at 16 000 x g, and the supernatant carefully transferred to a spin column. Another centrifugation took place, this time for 1 min, at the same speed. The flow-through was discarded and 200 µL Wash Buffer 1 was added, leaving the tube incubating at room temperature for 5 min, before centrifuging again for 1 min, at 16 000 x g. After the flow-through was again discarded, 400 µL Wash Buffer 2 was added, and the tube centrifuged again for 1 min, at 16 000 x g. The column was then transferred to a fresh 1.5 mL tube, and 30 µL pre-warmed (50 ºC) Elution Buffer was added to the column, and allowed to rest for 3 min, before a final 16 000 x g centrifugation, for 1 min, to elute the plasmid DNA.

For larger scale preparations, the selected protocol was that of the QIAfilter Plasmid Maxi Kit, from QIAGEN, performed to their specifications. Pre-cultures were grown by inoculating 10 µL of bacterial glycerol stock in 5 mL LB-antibiotic medium, and incubating for 24 h, at 30 ºC, with 300 rpm shaking. 200 µL of pre-culture were then pipetted into 100 mL LB-antibiotic medium, inside a sterile cotton-capped 500 mL Erlenmeyer flask, later incubated for another 24 h, at 30 ºC, and 300 rpm. The total amount of bacterial culture was then centrifuged for 15 min, at 6 000 x g, at 4 ºC, and the resulting supernatant discarded. 10 mL of Buffer P1 were used to resuspend the bacterial pellets, and 10 mL Buffer P2 were added and thoroughly mixed until the solution turned homogenously blue, at which point it was left for 5 min, at room temperature. 10 mL of pre-chilled (4 ºC) Buffer P3 were then added and mixed immediately by inverting the tube until the solution lost its blue colour and viscosity. The lysate was then poured into the barrel of a pre-capped QIAfilter Maxi Cartridge, where it was incubated for 10 min, before removing the cap, and filtering the solution into a pre-equilibrated QIAGEN tip 500, allowing it to enter the resin by gravity flow. The tip was then washed twice using 30 mL of Buffer QC, and finally the DNA eluted using 15 mL Buffer QF. 10.5 mL room--temperature isopropanol were then added to the eluate, and the contents of the tube mixed, before being centrifuged for 30 min, at 15 000 x g, at 4 ºC. The supernatant was carefully decanted, and the DNA pellet washed using 70 % ethanol, anticipating a new 15 000 x g centrifugation step, at 4 ºC, for 10 min, after which the supernatant was discarded and the final pellet airdried and resuspended in a suitable volume of Tris-EDTA (TE) buffer.

2.2.3.4. Site-directed mutagenesis

The QuikChange Lightning Site-Directed Mutagenesis Kit, from Agilent Technologies, was chosen to insert the p.Ile1061Thr, p.Ala1035Val and p.Ile858Val variants into the pBABE-puro+NPC1-mNeonGreen expression vector. According to the manufacturer's instructions, two complementary oligonucleotides containing the desired mutation were designed and synthesized for each variant of interest. In a PCR tube, 5 µL of 10X Reaction Buffer, 1.00 ng/µL pBABE-puro+NPC1-mNeonGreen plasmid, 0.66 µL of 20 µM mutagenic forward primer, 0.66 µL of 20 µM mutagenic reverse primer, 1 µL of 10 mM dNTP mix, 1.50 µL of QuikSolution Reagent, the volume was then brought to 49 µL with Nuclease-free water, and finally 1 µL QuikChange Lightning Enzyme was added to the reaction tube. Cycling conditions are described in Table 15.

Table 15 – Cycling conditions for the site-directed mutagenesis PCR.

Temperature	Time	Cycles
95 ºC	60 s	1
95 ºC	30 s	12
55 ºC	30 s	
68 ºC	300 s	

Digestion followed suit, by adding 2 µL *Dpn* I restriction enzyme, and incubating them for 5 min, at 37 ºC. Once the non-mutated and methylated DNA template was digested, transformation took place using XL10-Gold® ultracompetent cells. A tube of cells was thawed on ice, and 45 µL of cells were transferred to a pre-chilled 13 mL round bottom tube. 2 µL of β-mercaptoethanol mix were added, and the tubes incubated for 2 min, on ice, before adding 2 µL of the mutated plasmid DNA, swirling to mix. After 30 min on ice, the tubes were heat-pulsed for 30 s in a 42 ºC water-bath, and chilled again for 2 min, on ice. 0.5 mL pre-heated (30 ºC) NZY^{+} broth were added, and the tubes incubated for 1 h, at 30 ºC, and 250 rpm. The mix was then plated in selection plates (LB-Ampicillin), which were incubated at 30 ºC, for 36 h, before picking and inoculating individual colonies onto fresh plates.

2.2.3.5. Sequencing PCR

In order to confirm the success of the mutagenesis, the *NPC1* gene fragment containing the mutated sequence was subject to a sequencing PCR, using the BigDye™ Terminator v3.1 Cycling Sequencing Kit, from Applied Biosystems™, followed by dye-terminator Sanger sequencing, which was performed at the Technology and Innovation Unit of the National Institute of Health Dr. Ricardo Jorge, in Lisbon.

Two tubes were prepared per sample, by adding in 1 µL BigDye™ terminator, 1 µL sequencing buffer, 5.5 µL Nuclease-free water, 2 µL of DNA template, and 0.5 µL of 100 µM forward or reverse primer. After placing the samples on the thermocycler, the program in Table 16 was run, and the samples were then sent to Lisbon, on ice, for dye-terminator Sanger sequencing in an ABI 3130XL DNA Analyzer.

Table 16 – Cycling conditions for the sequencing PCR.

Temperature	Time	Cycles
96 ºC	600 s	1
96 ºC	10 s	25
50 ºC	5 s	
60 ºC	240 s	

2.2.3.6. Whole plasmid sequencing

After an initial confirmation of the site-directed mutagenesis by Sanger sequencing of the target *NPC1* fragment, the plasmids were sent to plasmidsaurus, in the United States of America, for whole plasmid sequencing.

2.2.3.7. Diagnostic restriction digest

The pCMV-VSV-G and pUMCV plasmids were sent to us as vectors expressed by bacterial stabs. Upon their arrival, the bacterial stabs were inoculated and seeded onto LB-Ampicillin or LB-Kanamycin plates, respectively, incubated for 24 h, at 37 ºC, from which individual colonies were then picked and grown in 5 mL LB-Ampicillin or LB-Kanamycin medium, proceeding with first small- and subsequently large-scale plasmid purification. The identity and purity of the plasmids were then confirmed through a diagnostic Restriction Digest of plasmid DNA protocol, from Addgene. For each plasmid, several reaction tubes were prepared, as portrayed in Table 17. The reaction mixes were then incubated for 1 h, at 37 ºC, before adding 10 µL of 6X TriTrack DNA Loading Dye and running 10 µL of each sample in a 1 % (w/V) agarose gel, containing ethidium bromide, alongside 10 µL of TrackIt™ 1 Kb Plus DNA Ladder. The run took 1 h, at 100 V, and the gel was then imaged in a GelDoc™ XR molecular imager.

Table 17 – Preparation of the reaction tubes for the diagnostic restriction digestion.

Tube	Plasmid DNA	10X Buffer		Restriction Enzyme	Nuclease-free water
1	1 µg	-	-	-	up to 50 µL
2		5 µL	NEBuffer 3	NotI	
3			rCutSmart Buffer	XhoI	
4			Buffer M	DraI	
5			Buffer R	NdeI	
6			SuRE/Cut Buffer H	NcoI	

2.2.3.8. Cell viability assay

ARPE-19 cells were cultured to around 80 % confluency in four 96-well tissue-culture treated plates. Puromycin was added to each of the four plates in serial dilutions, as exemplified in Figure 6. The plates were incubated at 37 ºC, 5 % CO_2, and, at each of the 48 h, 72 h, 96 h and 120 h timepoints, one plate was removed from the incubator, 10 µL alamarBlue® reagent was added to all its wells, and it was placed back in the incubator for 1 h, before measuring fluorescence in a SpectraMax® iD3 microplate reader ($\lambda_{excitation}$ = 570 nm; $\lambda_{emission}$ = 610 nm). After subtracting the "blank" (culture medium + puromycin) wells' value, fluorescence intensity was plotted versus puromycin concentration, to attain puromycin kill curves. Technical triplicates were obtained for each condition.

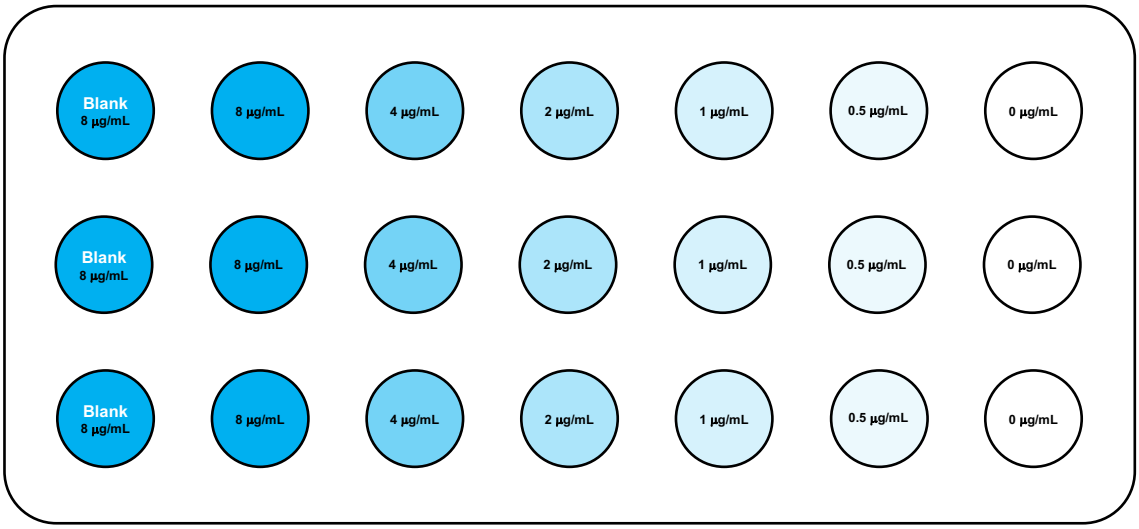


Figure 6 – Scheme of the puromycin serial dilutions for the cell viability assay. Puromycin was added to cell culture medium, and the mix was added to the blank wells (without cells) and to the test wells (containing APRE-19 cells) in serial dilutions as described in this scheme.

2.2.3.9. Transient transfection of HEK293T cells and γ-retroviral collection

HEK293T cells were grown in 12-well tissue-culture treated plates up to 70 % confluency, before initiating the transfection. The pBABE-puro+NPC1-mNeonGreen plasmid was used for the transfer of genetic material, in combination with the pCMV-VSV-G and pUMVC plasmids, which encode components of the murine leukemia retroviral (MuLV) particles. Various features of the protocol were thoroughly optimized before the ultimate transfection, namely the ratio of envelope:packaging:transfer plasmids and the proportions of plasmid DNA mix, culture medium and transfection reagent. Taking into account the results of said optimization, several envelope,

packaging and transfer plasmid DNA mixes – corresponding to the differently mutated pBABE-puro+NPC1-mNeonGreen plasmids – were prepared according to the ratios depicted in Table 18. 10 µL of the appropriate 1 µg/µL plasmid DNA mix were then added with 37 µL of room-temperature Opti-MEM medium, before vortexing and adding in 3 µL of room-temperature FuGENE® HD transfection reagent. The different mixes were incubated for 5 – 15 min, at room temperature, before adding them, dropwise, to the corresponding well on the 12-well plate. The plates were rocked back and forth to mix, and incubated for 16 h, at 37 ºC, 5 % CO_2. Experiments were performed between passages 4 to 10.

Table 18 – Plasmid ratios for the transient transfection.

Plasmid	Relative Concentration
pCMV-VSV-G	1
pUMCV	2
pBABE-puro+NPC1-mNeonGreen	3

Viral collection took place in a Biosafety Level 3 (BSL-3) laboratory. After the 16 h incubation, 1 mL Viral Collection Medium (VCM; 20 µM HEPES in DMEM supplemented with 10 % FBS) was added to each well of the 12-well plate. 32 h after adding the VCM, the Virus-Rich Medium (VRM) was collected (and stored at 4 ºC), and 1 mL of fresh VCM was added to the adherent cell layer. A final VRM collection took place 24 h after the first, and the virus-rich media were filtered through a 0.45 µm filter.

2.2.3.10. Retroviral transduction of *NPC1*$^{-/-}$ ARPE-19 cells

NPC1$^{-/-}$ ARPE-19 cells were grown on 6-well plates to approximately 80 % confluency, and transduced using 500 µL of filtered VRM, mixed with 500 µL DMEM/F-12 with 16 µg/mL polybrene, so that the final polybrene concentration in the wells came to 8 µg/mL. After 3 h incubating at 37 ºC, 5 % CO_2, 1 mL of fresh DMEM/F-12 was added to each well, and the cells were re-incubated for 48 h at 37 ºC, and 5 % CO_2. At this point, the old medium was replaced with DMEM/F-12 supplemented with 10 % FBS and 1 µg/mL puromycin, to begin the selection of the infected cells. This medium was replaced every 48 h, and once the cells reached the proper confluency, they were finally seeded in 25 cm^2 polystyrene flasks, for the bafilomycin A1 experiment, or in 8-well microscopy slide chambers, for subsequent filipin staining and immunofluorescence assays.

This protocol was also used for the stable transduction of these γ-retroviral particles in patient-derived skin fibroblasts expressing the c.3591+1G>A *NPC1* variant in homozygosity – the only difference being the use of DMEM instead of DMEM/F-12.

2.2.3.11. Bafilomycin A_1 Assay

Infected *NPC1*$^{-/-}$ ARPE-19 cells were grown to 80 % confluency in two 25 cm^2 polystyrene flasks for each *NPC1* variant (including non-transduced cells, and cells infected with the unmutated, wildtype *NPC1* construct). Next, the medium in each flask was replaced with either Baf (DMEM/F-12, supplemented with 10 % FBS, and 100 nM bafilomycin A_1), or Veh (DMEM/F-12, supplemented with 10 % FBS, and the same volume in vehicle – DMSO). The cells were then incubated for 24 h, at 37 ºC, and 5 % CO_2, before proceeding with pelleting, protein extraction, protein quantification, SDS-PAGE and western blot.

2.2.3.12. Filipin staining

At 80 % confluency, transduced *NPC1*$^{-/-}$ ARPE-19 cells seeded in the 8-well slide chambers were washed thrice with 1X PBS, and fixed with 4 % PFA, for 15 min, at room temperature. After 3 new washes with 1X PBS, the cells were incubated with 50 µg/mL filipin complex for 4 h, at room temperature, protected from the light. Once the 4 h passed, the fixed cells were washed 3 times with 1X PBS, and once with MiliQ water. The water was removed, the chamber was dismounted, and 1 drop of ProLong™ Diamond Antifade Mountant was added to each slot, before covering the slide with one long 17 mm thick coverslip. After 24 h curing in the dark, the slides were observed under a Leica DM 4000 B fluorescence microscope, using the DAPI filter and the 40X dry objective lens, and images were acquired at 1200 X 1200 pixels, 174.60 nm X 174.60 nm pixel size.

This protocol was also employed for the filipin staining of patient-derived skin fibroblasts with the c.3591+1G>A *NPC1* variant in homozygosity, after being transduced with the same NPC1-mNeonGreen constructs – the only difference being the use of DMEM instead of DMEM/F-12.

2.2.3.13. Immunofluorescence assays

Infected *NPC1*$^{-/-}$ ARPE-19 cells were grown in 8-well slide chambers up to 80 % confluency, before being washed 3 times using 1X PBS, and being incubated for 30 min, at room temperature, with 4 % PFA. The monolayer was then washed 3 new times using 1X PBS, and incubated with 50 mM NH_4Cl for 10 min, after which it was washed 3 more times with 1X PBS. Next, permeabilization was achieved by incubating the cells with either ice-cold methanol. 10 min later, the permeabilizing agent was removed and washed off using 1X PBS three more times. Blocking Solution (5 % BSA in 1X PBS) was added and left for 1 h, at room temperature, before adding the adequate primary or conjugate antibodies (diluted in Blocking Solution).

The primary α-LAMP1 antibody was then left overnight, at 4 ºC, in a wet chamber, before triple washing the slide with 1X PBS, and adding the secondary antibody, which incubated for 1 h, protected from the light.

Both slides were then washed with 1X PBS for 3 times, and once with MiliQ water, before removing the excess water, disassembling the chamber, adding 1 drop of EverBrite™ Mounting Medium with DAPI, and covering with a long coverslip and curing for 24 h. The slides were observed, and images were acquired at 2.5X zoom, using the 63X glycerol immersion objective lens of a Leica TCS SP5II scanning confocal microscope, with the following settings: 1024 X 1024 pixels; 96.20 nm X 96.20 nm pixel size; 6X line average.

2.2.3.14. Lysosome clustering scoring

Perinuclear clustering of lysosomes in transduced *NPC1*$^{-/-}$ ARPE cells was scored in an unbiased manner, by observing the LAMP1 immunofluorescence slides under a Leica DM 4000 B fluorescence microscope, with its 40X dry objective, selecting various random fields and counting cells with and without a clustering pattern (more than 300 cells were analysed for each condition). Finally, the number of cells displaying lysosomal clustering was divided by the total number of cells analysed for each condition to obtain the ratio of this phenomenon for each variant.

2.2.3.15. Colocalization quantification

Over 50 regions of interest were selected for each condition of differently transduced *NPC1*$^{-/-}$ ARPE-19 cells, and the LAMP1 and NPC1-mNeonGreen signal's cross correlation was determined using the Coloc2 plugin on the Fiji software, obtaining the Pearson's correlation coefficient for each region of interest.

2.2.4. RNA-based studies on NPC patients' fibroblasts and sera

2.2.4.1. Blood serum separation

Peripheral blood from NPC patients and healthy controls was collected in micronized silica-coated tubes, and processed within 90 min. The tubes were centrifuged for 10 min, at 1900 x g, at 4 ºC, and the supernatant was transferred to RNase-free tubes, stored at -80 ºC until further use. During this process, haemolysis can occur, which could mean a skewing of the results. To avoid this, the absorbance of samples was measured at λ = 414 nm (the peak wavelength for free haemoglobin), using a NanoDrop™ 1000 spectrophotometer. Samples that displayed Abs_{414} readings above 0.20 were excluded from this study.

2.2.4.2. RNA extraction

RNA was extracted from patient-derived skin fibroblasts and control cell lines using the miRNeasy Micro Kit, and from serum samples of patients and controls using the miRNeasy Serum/Plasma Kit, both from QIAGEN, according to the manufacturer's instructions. RNA samples were kept at -20 ºC in between uses.

For skin fibroblasts, the pellets were first disrupted using 700 µL of QIAzol Lysis Reagent, and thorough homogenization, after which the lysates were incubated for 5 min, at room temperature. For the serum samples, 1 mL QIAzol Lysis Reagent was added to 200 µL of the thawed serum samples, vortexed and incubated for 5 min, at room temperature.

Then, 0.2 volumes of chloroform were added to all the tubes, vortexed, and incubated again for 3 min, before centrifuging the samples for 15 min, at 12 000 x g, and 4 ºC. After phase separation, the upper aqueous phase was transferred to a new tube, where 1.5 volumes of pure ethanol were added, pipetting up and down to dissolve. 700 µL of the new mix were passed at a time through the RNeasy MinElute spin column,

by centrifuging for 15 s, at 12 000 x g, room temperature, discarding the flow-through each time. 700 µL of Buffer RWT were washed through the column with the same centrifugation settings, followed by 500 µL of Buffer RPE. A third wash-through was done using 800 µL of 80 % ethanol, centrifuging at 12 000 x g, for 2 min. The column was then dried by centrifuging it with an open lid, for 5 min, at 16 1000 x g. It was then placed inside the final 1.5 mL RNase-free collection tube, and 14 µL of RNase-free water were passed through the column to elute the RNA, by spinning for 1 min, at the same speed.

2.2.4.3. RNA quantification

Extracted RNA samples were quantified in a NanoDrop™ 1000 spectrophotometer, by measuring their absorbance at λ = 260 nm. Nucleic acid purity was ensured by confirming the 260/230 nm and 260/280 nm absorbance ratios were between 1.80 and 2.00, thereby avoiding any organic salt or protein contamination, respectively.

2.2.4.4. cDNA synthesis

For the RNA samples extracted from skin fibroblasts, the complementary DNA (cDNA) was synthesized using the Cytiva Ready-To-Go™ You-Prime First-Strand Beads. 1 µg of total RNA was dissolved to a total volume of 30 µL RNase-free water, and heated for 10 min, at 65 ºC, and then chilled for 2 min, on ice. This RNA solution was then transferred to the supplied tube of first-strand reaction beads, where 1 µL of primer and 2 µL of RNase-free water were added, to a final volume of 33 µL. The tubes were incubated for 1 min, before gently vortexing, spinning-down, and incubating them for 1 h, at 37 ºC.

Regarding the RNA samples extracted from serum, cDNA was synthesized using the TaqMan™ MicroRNA Reverse Transcription Kit, from Applied Biosystems. First, RNA samples were diluted to 2 ng/µL, using RNase-free water, and 5 µL of the solution was transferred to the bottom of a microtube. A MasterMix was prepared, according to the specifications in Table 19, and 7 µL of it were added to the microtubes, alongside 3 µL of the appropriate primers 5X Reverse Transcription primers, specific for each target miRNA.

Table 19 – Preparation of the cDNA MasterMix.

Component	Volume per reaction
100 mM dNTPs	0.15 µL
10X RT Buffer	1.50 µL
20 U/µL RNase Inhibitor	0.19 µL
50 U/µL Reverse Transcriptase	1.00 µL
RNase-free water	up to 7 µL

The tubes were then placed in a Biometra TProfessional Basic thermocycler, with the program described in Table 20.

Table 20 – Cycling conditions for the cDNA synthesis.

Temperature	Time	Cycles
16 ºC	30 min	1
42 ºC	30 min	1
85 ºC	5 min	1

2.2.4.5. Disease-causing variant confirmation

After cDNA synthesis, the extracted samples from patient-derived skin fibroblasts were purified using the illustra™ ExoProStar™ 1-Step Kit, from Cytiva, to clean-up any excessive primers and dNTPs, by adding 3 µL ExoProStar™ to 1 µL of cDNA. The reaction was then incubated at 37 ºC for 15 min, and then 80 ºC for another 15 min.

After purification, a sequencing PCR was performed as described in section 2.2.11.

2.2.4.6. Next-generation RNA sequencing

To identify differentially expressed miRNAs in NPC patients' fibroblasts (compared to healthy controls), a small RNA-Seq (sRNA-Seq) pipeline was followed. Small RNA (sRNA) yields and quality were first assessed using a NanoDrop™ 1000 spectrophotometer. The RNA 6000 Pico Kit was used to evaluate the RNA integrity number (RIN) of the samples in a 2100 Bioanalyzer automated electrophoresis tool, with a quality cut-off of RIN ≥ 7.5.

RNA libraries from a total of 14 samples (3 controls, 4 patients, 2 replicates each) were prepared using the TruSeq® small RNA Library Prep Kit, from illumina®, according to the manufacturer's instructions, and were then sequenced in a NextSeq 2000 system, also from illumina®. sRNA-Seq data analysis was performed by two separate teams: one from Novogene, and another from the Research and Development Unit of the National Institute of Health Dr. Ricardo Jorge.

Novogene trailed the following steps: 1 – raw data was processed in order to remove reads with contaminants and low quality reads; 2 – sRNA tags were mapped to the reference sequence; 3 – mapped sRNA tags were used to look for known miRNAs, using the miRbase 20.0 database as reference, and Novogene custom scripts were used to obtain miRNA counts and base bias for the first position of identified miRNAs; 4 – tags were removed from protein-coding genes, repeated sequences, ribosomal RNA (rRNA), transfer RNA (tRNA), small nuclear RNA (snRNA) and small nucleolar RNA (snoRNA); 5 – small RNA annotation; 6 – miRNA family analysis; 7 – target gene prediction; 8 – miRNA quantification; 9 – assessment of differential quantification; 10 – gene ontology (GO) KEGG (Kyoto Encyclopedia of Genes and Genomes) enrichment analysis.

The Portuguese team followed a parallel approach, using the smallRNA toolbox [156], namely the sRNA bench and the sRNAde tools. Differential expression was calculated through the DESeq2 method [157].

2.2.4.7. Quantitative real-time polymerase chain reaction

Differentially expressed miRNA hits were further validated by qRT-PCR both for fibroblasts and sera. This process was carried out in a Bio-Rad Laboratories' CFX96™ thermocycler, using Applied Biosystems' TaqMan™ MicroRNA Assays, and NZYtech's NZSpeedy qPCR Green MasterMix.

To start, a qRT-PCR mix was prepared, according to Table 21, and 7 µL of it were added to 1 µL of the appropriate cDNA template.

Table 21 – Preparation of the qRT-PCR mix.

Component	Volume per reaction
2X NZYSpeedy qPCR Green MasterMix	4.00 µL
5X TaqMan™ probes + primers	1.60 µL
RNase-free water	1.40 µL

The 96-well plate was then closed using and adhesive seal for a spin-down, and, after removing the seal again, placed in the thermocycler, for amplification following the program described in Table 22.

Table 22 – Cycling conditions for the qRT-PCR.

Temperature	Time	Cycles
95 ºC	600 s	1
92 ºC	15 s	50
58 ºC	40 s	
72 ºC	20 s	

Intracellular and circulating miRNA expression relative fold-change was quantified through the $2^{-\Delta\Delta Ct}$ method [158], using the ubiquitous small nuclear RNA RNU6B as an internal control for normalization in the case of skin fibroblasts [159], or a theoretical normalization for serum samples, seeing this cell-free bodily fluid is not associated with reliably constant levels of any particular RNA species. Such normalization was attained by uniformizing sample volumes and reaction conditions throughout all assays, and by setting the same baseline and threshold cycle for each target miRNA [160].

2.2.5. Bioinformatic data treatment

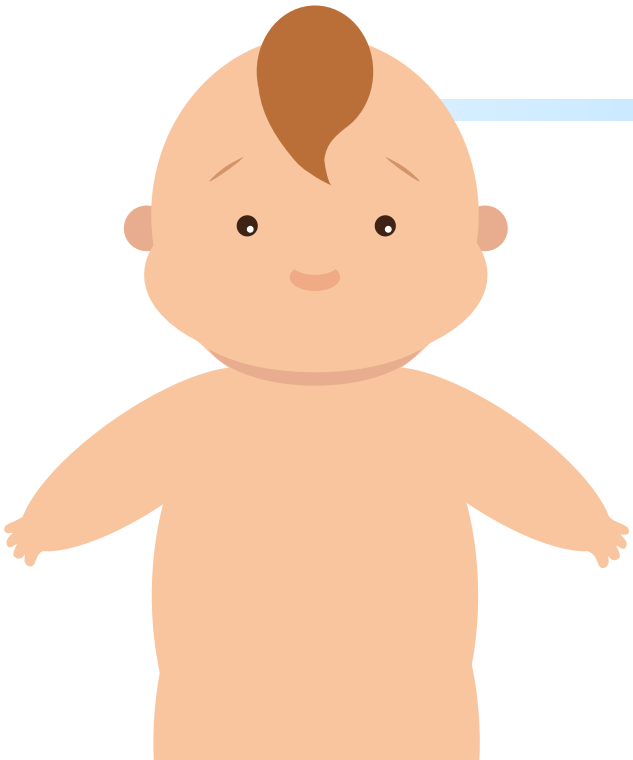
2.2.5.1. Image processing

Fluorescence microscopy images were processed using the Leica Application Suite X and Fiji software. The gels and membranes imaged using the GelDoc™ XR and ChemiDoc™ XRS+ imagers were handled using the Image Lab software.

2.2.5.2. Statistical analysis

Statistical analysis was performed using SPSS Statistics, and graphics were built with the Microsoft Excel software.

The first step was to verify the normality of each distribution of results, using the Shapiro-Wilk test for groups that had up to 25 elements, or the Kolmogorov-Smirnov test for groups that exceeded that number. Then, test parameters were compared between different groups using the t-student test for variables that displayed a normal distribution, setting the statistical significance alpha level at $p < 0.05$.



Results & Discussion

The monogenic perspective is very constricting when grappling such heterogenous and intricate disorders as LSDs. Recent scientific literature has highlighted the impact of several other elements on the phenotype of NPC patients. Epigenetic variations, post-zygotic mutagenesis, sex, environmental factors and additional genetic variants either within the same gene or in peripheral modifier genes and pathways may all influence the phenotypic manifestation of this disease [126].

Aiming to explore some of these routes, we developed and employed several tools to assess the effect of a polymorphic variant observed in *cis* in the *NPC1* gene of the analysed Portuguese patients carrying the p.Ala1035Val variant – p.Ile858Val. The 858 residue seems to be fully conserved as an isoleucine in mammals, hinting to a potential modifying effect of this semiconservative amino acid substitution (or its encompassing haplotype) on the expression of the p.Ala1035Val-NPC1 variant [161].

Patient-derived skin fibroblasts are a tried-and-true disease model of NPC, and they have often been used to investigate the subcellular trafficking and degradation routes prompted by different NPC1 missense mutants [89]. Yet, these *in vitro* models convey some limitations, such as the fact that they become senescent after a limited number of subculturing passages, rendering results irreproducible. Restricted availability of adequate antibodies against NPC1 is another caveat when using these cell models for immunofluorescence assays. In order to address these limitations, we established stable cell populations expressing the wild type (WT), p.Ile1061Thr and p.Ala1035Val (both with and without the p.Ile858Val SNP) variants of the NPC1 protein, fused to a mNeonGreen fluorescent tag. These cell lines were then used, alongside patient-derived skin fibroblasts (whenever appropriate) to survey the trafficking and degradation routes elicited by these different NPC1 variants, as well as their impact on lysosome biogenesis and positioning (Figure 7).

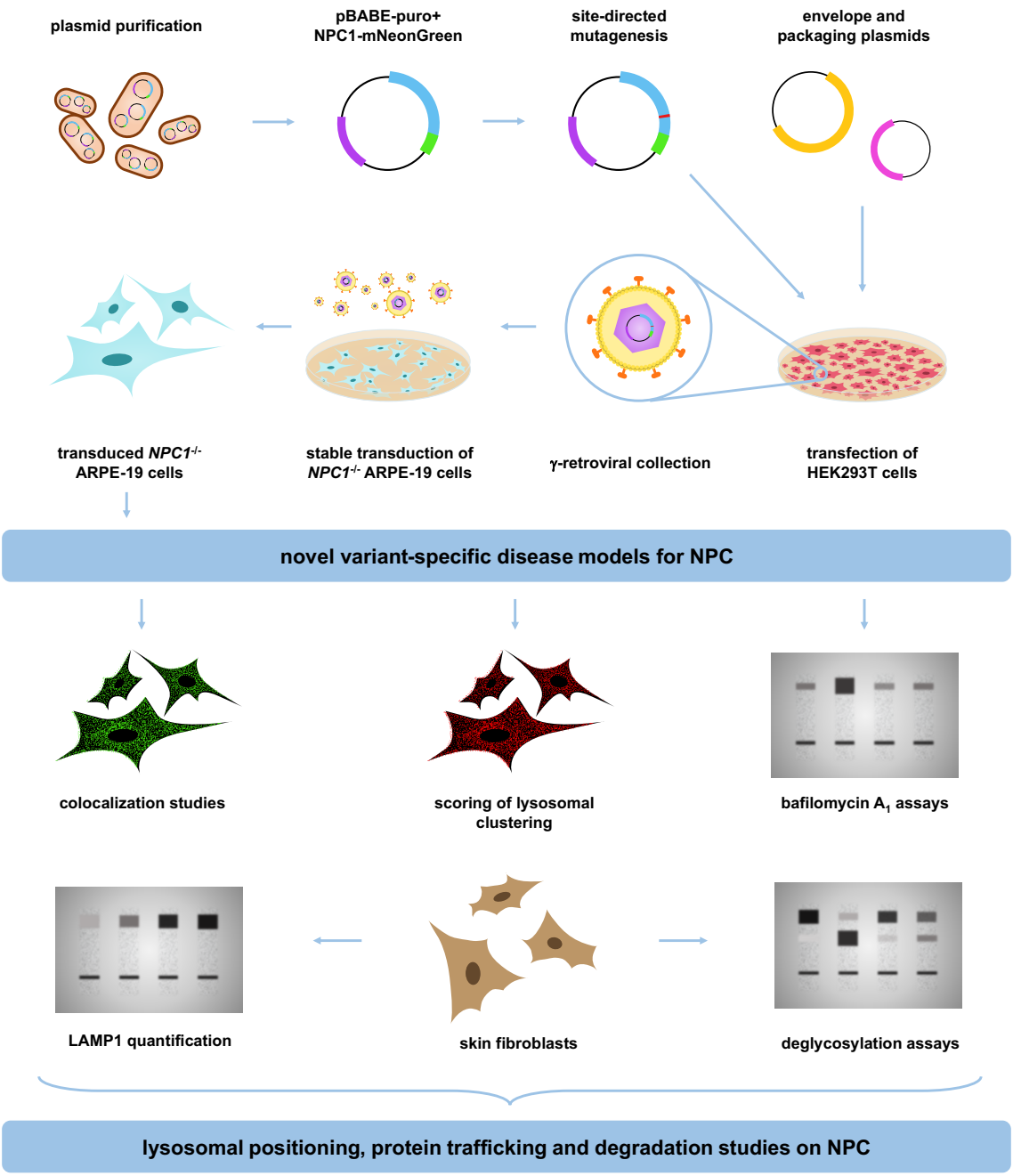


Figure 7 – Schematic view of the different methodologies used to develop a new, variant-specific disease model for NPC and to study lysosomal positioning and NPC1 protein trafficking and degradation routes.

Another way in which we tried exploring the many factors that doubtlessly influence NPC pathogenesis was through epigenetics. Taking advantage of state-of-the-art sequencing technologies, we submitted RNA samples extracted from patient-derived skin fibroblasts to next-generation sRNA-Seq. Even despite the small number of biological samples obtained for this analysis, we were able to identify two miRNA species that appeared to be upregulated in NPC patient cells. We then set out to validate these results through qRT-PCR, which did not confirm the next generation sequencing

(NGS)-based analysis on NPC skin fibroblasts, but indicated that both of these miRNAs seem to be significantly upregulated in NPC patients' sera, paving the way for long-awaited new putative biomarker candidates for this disorder, that combine high-specificity and minimally intrusive collection methods with time- and cost-effectively screening options for NPC (Figure 8).

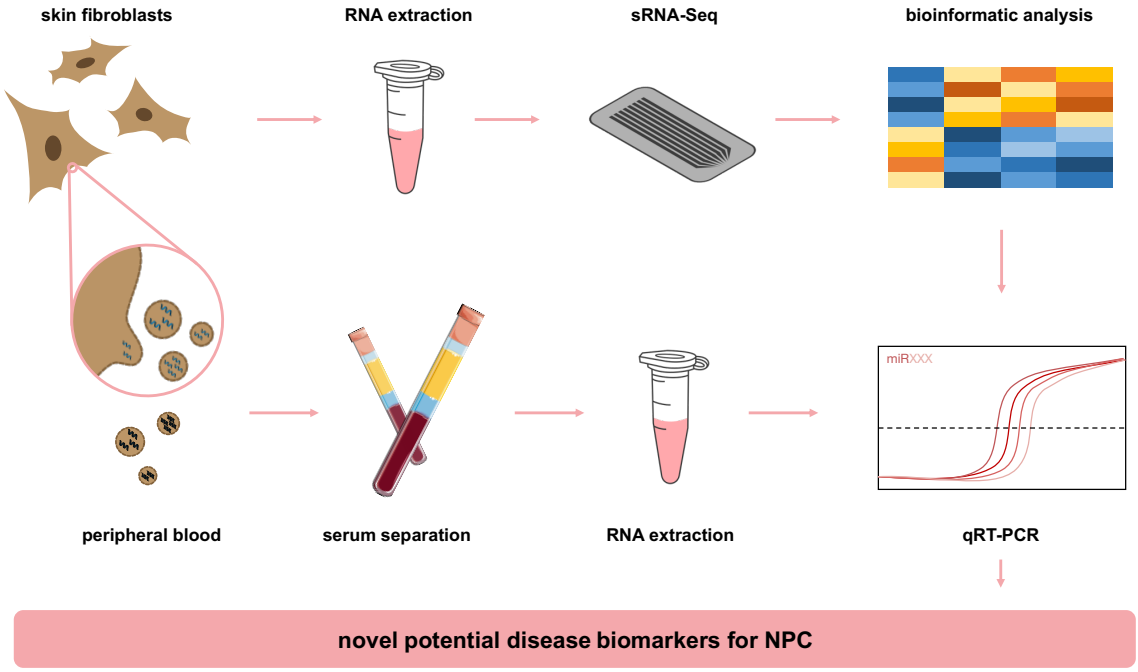


Figure 8 – Schematic view of the different methodologies employed to survey the miRNA expression profile of NPC patients and to explore new putative disease biomarkers for NPC.

3.1. Establishment of stably transduced *NPC1*$^{-/-}$ ARPE-19 cell lines

Cell lines have taken the stage in research involving molecular pathways related to NPC1 and its dysfunction, and they represent a comparable *in vitro* model to explore disease-relevant genetic variants and their significance [118,162].

Genetically engineered *NPC1*$^{-/-}$ ARPE-19 cells recapitulate the cellular pathogenic phenotype of NPC disease [123]. We took advantage or their ease of transduction to infect them using γ-retroviral particles generated in-house, carrying the different variants under study in a pBABE-puro construct that contained the *NPC1* cDNA sequence, fused with that of the mNeonGreen fluorescent protein. We also confirmed that cell lines transduced with the WT form of the biosynthetic NPC1 protein reverted the NPC cellular phenotype of *NPC1*$^{-/-}$ ARPE-19 cells, and detected NPC1-mNeonGreen expression in all

transduced cell lines using fluorescence microscopy, before proceeding with further analyses.

3.1.1. γ-retroviral plasmid identity was confirmed by diagnostic restriction digest

Upon arrival, the envelope (pCMV-VSV-G) and packaging (pUMVC) retroviral plasmids were purified, and their identity was confirmed through a diagnostic restriction digest, using different restriction enzymes to cut the plasmids into a precise number of fragments with specific sizes (Figure 9), and running the reactions in an agarose gel.

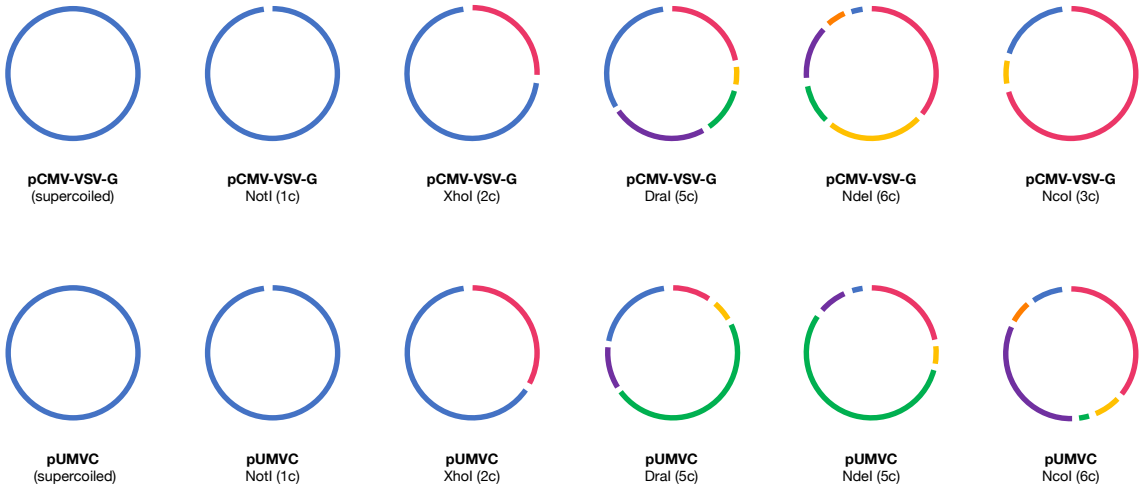


Figure 9 – Enzymatic restrictions of pCMV-VSV-G and pUMVC. The scheme depicts the predicted cut sites and fragments sizes of the NotI, XhoI, DraI, NdeI and NcoI restriction enzymes on the pCMV-VSV-G and pUMVC plasmids.

Figure 10 depicts the results of this test (top panel) and overlaps them with the expected DNA fingerprint pattern of these plasmids (bottom panel), confirming the identity and purity of the γ-retroviral envelope and packaging plasmids. Some of the lower molecular weight bands are not visible, because of certain components in the loading dye, and there is an unexpected band on lane 12 – that, on closer analysis, was found to have the exact same weight as the nicked plasmid (lane 9), meaning simply that the restriction reaction was incomplete for this enzyme. Nonetheless, plasmid identity was a perfect match for both plasmids.

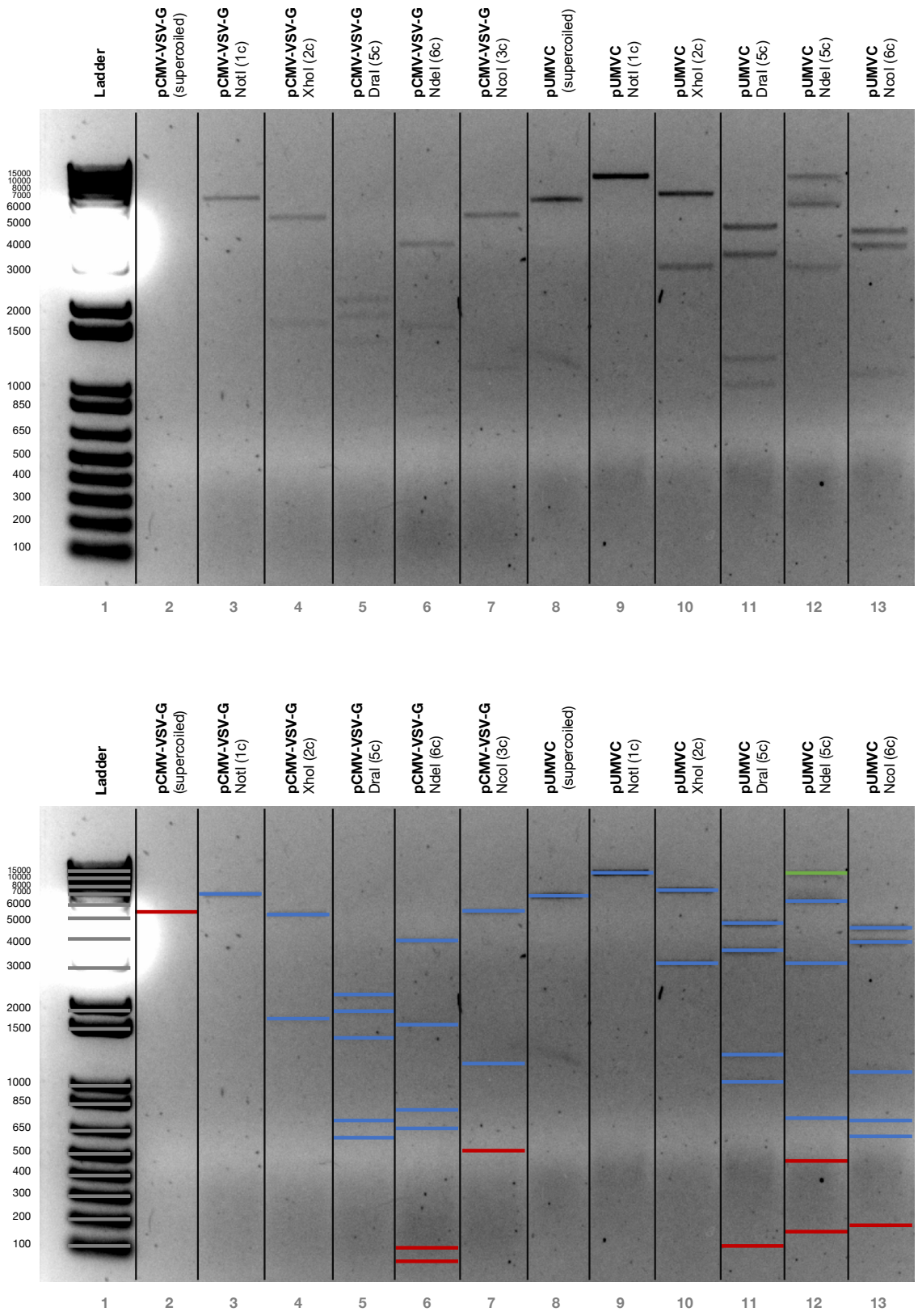


Figure 10 – Diagnostic restriction digest of pCMV-VSV-G and pUMVC. The top panel displays the agarose gel on which the enzymatic restriction reactions were run. The bottom panel represents the same gel overlapped with the expected DNA fingerprint pattern of the pCMV-VSV-G and pUMV plasmids. Blue lines are expected lines that were visible in the gel, red lines are expected lines that were not visible upon UV revelation, and the green line highlights an unexpected band, that evidences an incomplete enzymatic restriction.

3.1.2. Site-directed mutagenesis of the pBABE-puro+NPC1-mNeonGreen constructs was validated by Sanger and whole plasmid sequencing

The vector chosen for this study was pBABE-puro+NPC1-mNeonGreen (Figure 11). This plasmid is a 9.7 kb retroviral vector for mammalian expression, which encodes the ampicillin bacterial resistance (*AmpR*) gene under the command of the *AmpR* promoter in one sense, and, in the other, it contains the *NPC1* cDNA sequence, C-terminally fused with the mNeonGreen fluorescent tag, and a strong (SV40) promoter, directing the expression of the puromycin resistance (*PuroR*) gene, which allows for subsequent selection of correctly transduced host cells. Its long terminal repeat (LTR) sequences allow for the sequence's stable integration into the host's genome.

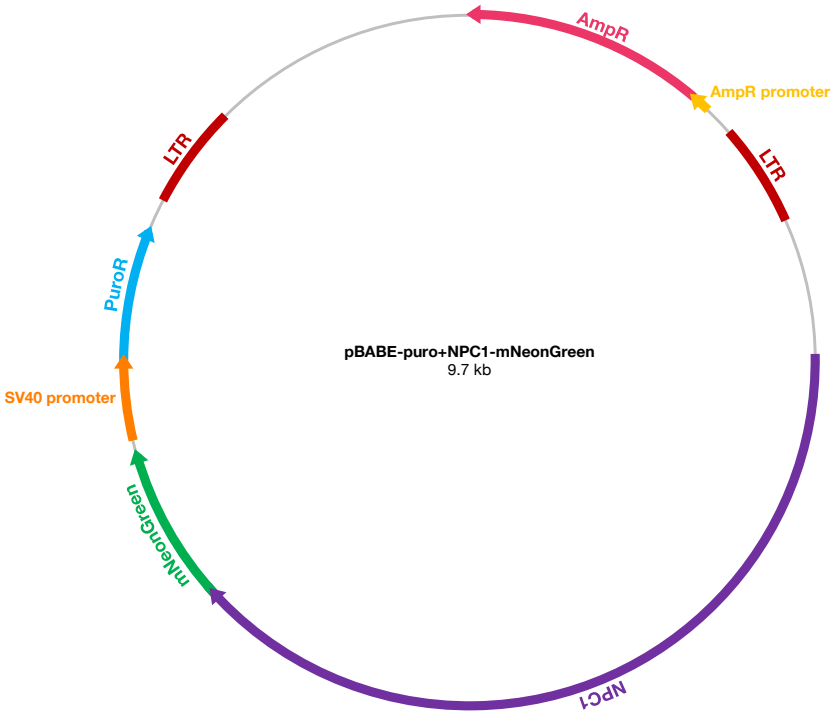


Figure 11 – pBABE-puro+NPC1-mNeonGreen annotated plasmid structure. The pBABE-puro+NPC1-mNeonGreen plasmid spans 9.7 kb, and includes an ampicillin resistance gene (*AmpR*) under the control of the *AmpR* promoter in one sense, and, in the opposite sense, it encodes the *NPC1* coding sequence, C-terminally fused with mNeonGreen, and a strong SV40 promoter, which operates the expression of the puromycin resistance gene (*PuroR*), all located in between two long terminal repeat (LTR) sequences.

Following the site-directed mutagenesis protocol, Sanger sequencing confirmed the insertion of the selected mutations within the *NPC1* cDNA sequence of the various pBABE-puro+NPC1-mNeonGreen constructs (Figure 12). When designing the p.Ile1061Thr oligonucleotide primers for this procedure, the Agilent QuikChange® Primer Design software automatically changed another nucleotide, c.3105A>G, for primer stability reasons. This additional polymorphism does not impact the encoded amino acid

in the resulting variant NPC1 protein, and is therefore considered a silent variant, without any impact on the protein's function.

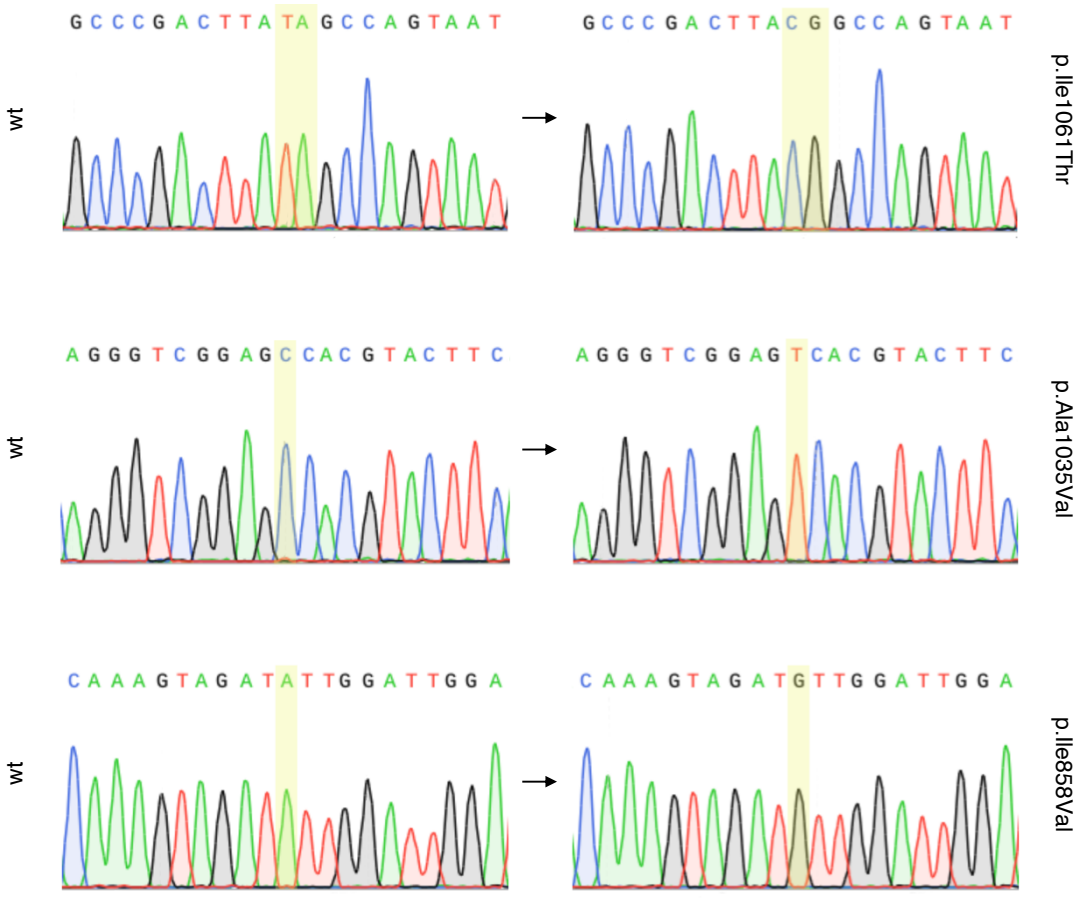


Figure 12 – DNA Sanger sequencing electropherograms highlighting (in yellow) the mutations inserted in different *NPC1* regions of the multiple pBABE-puro+NPC1-mNeonGreen constructs through site-directed mutagenesis.

Upon receiving the whole plasmid sequencing results from plasmidsaurus, the unedited and mutated pBABE-puro+NPC1-mNeonGreen sequences were aligned with the *NPC1* cDNA reference sequence, which confirmed the success of the site-directed mutagenesis in performing only the intended alterations (Figure 13), with no off-target mutations. The absence of any other unexpected modifications to the viral vectors was confirmed by aligning the obtained sequences with those of the *PuroR*, the *mNeonGreen* cDNA, and the *AmpR* gene (not shown).

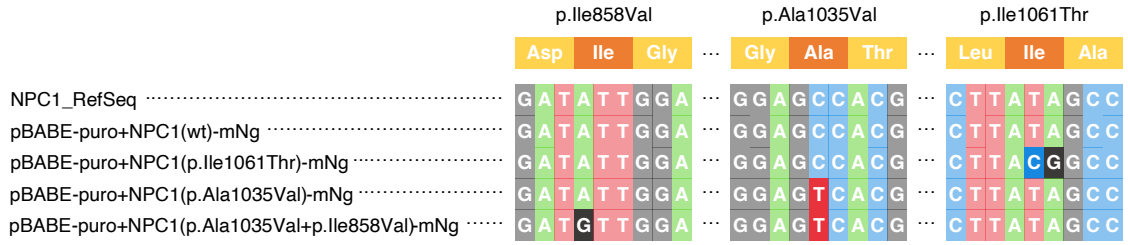


Figure 13 – Multiple sequence alignment of the different pBABE-puro+NPC1-mNeonGreen constructs (after site-directed mutagenesis) with the *NPC1* cDNA reference sequence (NPC1_RefSeq), obtained from NCBI (NM_000271.5).

3.1.3. Puromycin selection concentration was determined through cell viability assays

Puromycin is a potent, naturally occurring aminonucleoside antibiotic that acts by inhibiting the peptidyl transfer reaction catalysed by ribosomes during protein biosynthesis [163,164]. The *pac* gene, isolated from *Streptomyces alboniger*, encodes puromycin *N*-acetyltransferase, an enzyme that confers resistance to this antibiotic. Since its first use in 1986, this system has often been employed for the selection of stably transduced mammalian cell cultures [165,166].

The transfer vector chosen for this study, pBABE-puro+NPC1-mNeonGreen, contains the puromycin resistance gene, which is transduced into the host cells' genome alongside the NPC1-mNeonGreen sequence, allowing us to select effectively transduced *NPC1*$^{-/-}$ ARPE-19 cells. Animal cell cultures are generally sensitive to puromycin in concentrations ranging between 1 to 10 µg/mL. To determine the lowest concentration that killed 100% of non-transduced cells, we performed cell viability assays on the ARPE-19 cell line, with different antibiotic concentrations (from 0.5 to 8 µg/mL) and different selection timepoints (from 48 to 120 h).

As can be observed in the puromycin kill curve drawn from our results (Figure 14), at 48 h, it would take 2 µg/mL of puromycin to kill all non-transduced cells. For 72 h of incubation, 1 µg/mL would be enough to kill 100 % of the non-resistant cells. And, for the 96 h and 120 h incubation times, 100 % mortality is achieved with as little as 0.5 µg/mL of puromycin.

Based on our data, we chose the 1 µg/mL puromycin concentration and the 72 h timeframe for selection of γ-retrovirally transduced *NPC1*$^{-/-}$ ARPE-19 cells.

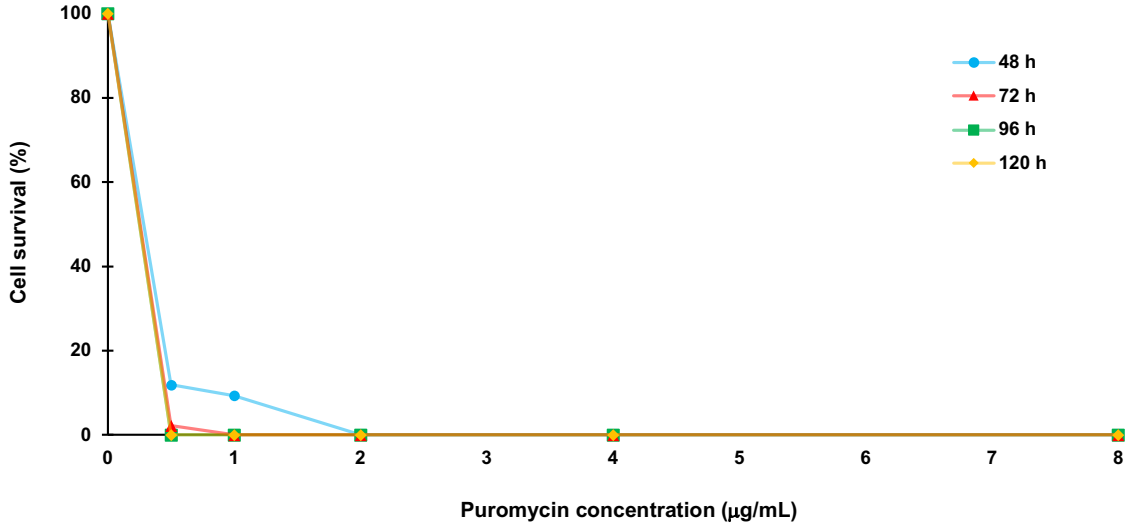


Figure 14 – Puromycin kill curve. The graph shows the percentage of cell survival of ARPE-19 cells after 48 h (blue), 72 h (red), 96 h (green) or 120 h (yellow) incubation with different concentrations of puromycin, determined through fluorescence detection of alamarBlue®.

3.1.4. NPC1-mNeonGreen expression was visualized using fluorescence microscopy

mNeonGreen is a yellow-green constitutively fluorescent protein, derived from *Branchiostoma lanceolatum*. Its high quantum yield, extinction coefficient and photostability substantiate its use as a fusion tag for fluorescence imaging [167]. In the vector we chose for this study, mNeonGreen is C-terminally fused to the *NPC1* cDNA sequence, in a pBABE-puro construct, in order to overcome the lack of appropriate antibodies for NPC1 immunofluorescence staining. This allowed us to track the expression and localization of the differently mutated NPC1 proteins, using the λ = 488 nm laser line.

After the stable transduction of *NPC1*$^{-/-}$ ARPE-19 cells with the γ-retroviral particles carrying the differently mutated plasmids, NPC1-mNeonGreen expression was observed by fluorescence microscopy. Images confirm the absence of mNeonGreen-NPC1 signal in non-transduced (NT) *NPC1*$^{-/-}$ ARPE-19 cells, and prove the expression of the successfully transduced NPC1-mNeonGreen constructs (Figure 15). As expected, cells transduced with the WT form of NPC1-mNeonGreen displayed a punctate pattern, consistent with its LE/Lys localization. On the other hand, cells transduced with the p.Ile1061Thr variant exhibited a less intense and much more diffuse pattern, consistent with its previously described retention and degradation in the ER [112,168]. Cells expressing the p.Ala1035Val variant (with and without the p.Ile858Val polymorphism) also presented

with a dim and disperse expression pattern, hinting at a conceivably similar targeting for degradation before reaching the LE/Lys compartment.

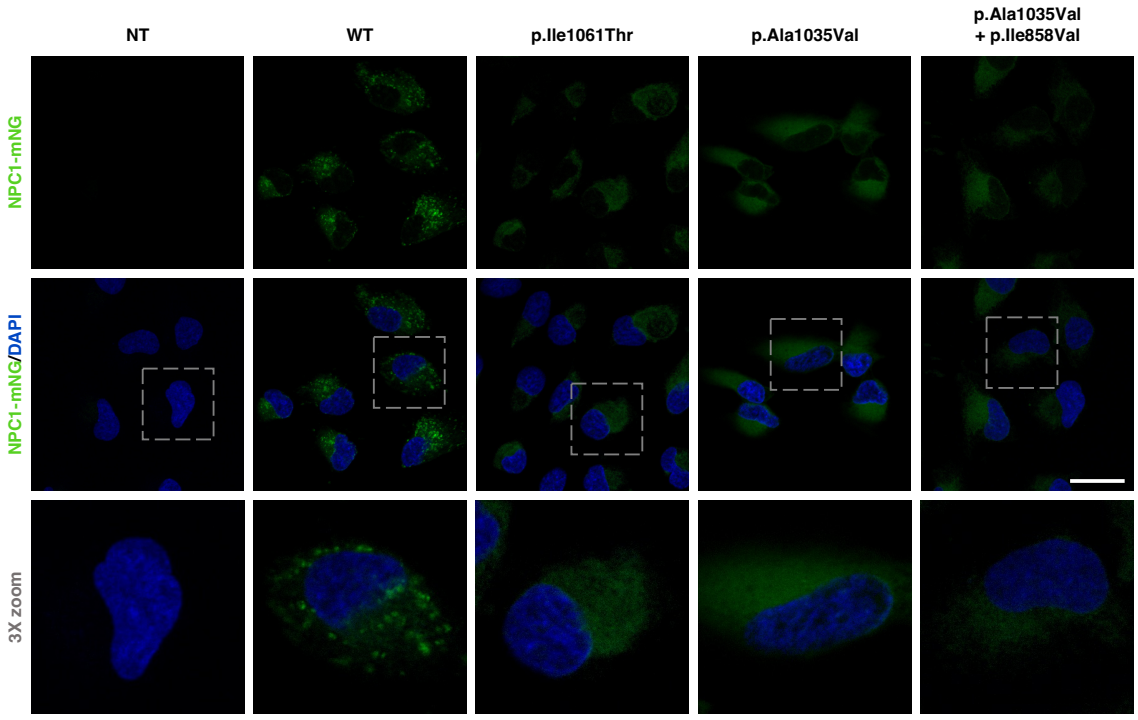


Figure 15 – NPC1-mNeonGreen expression in non-transduced and transduced *NPC1*$^{-/-}$ ARPE-19 cells. The top panel shows the NPC1-mNeonGreen signal (green), the middle panel displays a merge of that signal with DAPI (blue), and the bottom panel is a 3X zoom of the merged image. From left to right, each column exemplifies a condition of *NPC1*$^{-/-}$ ARPE--19 cells, the first column shows non-transduced (NT) cells, while the rest represent cells infected with retroviral particles containing either the wild type (WT), p.Ile1061Thr, p.Ala1035Val or p.Ala1035Val + p.Ile858Val constructs. These are representative images, obtained through confocal fluorescence microscopy. The scale bar (white) represents 25 µm.

3.1.5. Characteristic free-cholesterol accumulation was observed through filipin staining

Filipin is a naturally fluorescent polyene antibiotic that binds specifically to unesterified cholesterol [169]. For decades, it has been extensively used in NPC diagnostic screenings, as it allows for the visualization of one of the main accumulated substrates in this LSD – free-cholesterol – within lysosomes [137].

The filipin staining protocol was performed on the transduced *NPC1*$^{-/-}$ ARPE-19 cell lines, aiming to substantiate their usefulness as NPC disease models, which are able to replicate this hallmark pathological feature of NPC patient cells. Unfortunately, the filipin incubation protocol we used did not seem efficient in staining free-cholesterol in this cell line. Thus, we tried it on patient-derived skin fibroblasts expressing the c.3591+1G>A *NPC1* variant in homozygosity (effectively producing no detectable NPC1 protein) which we transduced using the same constructs.

Patient-derived fibroblasts carrying the c.3591+1G>A variant transduced with the p.Ile1061Thr, p.Ala1035Val and p.Ala1035Val + p.Ile858Val NPC1 constructs displayed a clear accumulation of unesterified cholesterol within vesicle-like structures that gather around the nuclei of those cells (Figure 16), consistent with the characteristic lysosomal accumulation of this undegraded substrate observed in most NPC patient cells, as a consequence of the intracellular cholesterol trafficking impairment due to NPC1 (or NPC2) dysfunction [170].

On the other hand, c.3591+1G>A fibroblasts expressing the WT-NPC1 construct fully recovered the physiological phenotype, exhibiting no accumulation of free-cholesterol within the LE/Lys compartment, as would be expected in cells expressing the native form of the NPC1 protein.

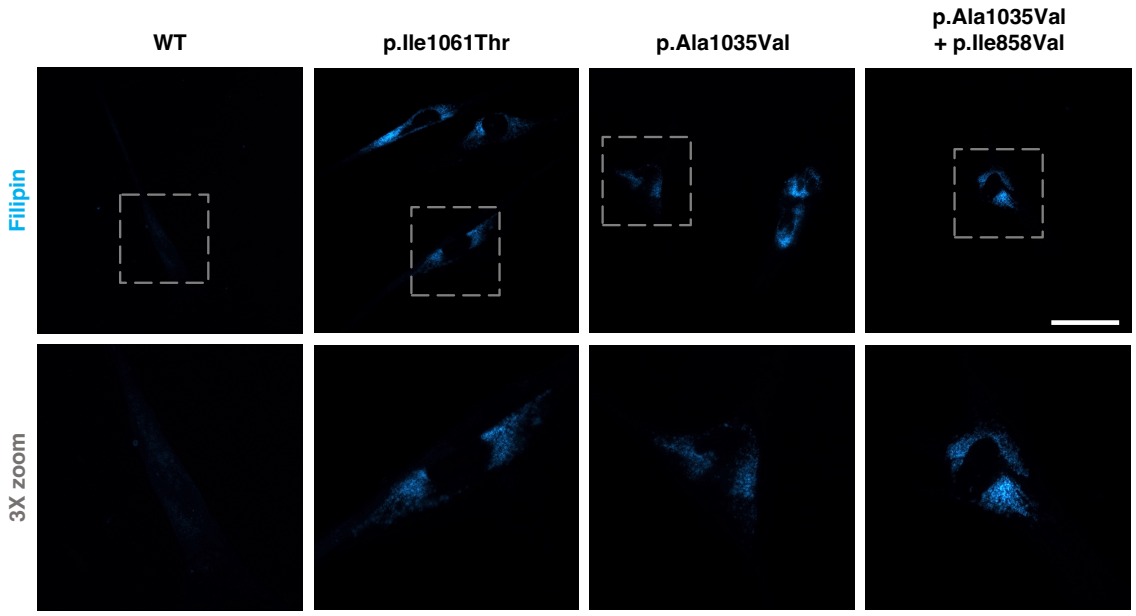


Figure 16 – Filipin staining in transduced c.3591+1G>A fibroblasts. The top panel shows the filipin signal (cyan), and the bottom panel is a 3X zoom of the same image. From left to right, each column exemplifies a condition of c.3591+1G>A patient-derived fibroblasts. From left to right, each column exemplifies a condition of c.3591G>A fibroblasts infected with retroviral particles containing either the wild type (WT), p.Ile1061Thr, p.Ala1035Val or p.Ala1035Val + p.Ile858Val constructs. These are representative images, obtained through fluorescence microscopy. The scale bar (white) represents 50 µm.

3.2. Altered lysosome biogenesis and positioning

3.2.1. Decreased lysosomal turnover

The lysosome-associated membrane protein 1 (LAMP1) is a highly glycosylated type I transmembrane protein, that, together with LAMP2, accounts for about 50 % of all lysosomal membrane protein content [171]. For this reason, LAMP1 is the most commonly used lysosome marker [172].

LAMP1 expression was detected by western blotting (Figure 17), for patient-derived skin fibroblasts with the different variants under study and compared with that of a primary human dermal fibroblast line (HDFa), used here as a control (CTRL). Results show a 3.40-fold (± 0.91) increase in LAMP1 expression in cells expressing NPC1 proteins with the p.Ile1061Thr variant. Cells with the p.Ala1035Val-NPC1 variant (in *cis* with the p.Ile858Val SNP) displayed an even higher, 4.14-fold (± 0.87) intensification in LAMP1 expression. The difference between LAMP1 expression of both NPC1 variants did not appear to be statistically significant. Such enlarged values have been previously reported [173], and seem to denote decelerated organelle turnover, rather than augmented lysosomal biogenesis, seeing as other studies have concluded that *LAMP1* mRNA levels do not account for the heightened protein expression [174].

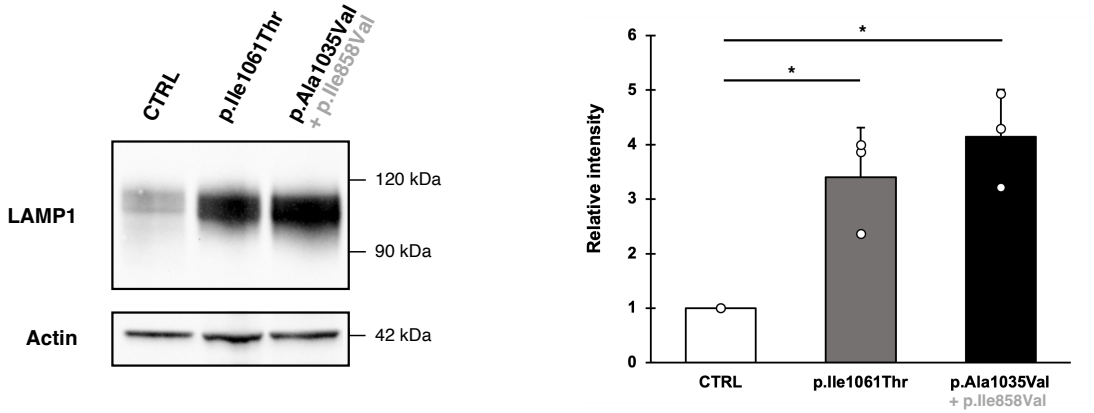


Figure 17 – LAMP1 quantification. The left panel displays a representative western blot showing LAMP1 protein levels in a human skin fibroblast cell line used as control (CTRL), and skin fibroblasts obtained from NPC patients homozygous for the p.Ile1061Thr and p.Ala1035Val (in *cis* with the p.Ile858Val SNP) variants in NPC1, and Actin as a loading control. The right panel displays the quantification of the relative LAMP1 protein levels, normalized using Actin, for 3 independent experiments (n=3). Comparisons between groups were analyzed using the t-student test (* $p < 0.05$).

3.2.2. Lysosomal clustering

Through immunofluorescence labelling of the LAMP1 protein, a significant accumulation and clustering of lysosomes was observed in the perinuclear region of

NPC1$^{-/-}$ ARPE-19 cells transduced with the mutant NPC1 constructs (Figure 18). Quantification of this clustering cells revealed an increase from 10.27 % (± 1.85 %) in cells transduced with the WT form of the protein to 66.27 % (± 3.82 %) in those expressing the p.Ile1061Thr variant, 83.13 % (± 0.97 %) for cells transduced with the p.Ala1035Val alone and 90.33 % (± 1.59 %) for those expressing p.Ala1035Val in *cis* with the p.Ile858Val. When compared between the different variants, all of these differences in lysosomal clustering displayed strong statistical significance (Figure 19). These results are consistent with the heightened LAMP1 protein detection observed through western blotting (Figure 17), and coincide with scientific literature, in which the lysosomes of NPC cells display a distinctive and perinuclearly concentrated pattern [175].

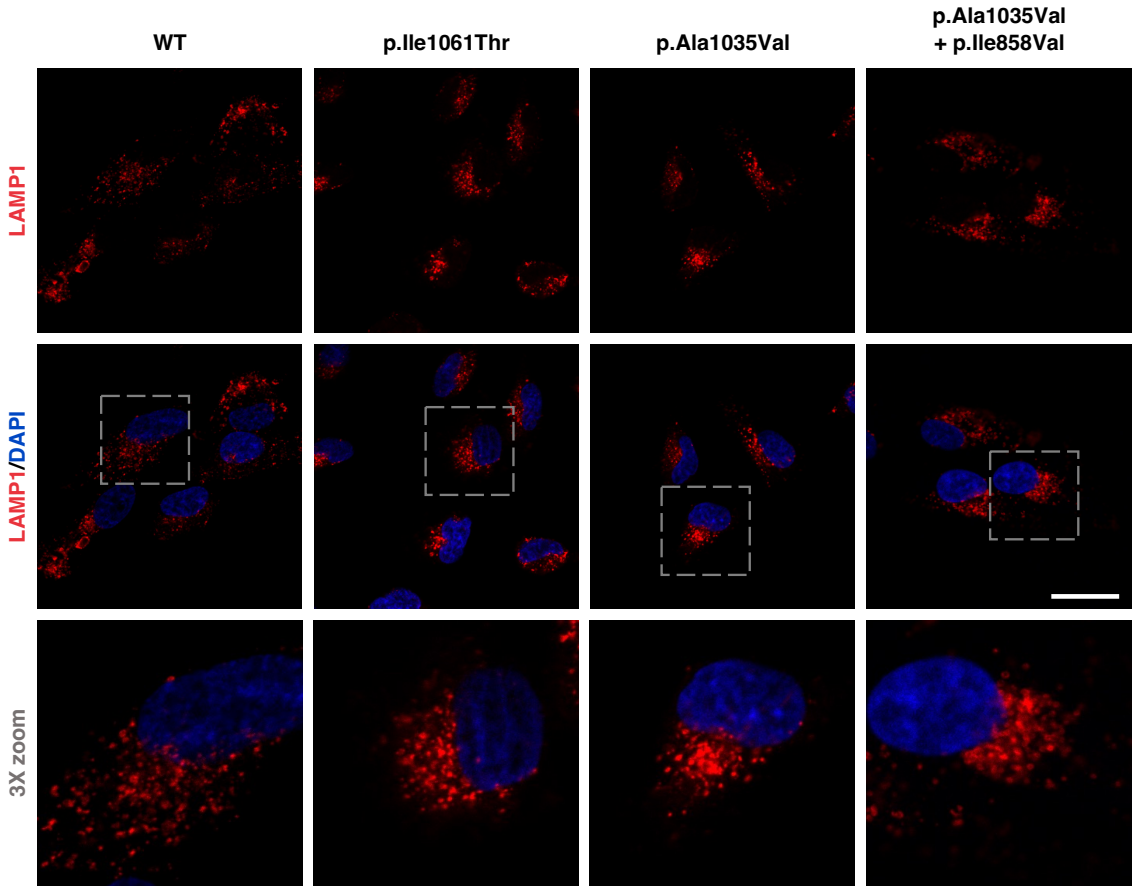


Figure 18 – Perinuclear lysosome clustering in transduced *NPC1*$^{-/-}$ ARPE-19 cells. The top panel shows the LAMP1 signal (red), the middle panel displays a merge of that signal with DAPI (blue), and the bottom panel represents a 3X zoom of the merged image. From left to right, each column exemplifies a condition of *NPC1*$^{-/-}$ ARPE-19 cells infected with retroviral particles carrying either the wild type (WT), p.Ile1061Thr, p.Ala1035Val or p.Ala1035Val + p.Ile858Val constructs. These are representative images, obtained through confocal fluorescence microscopy. The scale bar (white) represents 25 µm.

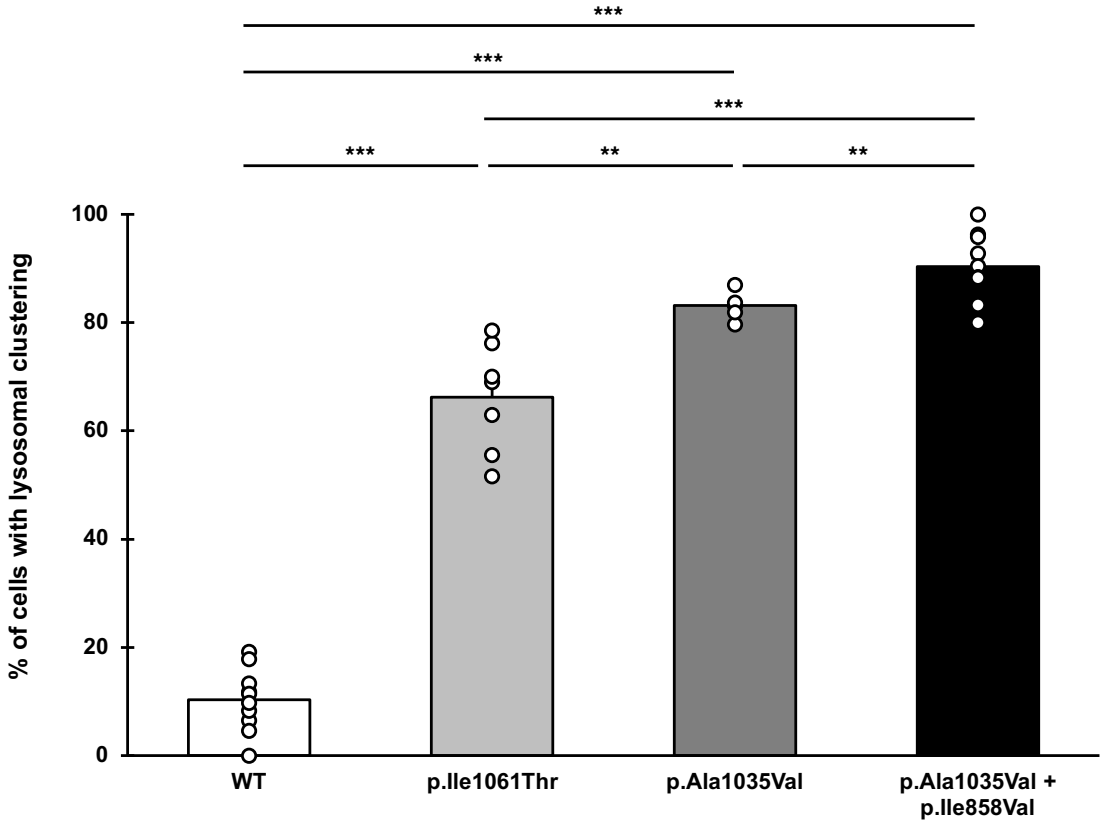


Figure 19 – Scoring of lysosome clustering in transduced *NPC1*$^{-/-}$ ARPE-19 cells. Various fields were selected in the LAMP1 microscopy slides in an unbiased manner for each cell line transduced with either the WT, p.Ile1061Thr, p.Ala1035Val or p.Ala1035Val + p.Ile858Val variants in NPC1, at least 300 cells were scored for lysosome clustering, and the percentage of cells presenting a clustered pattern was calculated for each field. Comparisons between groups were analyzed using the t-student test (** $p < 0.01$; *** $p < 0.001$).

Most lysosomal functions depend on their correct positioning and motility, both tightly orchestrated through complex mechanisms [97]. Many LSDs are characterized by a centripetal clustering of enlarged, substrate-filled lysosomes [9], which tend to establish more membrane contact sites with the ER limiting membrane, thus severely constraining lysosomal motility, and hindering their function [176].

A study on NPC disease has also described how the aberrant cholesterol accumulation within the LE/Lys compartment (here demonstrated by the filipin staining test for c.3591+1G>A fibroblasts transfected with the different NPC1-mNeonGreen constructs) elicits a juxtanuclear clustering of lysosomes [177,178], thus inhibiting mTORC1 signalling, and stimulating catabolism (e.g. autophagy) [179,180].

3.3. Anomalous NPC1 trafficking and degradation

3.3.1. NPC1 variants are retained and likely degraded in the ER

N-glycosylation takes place as the NPC1 protein is synthetized and folded within the ER [181]. Preassembled high-mannose oligosaccharides are co-translationally added to select asparagine residues within the growing polypeptide sequence, which is then transported to the GA, where its *N*-linked glycans are processed and matured, as their mannose residues are progressively replaced with other sugar monomers, turning NPC1 into a complex glycosylated protein, which is ultimately targeted to the LE/Lys membrane [52].

Seeing as this addition and maturation of *N*-linked glycans occurs gradually as NPC1 is transported through different organelles, we can infer the protein's subcellular localization by identifying its state of glycosylation. This can be achieved through deglycosylation assays using different enzymes.

Peptide-*N*-glycosidase F (PNGase F) is an amidase enzyme that cleaves virtually all asparagine-linked oligosaccharides from simple to more complex glycoproteins. Endoglycosidase H (Endo H), on the other hand, is only able to catalyze the cleavage of high-mannose *N*-linked glycans from simple to hybrid glycoproteins (Figure 20) [182]. In normal circumstances, most NPC1 protein within cells is already at its ultimate destination (the LE/Lys compartment), and therefore under its complex and mature glycosylation state. Thus, in healthy cells, virtually all NPC1 is expected to be PNGase F-sensitive, but Endo H-resistant.

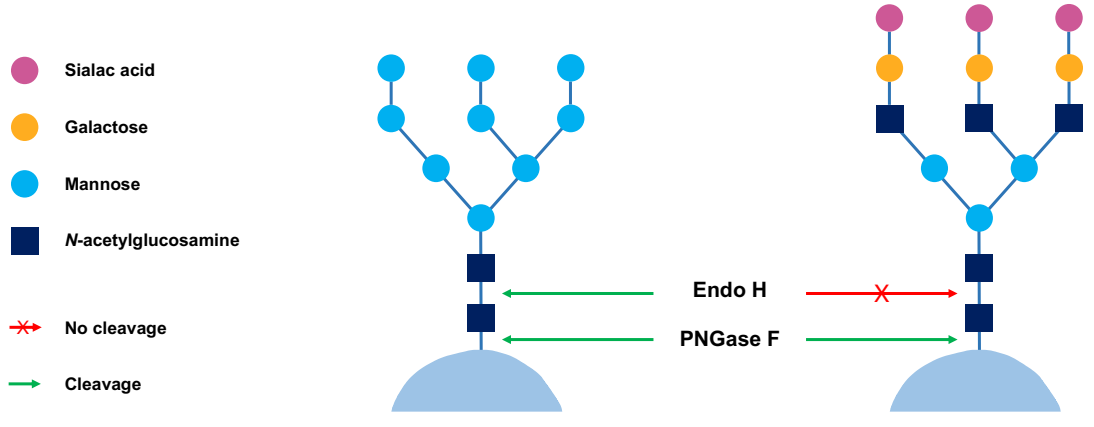


Figure 20 – PGNase F- and Endo H-mediated cleavage of simple and complex glycoproteins. Schematic representation of how the PGNase F and Endo H enzymes catalyze the cleavage of glycoproteins throughout their maturation stages.

In this study, we confirmed this glycosylation pattern for healthy control cells, which displayed a mere 21.91 % (± 1.01 %) mean Endo H-sensitive form. Patient-derived skin fibroblasts with the p.Ile1061Thr and with the p.Ala1035Val (alongside the p.Ile858Val SNP) NPC1 variants both exhibited around 3.50-fold increases in Endo H-sensitivity when compared to controls, with levels around 69.46 % (± 4.79 %) for the p.Ile1061Thr variant, and 82.19 % (± 2.26 %) for p.Ala1035Val (Figure 21).

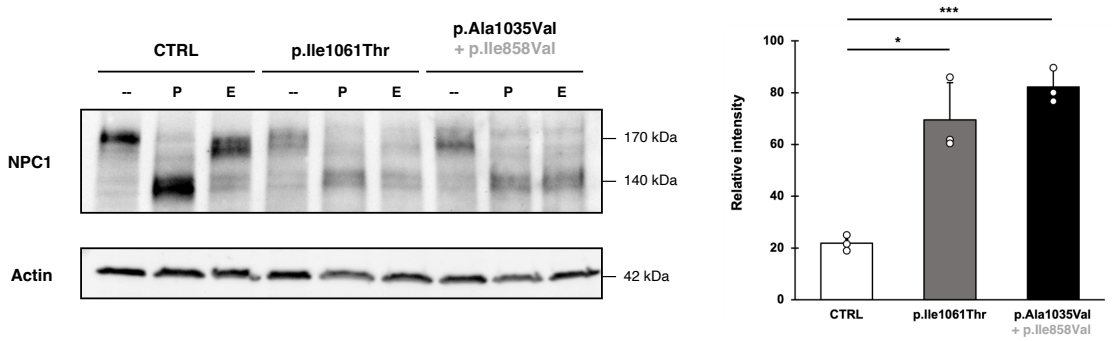


Figure 21 – Endo H-sensitivity quantification. The left panel displays a representative western blot showing both glycosylated and deglycosylated NPC1 protein levels in a human skin fibroblast cell line used as control (CTRL) and skin fibroblasts obtained from NPC patients with the p.Ile1061Thr and p.Ala1035Val (and p.Ile858Val) variants in NPC1, each incubated with no treatment (-), PNGase F (P) or Endo H (E) and Actin as a loading control. The right panel displays the quantification of the deglycosylated (Endo H-sensitive) NPC1 protein : total NPC1 protein, for 3 independent experiments (n=3). Comparisons between groups were analyzed using the t-student test (* $p < 0.05$; *** $p < 0.001$).

Immunofluorescence assays on *NPC1*$^{-/-}$ ARPE-19 cells infected with the different NPC1 constructs revealed that, unlike the wild type protein, the p.Ile1061Thr and p.Ala1035Val variants fail to traffic through the Golgi, being retained and likely degraded in the ER (Figure 22). Cells expressing the native form of the NPC1 protein, display a close to total colocalization of NPC1-mNeonGreen with LE/Lys vesicles (LAMP1-positive organelles), with an average Pearson's correlation coefficient of 0.82 (± 0.01). Mutant NPC1 proteins presented progressively attenuated LAMP1 colocalization figures: 0.47 (± 0.01) for p.Ile1061Thr, 0.33 (± 0.01) for p.Ala1035Val, and 0.07 (± 0.01) for p.Ala1035Val + p.Ile858Val (Figure 23).

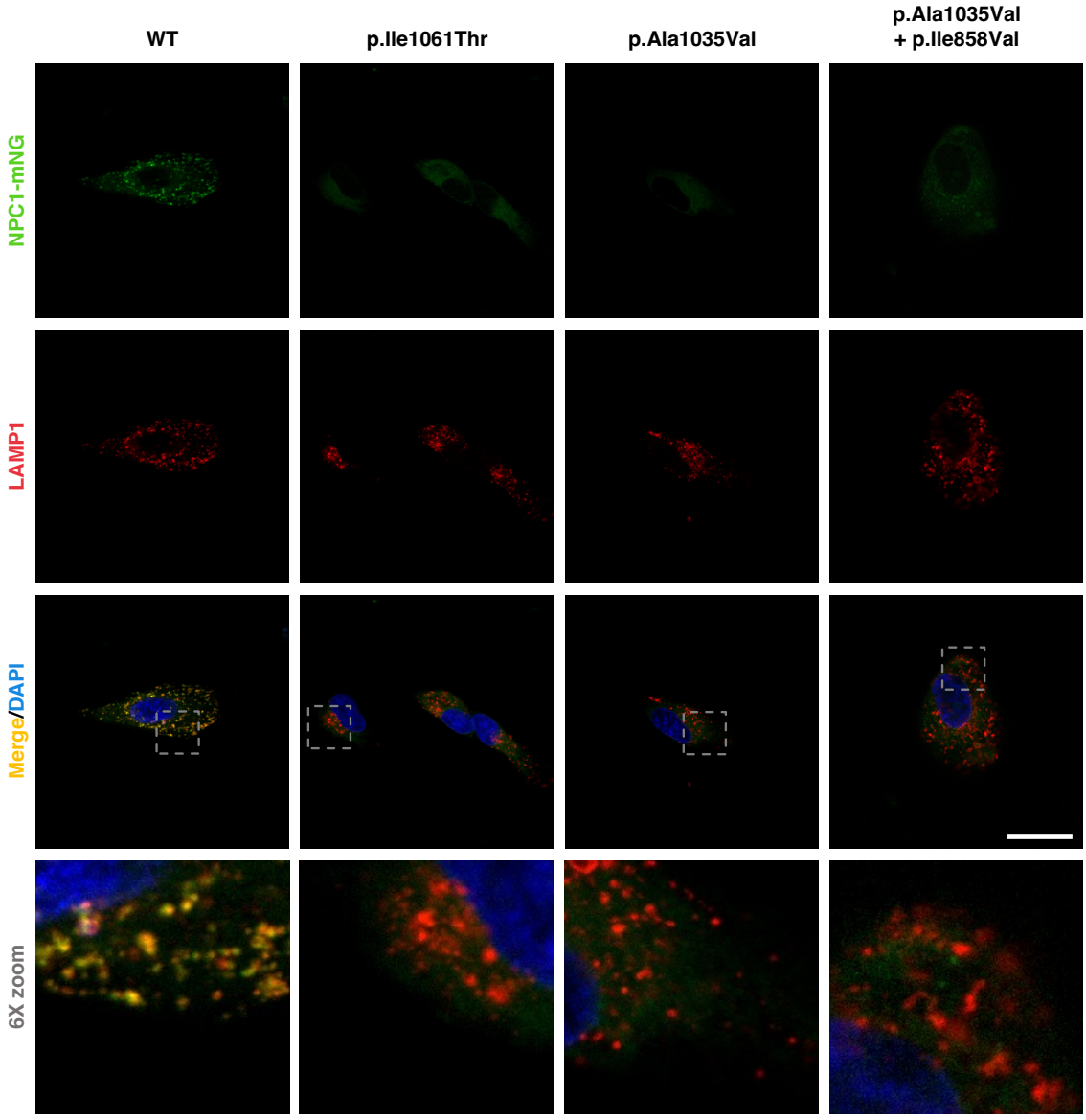


Figure 22 – LAMP1 and NPC1-mNeonGreen colocalization in transduced *NPC1*$^{-/-}$ ARPE-19 cells. The first line shows the NPC1-mNeonGreen signal (green), the second line represents the LAMP1 signal (red), the third line displays a merge of both of those signals, as well as DAPI (blue), and the bottom line represents a 6X zoom of the merged image. From left to right, each column exemplifies a condition of *NPC1*$^{-/-}$ ARPE-19 cells infected with either the wild type (WT), p.Ile1061Thr, p.Ala1035Val or p.Ala1035Val + p.Ile858Val constructs. These are representative images, obtained through confocal fluorescence microscopy. The scale bar (white) represents 25 µm.

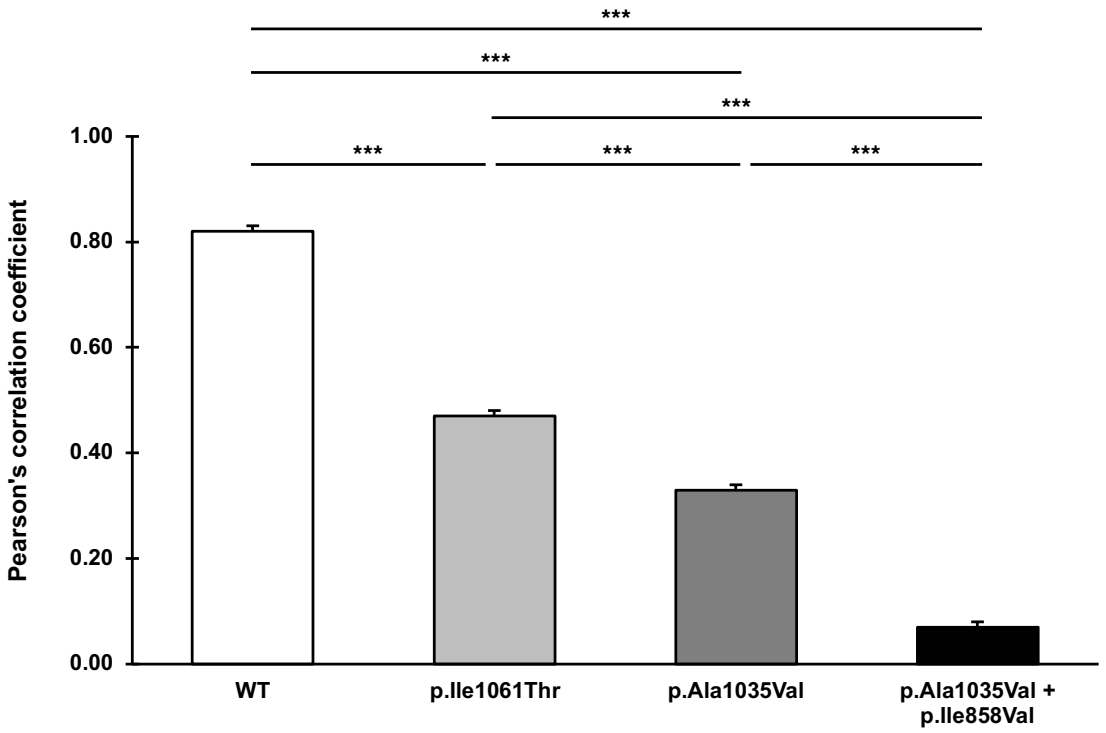


Figure 23 – Cross colocalization of LAMP1 with NPC1-mNeonGreen in transduced *NPC1*$^{-/-}$ ARPE-19 cells. Various regions of interest were selected in the LAMP1 microscopy slides in an unbiased manner for each cell line transduced with either the WT, p.Ile1061Thr, p.Ala1035Val or p.Ala1035Val + p.Ile858Val variants in NPC1, at least 50 regions of interest were analyzed, and the Pearson's correlation coefficient was calculated for each region. Comparisons between groups were analyzed using the t-student test (** $p < 0.01$; *** $p < 0.001$).

Such results endorse previously published reports where the p.Ile1061Thr-NPC1 protein failed to colocalize with LAMP1-positive organelles, contrary to the native NPC1 form [93,162,183], and show, for the first time, that the p.Ala1035Val variant seems to be retained and degraded in a similar – if not more extensive – manner to p.Ile1061Thr. The statistically significant ($p < 0.001$) difference between NPC1-mNeonGreen : LAMP1 colocalization for the p.Ala1035Val variant with and without the p.Ile858Val SNP implies a slightly altered trafficking pattern, which may account for at least some of the severe phenotype observed in patients within our cohort, that can otherwise not be fully predicted by functionality score algorithms for the alanine to valine substitution on position 1035 [184].

The high Endo H-sensitivity observed in NPC patients' cells, and the failure to colocalize with the LE/Lys compartment, suggest that the mutant proteins are misfolded in the ER, where they are flagged and retained by ERQC mechanisms and probably targeted for degradation, such as ERAD [168]. Our results regarding the p.Ile1061Thr variant corroborate those obtained by Schultz *et al* in 2022 [112], and imply a similar, if not

more severe, pattern for the p.Ala1035Val variant, especially when combined with the p.Ile858Val SNP.

3.3.2. NPC1 variants trigger different degradation pathways

Bafilomycin A_1 is a macrolide antibiotic that specifically inhibits lysosomal acidification by targeting the vacuolar H^+-ATPase, i.e. the lysosomal proton pump, blocking the fusion of lysosomes with autophagosomes, thus preventing catabolic degradation within the lysosome [185–187].

Using bafilomycin A_1, in 2018, Schultz *et al* described p.Ile1061Thr-NPC1 as being partly degraded by the lysosome itself – through selective ER-phagy – concurrently with the proteasome – following ERAD [83]. Employing a similar approach, we set out to investigate whether the ER-phagy degradation pathways is also recruited by the p.Ala1035Val-NPC1 variant.

As reported in that same study, treatment with bafilomycin A_1 significantly increased WT-NPC1 protein levels, around 2.38-fold (± 0.19), consistent with the inhibition of its degradation in the lysosome, implying that this organelle plays a significant role in the degradation of the native NPC1 protein. But, regarding p.Ile1061Thr, our data is not totally in accordance with the results obtained by Schultz *et al* in 2018, which pointed to a greater involvement of the lysosome in this variant's degradation than in that of the WT form of the protein.

Despite confirming the lysosome's involvement in the degradation of all forms of the protein, we achieved a lower recovery of p.Ile1061Thr-NPC1 following bafilomycin A_1 treatment – 1.59-fold (± 0.09) – denoting less involvement of the lysosome in p.Ile1061Thr-NPC1 degradation, when compared to the WT. Despite differing with the results of the aforementioned study, our data is in agreement with numerous other reports, that found lysosomal inhibition (by chloroquine) to not have a major effect on p.Ile1061Thr-NPC1 protein levels, questioning the theory that this variant is degraded mostly in the lysosome [89,93,188].

Similarly, p.Ala1035Val-NPC1 levels showed a comparable, 1.60-fold (± 0.11), recovery following incubation with bafilomycin A_1, indicating that this pathogenic variant is also degraded by ER-phagy, in the lysosome, but probably in a lesser extent than by the proteasome, through ERAD. Unfortunately, scarcity of p.Ala1035Val + p.Ile858Val cells following bafilomycin A_1 treatment incumbered us from attaining more than one data

set for this cell line, which yielded an even smaller, but ultimately uninformative, 1.23-fold recovery (not shown in Figure 24) of NPC1.

Taken together, these results suggest that NPC1 variants elicit diverse degradation pathways. While the native form of the protein is degraded in a similar ratio by the lysosome and the proteasome, a larger fraction of both the p.Ile1061Thr and the p.Ala1035Val forms seem to be triaged to ERAD rather than ER-phagy. Further analysis – such as proteasome inhibition assays – would be required to estimate the proportion of NPC1 protein degraded by each pathway.

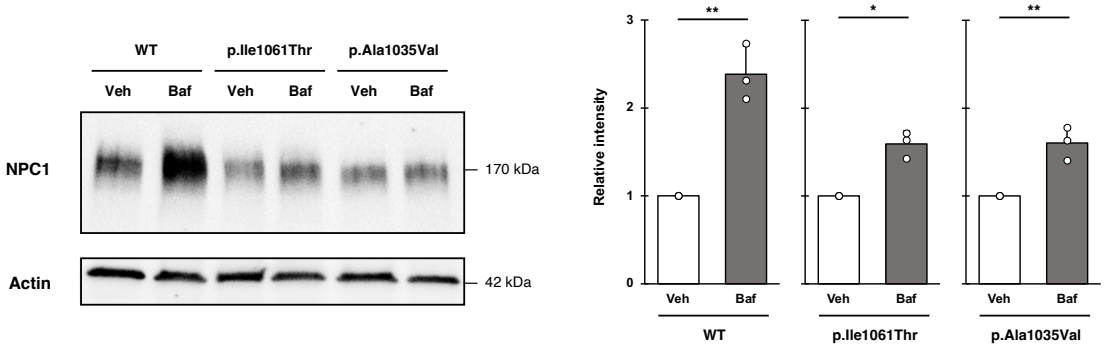


Figure 24 – Bafilomycin A_1 recovery quantification. The left panel displays a representative western blot showing NPC1 protein levels in *NPC1*$^{-/-}$ ARPE-19 cells transduced with either the wild type (WT) construct, the p.Ile1061Thr or the p.Ala1035Val variants, after treatment with 100 nM bafilomycin A_1 (Baf) or an equivalent volume of vehicle (Veh), and Actin as a loading control. The right panel displays the quantification of the recovery of NPC1 protein following Baf treatment (relative to Veh), for 3 independent experiments (n=3). Comparisons between groups were analyzed using the t-student test (* $p < 0.05$; ** $p < 0.01$).

3.4. Differentially expressed miRNAs in NPC

When tackling phenotypically diverse disorders, epigenetics is often one of the major players in the intricate network of pathophysiological mechanisms involved in disease progression and phenotypic expression [138]. The dysregulation of miRNAs in particular, has been frequently associated with countless diseases, and their levels in circulation can inform about an individual's physiological state [146]. In fact, their potential as novel biomarkers is currently under examination for other LSDs, including Pompe and Fabry diseases [150,152].

Here, we ventured out to define the miRNA expression profile of NPC patients using high-throughput small RNA sequencing methodologies, validating the main upregulated hits using qRT-PCR, and evaluating their diagnostic potential for NPC.

3.4.1. Disease-causing variants in *NPC1* were confirmed by dye-terminator sequencing

Since the patients included in the sRNA-Seq study either harboured splicing defects or mutations in exonic regions of the *NPC1* gene, confirmation of those variants was performed at the cDNA level, synthesizing the complementary strand after RNA extraction from patient-derived skin fibroblasts. As expected, dye-terminator Sanger sequencing results confirmed all the disease-causing variants for the included NPC patients (Figure 25).

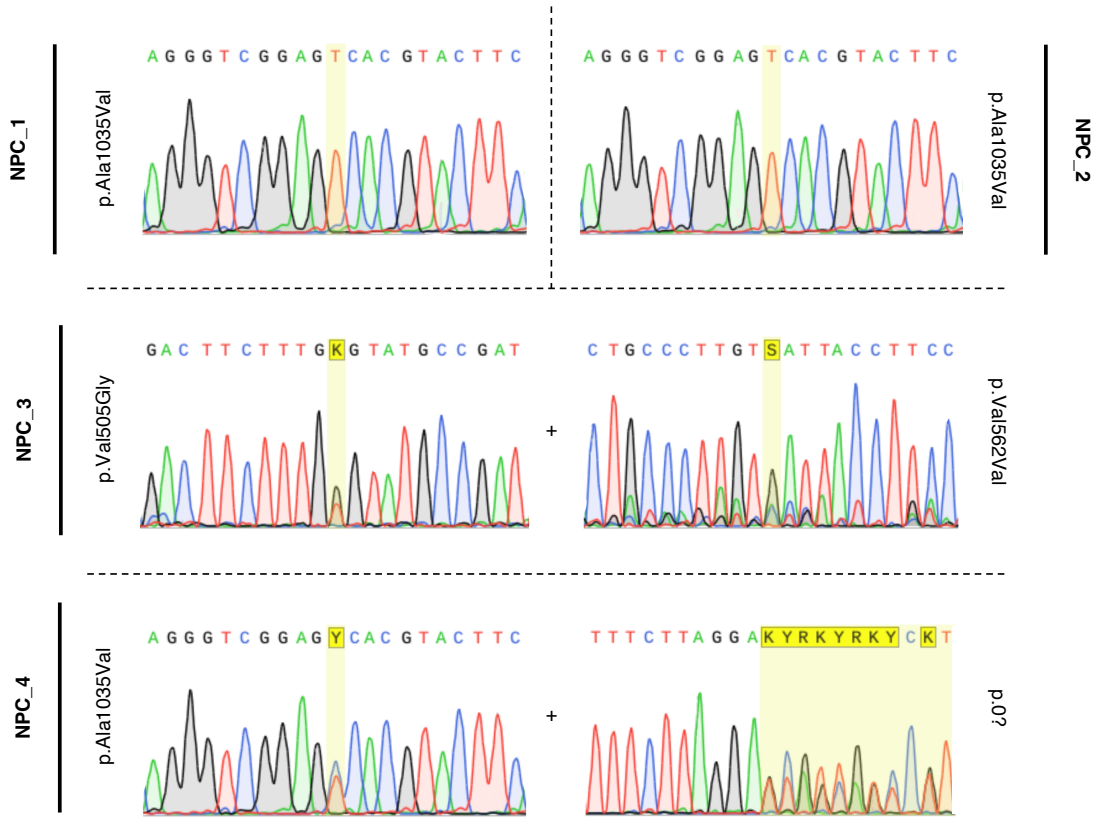


Figure 25 – DNA dye-terminator Sanger sequencing electropherograms highlighting (in yellow) the variations present in different *NPC1* regions of the multiple NPC patients included in the sRNA-Seq analysis. The NPC_1 and NPC_2 patients carry the c.3104C>T (p.Ala1035Val) variant in homozygosity. NPC_3 is heterozygous for the c.1514T>G (p.Val505Gly) and c.1686G>A (p.Val562Val) variants, the latter of which induces the skipping of exon 11, leading to a less abundant transcript, not always visible in cDNA analysis. NPC_4 displays the c.3104C>T (p.Ala1035Val) variant in heterozygosity with the c.1554-1009G>A (p.0?) variant, which results in aberrant splicing, giving rise to a 194 bp pseudoexon and a frameshift.

3.4.2. NPC patients display different miRNA expression patterns

After statistical and bioinformatic treatment, normalization and quality control, 19 differentially expressed miRNAs were identified between NPC patients and controls following Novogene's analysis pipeline (Table 23). Of those, miR-199a-3p was found to be the most upregulated species in NPC patients, with the highest statistical significance.

Table 23 – Differentially expressed cellular miRNAs in NPC patients vs. controls.

miRNA	Fold-change	Statistical significance
miR-101-39	1.97	< 0.05
miR-136-3p	1.52	< 0.01
miR-136-5p	1.83	< 0.05
miR-181c-5p	2.30	< 0.05
miR-199a-3p	5.66	< 0.0001
miR-210-3p	2.34	< 0.05
miR-214-3p	2.24	< 0.05
miR-29a-3p	1.55	< 0.05
miR-382-5p	1.63	< 0.05
miR-99b-3p	3.20	< 0.05
let-7a-3p	0.52	< 0.05
miR-1268a	0.21	< 0.05
miR-140-3p	0.63	< 0.05
miR-196-5p	0.03	< 0.0001
miR-222-3p	0.78	< 0.01
miR-505-3p	0.23	< 0.05
miR-561-5p	0.24	< 0.05
miR-708-3p	0.43	< 0.05
miR-98-5p	0.79	< 0.05

Another approach employed in the bioinformatic inquiry performed by Novogene was cluster analysis – a tool used to find miRNAs (or genes) with similar expression patterns, possibly revealing relationships between groups of miRNAs (or genes), in order to select the most remarkable ones for subsequent analyses (Figure 26).

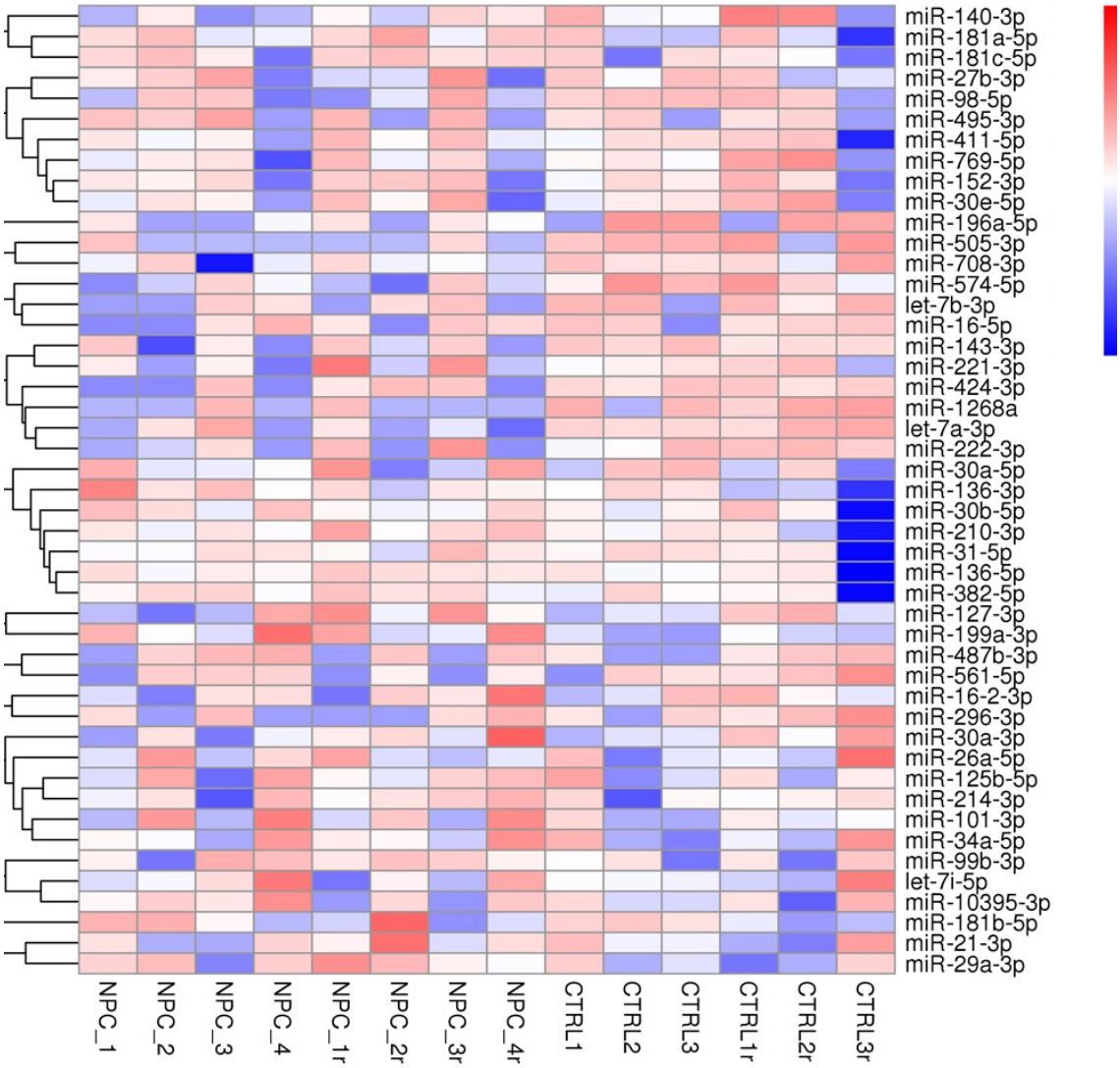


Figure 26 – Cluster analysis of differentially expressed miRNAs. The overall transcripts per million (TPM) results are clustered by $\log_{10}$(TPM+1). The red to blue scale represents high to low expression levels.

Finally, enrichment analysis was performed, to emphasize which cellular processes and pathways were most affected by the differing small RNA expression patterns in NPC patients and controls (Figure 27). Overall, this data suggested axon development, plasma membrane events, enzymatic activity and cell-to-cell adhesion as the most impacted pathways in NPC.

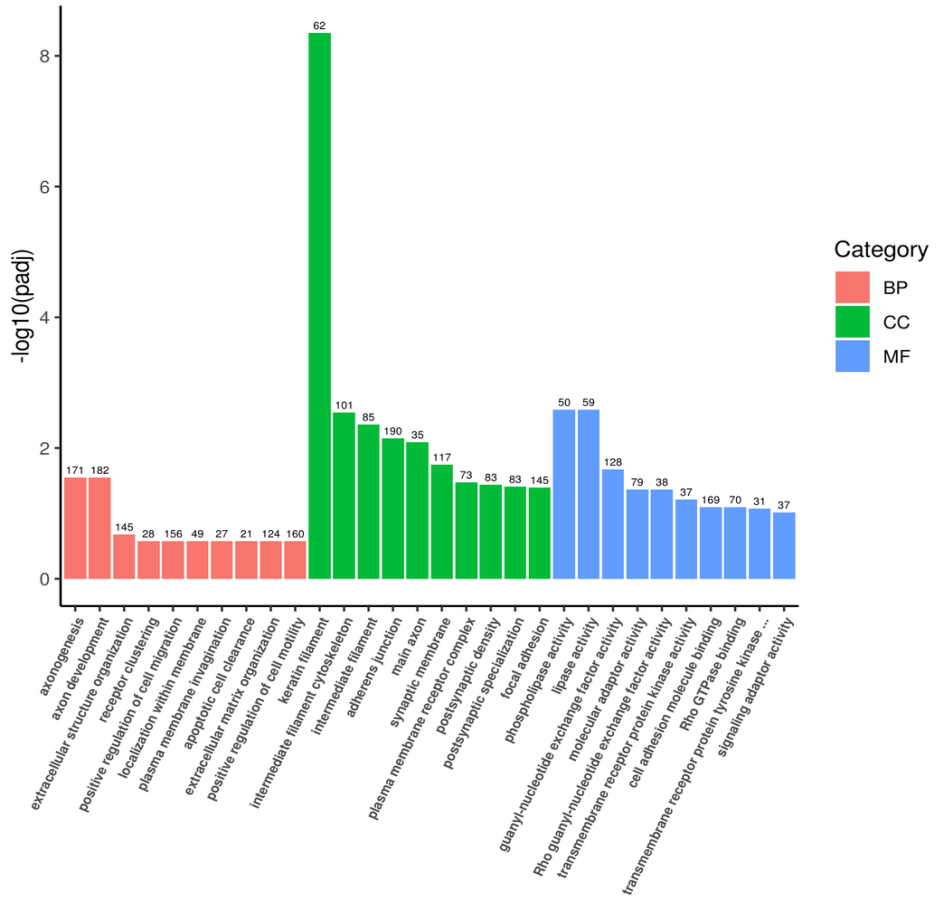


Figure 27 – Histogram of target gene candidates. This graph displays the pathways predicted to be most significantly targeted by the NPC differential miRNA profile, grouped as biological processes (BP, in red), cellular components (CC, in green) and molecular functions (MF, in blue). The number above each bar represents the number of predicted target genes related to that cellular process or pathway, and bar height represents the $\log_{10}$ of the respective average adjusted p value.

A different analysis pipeline followed at the Technology and Innovation Unit of the National Institute of Health Dr. Ricardo Jorge, identified other differentially expressed miRNA species in NPC patients, of which miR-143-3p was the most upregulated and the most statistically significantly so (data not shown).

Seeing as these two methods yielded disputing results, we selected the two most upregulated miRNAs identified by each method – miR-199a-3p and miR-143-3p – for further validation.

3.4.3. Differentially expressed miRNA hits were validated in patient cells and sera

miR-143-3p and miR-199a-3p levels were first quantified in patient-derived skin fibroblasts from 4 NPC patients and compared to corresponding levels in skin fibroblasts of 2 healthy controls. qRT-PCR results did not appear coincident with the sRNA-Seq

analysis, as no statistically significant differences were identified in these cells (Figure 28). This could be a result of miRNA degradation that might have occurred after several freeze-thaw cycles, or even indicative of possible contamination. In either case, further validation and optimization of cDNA synthesis and qRT-PCR conditions would be necessary to confirm the validity of these results.

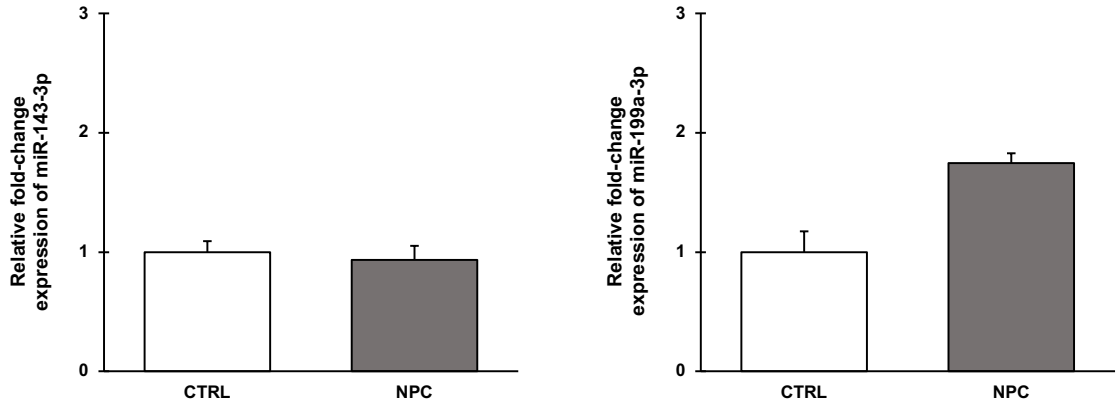


Figure 28 – Expression levels of miR-143-3p and miR-199a-3p in fibroblasts. Cellular levels of miR-143-3p (left) and miR-199a-3p (right) in patient-derived skin fibroblasts (NPC) and control cell lines (CTRL) were quantified through qRT-PCR, for 2 independent experiments (n=2), normalized using the RNU6B endogenous control, and expressed in relative fold-change. Comparisons between groups were analyzed using the t-student test.

Nonetheless, we moved onto serum samples obtained from 3 healthy controls and 4 NPC patients, and the results were quite different. Both species of miRNAs were found to be significantly upregulated ($p < 0.001$) in the sera of NPC patients when compared to that of controls – with a relative change of 19.50-fold for miR-143-3p and 15.79-fold for miR-199a-3p (Figure 29).

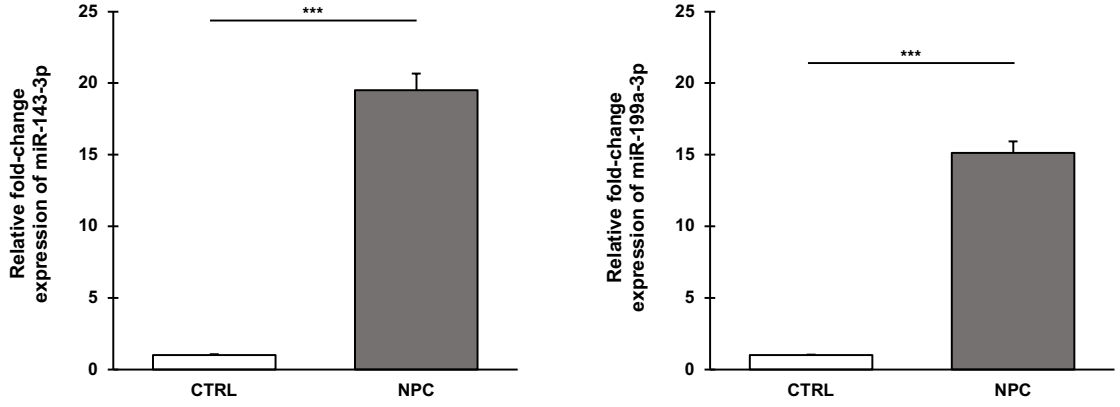


Figure 29 – Expression levels of miR-143-3p and miR-199a-3p in serum. Circulating levels of miR-143-3p (left) and miR-199a-3p (right) in patient (NPC) and control (CTRL) sera were quantified through qRT-PCR, for 3 independent experiments (n=3), theoretically normalized and expressed in relative fold-change. Comparisons between groups were analyzed using the t-student test (*** $p < 0.001$).

This finding poses circulating levels of miR-143-3p and miR-199a-3p as possible novel, minimally-invasive, time- and cost-effective diagnostic biomarkers for NPC disease, as alternatives to existing screening methods which are often unspecific and require complex and costly detection procedures. The quantification of their levels in patient serum could even eventually be useful to evaluate disease progression and response to therapy, but larger, more varied cohorts and further data regarding the patients' clinical information would be required.

In 2010, Ozsait *et al* published the only other study to trace the miRNA profile in NPC to date. Their survey evaluated the expression of several miRNA species in NPC patients' fibroblasts using a low-density array system. They reported both miR-143-3p and miR-199a-3p as downregulated in NPC fibroblasts, when compared to controls [141]. Our results appear to diverge from those, with RNA-Seq analysis finding significant upregulations of both miRNA species in patient cell-derived RNA, even though qRT-PCR validation did not appear consistent. On the other hand, qRT-PCR data from the serum samples of a different set of NPC patients and controls encouragingly corroborated the RNA-Seq results, revealing statistically significant differences in circulating levels of miR-143-3p and miR-199a-3p in these two groups.

Even though the role of these two miRNA species has not been extensively described in lysosomal storage disorders, a number of studies regarding their functions in other diseases and pathways could be extrapolated for the purpose of this discussion.

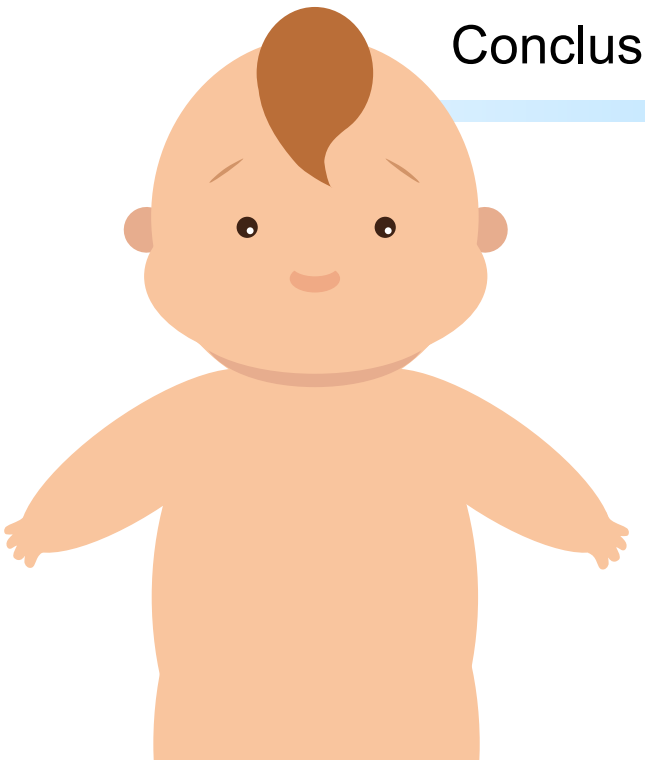
miR-143-3p was found to be overexpressed in diabetic (and prediabetic) mice, as well as in human adipocytes (when compared to preadipocytes), hinting at its important part in lipid homeostasis, namely by directing adipocyte differentiation, modulating atherosclerosis, and integrating metabolic signalling [189–191]. This miRNA is also reported to suppress autophagy by targeting *ATG2* (directly affecting autophagosome formation and potentiating inflammatory response) [192], *ATG7* (a mediator of oxidative-stress response) [193], *GABARAPL1* (an activator of autophagic flux) [194]. Lastly, it has also been reported that miR-143 inhibits the cation-independent mannose-6-phosphate receptor, severely hampering the transport of lysosomal enzymes across the blood-brain barrier – – a factor linked with therapy effectiveness in various lysosomal storage disorders [195].

The function(s) of miR-199a-3p have been the subject of several recent publications. Most interestingly, an 18.82-fold upregulation of miR-199a-3p was recently described in Gaucher disease whole blood samples [196]. Gaucher disease is the most commonly reported LSD, and some of its symptomatology overlaps with that of NPC, including hepato- and splenomegaly, motor and cognitive impairment, skeletal problems, and

respiratory complications[197]. Like Gaucher and other LSDs, NPC is characterized lipid trafficking dysfunction. miR-199a-3p promotes lipid accumulation in adipocytes (by targeting of transcription factors related to cell differentiation and metabolism) [198], it mediates cholesterol uptake in neurons (by targeting apolipoprotein E expression) [199], and it reduces cholesterol efflux from cells (by negatively regulating the expression of the ATP-binding cassette transporter ABCA1) [200]. This miRNA is additionally thought to inhibit receptor-mediated endocytosis in human cells [201], playing a role in intracellular trafficking and impairing autophagy through mTORC1 activation [202–204].

Plenty of these mechanisms seem to be at least tangentially related to the NPC pathogenesis, and the upregulation of both of these miRNA species could explain some of the features observed in NPC patients, such as the lipid accumulation, autophagy and intracellular trafficking impairments.

In summary, our data regarding these two apparently differentially expressed miRNAs in blood serum could be useful not just for the diagnostic and prognostic analysis of NPC disease, but also to further unveil and better understand its underlying pathogenic mechanisms, and even to improve and evaluate the therapeutic efficacy of available treatments.



Conclusions & Future Perspectives

Ever since its first description, NPC has been the subject of many publications, but most aspects of this disease still remain a mystery. The discovery that NPC1 – the affected lysosomal protein in about 95 % of cases – is a cellular receptor for a plethora of pathogenic agents shortly brought this protein to the spotlight, but a lot is still to be unveiled and understood concerning NPC disease.

One of the puzzling traits of this disorder is the great phenotypic variability observed in patients with both differing and coinciding genotypes, and even within affected members of the same family. Out of sundry factors that potentially influence the phenotypic manifestation of NPC, in the context of this thesis, we have addressed two: the p.Ala1035Val + p.Ile858Val complex allele in *NPC1* – for which no functional studies have been reported – and the miRNA expression profile of NPC patients – which has seldom been explored.

Among the over 660 disease-causing variants reported in the *NPC1* gene, p.Ile1061Thr is by far the most studied one. It is neither the most common, nor the most severe, but its substantial prevalence in patients of Western European descent has warranted it unrivalled attention in NPC literature. Recent studies have found the p.Ile1061Thr-NPC1 protein to be functional, could it bypass the ER's quality control machinery and be delivered to the lysosome, leading researchers to investigate NPC therapeutic approaches that modulate cellular proteostasis, alike others already in use for different LSDs. Arimoclomol is one such molecule currently in clinical trials, which acts by eliciting molecular chaperones to prevent mutant NPC1 protein misfolding and degradation. The trafficking and degradation routes of the p.Ala1035Val variant (specially with the p.Ile858Val SNP in *cis*) – the most frequent in Portugal and Latin America, and the second most recurrent worldwide – have not been surveyed yet.

Undoubtedly, NPC1 variants have emerged as latent targets for proteostasis modulators, but drug development efforts have so far been unsuccessful in mouse models. The issue may be that those models may not be appropriate for the translational study of NPC1 protein trafficking and degradation.

Taking into account all of these difficulties, we created stable *NPC1*$^{-/-}$ ARPE-19 cell lines transduced with the WT, p.Ile1061Thr, p.Ala1035Val and p.Ala1035Val + p.Ile858Val NPC1 variants. Unlike skin fibroblasts, *NPC1*$^{-/-}$ ARPE-19 cells mimic several features of the pathological cellular phenotype of NPC, including the accumulation of unesterified cholesterol, sphingosine and glycosphingolipids, and enlarged LE/Lys with anomalous morphology and positioning. These new cell models of NPC that we established enable the study of variant-specific trafficking patterns, and

their potential application in NPC research is even broader, including large-scale drug screenings. One caveat of our study was the missing filipin staining of these transduced cell lines, which needs to be performed in the future, to further endorse their use as versatile and accurate models of NPC.

Using these cells, alongside patient-derived skin fibroblasts, we surveyed the trafficking routes and degradation pathways of the p.Ala1035Val variant and revealed a possible disease-modifying effect for the p.Ile858Val SNP found in *cis*, in all the analyzed Portuguese p.Ala1035Val alleles. Our data collectively suggests that this variant leads to decreased lysosomal turnover and altered positioning (upheld by LAMP1 western blot quantification in patient-derived skin fibroblasts and by the scoring of lysosomal clustering following immunofluorescence assays on transduced *NPC1*$^{-/-}$ ARPE-19 cells) and to mutant NPC1 retention and likely degradation in the ER (as inferred from deglycosylation assays in skin fibroblasts from patients and controls, through LAMP1:NPC1-mNeonGreen colocalization observed using fluorescence microscopy, and bafilomycin A_1 recovery assays in stably transduced *NPC1*$^{-/-}$ ARPE-19 cells).

This poses patients carrying p.Ala1035Val – one of the most prevalent *NPC1* pathogenic variants worldwide – as candidates for which proteostasis modulator-based approaches might be effective therapeutic options.

NPC is a devastating disease, for which there is still no cure. *N*-butyldeoxynojirimycin (or miglustat) is the first therapy for which there is data supporting a disease modifying benefit for NPC patients. However, besides its many secondary effects, this drug is not recommended for patients with profound neurological symptomatology, nor has it received worldwide approval for the treatment of NPC. In most cases, treatment of this progressive disease is symptomatic, making a correct and prompt diagnosis of the utmost priority, to avoid extensive and irreversible neurodegenerative damage.

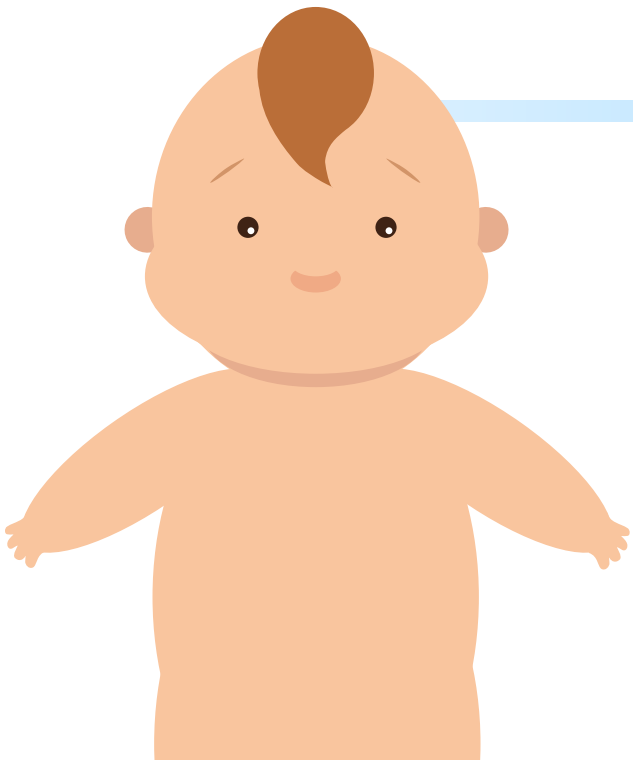
The issue remains that no single biomarker is specific for NPC, underscoring once again the vast phenotypic variability observed in this disorder, which is often a confounding factor in NPC diagnosis, leading to prolonged diagnostic odysseys for many of these patients. Besides possibly uncovering previously unidentified mechanisms involved in NPC pathogenesis, high-throughput transcriptome-wide sequencing technologies, such as sRNA-Seq, may be used to identify differentially expressed miRNAs in NPC patients, which can later be validated through qRT-PCR, for future use as diagnostic biomarkers.

Up to this point, only two studies have been published where miRNAs were evaluated in NPC patient cells, and, to our knowledge, no circulating miRNA levels were ever quantified in these individuals. This shortage of studies addressing the various factors that may impact phenotypic manifestation of NPC disease, namely the differential miRNA profile of NPC patients, alongside this impelling demand for minimally-intrusive, sensitive, specific, time- and cost-effective biomarker candidates for NPC, lead us to also explore this route in the context of this dissertation.

sRNA-Seq analysis indicated several possibly dysregulated miRNAs in NPC patients' fibroblasts, even though further validation is still needed to confirm their differential expression. qRT-PCR validation of some of these hits in patient and control serum yielded two promising circulating miRNA biomarker candidates: miR-143-3p and miR-199a-3p, which might be implicated in lipid accumulation, autophagy and intracellular trafficking impairment.

As a whole, these comprehensive molecular and functional studies contributed to the continuous effort in unveiling the pathological mechanisms which underly NPC disease. More specifically, we generated a new *in vitro* model to study the effect of *NPC1* variants on protein trafficking and degradation, which could even be used in drug screenings; we retraced the miRNA expression profile of NPC patients; and we proposed two serum miRNAs as new putative biomarkers of this disease.

As future perspectives, the evaluation of the filipin staining pattern of the different *NPC1*$^{-/-}$ ARPE-19 cell lines transduced with the various constructs is surely a priority, to further sustain the usefulness of these models. The creation of a stable *NPC1*$^{-/-}$ ARPE-19 cell line transduced with an NPC1-mNeonGreen construct expressing the p.Ile858Val NPC1 variant alone would be useful to assess whether the observed effect of this SNP was indeed an aggravation of the phenotype observed for p.Ala1035Val. Studying the lipid profile of the various created cell lines would also be of great interest, not just to further validate their usefulness as trustworthy disease models of NPC, but also to elucidate the accumulated lipid pattern of the different NPC1 variants. Further validation of the sRNA-Seq miRNA hits and their respective mRNA targets at the cellular level (through western blot and qRT-PCR) is definitely an imperative moving forward with these studies, as is the recruitment of more (national and international) NPC patients (with different genotypes) and controls to study the upregulated miRNAs in blood serum. It may also be interesting to validate these (and other eventual) differentially expressed miRNA hits in other bodily fluids, namely cerebrospinal fluid.



References

1. Berthet, J. & de Duve, C. (**1951**) Tissue fractionation studies. 1. The existence of a mitochondria-linked, enzymically inactive form of acid phosphatase in rat-liver tissue. *Biochem. J.* ***50***, 174–181.

2. Berthet, J., Berthet, L., Appelmans, F. & De Duve, C. (**1951**) Tissue fractionation studies. 2. The nature of the linkage between acid phosphatase and mitochondria in rat-liver tissue. *Biochem. J.* ***50***, 182–189.

3. Appelmans, F., Wattiaux, R. & de Duve, C. (**1955**) Tissue fractionation studies. 5. The association of acid phosphatase with a special class of cytoplasmic granules in rat liver. *Biochem. J.* ***59***, 438–445.

4. Novikoff, A. B., Beaufay, H. & De Duve, C. (**1956**) Electron microscopy of lysosome-rich fractions from rat liver. *J. Biophys. Biochem. Cytol.* ***2***, 179.

5. de Duve, C., Pressman, B. C., Gianetto, R., Wattiaux, R. & Appelmans, F. (**1955**) Tissue fractionation studies. 6. Intracellular distribution patterns of enzymes in rat-liver tissue. *Biochem. J.* ***60***, 604–617.

6. Parenti, G., Medina, D. L. & Ballabio, A. (**2021**) The rapidly evolving view of lysosomal storage diseases. *EMBO Mol. Med.* ***13***,.

7. Ballabio, A. & Bonifacino, J. S. (**2019**) Lysosomes as dynamic regulators of cell and organismal homeostasis. *Nat. Rev. Mol. Cell Biol. 2019 212* ***21***, 101–118.

8. Saftig, P. & Klumperman, J. (**2009**) Lysosome biogenesis and lysosomal membrane proteins: trafficking meets function. *Nat. Rev. Mol. Cell Biol. 2009 109* ***10***, 623–635.

9. Scerra, G. *et al.* (**2022**) Lysosomal positioning diseases: beyond substrate storage. *Open Biol.* ***12***,.

10. Perera, R. M., Di Malta, C. & Ballabio, A. (**2019**) MiT/TFE Family of Transcription Factors, Lysosomes, andCancer. *Annu. Rev. cancer Biol.* ***3***, 203.

11. Meras, I., Maes, J. & Lefrancois, S. (**2022**) Mechanisms regulating the sorting of soluble lysosomal proteins. *Biosci. Rep.* ***42***,.

12. Trivedi, P. C., Bartlett, J. J. & Pulinilkunnil, T. (**2020**) Lysosomal Biology and Function: Modern View of Cellular Debris Bin. *Cells 2020, Vol. 9, Page 1131* ***9***, 1131.

13. Braulke, T. & Bonifacino, J. S. (**2009**) Sorting of lysosomal proteins. *Biochim.*

Biophys. Acta - Mol. Cell Res. ***1793***, 605–614.

14. Owada, M. & Neufeld, E. F. (**1982**) Is there a mechanism for introducing acid hydrolases into liver lysosomes that is independent of mannose 6-phosphate recognition? evidence from I-cell disease. *Biochem. Biophys. Res. Commun.* ***105***, 814–820.

15. Dittmer, F. *et al.* (**1999**) Alternative mechanisms for trafficking of lysosomal enzymes in mannose 6-phosphate receptor-deficient mice are cell type-specific. *J. Cell Sci.* ***112***, 1591–1597.

16. Reczek, D. *et al.* (**2007**) LIMP-2 Is a Receptor for Lysosomal Mannose-6-Phosphate-Independent Targeting of β-Glucocerebrosidase. *Cell* ***131***, 770–783.

17. Janvier, K. & Bonifacino, J. S. (**2005**) Role of the Endocytic Machinery in the Sorting of Lysosome-associated Membrane Proteins. *Mol. Biol. Cell* ***16***, 4231.

18. Yang, C. & Wang, X. (**2021**) Lysosome biogenesis: Regulation and functions. *J. Cell Biol.* ***220***,.

19. Kühnel, W. (Thieme, 2003). *Color Atlas of Cytology, Histology, and Microscopic Anatomy*.

20. Udayar, V., Chen, Y., Sidransky, E. & Jagasia, R. (**2022**) Lysosomal dysfunction in neurodegeneration: emerging concepts and methods. *Trends Neurosci.* ***45***, 184–199.

21. Platt, F. M., d'Azzo, A., Davidson, B. L., Neufeld, E. F. & Tifft, C. J. (**2018**) Lysosomal storage diseases. *Nat. Rev. Dis. Prim. 2018 41* ***4***, 1–25.

22. Platt, F. M. (**2018**) Emptying the stores: lysosomal diseases and therapeutic strategies. *Nat. Rev. Drug Discov.* ***17***, 133–150.

23. Pinto, R. *et al.* (**2003**) Prevalence of lysosomal storage diseases in Portugal. *Eur. J. Hum. Genet. 2004 122* ***12***, 87–92.

24. Beck, M. (**2001**) Variable clinical presentation in lysosomal storage disorders. *J. Inherit. Metab. Dis.* ***24 Suppl 2***, 47–51.

25. Parenti, G., Andria, G. & Ballabio, A. (**2015**) Lysosomal Storage Diseases: From Pathophysiology to Therapy. *https://doi.org/10.1146/annurev-med-122313-085916* ***66***, 471–486.

26. Wraith, J. E. (**2002**) Lysosomal disorders. *Semin. Neonatol.* ***7***, 75–83.

27. Ballabio, A. & Gieselmann, V. (**2009**) Lysosomal disorders: from storage to cellular damage. *Biochim. Biophys. Acta **1793***, 684–696.

28. Niemann, A. (**1914**) Ein unbekanntes Krankheitsbild [An unknown disease picture]. *Jahrb. für Kinderheilkd. **79***, 1–10.

29. Pick, L. (**1926**) Der Morbus Gaucher und die ihm ähnlichen Krankheiten (die lipoidzellige Splenohepatomegalie Typus Niemann und die diabetische Lipoidzellenhypoplasie der Milz) [Gaucher's disease and similar diseases (type Niemann lipoid cell splenohepatomegaly and spleen . *Ergeb. Inn. Med. Kinderheilkd. **29***, 519–627.

30. Crocker, A. C. (**1961**) The cerebral defect in Tay-Sachs disease and Niemann-Pick disease. *J. Neurochem. **7***, 69–80.

31. Takahashi, T. *et al.* (**1995**) Identification and expression of a missense mutation (Y446C) in the acid sphingomyelinase gene from a Japanese patient with type A Niemann-Pick disease. *Tohoku J. Exp. Med. **177***, 117–123.

32. Graber, D., Salvayre, R. & Levade, T. (**1994**) Accurate Differentiation of Neuronopathic and Nonneuronopathic Forms of Niemann-Pick Disease by Evaluation of the Effective Residual Lysosomal Sphingomyelinase Activity in Intact Cells. *J. Neurochem. **63***, 1060–1068.

33. Desnick, J. P. *et al.* (**2010**) Identification and characterization of eight novel SMPD1 mutations causing types A and B Niemann-Pick disease. *Mol. Med. **16***, 316–321.

34. Patterson, M. (**2020**) Niemann-Pick Disease Type C. *GeneReviews®*.

35. Lloyd-Evans, E. & Platt, F. M. (**2010**) Lipids on Trial: The Search for the Offending Metabolite in Niemann-Pick type C Disease. *Traffic **11***, 419–428.

36. Greer, W. L. *et al.* (**1998**) The Nova Scotia (type D) form of Niemann-Pick disease is caused by a G3097-->T transversion in NPC1. *Am. J. Hum. Genet. **63***, 52.

37. Geberhiwot, T. *et al.* (**2018**) Consensus clinical management guidelines for Niemann-Pick disease type C. *Orphanet J. Rare Dis. **13***, 1–19.

38. Evans, W. *et al.* (**2021**) International consensus on clinical severity scale use in evaluating Niemann–Pick disease Type C in paediatric and adult patients: results from a Delphi Study. *Orphanet J. Rare Dis. **16***, 1–22.

39. Patterson, M. C. *et al.* (**2013**) Disease and patient characteristics in NP-C patients: findings from an international disease registry. *Orphanet J. Rare Dis.* ***8***, 12.

40. Vanier, M. T. (**2010**) Niemann-Pick disease type C. *Orphanet J. Rare Dis.* ***5***, 16.

41. Spiegel, R. *et al.* (**2009**) The clinical spectrum of fetal Niemann-Pick type C. *Am. J. Med. Genet. A* ***149A***, 446–450.

42. Kelly, D. A., Portmann, B., Mowat, A. P., Sherlock, S. & Lake, B. D. (**1993**) Niemann-Pick disease type C: diagnosis and outcome in children, with particular reference to liver disease. *J. Pediatr.* ***123***, 242–247.

43. Bolton, S. C. *et al.* (**2022**) Clinical disease characteristics of patients with Niemann-Pick Disease Type C: findings from the International Niemann-Pick Disease Registry (INPDR). *Orphanet J. Rare Dis.* ***17***, 1–10.

44. Klarner, B., Klünemann, H. H., Lürding, R., Aslanidis, C. & Rupprecht, R. (**2007**) Neuropsychological profile of adult patients with Niemann-Pick C1 (NPC1) mutations. *J. Inherit. Metab. Dis.* ***30***, 60–67.

45. Pineda, M., Walterfang, M. & Patterson, M. C. (**2018**) Miglustat in Niemann-Pick disease type C patients: a review. *Orphanet J. Rare Dis. 2018 131* ***13***, 1–21.

46. Platt, F. M., Neises, G. R., Dwek, R. A. & Butters, T. D. (**1994**) N-butyldeoxynojirimycin is a novel inhibitor of glycolipid biosynthesis. *J. Biol. Chem.* ***269***, 8362–8365.

47. Zervas, M., Somers, K. L., Thrall, M. A. & Walkley, S. U. (**2001**) Critical role for glycosphingolipids in Niemann-Pick disease type C. *Curr. Biol.* ***11***, 1283–1287.

48. Committee for Medicinal Products for Human Use. https://www.ema.europa.eu/en/documents/variation-report/zavesca-h-c-435-ii-0029-epar-assessment-report-variation_en.pdf (2008) *Assessment Report for Zavesca | Procedure No: EMEA/H/C/000435/II/0029*.

49. Carstea, E. D. *et al.* (**1993**) Linkage of Niemann-Pick disease type C to human chromosome 18. *Proc. Natl. Acad. Sci. U. S. A.* ***90***, 2002–2004.

50. Carstea, E. D. *et al.* (**1997**) Niemann-Pick C1 disease gene: homology to mediators of cholesterol homeostasis. *Science* ***277***, 228–231.

51. Watari, H. *et al.* (**1999**) Mutations in the leucine zipper motif and sterol-sensing domain inactivate the Niemann-Pick C1 glycoprotein. *J. Biol. Chem.* ***274***, 21861–

21866.

52. Ferris, S. P., Kodali, V. K. & Kaufman, R. J. (**2014**) Glycoprotein folding and quality-control mechanisms in protein-folding diseases. *Dis. Model. Mech.* ***7***, 331–341.

53. Davies, J. P. & Ioannou, Y. A. (**2000**) Topological analysis of Niemann-Pick C1 protein reveals that the membrane orientation of the putative sterol-sensing domain is identical to those of 3-hydroxy-3-methylglutaryl-CoA reductase and sterol regulatory element binding protein cleavage-activating protein. *J. Biol. Chem.* ***275***, 24367–24374.

54. Infante, R. E. *et al.* (**2008**) Purified NPC1 protein. I. Binding of cholesterol and oxysterols to a 1278-amino acid membrane protein. *J. Biol. Chem.* ***283***, 1052–1063.

55. Infante, R. E. *et al.* (**2008**) Purified NPC1 protein: II. Localization of sterol binding to a 240-amino acid soluble luminal loop. *J. Biol. Chem.* ***283***, 1064–1075.

56. Kwon, H. J. *et al.* (**2009**) Structure of N-terminal domain of NPC1 reveals distinct subdomains for binding and transfer of cholesterol. *Cell* ***137***, 1213–1224.

57. Millat, G. *et al.* (**2001**) Niemann-Pick C1 Disease: Correlations between NPC1 Mutations, Levels of NPC1 Protein, and Phenotypes Emphasize the Functional Significance of the Putative Sterol-Sensing Domain and of the Cysteine-Rich Luminal Loop. *Am. J. Hum. Genet.* ***68***, 1373.

58. Greer, W. L. *et al.* (**1999**) Mutations in NPC1 Highlight a Conserved NPC1-Specific Cysteine-Rich Domain. *Am. J. Hum. Genet.* ***65***, 1252.

59. Li, X. *et al.* (**2016**) Structure of human Niemann-Pick C1 protein. *Proc. Natl. Acad. Sci. U. S. A.* ***113***, 8212–8217.

60. Infante, R. E. *et al.* (**2008**) NPC2 facilitates bidirectional transfer of cholesterol between NPC1 and lipid bilayers, a step in cholesterol egress from lysosomes. *Proc. Natl. Acad. Sci. U. S. A.* ***105***, 15287–15292.

61. Scott, C. & Ioannou, Y. A. (**2004**) The NPC1 protein: structure implies function. *Biochim. Biophys. Acta - Mol. Cell Biol. Lipids* ***1685***, 8–13.

62. Schneede, A. *et al.* (**2011**) Role for LAMP-2 in endosomal cholesterol transport. *J. Cell. Mol. Med.* ***15***, 280–295.

63. Heybrock, S. *et al.* (**2019**) Lysosomal integral membrane protein-2 (LIMP-2/SCARB2) is involved in lysosomal cholesterol export. *Nat. Commun. 2019 101* ***10***, 1–12.

64. Chu, T. T. *et al.* (**2021**) Tonic prime-boost of STING signalling mediates Niemann-Pick disease type C. *Nature* ***596***, 570–575.

65. Rus, A. A. *et al.* (**2023**) NPC1 plays a role in the trafficking of specific cargo to melanosomes. *J. Biol. Chem.* ***299***, 105024.

66. Weng, Y. *et al.* (**2022**) Inhibition of the Niemann-Pick C1 protein is a conserved feature of multiple strains of pathogenic mycobacteria. *Nat. Commun. 2022 131* ***13***, 1–16.

67. García-Dorival, I. *et al.* (**2021**) Identification of Niemann-Pick C1 protein as a potential novel SARS-CoV-2 intracellular target. *Antiviral Res.* ***194***, 105167.

68. Sabino, C. *et al.* (**2019**) Bafilomycin A1 and U18666A Efficiently Impair ZIKV Infection. *Viruses* ***11***,.

69. Jupatanakul, N., Sim, S. & Dimopoulos, G. (**2014**) Aedes aegypti ML and Niemann-Pick type C family members are agonists of dengue virus infection. *Dev. Comp. Immunol.* ***43***, 1.

70. Osuna-Ramos, J. F., Reyes-Ruiz, J. M. & del Ángel, R. M. (**2018**) The Role of Host Cholesterol During Flavivirus Infection. *Front. Cell. Infect. Microbiol.* ***8***, 388.

71. Carette, J. E. *et al.* (**2011**) Ebola virus entry requires the cholesterol transporter Niemann-Pick C1. *Nature* ***477***, 340.

72. Côté, M. *et al.* (**2011**) Small molecule inhibitors reveal Niemann-Pick C1 is essential for ebolavirus infection. *Nature* ***477***, 344.

73. Wichit, S. *et al.* (**2017**) Imipramine Inhibits Chikungunya Virus Replication in Human Skin Fibroblasts through Interference with Intracellular Cholesterol Trafficking. *Sci. Rep.* **7**,.

74. Stoeck, I. K. *et al.* (**2018**) Hepatitis C Virus Replication Depends on Endosomal Cholesterol Homeostasis. *J. Virol.* ***92***, 1196–1213.

75. Tang, Y., Leao, I. C., Coleman, E. M., Broughton, R. S. & Hildreth, J. E. K. (**2009**) Deficiency of Niemann-Pick Type C-1 Protein Impairs Release of Human Immunodeficiency Virus Type 1 and Results in Gag Accumulation in Late

Endosomal/Lysosomal Compartments. *J. Virol.* ***83***, 7982.

76. Stenson, P. D. *et al.* (**2003**) Human Gene Mutation Database (HGMD): 2003 update. *Hum. Mutat.* ***21***, 577–581.

77. Anthony, K. & Gallo, J. M. (**2010**) Aberrant RNA processing events in neurological disorders. *Brain Res.* ***1338***, 67–77.

78. Paron, F., Dardis, A. & Buratti, E. (**2020**) Pre-mRNA splicing defects and RNA binding protein involvement in Niemann Pick type C disease. *J. Biotechnol.* ***318***, 20–30.

79. Pagani, F., Buratti, E., Stuani, C. & Baralle, F. E. (**2003**) Missense, nonsense, and neutral mutations define juxtaposed regulatory elements of splicing in cystic fibrosis transmembrane regulator exon 9. *J. Biol. Chem.* ***278***, 26580–26588.

80. Bychkov, I. *et al.* (**2021**) Additive effect of frequent polymorphism and rare synonymous variant alters splicing in twin patients with Niemann-Pick disease type C. *Eur. J. Hum. Genet. 2021 301* ***30***, 133–136.

81. Schieweck, R., Ninkovic, J. & Kiebler, M. A. (**2021**) RNA-binding proteins balance brain function in health and disease. *Physiol. Rev.* ***101***, 1309–1370.

82. Brogden, G. *et al.* (**2020**) Different Trafficking Phenotypes of Niemann-Pick C1 Gene Mutations Correlate with Various Alterations in Lipid Storage, Membrane Composition and Miglustat Amenability. *Int. J. Mol. Sci.* ***21***, 2101.

83. Schultz, M. L. *et al.* (**2018**) Coordinate regulation of mutant NPC1 degradation by selective ER autophagy and MARCH6-dependent ERAD. *Nat. Commun.* ***9***,.

84. Shammas, H., Kuech, E. M., Rizk, S., Das, A. M. & Naim, H. Y. (**2019**) Different Niemann-Pick C1 Genotypes Generate Protein Phenotypes that Vary in their Intracellular Processing, Trafficking and Localization. *Sci. Rep.* ***9***,.

85. Millat, G. *et al.* (**1999**) Niemann-Pick C1 Disease: The I1061T Substitution Is a Frequent Mutant Allele in Patients of Western European Descent and Correlates with a Classic Juvenile Phenotype. *Am. J. Hum. Genet.* ***65***, 1321.

86. Ribeiro, I. *et al.* (**2001**) Niemann-Pick type C disease: NPC1 mutations associated with severe and mild cellular cholesterol trafficking alterations. *Hum. Genet.* ***109***, 24–32.

87. Kubaski, F. *et al.* (**2022**) Experience of the NPC Brazil Network with a

Comprehensive Program for the Screening and Diagnosis of Niemann-Pick Disease Type C. *Int. J. Neonatal Screen.* ***8***,.

88. Guatibonza Moreno, P. *et al.* (**2023**) At a glance: the largest Niemann-Pick type C1 cohort with 602 patients diagnosed over 15 years. *Eur. J. Hum. Genet.* doi:10.1038/S41431-023-01408-7.

89. Gelsthorpe, M. E. *et al.* (**2008**) Niemann-Pick Type C1 I1061T Mutant Encodes a Functional Protein That Is Selected for Endoplasmic Reticulum-associated Degradation Due to Protein Misfolding. *J. Biol. Chem.* ***283***, 8229.

90. Mu, T. W., Fowler, D. M. & Kelly, J. W. (**2008**) Partial Restoration of Mutant Enzyme Homeostasis in Three Distinct Lysosomal Storage Disease Cell Lines by Altering Calcium Homeostasis. *PLoS Biol.* ***6***, 0253–0265.

91. Ong, D. S. T., Mu, T. W., Palmer, A. E. & Kelly, J. W. (**2010**) Endoplasmic Reticulum Ca2+ Increases Enhance Mutant Glucocerebrosidase Proteostasis. *Nat. Chem. Biol.* ***6***, 424.

92. Wang, F., Agnello, G., Sotolongo, N. & Segatori, L. (**2011**) Ca2+ homeostasis modulation enhances the amenability of L444P glucosylcerebrosidase to proteostasis regulation in patient-derived fibroblasts. *ACS Chem. Biol.* ***6***, 158–168.

93. Yu, T., Chung, C., Shen, D., Xu, H. & Lieberman, A. P. (**2012**) Ryanodine receptor antagonists adapt NPC1 proteostasis to ameliorate lipid storage in Niemann–Pick type C disease fibroblasts. *Hum. Mol. Genet.* ***21***, 3205.

94. Mengel, E. *et al.* (**2021**) Efficacy and safety of arimoclomol in Niemann-Pick disease type C: Results from a double-blind, randomised, placebo-controlled, multinational phase 2/3 trial of a novel treatment. *J. Inherit. Metab. Dis.* ***44***, 1463–1480.

95. Committee for Medicinal Products for Human Use. www.ema.europa.eu/contact (2023) *MIPLYFFA - Withdrawal assessment report*.

96. Schrader, M., Godinho, L. F., Costello, J. L. & Islinger, M. (**2015**) The different facets of organelle interplay—an overview of organelle interactions. *Front. Cell Dev. Biol.* ***3***, 56.

97. Oyarzún, J. E. *et al.* (**2019**) Lysosome motility and distribution: Relevance in health and disease. *Biochim. Biophys. Acta - Mol. Basis Dis.* ***1865***, 1076–1087.

98. Rocha, N. *et al.* (**2009**) Cholesterol sensor ORP1L contacts the ER protein VAP to control Rab7-RILP-p150 Glued and late endosome positioning. *J. Cell Biol.* ***185***, 1209–1225.

99. Gerasimenko, J. V., Tepikin, A. V., Petersen, O. H. & Gerasimenko, O. V. (**1998**) Calcium uptake via endocytosis with rapid release from acidifying endosomes. *Curr. Biol.* ***8***, 1335–1338.

100. Medina, D. L. & Ballabio, A. (**2015**) Lysosomal calcium regulates autophagy. *Autophagy* ***11***, 970.

101. Medina, D. L. *et al.* (**2015**) Lysosomal calcium signaling regulates autophagy via calcineurin and TFEB. *Nat. Cell Biol.* ***17***, 288.

102. Lloyd-Evans, E. *et al.* (**2008**) Niemann-Pick disease type C1 is a sphingosine storage disease that causes deregulation of lysosomal calcium. *Nat. Med.* ***14***, 1247–1255.

103. Xu, M. *et al.* (**2012**) δ-Tocopherol reduces lipid accumulation in Niemann-Pick type C1 and Wolman cholesterol storage disorders. *J. Biol. Chem.* ***287***, 39349–39360.

104. Visentin, S. *et al.* (**2013**) The stimulation of adenosine A2A receptors ameliorates the pathological phenotype of fibroblasts from Niemann-Pick type C patients. *J. Neurosci.* ***33***, 15388–15393.

105. Höglinger, D. *et al.* (**2015**) Intracellular sphingosine releases calcium from lysosomes. *Elife* ***4***,.

106. Newton, J., Milstien, S. & Spiegel, S. (**2018**) Niemann-Pick type C disease: The atypical sphingolipidosis. *Adv. Biol. Regul.* ***70***, 82.

107. Wheeler, S. & Sillence, D. J. (**2020**) Niemann–Pick type C disease: cellular pathology and pharmacotherapy. *J. Neurochem.* ***153***, 674–692.

108. Sun, H. *et al.* (**2021**) Next-Generation Sequencing Technologies and Neurogenetic Diseases. *Life* ***11***,.

109. Satam, H. *et al.* (**2023**) Next-Generation Sequencing Technology: Current Trends and Advancements. *Biol. 2023, Vol. 12, Page 997* ***12***, 997.

110. Piñero, J., Berenstein, A., Gonzalez-Perez, A., Chernomoretz, A. & Furlong, L. I. (**2016**) Uncovering disease mechanisms through network biology in the era of Next Generation Sequencing. *Sci. Reports 2016 61* ***6***, 1–12.

111. Pallottini, V. & Pfrieger, F. W. (**2020**) Understanding and Treating Niemann–Pick Type C Disease: Models Matter. *Int. J. Mol. Sci. 2020, Vol. 21, Page 8979* ***21***, 8979.

112. Schultz, M. L. *et al.* (**2022**) Species-specific differences in NPC1 protein trafficking govern therapeutic response in Niemann-Pick type C disease. *JCI insight* ***7***,.

113. Sloan, H. R., Uhlendorf, B. W., Kanfer, J. N., Brady, R. O. & Fredrickson, D. S. (**1969**) Deficiency of sphingomyelin-cleaving enzyme activity in tissue cultures derived from patients with Niemann-Pick disease. *Biochem. Biophys. Res. Commun.* ***34***, 582–588.

114. Ray, B., Chopra, N., Long, J. M. & Lahiri, D. K. (**2014**) Human primary mixed brain cultures: Preparation, differentiation, characterization and application to neuroscience research. *Mol. Brain* ***7***, 1–15.

115. Kobold, S., Guhr, A., Kurtz, A. & Löser, P. (**2015**) Human Embryonic and Induced Pluripotent Stem Cell Research Trends: Complementation and Diversification of the Field. *Stem Cell Reports* ***4***, 914.

116. Yamanaka, S. (**2020**) Pluripotent Stem Cell-Based Cell Therapy-Promise and Challenges. *Cell Stem Cell* ***27***, 523–531.

117. Castellano, B. M. *et al.* (**2017**) Lysosomal cholesterol activates mTORC1 via an SLC38A9-Niemann-Pick C1 signaling complex. *Science* ***355***, 1306–1311.

118. Vanharanta, L. *et al.* (**2020**) High-content imaging and structure-based predictions reveal functional differences between Niemann-Pick C1 variants. *Traffic* ***21***, 386–397.

119. Bartz, F. *et al.* (**2009**) Identification of cholesterol-regulating genes by targeted RNAi screening. *Cell Metab.* ***10***, 63–75.

120. Dunn, K. C., Aotaki-Keen, A. E., Putkey, F. R. & Hjelmeland, L. M. (**1996**) ARPE-19, a human retinal pigment epithelial cell line with differentiated properties. *Exp. Eye Res.* ***62***, 155–170.

121. Hwang, A. R., Park, S. & Woo, C. H. (**2023**) Lyso-globotriaosylsphingosine induces endothelial dysfunction via autophagy-dependent regulation of necroptosis. *Korean J. Physiol. Pharmacol.* ***27***, 231–240.

122. Li, J. K. *et al.* (**2022**) Proteomic analysis of s-acylated proteins in human retinal pigment epithelial cells and the role of palmitoylation of Niemann-Pick type C1

protein in cholesterol transport. *Front. Aging Neurosci.* ***14***, 965943.

123. Pastore, R., Ballabio, A. (supervisor), Parenti, G. (internal supervisor) & Platt, F. M. (external supervisor). (Università Degli Studi di Milano, 2019). Development of ARPE19 Cellular Models of Niemann-Pick Disease Type C1 and C2 and their Application to High Content Drug Screening. doi:10.13130/pastore-raffaele_phd2019-01-28.

124. Wassif, C. A. *et al.* (**2016**) High incidence of unrecognized visceral/neurological late-onset Niemann-Pick disease, type C1, predicted by analysis of massively parallel sequencing data sets. *Genet. Med.* ***18***, 41–48.

125. Imrie, J., Heptinstall, L., Knight, S. & Strong, K. (**2015**) Observational cohort study of the natural history of Niemann-Pick disease type C in the UK: a 5-year update from the UK clinical database. *BMC Neurol.* ***15***,.

126. Las Heras, M. *et al.* (**2023**) Understanding the phenotypic variability in Niemann-Pick disease type C (NPC): a need for precision medicine. *NPJ genomic Med.* ***8***,.

127. Patterson, M. C. *et al.* (**2017**) Recommendations for the detection and diagnosis of Niemann-Pick disease type C: An update. *Neurol. Clin. Pract.* ***7***, 499.

128. Kruth, H. S. *et al.* (**1986**) Type C Niemann-Pick disease. Abnormal metabolism of low density lipoprotein in homozygous and heterozygous fibroblasts. *J. Biol. Chem.* ***261***, 16769–16774.

129. Wraith, J. E. *et al.* (**2009**) Recommendations on the diagnosis and management of Niemann-Pick disease type C. *Mol. Genet. Metab.* ***98***, 152–165.

130. Degtyareva, A. V. *et al.* (**2019**) Oxysterol/chitotriosidase based selective screening for Niemann-Pick type C in infantile cholestasis syndrome patients. *BMC Med. Genet.* ***20***,.

131. Porter, F. D. *et al.* (**2010**) Cholesterol oxidation products are sensitive and specific blood-based biomarkers for Niemann-Pick C1 disease. *Sci. Transl. Med.* ***2***, 56ra81.

132. Zhang, H. *et al.* (**2014**) Diagnosis of Niemann-Pick disease type C with 7-ketocholesterol screening followed by NPC1/NPC2 gene mutation confirmation in Chinese patients. *Orphanet J. Rare Dis.* ***9***, 82.

133. Giese, A. K. *et al.* (**2015**) A novel, highly sensitive and specific biomarker for Niemann-Pick type C1 disease. *Orphanet J. Rare Dis.* ***10***,.

134. Sidhu, R. *et al.* (**2020**) Application of N-Palmitoyl-O-Phosphocholineserine for Diagnosis and Assessment of Response to Treatment in Niemann-Pick Type C disease. *Mol. Genet. Metab.* ***129***, 292.

135. Mazzacuva, F. *et al.* (**2016**) Identification of novel bile acids as biomarkers for the early diagnosis of Niemann-Pick C disease. *Febs Lett.* ***590***, 1651.

136. Jiang, X. *et al.* (**2016**) Development of a Bile Acid-Based Newborn Screen for Niemann-Pick C Disease. *Sci. Transl. Med.* ***8***, 337ra63.

137. Vanier, M. T. *et al.* (**2016**) Diagnostic tests for Niemann-Pick disease type C (NP-C): A critical review. *Mol. Genet. Metab.* ***118***, 244–254.

138. Hassan, S., Sidransky, E. & Tayebi, N. (**2017**) The role of epigenetics in lysosomal storage disorders: Uncharted territory. *Mol. Genet. Metab.* ***122***, 10–18.

139. Bartel, D. P. (**2004**) MicroRNAs: Genomics, Biogenesis, Mechanism, and Function. *Cell* ***116***, 281–297.

140. Esteller, M. (**2011**) Non-coding RNAs in human disease. *Nat. Rev. Genet. 2011 1212* ***12***, 861–874.

141. Ozsait, B. *et al.* (**2010**) Niemann-Pick type C fibroblasts have a distinct microRNA profile related to lipid metabolism and certain cellular components. *Biochem. Biophys. Res. Commun.* ***403***, 316–321.

142. Pergande, M. R., Cougnoux, A., Rathnayake, R. A. C., Porter, F. D. & Cologna, S. M. (**2019**) Differential Proteomics Reveals miR-155 as a Novel Indicator of Liver and Spleen Pathology in the Symptomatic Niemann-Pick Disease, Type C1 Mouse Model. *Molecules* ***24***,.

143. Cortez, M. A. *et al.* (**2011**) MicroRNAs in body fluids--the mix of hormones and biomarkers. *Nat. Rev. Clin. Oncol.* ***8***, 467–477.

144. Creemers, E. E., Tijsen, A. J. & Pinto, Y. M. (**2012**) Circulating MicroRNAs - Novel Biomarkers and Extracellular Communicators in Cardiovascular Disease. *Circ. Res.* ***110***, 483–495.

145. Chen, X. *et al.* (**2008**) Characterization of microRNAs in serum: a novel class of biomarkers for diagnosis of cancer and other diseases. *Cell Res. 2008 1810* ***18***, 997–1006.

146. Wu, Y. *et al.* (**2021**) Circulating microRNAs: Biomarkers of disease. *Clin. Chim.*

Acta ***516***, 46–54.

147. La Cognata, V., Guarnaccia, M., Polizzi, A., Ruggieri, M. & Cavallaro, S. (**2020**) Highlights on Genomics Applications for Lysosomal Storage Diseases. *Cells 2020, Vol. 9, Page 1902* ***9***, 1902.

148. Siebert, M. *et al.* (**2014**) Identification of miRNAs that modulate glucocerebrosidase activity in Gaucher disease cells. *RNA Biol.* ***11***, 1291–1300.

149. Ginns, E. I. *et al.* (**2014**) Neuroinflammation and α-synuclein accumulation in response to glucocerebrosidase deficiency are accompanied by synaptic dysfunction. *Mol. Genet. Metab.* ***111***, 152–162.

150. Tarallo, A. *et al.* (**2019**) microRNAs as biomarkers in Pompe disease. *Genet. Med.* ***21***, 591–600.

151. Carrasco-Rozas, A. *et al.* (**2019**) Identification of serum microRNAs as potential biomarkers in Pompe disease. *Ann. Clin. Transl. Neurol.* ***6***, 1214–1224.

152. Cammarata, G. *et al.* (**2018**) A pilot study of circulating microRNAs as potential biomarkers of Fabry disease. *Oncotarget* ***9***, 27333–27345.

153. Encarnação, M. *et al.* (**2020**) NPC1 silent variant induces skipping of exon 11 (p.V562V) and unfolded protein response was found in a specific Niemann-Pick type C patient. *Mol. Genet. genomic Med.* ***8***,.

154. Fernandez-Valero, E. M. *et al.* (**2005**) Identification of 25 new mutations in 40 unrelated Spanish Niemann-Pick type C patients: genotype-phenotype correlations. *Clin. Genet.* ***68***, 245–254.

155. Rodríguez-Pascau, L., Coll, M. J., Vilageliu, L. & Grinberg, D. (**2009**) Antisense oligonucleotide treatment for a pseudoexon-generating mutation in the NPC1 gene causing Niemann-Pick type C disease. *Hum. Mutat.* ***30***,.

156. Aparicio-Puerta, E. *et al.* (**2022**) sRNAbench and sRNAtoolbox 2022 update: accurate miRNA and sncRNA profiling for model and non-model organisms. *Nucleic Acids Res.* ***50***, W710–W717.

157. Love, M. I., Huber, W. & Anders, S. (**2014**) Moderated estimation of fold change and dispersion for RNA-seq data with DESeq2. *Genome Biol.* ***15***, 1–21.

158. Livak, K. J. & Schmittgen, T. D. (**2001**) Analysis of Relative Gene Expression Data Using Real-Time Quantitative PCR and the 2−ΔΔCT Method. *Methods* ***25***, 402–

408.

159. Donati, S., Ciuffi, S. & Brandi, M. L. (**2019**) Human Circulating miRNAs Real-time qRT-PCR-based Analysis: An Overview of Endogenous Reference Genes Used for Data Normalization. *Int. J. Mol. Sci. 2019, Vol. 20, Page 4353* ***20***, 4353.

160. Wang, G. *et al.* (**2010**) Serum and urinary cell-free MiR-146a and MiR-155 in patients with systemic lupus erythematosus. *J. Rheumatol.* ***37***, 2516–2522.

161. Bauer, P. *et al.* (**2002**) NPC1: Complete genomic sequence, mutation analysis, and characterization of haplotypes. *Hum. Mutat.* ***19***, 30–38.

162. Pipalia, N. H. *et al.* (**2017**) Histone deacetylase inhibitors correct the cholesterol storage defect in most Niemann-Pick C1 mutant cells. *J. Lipid Res.* ***58***, 695–708.

163. Tercero, J. A., Espinosa, J. C., Lacalle, R. A. & Jiménez, A. (**1996**) The biosynthetic pathway of the aminonucleoside antibiotic puromycin, as deduced from the molecular analysis of the pur cluster of Streptomyces alboniger. *J. Biol. Chem.* ***271***, 1579–1590.

164. Leung, E. K. Y., Suslov, N., Tuttle, N., Sengupta, R. & Piccirilli, J. A. (**2011**) The mechanism of peptidyl transfer catalysis by the ribosome. *Annu. Rev. Biochem.* ***80***, 527–555.

165. Vara, J. A., Portela, A., Ortìn, J. & Jimènez, A. (**1986**) Expression in mammalian cells of a gene from Streptomyces alboniger conferring puromycin resistance. *Nucleic Acids Res.* ***14***, 4617–4624.

166. Caputo, A. T. *et al.* (**2021**) Structure-guided selection of puromycin N-acetyltransferase mutants with enhanced selection stringency for deriving mammalian cell lines expressing recombinant proteins. *Sci. Reports 2021 111* ***11***, 1–11.

167. Shaner, N. C. *et al.* (**2013**) A bright monomeric green fluorescent protein derived from Branchiostoma lanceolatum. *Nat. Methods 2013 105* ***10***, 407–409.

168. Schultz, M. L., Krus, K. L. & Lieberman, A. P. (**2016**) Lysosome and endoplasmic reticulum quality control pathways in Niemann-Pick type C disease. *Brain Res.* ***1649***, 181–188.

169. Maxfield, F. R. & Wüstner, D. (**2012**) Analysis of cholesterol trafficking with fluorescent probes. *Methods Cell Biol.* ***108***, 367.

170. Vanier, M. T. *et al.* (**1991**) Type C Niemann-Pick disease: spectrum of phenotypic variation in disruption of intracellular LDL-derived cholesterol processing. *Biochim. Biophys. Acta* ***1096***, 328–337.

171. Eskelinen, E. L. (**2006**) Roles of LAMP-1 and LAMP-2 in lysosome biogenesis and autophagy. *Mol. Aspects Med.* ***27***, 495–502.

172. Barral, D. C. *et al.* (**2022**) Current methods to analyze lysosome morphology, positioning, motility and function. *Traffic* ***23***, 238–269.

173. Sarkar, S. *et al.* (**2013**) Impaired autophagy in the lipid storage disorder Niemann–Pick type C1 disease. *Cell Rep.* ***5***, 1302.

174. Kleinecke, S. *et al.* (**2017**) Peroxisomal dysfunctions cause lysosomal storage and axonal Kv1 channel redistribution in peripheral neuropathy. *Elife* ***6***,.

175. Pentchev, P. G. (**2004**) Niemann-Pick C research from mouse to gene. *Biochim. Biophys. Acta* ***1685***, 3–7.

176. Scerra, G. *et al.* (**2021**) Early onset effects of single substrate accumulation recapitulate major features of LSD in patient-derived lysosomes. *iScience* ***24***,.

177. Höglinger, D. *et al.* (**2019**) NPC1 regulates ER contacts with endocytic organelles to mediate cholesterol egress. *Nat. Commun. 2019 101* ***10***, 1–14.

178. Daniele, T. *et al.* (**2011**) A role for Rab7 in the movement of secretory granules in cytotoxic T lymphocytes. *Traffic* ***12***, 902–911.

179. Korolchuk, V. I. *et al.* (**2011**) Lysosomal positioning coordinates cellular nutrient responses. *Nat. Cell Biol. 2011 134* ***13***, 453–460.

180. Hong, S. & Inoki, K. (**2017**) Evaluating the mTOR Pathway in Physiological and Pharmacological Settings. *Methods Enzymol.* ***587***, 405–428.

181. Schoberer, J., Shin, Y. J., Vavra, U., Veit, C. & Strasser, R. (**2018**) Protein glycosylation in the ER. *Methods Mol. Biol.* ***1691***, 205.

182. Freeze, H. H. & Kranz, C. (**2010**) Endoglycosidase and Glycoamidase Release of N-Linked Glycans. *Curr. Protoc. Mol. Biol.* ***89***, 17.13A.1-17.13A.25.

183. Praggastis, M. *et al.* (**2015**) A Murine Niemann-Pick C1 I1061T Knock-In Model Recapitulates the Pathological Features of the Most Prevalent Human Disease Allele. *J. Neurosci.* ***35***, 8091.

184. Erwood, S. *et al.* (**2022**) Saturation variant interpretation using CRISPR prime editing. *Nat. Biotechnol. 2022 406* ***40***, 885–895.

185. Werner, G., Hagenmaier, H., Drautz, H., Baumgartner, A. & Zähner, H. (**1984**) Metabolic products of microorganisms. 224. Bafilomycins, a new group of macrolide antibiotics. Production, isolation, chemical structure and biological activity. *J. Antibiot. (Tokyo).* ***37***, 110–117.

186. Bowman, E. J., Siebers, A. & Altendorf, K. (**1988**) Bafilomycins: a class of inhibitors of membrane ATPases from microorganisms, animal cells, and plant cells. *Proc. Natl. Acad. Sci. U. S. A.* ***85***, 7972–7976.

187. Yamamoto, A. *et al.* (**1998**) Bafilomycin A1 prevents maturation of autophagic vacuoles by inhibiting fusion between autophagosomes and lysosomes in rat hepatoma cell line, H-4-II-E cells. *Cell Struct. Funct.* ***23***, 33–42.

188. Nakasone, N. *et al.* (**2014**) Endoplasmic Reticulum-associated Degradation of Niemann-Pick C1: Evidence for the Role of Heat Shock Proteins and Identification of Lysine Residues that Accept Ubiquitin. *J. Biol. Chem.* ***289***, 19714.

189. Esau, C. *et al.* (**2004**) MicroRNA-143 regulates adipocyte differentiation. *J. Biol. Chem.* ***279***, 52361–52365.

190. Sala, F. *et al.* (**2014**) MiR-143/145 deficiency protects against progression of atherosclerosis in Ldlr−/− mice. *Thromb. Haemost.* ***112***, 796.

191. Jordan, S. D. *et al.* (**2011**) Obesity-induced overexpression of miRNA-143 inhibits insulin-stimulated AKT activation and impairs glucose metabolism. *Nat. Cell Biol.* ***13***, 434–448.

192. Lin, X. T. *et al.* (**2018**) MicroRNA-143 Targets ATG2B to Inhibit Autophagy and Increase Inflammatory Responses in Crohn's Disease. *Inflamm. Bowel Dis.* ***24***, 781–791.

193. Ma, W. *et al.* (**2018**) By Targeting Atg7 MicroRNA-143 Mediates Oxidative Stress-Induced Autophagy of c-Kit+ Mouse Cardiac Progenitor Cells. *EBioMedicine* ***32***, 182–191.

194. Du, F., Feng, Y., Fang, J. & Yang, M. (**2015**) MicroRNA-143 enhances chemosensitivity of Quercetin through autophagy inhibition via target GABARAPL1 in gastric cancer cells. *Biomed. Pharmacother.* ***74***, 169–177.

195. Lin, Y. *et al.* (**2020**) miR-143 Regulates Lysosomal Enzyme Transport across the

Blood-Brain Barrier and Transforms CNS Treatment for Mucopolysaccharidosis Type I. *Mol. Ther.* ***28***, 2161.

196. Pawliński, Ł. *et al.* (**2020**) MiRNA Expression in Patients with Gaucher Disease Treated with Enzyme Replacement Therapy. *Life 2021, Vol. 11, Page 2* ***11***, 2.

197. Stirnemann, J. Ô. *et al.* (**2017**) A Review of Gaucher Disease Pathophysiology, Clinical Presentation and Treatments. *Int. J. Mol. Sci.* ***18***, 441.

198. Wada, K. *et al.* (**2022**) MiR-126-3p and MiR-199a-3p Promote Lipid Accumulation in 3T3-L1 Adipocytes via Regulating HIF-1α and C/EBPα Expression. *Shimane J. Med. Sci.* ***39***, 123–133.

199. Pencheva, N. *et al.* (**2012**) Convergent multi-miRNA Targeting of ApoE Drives LRP1/LRP8-Dependent Melanoma Metastasis and Angiogenesis. *Cell* ***151***, 1068.

200. Aranda, J. F. *et al.* (**2022**) Role of miR-199a-5p in the post-transcriptional regulation of ABCA1 in response to hypoxia in peritoneal macrophages. *Front. Cardiovasc. Med.* ***9***, 994080.

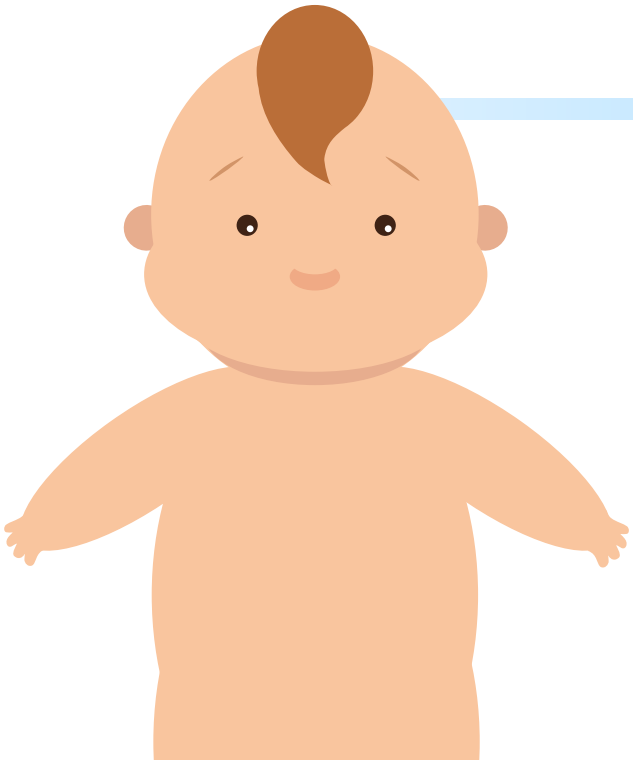
201. Aranda, J. F., Canfrán-Duque, A., Goedeke, L., Suárez, Y. & Fernández-Hernando, C. (**2015**) The miR-199-dynamin regulatory axis controls receptor-mediated endocytosis. *J. Cell Sci.* ***128***, 3197–3209.

202. Li, Z. *et al.* (**2017**) miR-199a impairs autophagy and induces cardiac hypertrophy through mTOR activation. *Cell Death Differ.* ***24***, 1205–1213.

203. Wang, Y., Luo, J., Wang, X., Yang, B. & Cui, L. (**2017**) MicroRNA-199a-5p Induced Autophagy and Inhibits the Pathogenesis of Ankylosing Spondylitis by Modulating the mTOR Signaling via Directly Targeting Ras Homolog Enriched in Brain (Rheb). *Cell. Physiol. Biochem.* ***42***, 2481–2491.

204. Ba, R. Q. *et al.* (**2020**) Effects of miR-199a on autophagy by targeting glycogen synthase kinase 3β to activate PTEN/AKT/mTOR signaling in an MPP+ in vitro model of Parkinson's disease. *Neurol. Res.* ***42***, 308–318.

Outputs



Publications in international peer-reviewed journals

REVIEW

Neurological Disease Modeling Using Pluripotent and Multipotent Stem Cells: A Key Step towards Understanding and Treating Mucopolysaccharidoses

Sofia Carvalho, Juliana Inês Santos, Luciana Moreira, Mariana Gonçalves, Hugo David, Liliana Matos, Marisa Encarnação, Sandra Alves & Maria Francisca Coutinho

Published in *Biomedicines* (21 April **2023**), 11(4):123
doi: 10.3390/biomedicines11041234

REVIEW

MicroRNA Profile, Putative Diagnostic Biomarkers and RNA-Based Therapies in the Inherited Lipid Storage Disease Niemann-Pick Type C

Marisa Encarnação, Hugo David, Maria Francisca Coutinho, Luciana Moreira & Sandra Alves

Published in *Biomedicines* (23 September **2023**), 11(10):2615
doi: 10.3390/biomedicines11102615

REVIEW

Challenges on the Definitive Diagnosis of Niemann-Pick type C – Leaky Variants and Alternative Transcripts

Marisa Encarnação, Isaura Ribeiro, Hugo David, Maria Francisca Coutinho, Dulce Quelhas & Sandra Alves

Published in *Genes* (25 October **2023**), 14(11):1990
doi: 10.3390/genes14111990

Communications in scientific conferences

ORAL COMMUNICATION

Help comes from unexpected places: How a tiny fairy and a tropical fish may help us model mucopolysccharidoses

M.F. Coutinho, S. Carvalho, L. Moreira, J. I. Santos, P. Gaspar, M. Gonçalves, L. Matos, H. David, M. Encarnação, D. Ribeiro, A. J. Duarte, O. Amaral, H. Rocha, L. Diogo, S. Ferreira, C. Santos, E. Martins, T. Neuparth, J. Soares, M. Ribeiro, B. Ribeiro Pinho, N. Oliveira, J. Ascenção Oliveira, M. Prata, M. Santos & S. Alves

Presented at the *19th International Symposium of the Portuguese Society for Metabolic Disorders* (30 March **2023**)

ORAL COMMUNICATION

Lost (and found) in Translation: the Potential of microRNAs

Hugo David, Isaura Ribeiro, Luís Vieira, Catarina Carneiro Silva, Maria Francisca Coutinho, Juliana Inês Santos, Esmeralda Martins, Anthony H. Futerman, Dulce Quelhas, Sandra Alves & Marisa Encarnação

Presented at the *VI CECA Meeting* (31 March **2023**)

ORAL COMMUNICATION

Inherited metabolic diseases in humans and in animals: mechanisms and therapies

Ana Joana Duarte, Diogo Ribeiro, Hugo David, Juliana Inês Santos, Liliana Matos, Luciana Moreira, Maria Francisca Coutinho, Mariana Gonçalves, Marisa Encarnação, Paula Figueira, Olga Amaral, Sofia Carvalho & Sandra Alves

Presented at the *VI CECA Meeting* (31 March **2023**)

ORAL COMMUNICATION

Gene-edited zebrafish: a promising animal model for Lysosomal Storage Disorders and beyond

Luciana Moreira, Maria Francisca Coutinho, Olga Martinez, Teresa Neuparth, Marta Ribeiro, Brigida Pinho, Nuno Oliveira, Paulo Gaspar, Sofia Carvalho, Juliana Santos, Mariana Gonçalves, Liliana Matos, Hugo David, Marisa Encarnação, Jorge Oliveira, Miguel Santos & Sandra Alves

Presented at the *VI CECA Meeting* (31 March **2023**)

ORAL COMMUNICATION

No Place Like the Lysosome: a Study on NPC1 Protein Trafficking

Hugo David, Isaura Ribeiro, Sofia Carvalho, Maria Francisca Coutinho, Dulce Quelhas, Sandra Alves & Marisa Encarnação

Presented at the *2nd Meeting of the AL4AnimalS* (12 April **2023**)

POSTER PRESENTATION

RNARARE – understanding RNA in Niemann-Pick type C disease

Marisa Encarnação, Hugo David, Isaura Ribeiro, Luís Vieira, Catarina Carneiro Silva, Maria Francisca Coutinho, Esmeralda Martins, Anthony H. Futerman, Dulce Quelhas & Sandra Alves

Presented at the *Lysosomal Diseases Gordon Research Conference* (14 -19 May **2023**)

POSTER PRESENTATION

Exosomal microRNAs as Possible Biomarkers for a Rare Disease Affecting Lipids

Marisa Encarnação, Hugo David, Isaura Ribeiro, Luís Vieira, Catarina Carneiro Silva, Esmeralda Martins, Maria Teresa Cardoso, Anthony H. Futerman, Dulce Quelhas & Sandra Alves

Presented at the *2nd Meeting of the Portuguese Network on Extracellular Vesicles* (22 -23 June **2023**)

ORAL COMMUNICATION

Tangled: a tale about NPC1 Protein Trafficking

Hugo David, Isaura Ribeiro, Maria Teresa Cardoso, Paulo Castro Chaves, Mariana Pintalhão, Esmeralda Martins, Luís Vieira, Catarina Carneiro Silva, Dulce Quelhas, Frances M. Platt, Andrea Ballabio, Sandra Alves & Marisa Encarnação

Presented at the *AL4AnimalS.biotech Meeting* (20 October **2023**)

Organization of scientific events

SEMINAR

CRISPR: Applications to Study Human Genetic Diseases

Marisa Encarnação, Hugo David & Rodrigo Leite de Oliveira

Member of the *Organizing Comittee* (22 November **2022**)

CONFERENCE

VI CECA Meeting

Hugo David, Mariana Gonçalves, Sandra Alves & José Manuel Costa

Member of the *Executive Comittee* (31 March – 1 April **2023**)

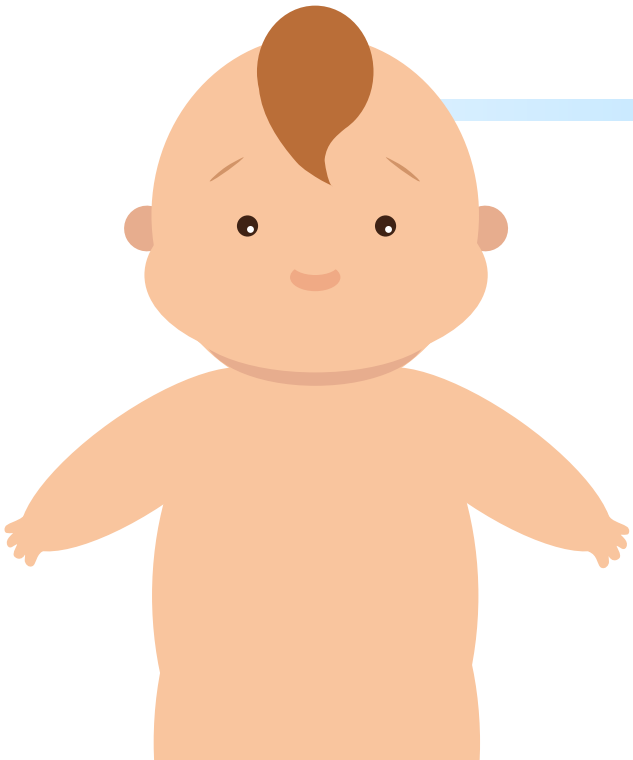
Other activities

FLYER

RNARARE Project

Hugo David, Sandra Alves & Marisa Encarnação

Designer of the *Flyer* (10 February **2023**)



Attachments

Attachment 1

MicroRNA Profile, Putative Diagnostic Biomarkers and RNA-Based Therapies in the Inherited Lipid Storage Disease Niemann-Pick Type C

Marisa Encarnação, Hugo David, Maria Francisca Coutinho, Luciana Moreira & Sandra Alves

Review published in *Biomedicines*, **2023**

biomedicines

MDPI

Review

MicroRNA Profile, Putative Diagnostic Biomarkers and RNA-Based Therapies in the Inherited Lipid Storage Disease Niemann-Pick Type C

Marisa Encarnação [1,2,3,*], Hugo David [1,2,3,4], Maria Francisca Coutinho [1,2,3], Luciana Moreira [1,2,3] and Sandra Alves [1,2,3,*]

[1] Research and Development Unit, Department of Human Genetics, National Institute of Health Doutor Ricardo Jorge, INSA I.P., Rua Alexandre Herculano 321, 4000-055 Porto, Portugal; hugo.david@insa.min-saude.pt (H.D.); francisca.coutinho@insa.min-saude.pt (M.F.C.); luciana.moreira@insa.min-saude.pt (L.M.)
[2] Center for the Study of Animal Science-Instituto de Ciências, Tecnologias e Agroambiente da Universidade do Porto, CECA-ICETA, University of Porto, Praça Gomes Teixeira, Apartado 55142, 4051-401 Porto, Portugal
[3] Associate Laboratory for Animal and Veterinary Sciences, AL4AnimalS, Faculdade de Medicina Veterinária Avenida da Universidade Técnica, 1300-477 Lisboa, Portugal
[4] Biology Department, Faculty of Sciences, University of Porto, Rua do Campo Alegre, 4169-007 Porto, Portugal
* Correspondence: marisa.encarnacao@insa.min-saude.pt (M.E.); sandra.alves@insa.min-saude.pt (S.A.)

Abstract: Lipids are essential for cellular function and are tightly controlled at the transcriptional and post-transcriptional levels. Dysregulation of these pathways is associated with vascular diseases, diabetes, cancer, and several inherited metabolic disorders. MicroRNAs (miRNAs), in particular, are a family of post-transcriptional gene repressors associated with the regulation of many genes that encode proteins involved in multiple lipid metabolism pathways, thereby influencing their homeostasis. Thus, this class of non-coding RNAs (ncRNAs) has emerged as a promising therapeutic target for the treatment of lipid-related metabolic alterations. Most of these miRNAs act at an intracellular level, but in the past few years, a role for miRNAs as intercellular signaling molecules has also been uncovered since they can be transported in bodily fluids and used as potential biomarkers of lipid metabolic alterations. In this review, we point out the current knowledge on the miRNA signature in a lysosomal storage disorder associated with lipid dysfunction, Niemann-Pick type C, and discuss the potential use of miRNAs as biomarkers and therapeutic targets for RNA-based therapies.

Keywords: microRNA; lipid storage disorders; metabolism; cholesterol trafficking; biomarkers; Niemann-Pick type C; RNA-based therapies

check for updates

Citation: Encarnação, M.; David, H.; Coutinho, M.F.; Moreira, L.; Alves, S. MicroRNA Profile, Putative Diagnostic Biomarkers and RNA-Based Therapies in the Inherited Lipid Storage Disease Niemann-Pick Type C. *Biomedicines* **2023**, *11*, 2615. https://doi.org/10.3390/biomedicines11102615

Academic Editors: Joan Carles Escolà-Gil and Noemí Rotllan

Received: 22 August 2023
Revised: 14 September 2023
Accepted: 21 September 2023
Published: 23 September 2023

Copyright: © 2023 by the authors. Licensee MDPI, Basel, Switzerland. This article is an open access article distributed under the terms and conditions of the Creative Commons Attribution (CC BY) license (https://creativecommons.org/licenses/by/4.0/).

1. Introduction

Lipids are key molecules not only for cellular membrane integrity and tissue physiology but also for energy storage and signaling. Phospholipids, glycolipids, and cholesterol constitute the major kinds of membrane lipids [1], and detrimental changes in lipid metabolism contribute to a variety of metabolic disorders, such as diabetes, obesity, liver disease, and atherosclerosis. Less frequent diseases related to lipid dysfunction include a subgroup of lysosomal storage disorders (LSDs). Lysosomal lipid storage disorders are rare inherited metabolic diseases that, among other mechanisms, cause the dysregulation of lipid metabolism and the accumulation of a broad range of lipids inside lysosomes, resulting in cellular toxicity [2–4]. Neurons are particularly sensitive to lipid accumulation, which leads to stunted brain development and neurodegeneration [5]. Over time, this excessive storage of fats can cause permanent cellular and tissue damage in the peripheral nervous system, liver, spleen, and bone marrow. Many of these monogenic diseases are fatal at a young age, and treatment options are limited [6]. The diagnostic timeline is generally very prolonged due to phenotypic overlapping and clinical heterogeneity [7–10],

which may happen even in monozygotic twins [11]. Furthermore, response to therapy, when existing, can be very variable among patients with the same genotype and even within the same family. That is why the traditional monogenic view may not be enough to explain LSD pathophysiology, and classical genotype/phenotype correlations may not be as straightforward as previously thought.

Recent genomic approaches have contributed to the understanding of the complexity and clinical variability observed in this group of monogenic disorders, namely epigenetic studies [12–16]. Overall, the field of epigenetics is gathering momentum, and correlating epigenetic changes with clinical parameters is a commonly used approach these days. Among the broad field of epigenetics, microRNA (miRNA) profiling holds great promise to identify biomarkers that correlate with disease severity and assist in monitoring disease progression and the effectiveness of therapies [13]. Ultimately, miRNAs can also be the target of RNA-based therapies.

miRNAs are a class of highly conserved [17–19] single-stranded non-coding RNA (ncRNA) molecules with 20–22 nucleotides. They direct the post-transcriptional regulation of target messenger RNAs (mRNAs) in diverse eukaryotic lineages [18], fine-tuning their levels. Each miRNA can target multiple mRNAs that contain the cognate miRNA-binding site, thus being able to regulate multiple cellular functions involved in disease development and progression—including metabolism [20]. Similarly, each single miRNA can target multiple effectors of pathways in a functional gene network. In most cases, miRNAs suppress gene expression by interacting with the 3′ untranslated region (UTR) of target mRNAs and repress protein production by destabilizing the mRNA and via translational silencing [21,22]. Although most miRNAs act in the tissue where they are produced, some miRNAs can also be secreted from cells into the circulatory system [23]. Those circulating miRNAs are disease-specific miRNAs that may also contribute to the development of precision treatments. In rare diseases, however, these studies have been mostly underexploited. Some recent reports related to changes in miRNA expression and their consequences on LSD physiopathology have been described for Gaucher (type I, MIM #230800) [24] and Fabry diseases (MIM #301500) [25]. Here, we summarize the current knowledge of the miRNA profile of another lipid LSD—Niemann-Pick type C (NPC, MIM #257220)—and discuss the identification of dysregulated miRNAs in NPC patients that correlate with their high clinical heterogeneity and their potential use as potential diagnostic and/or prognostic biomarkers for NPC. We end on a brief note regarding the promising emerging ncRNA therapeutic approaches.

2. MicroRNA (miRNA) Biogenesis

The biogenesis of miRNAs can be classified into canonical and non-canonical pathways [22]. Overall, miRNA biosynthesis pathways are under tight temporal and spatial control, and their dysregulation is associated with many human diseases [26].

Currently, there are 576 *bona fide* miRNA genes annotated in the human genome [27,28], with a significant proportion exhibiting non-ubiquitous, cell type-specific expression patterns [29]. These genes range from independent transcription units (intergenic miRNAs) to intron-contained, protein-coding gene-associated genomic *loci* (intragenic miRNAs). In humans, most miRNAs are intragenic [30] and located within introns [31], often being functionally connected to their host genes as a gene network [32].

The canonical biogenesis of miRNAs, depicted in Figure 1, begins in the nucleus, where both intergenic and intragenic miRNAs are transcribed by RNA polymerase II into long primary miRNA transcripts (pri-miRNAs) [33] before being cleaved by the Drosha ribonuclease (RNase) III enzyme and its interacting protein DGCR8, to generate a hairpin-structure where miRNAs are embedded (pre-miRNA). This molecule is then exported to the cytoplasm via the Exportin5 (XPO-5)-RanGTP system [26], where it is then cleaved by the Dicer RNase III enzyme and its interacting protein TRBP, releasing a ~22 nt mature miRNA duplex (miRNA-3p/miRNA-5p), which is loaded onto a member of the Argonaute (AGO) protein family to form the RNA-induced silencing complex

(RISC) [26,34,35]. Typically, one particular strand of the miRNA duplex is favored by the RISC, while the other is ejected from the complex and degraded [26,36,37]. miRNAs often exert their effect by downregulating mRNA levels, but they may also directly repress the translation of hundreds of genes [38–40], fine-tuning protein synthesis. One such example is their ability to target components of the epigenetic machinery such as DNA methyltransferases (DNMTs), ten-eleven translocation (TET) proteins, histone deacetylases (HDACs) and histone methyltransferases (HMTs) [41], thus indirectly regulating DNA methylation and histone modifications.

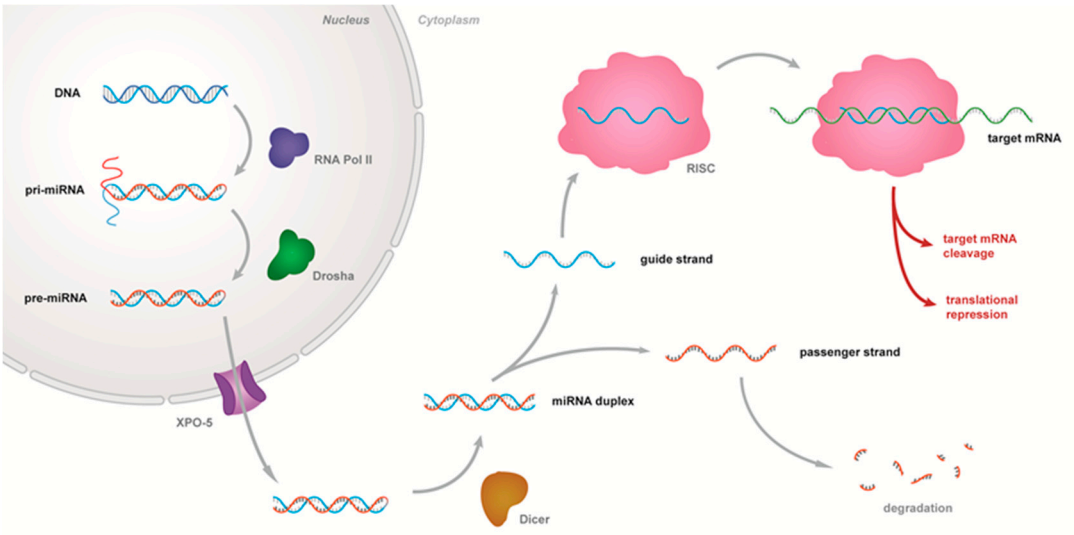


Figure 1. Canonical miRNA biosynthesis. MicroRNAs (miRNAs) function as guide molecules in RNA silencing. In animals, miRNAs are ~22 nucleotides in length, and they are processed by the sequential action of two RNase III enzymes—Drosha and Dicer. miRNA biogenesis is regulated at multiple levels, including at the transcriptional level and upon their cleavage by Drosha and Dicer in the nucleus and cytoplasm, respectively.

Apart from the well-known canonical pathway, non-canonical pathways for miRNA biogenesis are also emerging, which can be generally grouped into Drosha/DGCR8- and Dicer-independent pathways [22,34]. Examples of pre-miRNAs generated by these independent pathways include mirtrons—which are produced from mRNA introns during splicing—and the 7-methylguanosine (m7G)-capped pre-miRNA, and directly exported to the cytoplasm via Exportin 1 without the need for Drosha cleavage [22].

3. miRNAs and Lipid Homeostasis

The liver plays a crucial role in the metabolism of most endogenous lipids, plasma apolipoproteins, and lipoproteins, keeping lipid biogenesis and turnover carefully controlled by regulating the distribution of lipoprotein particles within the body. Low-density lipoprotein (LDL) particles are synthesized mainly in hepatocytes and transport cholesterol, triglycerides, and phospholipids to cells in the periphery. Hepatocytes are also the main source of high-density lipoprotein (HDL) particles released into circulation. The balance of LDL and HDL in circulation is critical for lipid homeostasis, namely that of cholesterol. Imbalances in the cellular cholesterol concentration promote vascular diseases, diabetes, and cancer but can also be observed in several monogenic diseases [42]. In fact, cholesterol homeostasis is tightly modulated by a complex network, which involves its synthesis, import, export, esterification, and metabolism. This balance is maintained by two key transcription factors: the membrane-bound transcription factor—sterol regulatory element-binding proteins SREBP1 and SREBP2 [43]—and the liver X receptor (LXR) [44], that activate genes encoding enzymes involved in cholesterol and fatty acid biosynthesis. The LXR—an oxysterol-activated transcription factor—regulates the expression of

genes involved in the efflux of cholesterol, such as the adenosine triphosphate-binding cassette (ABC) transporters ABCA1 and ABCG1. Extracellular cholesterol absorption and distribution into cells requires an appropriate endosomal trafficking system. LDL binds to its receptor on the cell surface and is then absorbed by clathrin-mediated endocytosis. Upon internalization, LDL is delivered to early sorting endosomes and then to late endolysosomes/lysosomes, where LDL and cholesteryl esters are hydrolyzed. The LDL receptor can then be recycled back to the plasma membrane. After the hydrolyzation of cholesteryl esters by lysosomal acid lipase (LAL), the lysosomal Niemann-Pick type C1 and C2 proteins mediate cholesterol export to the cytosol. The small soluble NPC2 protein picks up cholesterol inside late endosomes/lysosomes and delivers it to NPC1—a lysosomal membrane protein—which is then thought to transport cholesterol into and/or across the lysosomal membrane [45–49]. The mechanism through which cholesterol is delivered to other membranes, such as those from the ER, endosomes, mitochondria, and the plasma membrane, is still largely unknown.

In addition to classic transcriptional regulation of cholesterol metabolism, several miRNAs have been identified to be potent post-transcriptional regulators of lipid metabolism genes, including let-7, miR-26, miR-33, miR-34a, miR-106, miR-122, miR-143, miR-148-a, miR-185 [50], miR-335, miR-370, miR-370, miR-378/378*, and miR-758 [44,51–53].

4. Niemann–Pick Type C Disease

Pathogenic variants in the *NPC1* or *NPC2* genes lead to cellular cholesterol trafficking impairment, triggering NPC disease. Additionally, *NPC1* gene variants are implicated in different common metabolic disorders, an observation that can be explained using NPC1 protein influence on steroid hormone production and/or lipid homeostasis [54]. Clinically, NPC is a devastating neurodegenerative disease with a wide range of phenotypes and differing ages of onset. Patients who develop NPC during early infancy frequently present mainly visceral manifestations such as splenomegaly, hepatomegaly, neonatal jaundice, and hyperbilirubinemia, with several degrees of neurologic signs [55,56]. Adolescent or adult-onset NPC patients, on the other hand, display varying combinations of progressive neurologic deficits, e.g., ataxia, dystonia, and/or dementia, vertical supranuclear gaze palsy (VSGP), or major psychiatric illness [56].

Classically, NPC diagnosis relied upon filipin staining of cultured fibroblasts from skin biopsies [57]. Filipin specifically binds to unsterified cholesterol, allowing the cholesterol accumulated in perinuclear vesicular compartments to be visualized [58]. That is why Filipin labeling was used for years as the gold standard for NPC diagnosis. Nevertheless, even the most severely affected patients may fail to be diagnosed using this method [59,60]. Recent advances in the field, such as the generalized use of next-generation sequencing (NGS) technologies, namely whole-exome sequencing (WES) or whole-genome sequencing (WGS), have been actively increasing the detection of NPC patients. The development of novel, rapid, and reliable biomarkers has also greatly contributed to this scenario. Among others, a biomarker with great potential to shorten the diagnostic odyssey of NPC patients is N-palmitoyl-O-phosphocholineserine (previously known as lysosphingomyelin-509), which has been shown to be elevated in plasma and dried blood spots of NPC patients [61,62].

Other studies have highlighted proteins as potential biomarkers, including GPNMB, that corresponds to the glycoprotein NMB, encoded by the *GPNMB* gene—a downstream target of the lysosomal transcription factor EB—TFEB. GPNMB was recently identified as a useful biomarker of treatment response in NPC disease [63]. Besides biochemical biomarkers, other kinds of blood biomarkers, particularly miRNAs, are already used for cancer and other diseases and should be explored for NPC.

4.1. MicroRNA Profile in NPC

Besides their putative use as biomarkers, knowledge of miRNA signatures can be useful in understanding the different clinical manifestations of NPC. Like in many other

LSDs, a strictly monogenic view is not enough to explain the significant clinical variability that occurs in this disease, and that may be seen even within members of the same family. Over the following paragraphs, we will review the current knowledge on the miRNA profile in NPC by summarizing the currently published results reported by different teams.

A previous study of miRNA profile was conducted in NPC skin fibroblasts using microarrays (Human microRNA Panel A), encompassing 365 mature human miRNAs, even though only 107 of them were shown to be expressed in NPC fibroblasts samples [64]. No information about the genotype was provided. Differences in gene expression between control and NPC fibroblasts (>3.5-fold difference, p-value < 0.05) were detected, and it was found that three miRNAs (miR-196a, miR-196b, and miR-296) were significantly upregulated, whereas 38 miRNAs (35.5%) were significantly downregulated in NPC cells (Table 1). The predicted target genes of the differentially expressed miRNAs were mostly related to the regulation of transcription, signal transduction, and vesicular transport, and only a small percentage was linked to cholesterol and lipid metabolism. Amongst the downregulated non-coding RNAs, miR-98 was the most downregulated, and its predicted target genes were found to be related to the lysosome and Golgi. miR-143, a lipid biosynthesis-associated miRNA, had a 20-fold decreased expression in NPC cells. The most upregulated one (near forty-fold) was miR-196a, which, as well as miR-98, was also found to be related to the lysosome and Golgi compartments in NPC cells. Altogether, the technology used in this study presents some caveats since microarrays have some well-known technical limitations. Furthermore, the predicted target genes of the differentially expressed miRNAs were not experimentally validated. Still, this is preliminary data, which surely deserves further validation. More recently, in the era of NGS-based methods, RNA sequencing (RNA-Seq) technologies allow a higher coverage and offer higher resolution, as well as a better range of detection and lower technical variability when compared with microarrays [65], and it is expected to find more dysregulated miRNAs in NPC patients' cells using RNA-Seq based approaches, namely ncRNA pipelines.

Table 1. Most differentially expressed miRNAs in NPC cells (human and *Npc1*$^{-/-}$ mice).

miRNA	RQ Value [1] (NPC/Control)	Expression	Tissue of Origin	Organism	Technology Applied	Ref
miR-98	−33.3	Decreased	Skin fibroblasts	NPC patients	TaqMan® low-density arrays	[64]
miR-143	−20	Decreased				
miR-196a	37.41	Increased				
miR-196b	6.68	Increased				
miR-296	3.53	Increased				
miR-155	n/a	Increased	Liver			
	n/a	Decreased	Spleen	*Npc1*$^{-/-}$ mice	qRT-PCR	[66]

[1] RQ = Relative quantity value.

Another study regarding miRNAs in NPC disease started with a proteomics analysis on an NPC-null mouse model (*Npc1*$^{-/-}$ mice) [66], which mimics human disease and presents progressive cerebellar neurodegeneration, ataxia, and hepatosplenomegaly. This study was conducted using liver and spleen samples, two of the organs that are strongly affected in the early infantile form of the NPC disease. Neurodegeneration has been studied more extensively, but severe liver disease is also a major symptom for a subset of patients and some of them died from acute liver failure by the first months of life [67,68]. In this context, capillary LC-MS/MS was used to perform label-free quantitative proteomics in *Npc1*$^{-/-}$ mice at an endpoint in disease progression. The differential proteome was analyzed to identify potential biomarkers and to unravel the mechanism leading to hepatosplenomegaly. Overall, the analysis of the datasets showed many altered pathways in the *Npc1*$^{-/-}$ mice and upstream transcriptional regulator analysis identified miR-155 as a possible modulator. For validation, the expression levels of miR-155 were

quantified by qRT-PCR in 9-week-old $Npc1^{+/+}$ and $Npc1^{-/-}$ mice and its levels were found to be significantly decreased in the spleen and increased in the liver of $Npc1^{-/-}$ mice [66]. This miRNA—which is involved in the regulation of multiple genes involved in lipid metabolism—was thereby proposed as a novel indicator of spleen and liver pathology in NPC disease.

Further, miR-155 enhances tyrosine-kinase-mediated signaling pathways in the immune system, playing a role in inflammation, which is a hallmark of NPC disease [69,70]. In fact, miR-155 targets the SHIP tyrosine phosphatase [71]—a well-known negative regulator of PI3P-AKT signaling. It has been described that tyrosine kinase levels are dysregulated in NPC neurons from transgenic mice, for instance [72]. Therefore, tyrosine-mediated signaling is enhanced in these cells. The aberrant activation of certain tyrosine kinases leads to premature neuroinflammation and neuronal loss in the forebrain of NPC transgenic mice [72].

Whether these differentially expressed intracellular miRNAs (detected in fibroblasts, liver, or spleen cells) could be used as biomarkers as a result of their association with extracellular vesicles (EVs) needs to be studied further. On the other hand, investigating if the expression of those miRNAs varies even among NPC patients with the same pathogenic variant in the *NPC1* gene could explain the large phenotypic spectrum characteristic of these patients.

4.2. miRNAs That Target the NPC1 Gene, Impacting Its Expression

Besides the miRNA signature associated with NPC disease, another point of interest in the scope of this review is to explore the miRNAs that regulate NPC1 levels. To the best of our knowledge, miR-33a/b, miR-25, and miR-200c bind to the 3′-UTR of the *NPC1* mRNA, thus repressing its expression (Figure 2). Over the following paragraphs, we will further elaborate on each one of these miRNAs and the original studies reporting their impact on the expression of NPC1.

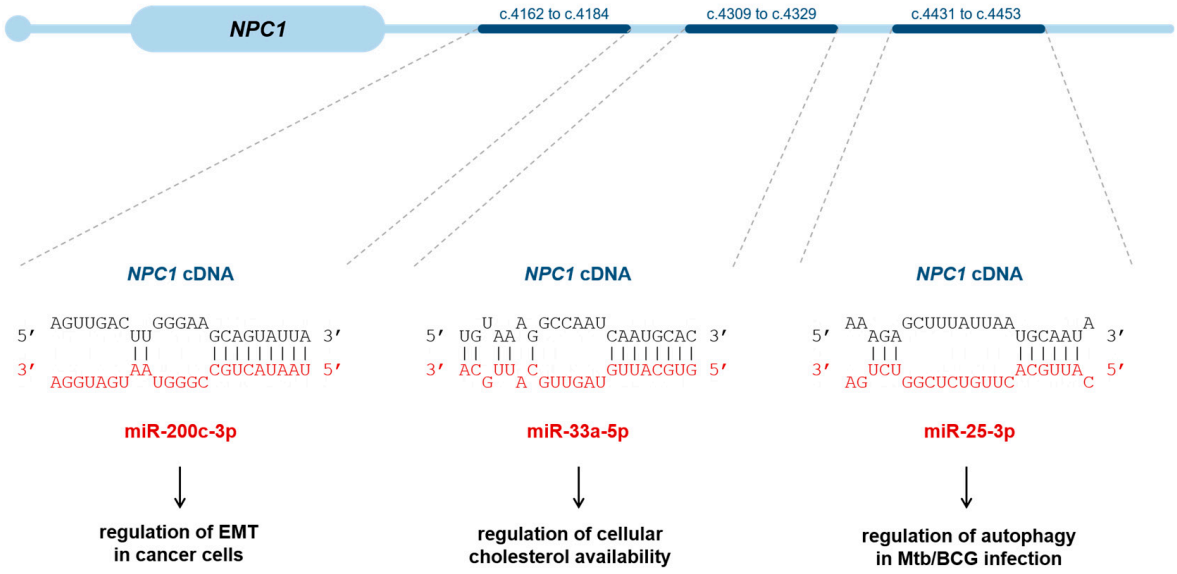


Figure 2. Different miRNAs target the *NPC1* gene under different physiological contexts. miR-200c-3p, a known repressor of EMT in cancer cells, binds to the -3′UTR of *NPC1;* miR-33a-5p targets the *NPC1* gene, regulating the cellular cholesterol availability, and miR-25-3p also represses *NPC1* expression, regulating autophagy in Mtb/BCG infection.

4.2.1. miR-33a/b

Among the most well-characterized key regulators of lipid metabolism are miR-33a and -b (miR-33 a/b) [73,74]—which are encoded within the introns of *SREBP2* and *SREBP1*, respectively—and constitute a master switch for genes involved in fatty acid and cholesterol

metabolism [73,75–79] and insulin regulation. miR-33a and miR-33b share the same seed sequence and differ in only two nucleotides. Both regulate cholesterol homeostasis and fatty acid metabolism in concert with their host genes, *SREBP2* and *SREBP1c*, in a negative feedback loop [80]. *SREBP1* encodes SREBP1a and SREBP1c, which regulate lipogenic genes, whereas *SREBP2* mainly modulates cholesterol-regulating genes.

miR-33a specifically targets the 3′-UTR of the *NPC1* mRNA, among others, thus playing an important role in cholesterol homeostasis. The 3′-UTR of human *NPC1* contains two miR-33a binding sites, resulting in the repression of NPC1 protein in hepatocytes and macrophages [76]. For example, under low intracellular cholesterol conditions, miR-33a is cotranscribed with SREBP2 and works to increase the cellular cholesterol levels via the inhibition of ABCA1 and ABCG1 transporters and NPC1 protein [73,75,76], thus reducing cholesterol export. On the other hand, in cholesterol-rich conditions, SREBP2 and miR-33a levels decreases, thus relieving ABCA1 suppression [80]. When the intracellular cholesterol levels are high, SREBP1-c is induced, miR-33b is co-transcribed and works to reduce cellular fatty acid oxidation by targeting carnitine O-octanoyl transferase (CROT), carnitine palmitoyltransferase 1A (CPT1a), hydroxyacyl coenzyme A (hydroxyacyl-CoA) dehydrogenase subunit beta (HADHB), and AMP kinase subunit alpha (AMPKα), as well as insulin signaling, by targeting insulin receptor substrate 2 (IRS2) and sirtuin 6 (SIRT6) [81].

In conclusion, SREBP's transcription factors, in concert with miR33a/b, prevent dramatic increases or reductions in cellular lipid levels by controlling lipid synthesis, uptake, and export. miR-33a and miR-33b help prevent further loss of lipids by targeting genes involved in cholesterol trafficking and efflux (*NPC1*, *ABCA1*, *ABCG1*) and fatty acid metabolism (*CPT1A*, *CROT*).

4.2.2. miR-25

miR-25 has a broad range of potential mRNA targets that participate in many cellular processes. Among those, autophagy plays an essential role, as it degrades cytoplasmic constituents and organelles, strongly contributing to the cell's homeostasis. Additionally, it was precisely the pivotal role of miR-25 in autophagy that was first brought to light. In fact, while studying miRNA effects on autophagy regulation during the progression of *Mycobacterium tuberculosis* (Mtb)/ Bacillus Calmette-Guérin (BCG) infection in macrophages, some miRNAs were identified as upregulated, including miR-25. Then, online software (TargetScan https://www.targetscan.org/vert_80/, accessed on 21 August 2023. miRDB http://www.mirdb.org/, miRanda https://bioweb.pasteur.fr/packages/pack@miRanda@3.3a, accessed on 21 August 2023) was used to predict the mRNA targets of miR-25, and those results were subsequently cross-linked with target autophagy pathway-related genes [82,83]. The results showed that miR-25—which is upregulated upon BCG/Mtb infection—directly targets the *NPC1* mRNA (binding the 3′-UTR), decreasing NPC1 at the transcriptional and protein levels and impairing autophagosome-lysosome fusion [84]. Accordingly, when the cells were transfected with a miR-25 inhibitor, NPC1 was upregulated, promoting autophagic flux. Ultimately, all the results suggested that miR-25 actively affects the intracellular survival of BCG and Mtb by regulating the autophagic pathway via its target—NPC1.

4.2.3. miR-200c

As we have already mentioned, miR-25 is not the only miRNA known to directly bind *NPC1* mRNA. miR-200c has also been shown to play its part. Additionally, again, the first reports on miR-200c, came from studies in cancer cells. It was initially shown to inhibit epithelial-mesenchymal transition (EMT)—a mechanism that facilitates metastasis in cancer cells. In order to unveil the genes affected by miR-200c, it was observed that the restoration of miR-200c to cancer cells reduces the levels of certain immune modulatory response genes and among them, *NPC1* was found [85]. Consistently, its silencing led to decelerated proliferation and decreased invasiveness, altered mitochondrial function and morphology, suppression of mTOR signaling and accumulation of autophagossomes [86].

Additionally, the *NPC1* gene has also been shown to be highly expressed and directly targeted by miR-200c in aggressive breast cancer [86].

5. Circulating miRNA as Putative Biomarkers

Extracellular miRNAs are remarkably stable, and since they can be used in intercellular communication [87], their characterization can provide important insights into health and disease. For neurodegenerative and metabolic diseases, such as NPC, it is expected to find informative miRNAs in bodily fluids, which can be used as reliable biomarkers for disease diagnosis and prognosis. The possibility of using miRNAs as disease biomarkers and treatment follow-ups has already been studied for another LSD, namely Pompe Disease (Glycogen storage disease type II: MIM #232300) [88].

Cell-free miRNAs can be transported using two tightly regulated and energy-demanding processes (Figure 3). The first one is active transport via EVs, which includes shedding vesicles/microvesicles/ectosomes and exosomes [23], which are released by almost all cell types under physiological and pathological conditions [89]. The second is transport as part of protein-miRNA complexes (RNA-binding proteins) (Figure 3). In some cases, there can also be passive leakage of miRNAs from broken and damaged cell membranes. For the uptake of circulating miRNAs, microvesicle (MV)-enclosed miRNAs are recognized by cellular surface molecules and internalized by endocytosis, phagocytosis, or direct fusion with the plasma membrane.

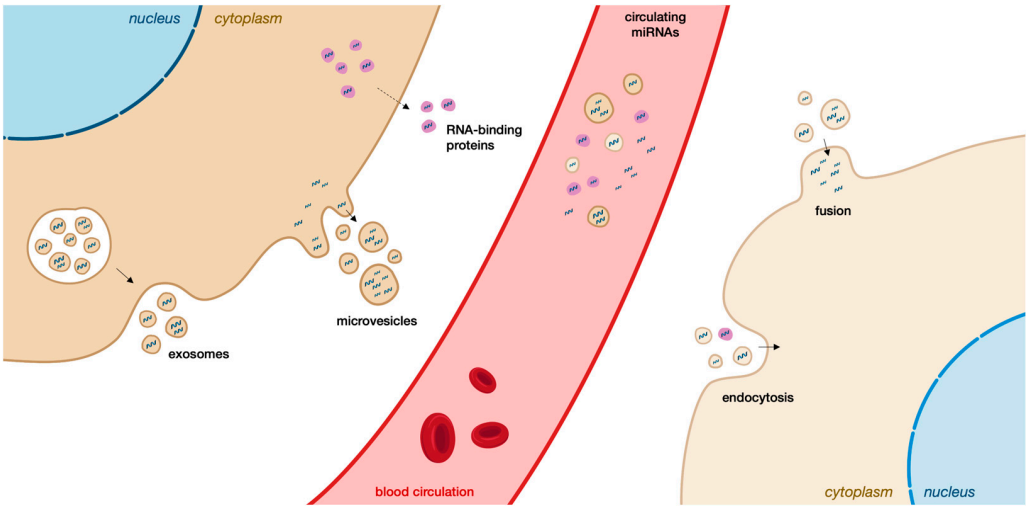


Figure 3. miRNAs Export, transport, and uptake. Extracellular microRNA can be transported in a regulated manner through exosomes (30–100 nm), microvesicles (100–1000 nm), and complexed with proteins. Circulating miRNAs can be used as biomarkers and function in intercellular communication.

Major cell types of the central nervous system (CNS) release EVs, namely exosomes. It was shown that patients harboring pathogenic NPC1 variants showed elevated exosomal cholesterol release, which could disrupt cholesterol homeostasis [90].

6. Therapeutic Metabolic Reprogramming to Use in LSDs—RNA-Based Therapeutics

Finally, there is yet another possibility to consider when discussing miRNAs: their potential as therapeutic targets for RNA-based therapies. In fact, a better understanding of the epigenome, especially regarding the role of miRNAs and their expression levels, namely if some of them are up or downregulated in NPC patients, can also lead to the development of tailored therapies. One possibility is the use of RNA-based therapeutics, a type of therapy that has merited significant attention in recent years due to their potential to treat a variety of diseases [91,92].

The most well-known RNA-based therapeutics rely on the use of modified oligonucleotides, also known as antisense oligonucleotides (ASOs) [93]. ASOs are single-stranded

oligonucleotides, some of which can also be used for target gene knockdown via the recruitment of endogenous RNAse H (gapmer ASOs). However, another type of ASO, designated steric block ASOs, exerts its function by binding to their target transcripts, thus masking specific sequences and interfering with RNA–RNA and/or RNA–protein interactions [93,94].

Steric block ASOs can either be used to competitively inhibit miRNAs via direct binding to these small RNA species (in which case they are known as anti-miRNA oligonucleotides, anti-miRs, or antagomirs), or they can be designed to mimic the activity of endogenous miRNAs (being referred to as miRNA mimics or agomirs) [93].

Importantly, these types of miRNA-targeting ASOs are under clinical development for a number of diseases, with ongoing clinical trials and some approved drugs, which further support their overall potential as effective therapeutic strategies as soon as their safety and toxicology profiles meet all the requirements. The first anti-miRNA drug to enter clinical trials was miravirsen—an antagomir to miR-122, a liver-specific microRNA that the hepatitis C virus (HCV) requires for replication. Despite having shown promising results, an escape mutation that renders the HCV genome refractory to miravirsen has also been reported [94,95].

However, many other approaches have entered development either to restore or to block miRNAs for a therapeutic purpose. Anti-miRNA oligonucleotide drugs are being developed for nonalcoholic steatohepatitis, cholestatic diseases, fibrogenesis of organs associated with Alport syndrome, lymphoma and leukemia, amyotrophic lateral sclerosis, and ischemic conditions. In turn, miRNA mimic approaches are being developed and are currently in clinical trials for fibrotic diseases, cancers, and malignant pleural mesothelioma [95].

To the best of our knowledge, the use of oligonucleotide drugs to modulate the function of miRNAs has never been tested, not even *in vitro*, for NPC or any other LSD in which certain miRNAs were found to be differentially expressed.

However, another type of RNA therapeutics that is based on the use of the entire coding mRNA molecule has been recently tested *in vitro* for NPC. Furtado et al. treated NPC patient fibroblasts with an engineered *NPC1* mRNA and observed the restoration of functional protein expression and the reversal of disease pathology [96]. Therefore, RNA therapies hold promise for the treatment of NPC, and they can be used to target both the genetic causes (mutations in the *NPC1* and *NPC2* genes) as well as the epigenetic causes, such as the dysregulation of miRNAs.

In summary, even though many issues still have to be addressed before the broader application of miRNA-based therapies (e.g., delivery, off-targets, immune system reactions), their potential for the treatment of a great panoply of diseases in which microRNAs are dysregulated (NPC and other LSDs included) is enormous.

7. Concluding Remarks

NPC is a neurovisceral disease, which means its main affected organs are all of great interest for targeted analyses since miRNA expression is cell-type specific. That catalog includes not only the brain but also the liver and spleen, just to mention the most significant ones. However, the few studies reported so far did not cover all of those major organs. Furthermore, most of them were assessed using microarray technologies, which have quite a few limitations. Recent advances in research, including the development of multi-omics methods, have made it possible to elucidate multiple transcriptomic and epigenetic pathways in eukaryotic organisms. Decreased sequencing costs and increased accessibility of data analysis make epigenetics research more affordable and achievable. For monogenic diseases with high clinical variability, such as LSDs in general and NPC in particular, epigenetics, namely ncRNAs, can explain the different disease outcomes observed in patients with the same genetic defect. In fact, it is predicted that miRNAs account for 1–5% of the human genome but regulate at least 30% of protein-coding gene expression, and they are not limited to intracellular activity. Due to their ability to be transported in EVs,

their detection in bodily fluids can provide important insights related to the disease and be used as biomarkers.

This review highlighted the microRNA profile associated with NPC and some of the few miRNAs that have been experimentally shown to target the *NPC1* gene, thus modulating relevant cellular mechanisms. However, most importantly, it also highlighted the need for additional studies and extended profiling in NPC patients. Overall, the potential of miRNAs is enormous, not just from a basic science point of view (by helping us unveil and understand the underlying pathophysiological mechanisms) but also from a more applied perspective (by acting as putative disease biomarkers or therapeutic targets). Either way, there is plenty of room and need for further research in the field.

Author Contributions: Conceptualization, M.E., H.D. and S.A.; NCBI PubMed search: M.E., H.D., M.F.C. and S.A.; manuscript structure: M.E., H.D., M.F.C. and S.A.; original draft preparation: M.E. and S.A.; additional writing: M.F.C., H.D. and L.M.; critical review: M.F.C., H.D., L.M. and S.A.; funding acquisition, M.E. and S.A. All authors have read and agreed to the published version of the manuscript.

Funding: This research was funded by FCT (Fundação para a Ciência e Tecnologia), grant number EXPL/BTM-TEC/1477/2021; UIDB/00211/2020—Centro de Estudos de Ciência Animal/Center for the Study of Animal Science; LA/P/0059/2020—Laboratório Associado para Ciência Animal e Veterinária/Associate Laboratory for Animal and Veterinary Sciences.

Conflicts of Interest: The authors declare no conflict of interest.

References

1. van Meer, G.; Voelker, D.R.; Feigenson, G.W. Membrane Lipids: Where They Are and How They Behave. *Nat. Rev. Mol. Cell Biol.* **2008**, *9*, 112–124. [CrossRef]
2. Platt, F.M.; Boland, B.; van der Spoel, A.C. The Cell Biology of Disease: Lysosomal Storage Disorders: The Cellular Impact of Lysosomal Dysfunction. *J. Cell Biol.* **2012**, *199*, 723–734. [CrossRef] [PubMed]
3. Lieberman, A.P.; Puertollano, R.; Raben, N.; Slaugenhaupt, S.; Walkley, S.U.; Ballabio, A. Autophagy in Lysosomal Storage Disorders. *Autophagy* **2012**, *8*, 719–730. [CrossRef] [PubMed]
4. Schulze, H.; Sandhoff, K. Lysosomal Lipid Storage Diseases. *Cold Spring Harb. Perspect. Biol.* **2011**, *3*, a004804. [CrossRef] [PubMed]
5. Shamim, A.; Mahmood, T.; Ahsan, F.; Kumar, A.; Bagga, P. Lipids: An Insight into the Neurodegenerative Disorders. *Clin. Nutr. Exp.* **2018**, *20*, 1–19. [CrossRef]
6. Platt, F.M. Emptying the Stores: Lysosomal Diseases and Therapeutic Strategies. *Nat. Rev. Drug Discov.* **2018**, *17*, 133–150. [CrossRef]
7. Encarnação, M.; Coutinho, M.F.; Silva, L.; Ribeiro, D.; Ouesleti, S.; Campos, T.; Santos, H.; Martins, E.; Cardoso, M.T.; Vilarinho, L.; et al. Assessing Lysosomal Disorders in the NGS Era: Identification of Novel Rare Variants. *Int. J. Mol. Sci.* **2020**, *21*, 6355. [CrossRef]
8. Encarnação, M.; Coutinho, M.F.; Cho, S.M.; Cardoso, M.T.; Ribeiro, I.; Chaves, P.; Santos, J.I.; Quelhas, D.; Lacerda, L.; Leão Teles, E.; et al. NPC1 Silent Variant Induces Skipping of Exon 11 (p.V562V) and Unfolded Protein Response Was Found in a Specific Niemann-Pick Type C Patient. *Mol. Genet. Genom. Med.* **2020**, *8*, e1451. [CrossRef]
9. Beck, M. Variable Clinical Presentation in Lysosomal Storage Disorders. *J. Inherit. Metab. Dis.* **2001**, *24* (Suppl. S2), 47–51. [CrossRef]
10. Las Heras, M.; Szenfeld, B.; Ballout, R.A.; Buratti, E.; Zanlungo, S.; Dardis, A.; Klein, A.D. Understanding the Phenotypic Variability in Niemann-Pick Disease Type C (NPC): A Need for Precision Medicine. *NPJ Genomic Med.* **2023**, *8*, 21. [CrossRef]
11. Benussi, A.; Alberici, A.; Premi, E.; Bertasi, V.; Cotelli, M.S.; Turla, M.; Dardis, A.; Zampieri, S.; Marchina, E.; Paghera, B.; et al. Phenotypic Heterogeneity of Niemann–Pick Disease Type C in Monozygotic Twins. *J. Neurol.* **2015**, *262*, 642–647. [CrossRef]
12. Hassan, S.; Sidransky, E.; Tayebi, N. The Role of Epigenetics in Lysosomal Storage Disorders: Uncharted Territory. *Mol. Genet. Metab.* **2017**, *122*, 10–18. [CrossRef] [PubMed]
13. Parenti, G.; Medina, D.L.; Ballabio, A. The Rapidly Evolving View of Lysosomal Storage Diseases. *EMBO Mol. Med.* **2021**, *13*, e12836. [CrossRef] [PubMed]
14. Ryan, E.; Seehra, G.K.; Sidransky, E. Mutations, Modifiers and Epigenetics in Gaucher Disease: Blurred Boundaries between Simple and Complex Disorders. *Mol. Genet. Metab.* **2019**, *128*, 10–13. [CrossRef] [PubMed]
15. Wang, C.; Scott, S.M.; Subramanian, K.; Loguercio, S.; Zhao, P.; Hutt, D.M.; Farhat, N.Y.; Porter, F.D.; Balch, W.E. Quantitating the Epigenetic Transformation Contributing to Cholesterol Homeostasis Using Gaussian Process. *Nat. Commun.* **2019**, *10*, 5052. [CrossRef] [PubMed]
16. Han, S.; Ren, M.; Kuang, T.; Pang, M.; Guan, D.; Liu, Y.; Wang, Y.; Zhang, W.; Ye, Z. Cerebellar Long Noncoding RNA Expression Profile in a Niemann-Pick C Disease Mouse Model. *Mol. Neurobiol.* **2021**, *58*, 5826–5836. [CrossRef]

17. Iwakawa, H.; Tomari, Y. The Functions of MicroRNAs: MRNA Decay and Translational Repression. *Trends Cell Biol.* **2015**, *25*, 651–665. [CrossRef] [PubMed]
18. Bartel, D.P. Metazoan MicroRNAs. *Cell* **2018**, *173*, 20–51. [CrossRef]
19. Ambros, V. The Functions of Animal MicroRNAs. *Nature* **2004**, *431*, 350–355. [CrossRef]
20. Gibson, M.S.; Noronha-Estima, C.; Gama-Carvalho, M. Therapeutic Metabolic Reprograming Using MicroRNAs: From Cancer to HIV Infection. *Genes* **2022**, *13*, 273. [CrossRef]
21. Cannell, I.G.; Kong, Y.W.; Bushell, M. How Do MicroRNAs Regulate Gene Expression? *Biochem. Soc. Trans.* **2008**, *36*, 1224–1231. [CrossRef] [PubMed]
22. O'Brien, J.; Hayder, H.; Zayed, Y.; Peng, C. Overview of MicroRNA Biogenesis, Mechanisms of Actions, and Circulation. *Front. Endocrinol.* **2018**, *9*, 402. [CrossRef] [PubMed]
23. Valadi, H.; Ekström, K.; Bossios, A.; Sjöstrand, M.; Lee, J.J.; Lötvall, J.O. Exosome-Mediated Transfer of MRNAs and MicroRNAs Is a Novel Mechanism of Genetic Exchange between Cells. *Nat. Cell Biol.* **2007**, *9*, 654–659. [CrossRef] [PubMed]
24. Pawliński, Ł.; Polus, A.; Tobór, E.; Sordyl, M.; Kopka, M.; Solnica, B.; Kieć-Wilk, B. MiRNA Expression in Patients with Gaucher Disease Treated with Enzyme Replacement Therapy. *Life* **2020**, *11*, 2. [CrossRef] [PubMed]
25. Xiao, K.; Lu, D.; Hoepfner, J.; Santer, L.; Gupta, S.; Pfanne, A.; Thum, S.; Lenders, M.; Brand, E.; Nordbeck, P.; et al. Circulating MicroRNAs in Fabry Disease. *Sci. Rep.* **2019**, *9*, 15277. [CrossRef] [PubMed]
26. Ha, M.; Kim, V.N. Regulation of MicroRNA Biogenesis. *Nat. Rev. Mol. Cell Biol.* **2014**, *15*, 509–524. [CrossRef] [PubMed]
27. Kang, W.; Fromm, B.; Houben, A.J.; Høye, E.; Bezdan, D.; Arnan, C.; Thrane, K.; Asp, M.; Johnson, R.; Biryukova, I.; et al. MapToCleave: High-Throughput Profiling of MicroRNA Biogenesis in Living Cells. *Cell Rep.* **2021**, *37*, 110015. [CrossRef]
28. Fromm, B.; Domanska, D.; Høye, E.; Ovchinnikov, V.; Kang, W.; Aparicio-Puerta, E.; Johansen, M.; Flatmark, K.; Mathelier, A.; Hovig, E.; et al. MirGeneDB 2.0: The Metazoan MicroRNA Complement. *Nucleic Acids Res.* **2020**, *48*, D132–D141. [CrossRef]
29. Halushka, M.K.; Fromm, B.; Peterson, K.J.; McCall, M.N. Big Strides in Cellular MicroRNA Expression. *Trends Genet.* **2018**, *34*, 165–167. [CrossRef]
30. Hinske, L.C.; França, G.S.; Torres, H.A.M.; Ohara, D.T.; Lopes-Ramos, C.M.; Heyn, J.; Reis, L.F.L.; Ohno-Machado, L.; Kreth, S.; Galante, P.A.F. MiRIAD-Integrating MicroRNA Inter- and Intragenic Data. *Database* **2014**, *2014*, bau099. [CrossRef]
31. Hinske, L.C.G.; Galante, P.A.F.; Kuo, W.P.; Ohno-Machado, L. A Potential Role for Intragenic MiRNAs on Their Hosts' Interactome. *BMC Genom.* **2010**, *11*, 533. [CrossRef] [PubMed]
32. Galatenko, V.V.; Galatenko, A.V.; Samatov, T.R.; Turchinovich, A.A.; Shkurnikov, M.Y.; Makarova, J.A.; Tonevitsky, A.G. Comprehensive Network of MiRNA-Induced Intergenic Interactions and a Biological Role of Its Core in Cancer. *Sci. Rep.* **2018**, *8*, 2418. [CrossRef] [PubMed]
33. Matsuyama, H.; Suzuki, H.I. Systems and Synthetic MicroRNA Biology: From Biogenesis to Disease Pathogenesis. *Int. J. Mol. Sci.* **2020**, *21*, 132. [CrossRef] [PubMed]
34. Treiber, T.; Treiber, N.; Meister, G. Regulation of MicroRNA Biogenesis and Its Crosstalk with Other Cellular Pathways. *Nat. Rev. Mol. Cell Biol.* **2018**, *20*, 5–20. [CrossRef]
35. Kim, Y.; Kim, V.N. MicroRNA Factory: RISC Assembly from Precursor MicroRNAs. *Mol. Cell* **2012**, *46*, 384–386. [CrossRef] [PubMed]
36. Meijer, H.A.; Smith, E.M.; Bushell, M. Regulation of MiRNA Strand Selection: Follow the Leader? *Biochem. Soc. Trans.* **2014**, *42*, 1135–1140. [CrossRef]
37. Medley, J.C.; Panzade, G.; Zinovyeva, A.Y. MicroRNA Strand Selection: Unwinding the Rules. *Wiley Interdiscip. Rev. RNA* **2021**, *12*, e1627. [CrossRef]
38. Selbach, M.; Schwanhäusser, B.; Thierfelder, N.; Fang, Z.; Khanin, R.; Rajewsky, N. Widespread Changes in Protein Synthesis Induced by MicroRNAs. *Nature* **2008**, *455*, 58–63. [CrossRef] [PubMed]
39. Baek, D.; Villén, J.; Shin, C.; Camargo, F.D.; Gygi, S.P.; Bartel, D.P. The Impact of MicroRNAs on Protein Output. *Nature* **2008**, *455*, 64–71. [CrossRef]
40. Naeli, P.; Winter, T.; Hackett, A.P.; Alboushi, L.; Jafarnejad, S.M. The Intricate Balance between MicroRNA-Induced MRNA Decay and Translational Repression. *FEBS J.* **2022**, *290*, 2508–2524. [CrossRef]
41. Yao, Q.; Chen, Y.; Zhou, X. The Roles of MicroRNAs in Epigenetic Regulation. *Curr. Opin. Chem. Biol.* **2019**, *51*, 11–17. [CrossRef] [PubMed]
42. Ikonen, E. Mechanisms for Cellular Cholesterol Transport: Defects and Human Disease. *Physiol. Rev.* **2006**, *86*, 1237–1261. [CrossRef] [PubMed]
43. Brown, M.S.; Goldstein, J.L. A Proteolytic Pathway That Controls the Cholesterol Content of Membranes, Cells, and Blood. *Proc. Natl. Acad. Sci. USA* **1999**, *96*, 11041–11048. [CrossRef] [PubMed]
44. Fernández-Hernando, C.; Suárez, Y.; Rayner, K.J.; Moore, K.J. MicroRNAs in Lipid Metabolism. *Curr. Opin. Lipidol.* **2011**, *22*, 86. [CrossRef]
45. Sturley, S.L.; Patterson, M.C.; Balch, W.; Liscum, L. The Pathophysiology and Mechanisms of NP-C Disease. *Biochim. Biophys.* **2004**, *1685*, 83–87. [CrossRef]
46. Li, X.; Saha, P.; Li, J.; Blobel, G.; Pfeffer, S.R. Clues to the Mechanism of Cholesterol Transfer from the Structure of NPC1 Middle Lumenal Domain Bound to NPC2. *Proc. Natl. Acad. Sci. USA* **2016**, *113*, 10079–10084. [CrossRef]

47. Long, T.; Qi, X.; Hassan, A.; Liang, Q.; De Brabander, J.K.; Li, X. Structural Basis for Itraconazole-Mediated NPC1 Inhibition. *Nat. Commun.* **2020**, *11*, 152. [CrossRef]
48. Brown, M.S.; Radhakrishnan, A.; Goldstein, J.L. Retrospective on Cholesterol Homeostasis: The Central Role of Scap. *Annu. Rev. Biochem.* **2018**, *87*, 783–807. [CrossRef] [PubMed]
49. Pfeffer, S.R. NPC Intracellular Cholesterol Transporter 1 (NPC1)-Mediated Cholesterol Export from Lysosomes. *J. Biol. Chem.* **2019**, *294*, 1706–1709. [CrossRef]
50. Jiang, H.; Zhang, J.; Du, Y.; Jia, X.; Yang, F.; Si, S.; Wang, L.; Hong, B. MicroRNA-185 Modulates Low Density Lipoprotein Receptor Expression as a Key Posttranscriptional Regulator. *Atherosclerosis* **2015**, *243*, 523–532. [CrossRef]
51. Du, H.; Zhao, Y.; Li, H.; Wang, D.W.; Chen, C. Roles of MicroRNAs in Glucose and Lipid Metabolism in the Heart. *Front. Cardiovasc. Med.* **2021**, *8*, 716213. [CrossRef] [PubMed]
52. Agbu, P.; Carthew, R.W. MicroRNA-Mediated Regulation of Glucose and Lipid Metabolism. *Nat. Rev. Mol. Cell Biol.* **2021**, *22*, 425–438. [CrossRef]
53. Desgagné, V.; Bouchard, L.; Guérin, R. MicroRNAs in Lipoprotein and Lipid Metabolism: From Biological Function to Clinical Application. *Clin. Chem. Lab. Med.* **2017**, *55*, 667–686. [CrossRef] [PubMed]
54. Lamri, A.; Pigeyre, M.; Garver, W.S.; Meyre, D. The Extending Spectrum of NPC1-Related Human Disorders: From Niemann-Pick C1 Disease to Obesity. *Endocr. Rev.* **2018**, *39*, 192–220. [CrossRef]
55. Pineda, M.; Mengel, E.; Jahnová, H.; Héron, B.; Imrie, J.; Lourenço, C.M.; van der Linden, V.; Karimzadeh, P.; Valayannopoulos, V.; Jesina, P.; et al. A Suspicion Index to Aid Screening of Early-Onset Niemann-Pick Disease Type C (NP-C). *BMC Pediatr.* **2016**, *16*, 107. [CrossRef]
56. Wijburg, F.A.; Sedel, F.; Pineda, M.; Hendriksz, C.J.; Fahey, M.; Walterfang, M.; Patterson, M.C.; Wraith, J.E.; Kolb, S.A. Development of a Suspicion Index to Aid Diagnosis of Niemann-Pick Disease Type C. *Neurology* **2012**, *78*, 1560–1567. [CrossRef] [PubMed]
57. Kruth, H.S.; Cupp, J.E.; Khan, M.A. Method for Detection and Isolation of Cholesteryl Ester-containing "Foam" Cells Using Flow Cytometry. *Cytometry* **1987**, *8*, 146–152. [CrossRef] [PubMed]
58. Boernig, H.; Geyer, G. Staining of Cholesterol with the Fluorescent Antibiotic "Filipin". *Acta Histochem.* **1974**, *50*, 110–115.
59. Vanier, M.T.; Latour, P. Laboratory Diagnosis of Niemann-Pick Disease Type C: The Filipin Staining Test. *Methods Cell Biol.* **2015**, *126*, 357–375. [CrossRef]
60. Probert, F.; Ruiz-Rodado, V.; Te Vruchte, D.; Nicoli, E.R.; Claridge, T.D.W.; Wassif, C.A.; Farhat, N.; Porter, F.D.; Platt, F.M.; Grootveld, M. NMR Analysis Reveals Significant Differences in the Plasma Metabolic Profiles of Niemann Pick C1 Patients, Heterozygous Carriers, and Healthy Controls. *Sci. Rep.* **2017**, *7*, 6320. [CrossRef]
61. Maekawa, M.; Jinnoh, I.; Matsumoto, Y.; Narita, A.; Mashima, R.; Takahashi, H.; Iwahori, A.; Saigusa, D.; Fujii, K.; Abe, A.; et al. Structural Determination of Lysosphingomyelin-509 and Discovery of Novel Class Lipids from Patients with Niemann-Pick Disease Type C. *Int. J. Mol. Sci.* **2019**, *20*, 5018. [CrossRef]
62. Sidhu, R.; Mondjinou, Y.; Qian, M.; Song, H.; Kumar, A.B.; Hong, X.; Hsu, F.-F.; Dietzen, D.J.; Yanjanin, N.M.; Porter, F.D.; et al. N-Acyl-O-Phosphocholineserines: Structures of a Novel Class of Lipids That Are Biomarkers for Niemann-Pick C1 Disease. *J. Lipid Res.* **2019**, *60*, 1410–1424. [CrossRef]
63. Rodriguez-Gil, J.L.; Baxter, L.L.; Watkins-Chow, D.E.; Johnson, N.L.; Davidson, C.D.; Carlson, S.R.; Incao, A.A.; Wallom, K.L.; Farhat, N.Y.; Platt, F.M.; et al. Transcriptome of HPβCD-Treated Niemann-Pick Disease Type C1 Cells Highlights GPNMB as a Biomarker for Therapeutics. *Hum. Mol. Genet.* **2021**, *30*, 2456–2468. [CrossRef] [PubMed]
64. Ozsait, B.; Komurcu-Bayrak, E.; Levula, M.; Erginel-Unaltuna, N.; Kähönen, M.; Rai, M.; Lehtimäki, T.; Laaksonen, R. Niemann-Pick Type C Fibroblasts Have a Distinct MicroRNA Profile Related to Lipid Metabolism and Certain Cellular Components. *Biochem. Biophys. Res. Commun.* **2010**, *403*, 316–321. [CrossRef] [PubMed]
65. Kukurba, K.R.; Montgomery, S.B. RNA Sequencing and Analysis. *Cold Spring Harb. Protoc.* **2015**, *2015*, 951–969. [CrossRef]
66. Pergande, M.R.; Cougnoux, A.; Rathnayake, R.A.C.; Porter, F.D.; Cologna, S.M. Differential Proteomics Reveals MiR-155 as a Novel Indicator of Liver and Spleen Pathology in the Symptomatic Niemann-Pick Disease, Type C1 Mouse Model. *Molecules* **2019**, *24*, 994. [CrossRef]
67. Imrie, J.; Heptinstall, L.; Knight, S.; Strong, K. Observational Cohort Study of the Natural History of Niemann-Pick Disease Type C in the UK: A 5-Year Update from the UK Clinical Database. *BMC Neurol.* **2015**, *15*, 257. [CrossRef] [PubMed]
68. Vanier, M.T. Niemann-Pick Diseases. *Handb. Clin. Neurol.* **2013**, *113*, 1717–1721. [CrossRef]
69. Platt, N.; Speak, A.O.; Colaco, A.; Gray, J.; Smith, D.A.; Williams, I.M.; Wallom, K.-L.; Platt, F.M. Immune Dysfunction in Niemann-Pick Disease Type C. *J. Neurochem.* **2016**, *136* (Suppl. S1), 74–80. [CrossRef]
70. Hammerschmidt, T.G.; Donida, B.; Faverzani, J.L.; Moura, A.P.; dos Reis, B.G.; Machado, A.Z.; Kessler, R.G.; Sebastião, F.M.; Reinhardt, L.S.; Moura, D.J.; et al. Cytokine Profile and Cholesterol Levels in Patients with Niemann-Pick Type C Disease Presenting Neurological Symptoms: In Vivo Effect of Miglustat and in Vitro Effect of N-Acetylcysteine and Coenzyme Q10. *Exp. Cell Res.* **2022**, *416*, 113175. [CrossRef]
71. O'Connell, R.M.; Chaudhuri, A.A.; Rao, D.S.; Baltimore, D. Inositol Phosphatase SHIP1 Is a Primary Target of MiR-155. *Proc. Natl. Acad. Sci. USA* **2009**, *106*, 7113–7118. [CrossRef] [PubMed]
72. Gonfloni, S.; Maiani, E.; Di Bartolomeo, C.; Diederich, M.; Cesareni, G. Oxidative Stress, DNA Damage, and c-Abl Signaling: At the Crossroad in Neurodegenerative Diseases? *Int. J. Cell Biol.* **2012**, *2012*, 683097. [CrossRef]

73. Najafi-Shoushtari, S.H.; Kristo, F.; Li, Y.; Shioda, T.; Cohen, D.E.; Gerszten, R.E.; Näär, A.M. MicroRNA-33 and the SREBP Host Genes Cooperate to Control Cholesterol Homeostasis. *Science* **2010**, *328*, 1566–1569. [CrossRef] [PubMed]
74. Rottiers, V.; Najafi-Shoushtari, S.H.; Kristo, F.; Gurumurthy, S.; Zhong, L.; Li, Y.; Cohen, D.E.; Gerszten, R.E.; Bardeesy, N.; Mostoslavsky, R.; et al. Micrornas in Metabolism and Metabolic Diseases. *Cold Spring Harb. Symp. Quant. Biol.* **2011**, *76*, 225–233. [CrossRef] [PubMed]
75. Marquart, T.J.; Allen, R.M.; Ory, D.S.; Baldán, Á. MiR-33 Links SREBP-2 Induction to Repression of Sterol Transporters. *Proc. Natl. Acad. Sci. USA* **2010**, *107*, 12228–12232. [CrossRef]
76. Rayner, K.J.; Suárez, Y.; Dávalos, A.; Parathath, S.; Fitzgerald, M.L.; Tamehiro, N.; Fisher, E.A.; Moore, K.J.; Fernández-Hernando, C. MiR-33 Contributes to the Regulation of Cholesterol Homeostasis. *Science* **2010**, *328*, 1570–1573. [CrossRef]
77. Dávalos, A.; Goedeke, L.; Smibert, P.; Ramírez, C.M.; Warrier, N.P.; Andreo, U.; Cirera-Salinas, D.; Rayner, K.; Suresh, U.; Pastor-Pareja, J.C.; et al. MiR-33a/b Contribute to the Regulation of Fatty Acid Metabolism and Insulin Signaling. *Proc. Natl. Acad. Sci. USA* **2011**, *108*, 9232–9237. [CrossRef]
78. Gerin, I.; Clerbaux, L.-A.; Haumont, O.; Lanthier, N.; Das, A.K.; Burant, C.F.; Leclercq, I.A.; MacDougald, O.A.; Bommer, G.T. Expression of MiR-33 from an SREBP2 Intron Inhibits Cholesterol Export and Fatty Acid Oxidation. *J. Biol. Chem.* **2010**, *285*, 33652–33661. [CrossRef]
79. Horton, J.D.; Goldstein, J.L.; Brown, M.S. SREBPs: Activators of the Complete Program of Cholesterol and Fatty Acid Synthesis in the Liver. *J. Clin. Investig.* **2002**, *109*, 1125–1131. [CrossRef]
80. Fernández-Hernando, C.; Moore, K.J. MicroRNA Modulation of Cholesterol Homeostasis. *Arterioscler. Thromb. Vasc. Biol.* **2011**, *31*, 2378–2382. [CrossRef]
81. Goedeke, L.; Vales-Lara, F.M.; Fenstermaker, M.; Cirera-Salinas, D.; Chamorro-Jorganes, A.; Ramírez, C.M.; Mattison, J.A.; de Cabo, R.; Suárez, Y.; Fernández-Hernando, C. A Regulatory Role for MicroRNA 33* in Controlling Lipid Metabolism Gene Expression. *Mol. Cell. Biol.* **2013**, *33*, 2339–2352. [CrossRef]
82. Feng, X.; Zou, B.; Nan, T.; Zheng, X.; Zheng, L.; Lan, J.; Chen, W.; Yu, J. MiR-25 Enhances Autophagy and Promotes Sorafenib Resistance of Hepatocellular Carcinoma via Targeting FBXW7. *Int. J. Med. Sci.* **2022**, *19*, 257–266. [CrossRef] [PubMed]
83. Yuan, W.; Zhan, X.; Liu, W.; Ma, R.; Zhou, Y.; Xu, G.; Ge, Z. Mmu-MiR-25-3p Promotes Macrophage Autophagy by Targeting DUSP10 to Reduce Mycobacteria Survival. *Front. Cell. Infect. Microbiol.* **2023**, *13*, 1120570. [CrossRef] [PubMed]
84. Dong, W.; Wang, G.; Feng, J.; Li, P.; Wang, R.; Lu, H.; Lu, W.; Wang, C.; Wang, X.; Chen, H.; et al. MiR-25 Blunts Autophagy and Promotes the Survival of Mycobacterium Tuberculosis by Regulating NPC1. *iScience* **2022**, *25*, 104279. [CrossRef]
85. Rogers, T.J.; Christenson, J.L.; Greene, L.I.; O'Neill, K.I.; Williams, M.M.; Gordon, M.A.; Nemkov, T.; D'Alessandro, A.; Degala, G.D.; Shin, J.; et al. Reversal of Triple-Negative Breast Cancer EMT by MiR-200c Decreases Tryptophan Catabolism and a Program of Immunosuppression. *Mol. Cancer Res.* **2019**, *17*, 30–41. [CrossRef] [PubMed]
86. O'Neill, K.I.; Kuo, L.-W.; Williams, M.M.; Lind, H.; Crump, L.S.; Hammond, N.G.; Spoelstra, N.S.; Caino, M.C.; Richer, J.K. NPC1 Confers Metabolic Flexibility in Triple Negative Breast Cancer. *Cancers* **2022**, *14*, 3543. [CrossRef]
87. Chen, X.; Liang, H.; Zhang, J.; Zen, K.; Zhang, C.-Y. Secreted MicroRNAs: A New Form of Intercellular Communication. *Trends Cell Biol.* **2012**, *22*, 125–132. [CrossRef]
88. Tarallo, A.; Carissimo, A.; Gatto, F.; Nusco, E.; Toscano, A.; Musumeci, O.; Coletta, M.; Karali, M.; Acampora, E.; Damiano, C.; et al. MicroRNAs as Biomarkers in Pompe Disease. *Genet. Med.* **2019**, *21*, 591–600. [CrossRef]
89. van Niel, G.; D'Angelo, G.; Raposo, G. Shedding Light on the Cell Biology of Extracellular Vesicles. *Nat. Rev. Mol. Cell Biol.* **2018**, *19*, 213–228. [CrossRef]
90. Strauss, K.; Goebel, C.; Runz, H.; Möbius, W.; Weiss, S.; Feussner, I.; Simons, M.; Schneider, A. Exosome Secretion Ameliorates Lysosomal Storage of Cholesterol in Niemann-Pick Type C Disease. *J. Biol. Chem.* **2010**, *285*, 26279–26288. [CrossRef]
91. Godfrey, C.; Desviat, L.R.; Smedsrød, B.; Piétri-Rouxel, F.; Denti, M.A.; Disterer, P.; Lorain, S.; Nogales-Gadea, G.; Sardone, V.; Anwar, R.; et al. Delivery Is Key: Lessons Learnt from Developing Splice-Switching Antisense Therapies. *EMBO Mol. Med.* **2017**, *9*, 545–557. [CrossRef] [PubMed]
92. Coutinho, M.F.; Matos, L.; Santos, J.I.; Alves, S. RNA Therapeutics: How Far Have We Gone? *Adv. Exp. Med. Biol.* **2019**, *1157*, 133–177. [CrossRef] [PubMed]
93. Hammond, S.M.; Aartsma-Rus, A.; Alves, S.; Borgos, S.E.; Buijsen, R.A.M.; Collin, R.W.J.; Covello, G.; Denti, M.A.; Desviat, L.R.; Echevarría, L.; et al. Delivery of Oligonucleotide-Based Therapeutics: Challenges and Opportunities. *EMBO Mol. Med.* **2021**, *13*, e13243. [CrossRef]
94. Roberts, T.C.; Langer, R.; Wood, M.J.A. Advances in Oligonucleotide Drug Delivery. *Nat. Rev. Drug Discov.* **2020**, *19*, 673–694. [CrossRef] [PubMed]
95. Ho, P.T.B.; Clark, I.M.; Le, L.T.T. MicroRNA-Based Diagnosis and Therapy. *Int. J. Mol. Sci.* **2022**, *23*, 7167. [CrossRef]
96. Furtado, D.; Cortez-Jugo, C.; Hung, Y.H.; Bush, A.I.; Caruso, F. MRNA Treatment Rescues Niemann-Pick Disease Type C1 in Patient Fibroblasts. *Mol. Pharm.* **2022**, *19*, 3987–3999. [CrossRef]

Disclaimer/Publisher's Note: The statements, opinions and data contained in all publications are solely those of the individual author(s) and contributor(s) and not of MDPI and/or the editor(s). MDPI and/or the editor(s) disclaim responsibility for any injury to people or property resulting from any ideas, methods, instructions or products referred to in the content.

Attachment 2

Challenges on the Definitive Diagnosis of Niemann-Pick Type C – Leaky Variants and Alternative Transcripts

Marisa Encarnação, Isaura Ribeiro, Hugo David, Maria Francisca Coutinho, Dulce Quelhas & Sandra Alves

Review published in *Genes*, **2023**

genes

MDPI

Review

Challenges in the Definitive Diagnosis of Niemann–Pick Type C—Leaky Variants and Alternative Transcripts

Marisa Encarnação [1,2,3], Isaura Ribeiro [4,5,6], Hugo David [1,2,3,7], Maria Francisca Coutinho [1,2,3], Dulce Quelhas [4,5,6] and Sandra Alves [1,2,3,*]

1 Research and Development Unit, Department of Human Genetics, National Institute of Health Doutor Ricardo Jorge, INSA I.P., Rua Alexandre Herculano, 321, 4000-055 Porto, Portugal; marisa.encarnacao@insa.min-saude.pt (M.E.); hugo.david@insa.min-saude.pt (H.D.); francisca.coutinho@insa.min-saude.pt (M.F.C.)
2 Center for the Study of Animal Science-Instituto de Ciências, Tecnologias e Agroambiente da Universidade do Porto, CECA-ICETA, University of Porto, Praça Gomes Teixeira, Apartado 55142, 4051-401 Porto, Portugal
3 Associate Laboratory for Animal and Veterinary Sciences, AL4AnimalS, Faculdade de Medicina Veterinária Avenida da Universidade Técnica, 1300-477 Lisboa, Portugal
4 Laboratório de Bioquímica Genética, Serviço de Genética Laboratorial, Centro de Genética Médica Jacinto Magalhães, Centro Hospitalar e Universitário de Santo António (CHUdSA), 4099-001 Porto, Portugal; isauraribeiro.cgm@chporto.min-saude.pt (I.R.); dulce.quelhas@chporto.min-saude.pt (D.Q.)
5 UMIB-Unit for Multidisciplinary Research in Biomedicine, ICBAS, University of Porto, 4099-002 Porto, Portugal
6 ITR—Laboratory for Integrative and Translational Research in Population Health, 4050-600 Porto, Portugal
7 Biology Department, Faculty of Sciences, University of Porto, Rua do Campo Alegre, 4169-007 Porto, Portugal
* Correspondence: sandra.alves@insa.min-saude.pt

Abstract: Niemann–Pick type C (NPC, ORPHA: 646) is a neuro-visceral, psychiatric disease caused predominantly by pathogenic variants in the *NPC1* gene or seldom in *NPC2*. The rarity of the disease, and its wide range of clinical phenotypes and ages of onset, turn the diagnosis into a significant challenge. Other than the detailed clinical history, the typical diagnostic work-up for NPC includes the quantification of pathognomonic metabolites. However, the molecular basis diagnosis is still of utmost importance to fully characterize the disorder. Here, the authors provide an overview of splicing variants in the *NPC1* and *NPC2* genes and propose a new workflow for NPC diagnosis. Splicing variants cover a significant part of the disease-causing variants in NPC. The authors used cDNA analysis to study the impact of such variants, including the collection of data to classify them as leaky or non-leaky pathogenic variants. However, the presence of naturally occurring spliced transcripts can misdiagnose or mask a pathogenic variant and make the analysis even more difficult. Analysis of the *NPC1* cDNA in NPC patients in parallel with controls is vital to assess and detect alternatively spliced forms. Moreover, nonsense-mediated mRNA decay (NMD) analysis plays an essential role in evaluating the naturally occurring transcripts during cDNA analysis and distinguishing them from other pathogenic variants' associated transcripts.

Keywords: Niemann–Pick type C; splicing variants; leaky variants; *NPC1* gene; molecular diagnosis

check for updates

Citation: Encarnação, M.; Ribeiro, I.; David, H.; Coutinho, M.F.; Quelhas, D.; Alves, S. Challenges in the Definitive Diagnosis of Niemann–Pick Type C—Leaky Variants and Alternative Transcripts. *Genes* **2023**, *14*, 1990. https://doi.org/10.3390/genes14111990

Academic Editor: Andreas R. Janecke

Received: 29 September 2023
Revised: 17 October 2023
Accepted: 23 October 2023
Published: 25 October 2023

Copyright: © 2023 by the authors. Licensee MDPI, Basel, Switzerland. This article is an open access article distributed under the terms and conditions of the Creative Commons Attribution (CC BY) license (https://creativecommons.org/licenses/by/4.0/).

1. Introduction

Lysosomal storage disorders (LSDs) are a group of about 70 inherited diseases, most of which are quite rare and present with vast clinical heterogeneity, ranging from severe, early-onset diseases to milder forms, of later onset. This remarkable variability may be observed not only between different diseases from the same group but also—and most importantly—amongst patients suffering from the same exact disease. Overall, this clinical heterogeneity has a direct impact on their diagnosis. Over the past several years, the number of available treatments for patients with LSDs has rapidly increased, namely, enzyme replacement and substrate reduction therapies, the use of molecular chaperones, gene therapy, and bone

marrow transplant, among others [1]. Nevertheless, molecular diagnosis is the ultimate and essential step to provide access to therapy. The identification of biallelic nonsense and frameshift variants, as well as missense variants in conserved regions, provides a straightforward direct gene target analysis. Nevertheless, next-generation sequencing (NGS)-targeted panels for LSD-associated genes or other NGS methodologies provide a quick way to identify the molecular defect underlying diseases with such clinical variability [2]. However, in specific cases, the molecular diagnosis timeline can be even longer, when such pathogenic variants affect splicing and mRNA processing. These situations represent an additional challenge, with the identification and effect prediction of abnormal transcripts. In addition, some naturally spliced forms can raise another layer of difficulty and even mimic the molecular defect and its impact on splicing. The *IDS*, *GNPTAB*, and *NPC1* genes—whose pathogenic variants underly Mucopolysaccharidosis type II, Mucolipidosis types II or III, and Niemann–Pick type C, respectively—are some examples of LSD-associated genes with naturally occurring spliced forms already reported in the databases (https://www.uniprot.org/uniprotkb/P22304/entry#sequences (accessed on 28 September 2023)); (https://www.uniprot.org/uniprotkb/Q3T906/entry#sequences (accessed on 28 September 2023)); and (https://www.uniprot.org/uniprotkb/O15118/entry#sequences (accessed on 28 September 2023)).

Niemann–Pick type C (NPC, ORPHA: 646) in particular is a devastating neurodegenerative LSD, caused by loss-of-function variants in either the *NPC1* gene (in approximately 95% of cases) [3] or the *NPC2* gene (in 5% of cases). Analysis of next-generation sequencing (NGS) data sets indicates that the incidence rate of NPC for the classical clinical manifestations is ~1:90,000 but suggests that, for the late-onset phenotype or variant forms, the frequency might be higher [4].

Overall, the wide range of clinical phenotypes and the different ages of onset it may present with, together with the rarity of the disease and the fact it may be caused by mutations in two different genes, make its diagnosis a significant challenge. At a clinical level, NPC's infantile forms present varying degrees of neurologic involvement and frequently present visceral manifestations, such as splenomegaly, hepatomegaly, neonatal jaundice, and hyperbilirubinemia [5,6]. Adolescent- or adult-onset NPC, on the other hand, presents with varying combinations of progressive neurologic deficits, e.g., ataxia, dystonia and/or dementia, vertical supranuclear gaze palsy (VSGP), or major psychiatric illness, including schizophrenia, depression, and psychosis, among others [6].

That is why a definitive NPC diagnosis must rely on additional laboratorial analyses. The classical method of establishing a NPC diagnosis relies on the filipin staining of cultured fibroblasts from skin biopsies [7]. This is a microscopy-based test that takes advantage of the fact that filipin specifically binds to unesterified cholesterol, allowing the evaluation of cholesterol accumulation in the perinuclear vesicular compartments [8]. This rationale is consistent with the current assumption that the impaired egress of cholesterol from the late endosome/lysosome (LE/L) is a key element of NPC pathogenesis. Nevertheless, even the most severely affected patients may fail to be diagnosed through this method [9,10]. In fact, patients with proven NPC disease may present with variable filipin patterns, from typical "classical" or "intermediate" to "atypical" or "variant" ones, which fail to be classified as a NPC by filipin staining alone. Recent advances in the field are actively contributing to an increase in the detection of NPC patients. Among those advances is the development of rapid and reliable biomarkers, including oxysterols [11–13], lysosphingomyelin derivatives [14,15], and bile acids [16,17], even though none of them are specific to NPC [18]. However, *N*-palmitoyl-*O*-phosphocholineserine, (PPCS, previously known as lysosphingomyelin-509) has been shown to be elevated in the plasma and dried blood spots of NPC patients [19,20]. But, these novel biomarkers are not the sole contributors to the increased recognition of this disorder and its more expedited diagnosis. The increased availability of NGS has also contributed to the update of the overall NPC diagnostic algorithm while actively contributing to an increase in the number of positive molecular NPC diagnoses. Currently, there are a number of fully described diagnostic

workflows for NPC [18], which may slightly vary between different labs depending on the tests each of them has available. However, *NPC1* and *NPC2* molecular analysis is mandatory in all of them and usually represents the ultimate step towards diagnosis [21]. Indeed, a rapid molecular diagnosis of a potential NPC patient is essential, not just for swift access to available therapies (currently miglustat is the only one approved within the European Union) but also to slow the progression of the disease and ultimately because it is the sole method of offering prenatal diagnosis to affected families [22].

2. A Brief Overview of the Diagnostic Workflow for Niemann-Pick Type C

2.1. The Picture in Black and White: Standard Workflows and Straightforward Diagnoses

In general, following a suspicious timeline of clinical manifestation and/or a biomarker profile consistent with NPC, the next step is the *NPC1* and *NPC2* sequencing of the index case (Figure 1) and subsequent segregation studies of the parents [18]. The *NPC1* gene (MIM# 607623) comprises 25 exons and over 600 disease-causing variants have been reported to date [23], most of which encode missense alleles. For the *NPC2* gene (MIM# 601015), thirty-four disease-causing variants have been described and four of them are splicing (https://my.qiagendigitalinsights.com/, HGMD Professional 2023.3, accessed on 17 October 2023). Among the most common *NPC1* pathogenic variants are p.Ile1061Thr, found in 20% of patients of Western European descent [24], and p.Pro1007Ala, associated with milder forms of the disease [25,26]. In Portugal, however, the most frequent disease-causing variant is the missense p.Ala1035Val, which accounts for 15–20% of the affected cases (unpublished data transmitted by Quelhas D and Ribeiro I); it was recently reported as the most common in patients from Latin America [27].

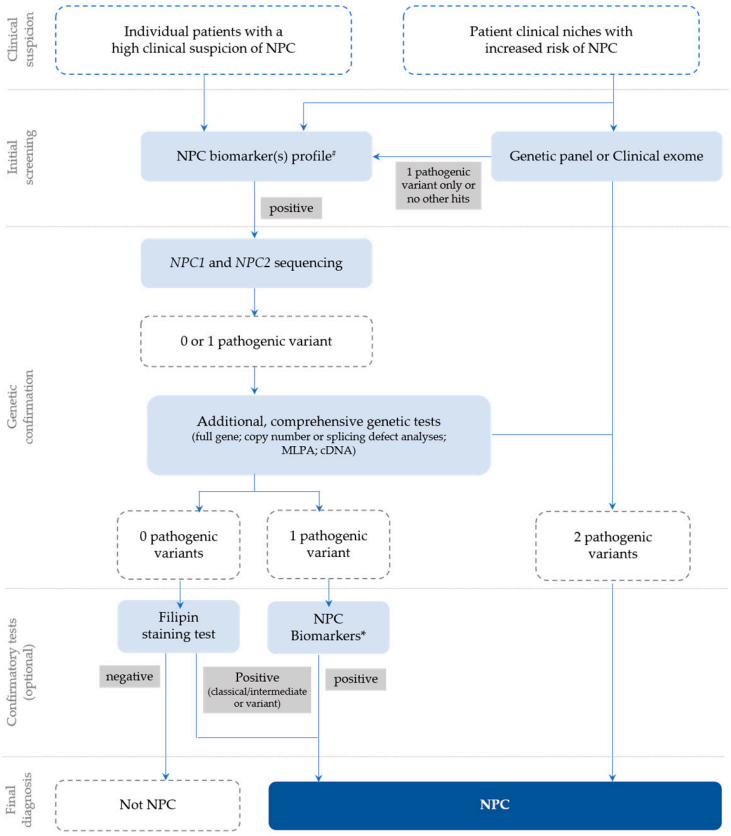


Figure 1. Recommendations for the detection and diagnosis of NPC, based on Patterson et al. [18] with slight updates to accommodate the most recent technologies, which are now commonly used for diagnostic purposes (e.g., clinical exome), as well as the current nomenclature. # Negative biomarkers may be suggestive that the diagnosis is not NPC; * Biomarker(s) profiling (if not initially conducted) or extended biomarker(s) profiling (in addition to those already conducted).

However, the highly polymorphic nature of *NPC1* can muddle diagnostic conclusions and turn the interpretation of novel variants of unknown significance (VUSs) into a challenge. In addition, cDNA sequencing is necessary to address mRNA processing in the presence of silent variants, or other VUSs, including missense variants near the (exonic or intronic) splicing regions.

More specifically, the cDNA analysis of exonic variants may help confirm the pathogenic effect of variants predicted to affect splice sites [28]. Several splice-site pathogenic variants have been identified in NPC and in many other LSDs [29]. In some instances, these variants do not allow the generation of functional mRNAs [30]. However, they are leaky and frequently produce a small percentage of correctly spliced and translated transcripts, leading to attenuated phenotypic expression of the disease [31].

Whenever conventional gDNA analysis leads to a single variant identification, the genetic study focuses on detecting the second damaging variant. For this reason, complementary studies, such as multiplex ligation-dependent probe amplification (MLPA) in gDNA to cover intragenic deletions or duplications or cDNA sequencing, may also be required for proper diagnosis of NPC [18,22]. As straightforward as this approach may sound, reaching a conclusive molecular diagnosis of NPC may, in some cases, be harder than it seems.

2.2. The Grayscale Image

Among the confounding factors that can either hinder or delay a definitive diagnosis of NPC is the presence of genetic variants affecting the normal *NPC1* and *NPC2* splicing patterns.

Several pathogenic variants affecting both *NPC1* and *NPC2* mRNA splicing, occurring in intronic and exonic regions, have already been described [32]. Although quite rare, three pathogenic intronic variants have been described in the *NPC2* gene [12,28,33]. One additional variant affecting splicing was found in both healthy controls and patients [4].

Interestingly, missense variants, such as the c.1553G>A (p.Arg518Gln), were proven to have an additional impact on the splicing mechanism in the *NPC1* gene, as long as they occur in the coding exons' splicing regulatory sequences [28,34–36].

Following a combined approach (gDNA and cDNA studies), we have previously proven the impact of a silent variant in the *NPC1* gene that leads to exon skipping—p.Val562= (Figure 2) [37]. This variant is located in Exon 11 and was initially reported in Spanish NPC patients and classified, at that time, as a VUS or polymorphism, after a genomic DNA study [38].



Figure 2. Schematic representation of the silent variants in the *NPC1* exonic region affecting splicing and the effect on splicing based on in silico predictions (Human Splicing Finder—HSF and EX-SKIP tools and Maxent). P.Val562= localization on Exon 11 (red) and the effect on splicing based on in silico predictions. EX-SKIP compares the Exonic Splicing Enhancer (ESE)/Exonic Splicing Silencer (ESS) profile of a wild type (WT) and a mutated allele to determine if a specific exonic variant increases the chance of exon skipping. It calculates the total number of ESSs, ESEs, and their ratio. The p.Val562= mutant is associated with a change in the ESE/ESS ratio, which is compatible with a higher chance of exon skipping than in the WT allele. In addition, the HSF (a tool to predict the effects of pathogenic variants on splicing signals or to identify splicing motifs in any human sequence) predicts that the p.Val562= mutant leads to the creation of an ESS site. It involves the cDNA sequences CTTGTAAT

(orange) [39] and CTTGTA (yellow) [40], which might be associated with a potential alteration of splicing. In the case of the silent variant p.Val562=, functional cDNA analysis was performed [19], confirming the bioinformatic prediction of Exon 11 skippings.

In our previous study, cDNA analysis of the affected patient and his mother (heterozygous carrier) made it possible to identify a transcript with the skipping of Exon 11. This caused a shift in the reading frame and the emergence of a premature termination codon [37], leading to its reclassification as a disease-causing variant. Importantly, the p.Val562= variant was found not only in three independent Portuguese families but also in previously reported Spanish [38] and French patients [41] (Table 1). In a French cohort, this variant was reported in heterozygosity with the p.Ile1061Thr in two siblings [41,42]; however, its functional consequence was not ascertained. Despite the sequencing of five overlapping *NPC1* cDNA fragments in the two siblings carrying the p.Val562=, the pathogenic effect of the variant was considered unknown (Supplementary Table S1, patients 25 and 25 from Nadjar et al. [41]). The most likely explanation is the degradation of the aberrant transcript by NMD. There is no information about the frequency of this variant in gnomAD. Looking to other repositories, this variant is only reported in a database from Tubingen University (NPC-db2; https://medgen.medizin.uni-tuebingen.de/NPC-db2/search.php (accessed on 28 September 2023))—it was found in one patient but not in the controls. No information was provided regarding the homo- or heterozygosity of that patient; however, both in the literature and in our cohort, only heterozygous patients were identified.

Table 1. Patients identified as compound heterozygous for the splicing variant c.1686G>A in the *NPC1* gene.

Patient	Origin	Genotype	Age at Neurologic Onset (Years)	Clinical Form	Filipin Staining	PPCS# (Control Range 0.3–3.9 MoM)	Reference
P1	Portugal	c.1514T>G (p.Val505Gly) c.1686G>A (p.Val562=)	6	Juvenile	Variant	12.4	[37]
P2	Portugal	c.1552C>T (p.Val518W) c.1686G>A (p.Val562=)	7	Juvenile	Variant	4.3	[37]
P2′	Portugal	c.1552C>T (p.Val518W) c.1686G>A (p.Val562=)	7	Juvenile	Variant	3.2	[37]
P3	Portugal	c.1686G>A (p.Val562=) c.3019C>G (p.Pro1007Ala)	18	Adult	n.a.	6.4	This study
P4	Spain	c.1436G>A (p.Cys479Tyr) c.1686G>A (p.Val562=)	9	Juvenile	Variant	n.a.	[38]
P5	France	c.1686G>A (p.Val562=) c.3182T>C (p.Ile1061Thr)	18	Adult	Intermediate	n.a.	[41]
P5′	France	c.1686G>A (p.Val562=) c.3182T>C (p.Ile1061Thr)	18	Adult	Intermediate	n.a.	[41]

Patients P2 and P2′, P5 and P5′ are siblings, GeneBank references: *NPC1*: NM_000271.5, Transcript ENST00000269228.10, n.a.: information not available/not applicable, MoM: multiple of median, # *N*-palmitoyl-*O*-phosphocholineserine (PPCS): formerly known as lyso-SM-509, n.a.: information not available/not applicable.

Another example of a NPC-causing variant associated with complex mRNA processing is the c.190+5G>A variant. This particular variant is located not in *NPC1*, the most obvious candidate to harbor a disease-causing mutation, but in Intron 2 of the *NPC2* gene. Again, this variant seems to be associated with a milder clinical course since both reported patients—two siblings homozygous for this variant—presented with a juvenile onset of the neurological disease and prolonged survival. A more detailed study showed that this splice variant generated multiple abnormal mRNAs [43]. However, in fibroblasts, a very small proportion of the correctly spliced transcript was also observed. Although this was not sufficient in producing enough NPC2 protein for Western Blot detection, the presence of low levels of functional protein presumably accounts for the milder clinical course. The

question of whether different tissues could display variable levels of abnormally/normally spliced RNA transcribed from the c.190+5G>A variant can also be raised.

Ideally, however, these variants should be easily detected whenever an adequate cDNA analysis of any of the involved genes is performed. Still, that is not always the case, as we will demonstrate with a few practical examples.

2.2.1. Splice Site Prediction Software

In light of a high NPC-suspicion index (a high suspicion score is assigned to patients who present with either two of seven key symptoms or VSGP alone) [44], the synonymous and nonsynonymous variants in either *NPC1* or *NPC2* should be studied. The predicted impact of potential splice site variants can be analyzed with the splicing prediction module of Alamut Visual software v.2.11 (Interactive Biosoftware, Rouen, France), which integrates data from three methods: Splice Site Prediction by Neural Network (NNSplice), MaxEntScan, and Human Splicing Finder (HSF) [39]. In the past few years, the SpliceAI algorithm has demonstrated the highest sensitivity and specificity when compared with other tools [45] and is nowadays the most widely recommended [46]. However, cDNA analysis is useful to study the effect of the novel variants on splicing, as well as to improve the current knowledge of the underlying molecular mechanisms and, essentially, to analyze if the variants are leaky. Other than cDNA analysis, other procedures can help to assess if a variant is leaky, namely, cloning procedures; allele-specific RNA expression quantification using PCR-based methods, among others; and procedures depending on the studied cases.

2.2.2. Naturally Occurring Spliced Forms of mRNA May Mask Disease-Associated Transcripts

While analyzing cDNA samples obtained from the skin fibroblasts of NPC patients and controls, we observed the presence of an additional amplification product comprising Exons 9, 12, and 13 and missing Exons 10 and 11. This was detected both with and without cycloheximide (CHX) treatment while the pathogenic transcript due to p.Val562= was responsive to CHX. CHX is a potent NMD inhibitor that can be used to prevent the degradation of PTC-containing transcripts. In the case of disease-causing variants that affect splicing, the visualization of the aberrant transcripts can be tricky and consequently overlooked. When patients' cells are available, the treatment of cell cultures with CHX can significantly increase the signal of the aberrant transcripts that have PTCs and are, thus, degraded by NMD but do not have any effect on the naturally occurring transcripts (a detailed protocol is described in Encarnação et al., 2020 [37].

This observation prompted us to further analyze the transcript, searching for its presence in other tissue samples. After a number of independent assessments with different primer sets and PCR conditions, it was possible to observe the presence of a smaller *NPC1* transcript, amplified in both controls and NPC patients, missing *NPC1* Exons 10 and 11. This alternative transcript may be detected after RT-PCR electrophoresis as a lower molecular weight band. This may be confusing when analyzing actual aberrant transcripts resulting from real pathogenic variants causing the constitutive splicing errors of the *NPC1* gene. This transcript lacking Exons 10 and 11 has already been reported in the Ensembl genome database (Transcript ID ENST00000591051.1).

Interestingly, this alternative skipping produces an in-frame transcript and the overall *NPC1* reading frame remains unaltered, despite missing 204 nucleotides, corresponding to 64 coding triplets.

In order to verify the expression levels of this transcript in other cells/tissues, RNA was extracted from blood samples. cDNA was then synthesized using the same amount of RNA as that used for fibroblasts samples and both transcripts were detected. Nevertheless, their expression levels in blood seemed significantly lower than those of fibroblasts. That pattern is in full agreement with previous reports on mRNA expression in normal human tissues.

The presence of this naturally occurring *NPC1* alternatively spliced mRNA is actually in accordance with the in silico estimates on splice junction strengths predicted by the MaxEntScan. This tool is based on the approach for modeling the sequences of short

sequence motifs, such as those involved in RNA splicing. It simultaneously scores non-adjacent as well as adjacent dependencies between positions [5]. Interestingly, when using the tool to evaluate these regions in *NPC1* Exons 9, 10, 11, and 12, we observed that the lowest 3′ss score was predicted for Exon 10 while the weakest 5′ss was predicted for Exon 11. This is in accordance with our data and can justify the existence of a naturally occurring *NPC1* transcript, which does not encompass Exons 10 and 11. If translated, one such differently spliced form would give rise to a protein, which would not include amino acids 519 to 586 (68 amino acids in total). That segment is located in Middle Luminal Domain 3 (MLD3), between transmembrane domains (TMDs) II and III of the NPC1 protein (Figure 3). MLD3 mediates the transfer of NPC2-bound cholesterol to the sterol binding domain located at the *N*-terminal domain of NPC1 and also the Ebola virus binding [47,48]. There are 20 disease-causing missense variants in this region (HGMD Professional 2023.3 in October 2023) but this is not the most conserved region of the NPC1 protein. Interestingly, however, the predicted size of that protein product would be 1210 aa but none of the transcripts listed in Ensembl match that prediction. Still, when a more detailed analysis of those transcripts is performed, namely, by Clustal omega multiple sequence alignment, it becomes evident that there is one *NPC1* transcript that does lack Exons 10 and 11 (ID ENST00000591051.1). Remarkably, however, that is not the only difference between this naturally occurring transcript and the wild type one. There is a significant difference between the transcription initiation of both transcripts, with the ENST00000591051.1 transcript Exon 1 corresponding to a sequence that partially overlaps Exon 6 of the wild-type transcript, thus comprising only 18 coding exons, in opposition to the wild-type one, which spans 25 exons.

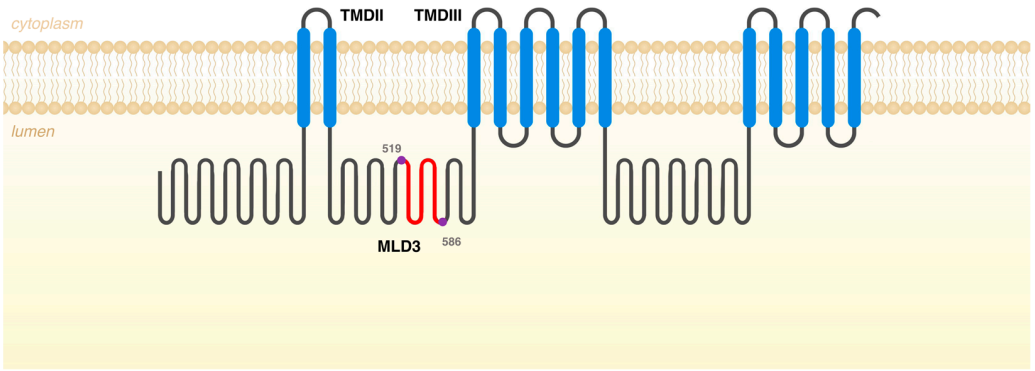


Figure 3. Schematic representation of NPC1 protein with the different domains. In red are the missing amino acids, if the differently spliced form would give rise to a protein. That segment is located in Middle Luminal Domain 3 (MLD3), between transmembrane domains (TMDs) II and III, and it contains the amino acids 519 to 586 (68 amino acids in total).

This is yet another reason for us to highlight its presence under some amplification conditions as it may confound the analysis of cDNA patterns in that region, with serious implications for the classification of pathogenic variants predicted to impact splicing.

3. Variants in the *NPC1* Gene That Affect Splicing

Pathogenic variants that affect pre-mRNA splicing account for at least 15% of disease-causing mutations [49]. Most of these variants affect 5′ and 3′ss, the polypyrimidine tract, the branch-point sequence, and also *cis*-acting elements (exonic/intronic splicing enhancers and silencers). Other variants create novel splicing sequences deeply within introns, causing the abnormal inclusion of intron sequences. All of these variants lead to the production of abnormal transcripts that usually contain PTCs and are degraded by nonsense-mediated mRNA decay (NMD) [50]. Even exonic variants (missense and synonymous) may affect splicing, having a completely different effect from what was expected [51]. Therefore, both gDNA and cDNA should be analyzed.

The *NPC1* gene contains 25 exons and spans 55 kb from the base pairs (23, 531, 442) to 23, 586, 506 on the reverse strand of chromosome 18 at 18q11.2 (NC_000018.10); here we report on 53 published pathogenic variants affecting splicing.

Seven of them are exonic, two are synonymous, five are missense (Tables 1 and 2), and forty-six are intronic variants (Table 3), mainly affecting the 3′ss and the 5′ss; however, there are also variants reported in the branch point as well as deep-intronic variants.

Table 2. Exonic splicing variants in the *NPC1* gene.

Splicing Variant	Location	Impact on mRNA and Protein Levels	Clinical Form	Reference
c.1553G>A	Exon 9	Changes amino acid and induces a splicing error. The variant occurs in the last nucleotide of Exon 9. It induces the skipping of Exon 9 (227 bp-deletion), leading to a 75 amino acid deletion and a frameshift, creating a premature termination codon (PTC) at position 499 of Exon 10.	Late infantile	[36]
c.2292G>A (also known as IVS16-82G>A)	Exon 15	Silent variant (p.Ala764=). Creation of a splice site in Exon 15, generating a transcript with a 48 bp in-frame deletion (750del16aa).	n.a.	[26]
c.2599C>T	Exon 17	Changes amino acid but also induces a splicing error. In silico prediction, only by Neural Network Splice Site Prediction.	n.a.	[28]
c.2911G>C	Exon 19	Changes amino acid but also induces a splicing error. In silico prediction, only by Neural Network Splice Site Prediction.	n.a.	[28]
c.3422T>G	Exon 22	Activation of a new donor splice site in which the 3′ end of Exon 22 is deleted.	n.a.	[34]
c.3754G>C (previously described as p.Gly1252Arg)	Exon 24	Affects the last nucleotide of Exon 24 generating skipping of Exon 24.	Late infantile	[38,52]

n.a.: information not available/not applicable.

Table 3. Intronic splicing variants in *NPC1* gene.

Genotype	Location	Impact on mRNA and Protein Levels (as Described in the Reference Paper)	Age at Neurologic Onset (Years)/Clinical Manifestation	Ref
c.57+4A>G	Intron 1	No cDNA analysis was performed. Only in silico analysis was described.	Ataxia at the age of 20.	[53]
c.58−3T>G	Intron 1	No cDNA analysis was published.	Identified in compound heterozygosity with p.Val1165Met in two siblings from an Italian cohort. One presents a late infantile form and the other a juvenile form.	[54]
c.58-3281C>G	Intron 1	Pseudoexon insertion, creating a novel acceptor region and activating a cryptic donor splice site.	n.a.	[52]
c.58-3290G>A	Intron 1	Partial retention of Intron 1.	At 12 years old when in compound heterozygosity with the p.Gly992Arg variant.	[41]
c.181-6T>A	Intron 2	Skipping of Exon 2.	At 20 years old when in compound heterozygosity with the p.Tyr475Cys variant.	[41]
c.181-2A>G	Intron 2	Generation of a novel splicing acceptor site located one nucleotide (NT) upstream of the canonical 3′ss. Thus, the last NT of Intron 2 is retained within the mature transcript, causing a frameshift in the open reading frame and the generation of a PTC that would eventually result in the synthesis of a truncated protein.	At 40 years when in compound heterozygosity with the variant Gly1012Cys.	[41,54]
c.287+1G>A	Intron 3	Located at the 5′ donor splice site of Intron 3. This location has a 0.98 score prediction as a splice site (Neural Network) and a confidence of 0.76 as a donor splice site (NetGene2), likely disturbing normal splicing and altering protein features (Mutation Taster). According to recommendations of the ACMG, this variant was classified as pathogenic.	At 4 months when in compound heterozygosity with the variant (p.Arg1186His). NPC was confirmed by a filipin test on a fibroblast cell culture at 4.5 years old.	[55]
c.464-2A>C	Intron 4	Affects the 3′ acceptor splice site of Intron 4, leading to the activation of the downstream cryptic splice site (score, 0.98), predicted to be a genomic region overlapping Exon–Intron 5. A possible consequence could be an unstable aberrantly spliced transcript, carrying a premature translation stop codon, possibly subjected to NMD. cDNA analysis showed degradation of the patient's mRNA.	Identified in two siblings. The second disease-causing variant was not identified. First neurologic symptoms at 2 and 3 years old.	[56]
c.882-40T>A	Intron 6	n.a.	At 12 years, identified in compound heterozygosity with the p.Ile1061Thr variant.	[57]

Table 3. *Cont.*

Genotype	Location	Impact on mRNA and Protein Levels (as Described in the Reference Paper)	Age at Neurologic Onset (Years)/Clinical Manifestation	Ref
c.882-28A>G	Intron 6	It occurs in a conserved adenosine of a putative branch point sequence. The Exon 6–Exon 8 junction in this mRNA causes a frameshift and a premature stop codon, predicted to result in a truncated protein. The skipping of Exon 7 was confirmed both in the patient´s fibroblasts (cDNA analysis) and in cells expressing minigenes.	Identified in two siblings in compound heterozygosity with p.Arg978Cys, both with the first neurological symptoms occurring during their 20 s.	[58]
c.882-28A>T	Intron 6	The conserved adenosine residue of the lariat branch point in Intron 6 causes an abnormally spliced mRNA with the complete skipping of Exon 7 (c.882_954del73). The loss of Exon 7 disrupts the reading frame, leading to a PTC, which activates mRNA degradation by the NMD process. This was confirmed by cDNA analysis.	Identified in one Spanish patient with the late infantile form in compound heterozygosity with p.Ser425X.	[52]
c.881+3A>G	Intron 6	No cDNA analysis was performed but bioinformatics analysis predicts that the variant affects the splicing donor.	Identified in two patients (two independent studies), both presenting development regression of movement and intelligence.	[59]
c.955+1G>A	Intron 7	No cDNA analysis was performed.	Identified in compound heterozygosity with p.Trp942Cys in one patient with severe infantile disease (symptoms at 1 year old).	[38]
c.955+5G>A	Intron 7	No cDNA analysis was performed.	Identified in compound heterozygosity with p.Pro1007Ala in a patient with their first neurological symptoms at 1 year old.	[60]
c.1554-1009G>A	Intron 9	Creates a cryptic donor splice site, resulting in the incorporation of 194 bp of Intron 9 as a new exon (pseudoexon) in the mRNA. This new transcript bears a premature termination codon and is degraded by the NMD mechanism. This was observed in the patient's fibroblasts and also in HeLa cells transfected with a mutant but not with a wild-type *NPC1* minigene.	Compound heterozygous with the in-frame deletion insertion p.Asn961_Phe966delinsSer.	[61]
c.1553+1G>C	Intron 9	n.a.	Identified in compound heterozygosity with p.Ser652Trp.	[62]
c.1553+1G>A	Intron 9	n.a.	Identified in one patient with the early infantile form and in compound heterozygosity with c.181-2A>G (p.Glu61GlyfsTer24).	[54]
c.1553+5G>A	Intron 9	cDNA analysis showed the skipping of Exon 9.	Identified in three Turkish cases from the same family.	[63]
c.1654+1G>T	Intron 10	n.a.	Infantile.	[3]
c.1757+2T>C	Intron 11	n.a.	n.a.	[64]
c.1757+5G>A	Intron 11	n.a.	Identified in a Chinese patient.	[65]
c.1947+2T>G	Intron 12	*In silico* by Neural Network Splice Site Prediction.	n.a.	[28]
c.1947+5G>C	Intron 12	Predicted disruption of the Intron 12 donor site and subsequent use of a cryptic donor site within Exon 12, resulting in an alternative transcript. As a consequence, there is a 25 amino acid in-frame deletion (p.Ile626_Val650del) that, based on in silico modeling, may disrupt the third transmembrane domain of the NPC1 protein. This was validated in *NPC1* cDNA.	Identified in a NPC1 cell line fibroblast maintained by the Coriell Repository (GM03123).	[66]
c.2130+1G>A	Intron 13	n.a.	Found in homozygosity in three patients from Saudi Arabia.	[67]
c.2130+2T>C	Intron 13	No cDNA analysis was conducted.	Found in two siblings in compound heterozygosity with the p.Pro1007Ala variant.	[12]
c.2246-2A>G	Intron 14	*In silico* by Neural NetworkSplice Site Prediction.	n.a.	[28]
c.2245+1G>A	Intron 14	n.a.	Found in compound heterozygosity with p.Pro543Leu in a patient with the early infantile form.	[68]
c.2374-1G>A	Intron 15	n.a.	Found in a Whole Genome Sequencing project of a large cohort.	[69]
c.2604+1G>A	Intron 17	n.a.	Found in an Indian patient in compound heterozygosity with p.Ile690Phe.	[70]
c.2604+2T>G	Intron 17	n.a.	Found in one Indian patient in homozygosity. The cohort included patients with predominant central nervous system white matter abnormalities.	[71]
c.2604+5G>A	Intron 17	Located in a conserved position of the donor splice site of Intron 17. Promotes the skipping of Exon 17.	Neonatal (when present in both alleles).	[52]

Table 3. *Cont.*

Genotype	Location	Impact on mRNA and Protein Levels (as Described in the Reference Paper)	Age at Neurologic Onset (Years)/Clinical Manifestation	Ref
c.2795+1G>C	Intron 18	Located in the 5′ donor splice site of Intron 18. qRT-PCR analysis of the *NPC1* mRNA from the patient´s fibroblasts showed that this splicing variant generates an unstable mRNA that is most likely degraded by NMD.	Identified in compound heterozygosity with the p.Val1165Met variant.	[72]
c.2795+5G>A	Intron 18	No cDNA analysis was conducted.	Identified in compound heterozygosity with p.Leu107CysfsTer5. Diagnosed at 1 year old.	[73]
c.2795+5G>C	Intron 18	It decreases the strength of the canonical donor splicing site and the strongest donor splice site is predicted to be 124 bp downstream. The analysis of cDNA sequence encompassing Exons 17–20 from a patient carrying this variant confirmed the inserted fragment of 124 bp (between Exons 18 and 19).	Identified in a Serbian patient in compound heterozygosity with the splicing c.2819C>T.	[74]
c.2912-3C>G	Intron 19	Predicted to alter the splicing acceptor site of Intron 19 (*in silico* analysis).	Identified in a Chinese patient with the late infantile form in compound heterozygosity with the c.2302_2303insG.	[75]
c.3041+5G>A	Intron 20	n.a.	n.a.	[12]
c.3246-2A>G	Intron 21	n.a.	Identified in compound heterozygosity with p.Arg978Cys in two siblings with NPC.	[76]
c.3477+1G>A	Intron 22	n.a.	Identified in a French patient in compound heterozygosity with p.Ala1174Val.	[3]
c.3477+4A>G	Intron 22	n.a.	Identified in compound heterozygosity with p.Pro1007Ala. The age at onset was 29 years old, with ataxic gait as the first symptom. Also presenting cerebellar ataxia, dysarthria/dysphagia, VSGP, pyramidal tract signs, executive dysfunction, and the magnetic resonance imaging showing cerebellar atrophy.	[77]
c.3591+1G>A	Intron 23	Activation of a splice site in Intron 23, which is predicted to lead to a 45 bp in-frame insertion and the activation of a splice site in Exon 23, leading to a 63 bp in-frame deletion. In cells from patients homozygous for the variant, no detectable band was observed in the NPC1 protein region, showing that none of the two predicted transcripts produces protein.	Identified in homozygosity in a Portuguese patient with the early infantile form (age at neurological onset was 2 years). Severe hepatosplenomegaly. Sibling deceased at 3 months from the severe neonatal rapidly fatal cholestatic form alongside pulmonary infiltration.	[26]
c.3591+1G>T		n.a.	n.a.	[78]
c.3591+3G>C	Intron 23	n.a.	Identified in compound heterozygosity with p.Asp944Asn.	[62]
c.3591+5G>A	Intron 23	Three abnormally spliced cDNAs were observed/identified: one with an insertion of the first 45 bp of Intron 23 (c.3591_3592ins45), another with a deletion of the last 63 bp of Exon 23 (c.3529_3591del63), and a third one with the skipping of Exon 23 (c.3478_3591del114).	Identified in homozygosity in a Spanish patient with a neonatal form.	[52]
c.3754+1G>A	Intron 24	n.a.	n.a.	[12]
c.3754+1G>C	Intron 24	Skipping of Exon 24, frameshift, and PTC.	Identified in heterozygosity with p.Leu724Pro. Late infantile clinical form.	[25]
c.3754+3A>C	Intron 24	n.a	n.a	[12]

n.a.: information not available/not applicable, PTC: premature termination codon.

Altogether, these observations call attention to the need for extensive mRNA studies in *NPC1*, or even *NPC2*, to establish a definitive NPC diagnosis. In this context, the presence of an alternatively spliced transcript may be somewhat confusing and even mask or mimic a real pathogenic variant that impacts splicing only in NPC patients and *NPC1* variant carriers.

As for tissue-specific differences in the relative abundance of the two *NPC1* splice isoforms, we observed a higher expression of the spliced isoform in fibroblasts than in blood. In fact, in the genotype-tissue expression project (GTEx), which studies tissue-specific gene expression and regulation in fibroblasts, they quantified 30 fragments per kilobase of exon per million fragments mapped; meanwhile, in whole blood, only 17 fragments were quantified (https://www.genecards.org/cgi-bin/carddisp.pl?gene=NPC1&keywords=npc1#expression (accessed on 28 September 2023)).

4. Conclusions

Altogether, our data highlight the fact that a naturally occurring spliced form of *NPC1* mRNA should be taken into consideration when analyzing the *NPC1* cDNA amplicons, especially when considering fibroblast cell cultures. Even though the traditional diagnostic workflows rely almost exclusively on targeted genomic DNA sequencing, the study of mRNA processing is often critical to understanding the real impact of the genomic variant. Therefore, cDNA analysis is highly recommended as the presence of an alternative transcript can muddle the results. Thus, one should be aware that, under certain conditions relying on the amount of total RNA used for in vitro cDNA synthesis, the transcript here reported is naturally occurring and not related to disease.

For now, the physiological role of such a transcript can only be a speculative assumption. However, the biological role of the NPC1 protein is still not fully understood. Specific efforts are striving to better understand how this protein, and others (including NPC2), take part in the egress of unesterified cholesterol from the LE/L compartment. Moreover, other important roles for NPC1, such as being the receptor of the Ebola virus, have recently been uncovered. Therefore, this transcript, as well as the encoding, may have a biological role that merits deeper research far beyond this technical recommendation for the diagnosis of NPC disease.

Author Contributions: Conceptualization, M.E. and S.A.; methodology, M.E., I.R. and M.F.C.; validation, S.A. writing—original draft preparation, M.E.; writing—review and editing, M.F.C., I.R., S.A., H.D. and D.Q.; supervision, D.Q. and S.A.; funding acquisition, M.E, D.Q. and S.A. All authors have read and agreed to the published version of the manuscript.

Funding: This research was funded by national funds through FCT—Fundação para a Ciência e a Tecnologia, I.P., in the scope of the project EXPL/BTM-TEC/1477/2021. This work was also financially supported with funding from FCT/MCTES (UIDB/00211/2020) through national funds.

Institutional Review Board Statement: Not applicable.

Informed Consent Statement: Not applicable.

Data Availability Statement: The data presented in this study are available on request from the corresponding author.

Conflicts of Interest: The authors declare no conflict of interest.

Abbreviations

ACMG	American College of Medical Genetics and Genomics
CHX	Cycloheximide
ESE	Exonic splicing enhancer
ESS	Exonic splicing silencer
GTEx	Genotype-tissue expression project
HSF	Human Splicing Finder
LE/L	Late endosome/lysosome
LSD	Lysosome storage disorder
MLPA	Multiplex ligation-dependent probe amplification
MoM	Multiple of median
MLD3	Middle luminal domain 3
NGS	Next-generation sequencing
NPC	Niemann-Pick type C
NMD	Nonsense-mediated mRNA decay
PPCS	N-palmitoyl-O-phosphocholineserine
PTC	Premature termination codon
TMD	Transmembrane domain
VUS	Variant of unknown significance
VSGP	Vertical supranuclear gaze palsy
wt	Wild type

References

1. Beck, M. Treatment Strategies for Lysosomal Storage Disorders. *Dev. Med. Child Neurol.* **2018**, *60*, 13–18. [CrossRef]
2. Encarnação, M.; Coutinho, M.F.; Silva, L.; Ribeiro, D.; Ouesleti, S.; Campos, T.; Santos, H.; Martins, E.; Cardoso, M.T.; Vilarinho, L.; et al. Assessing Lysosomal Disorders in the NGS Era: Identification of Novel Rare Variants. *Int. J. Mol. Sci.* **2020**, *21*, 6355. [CrossRef]
3. Millat, G.; Baïlo, N.; Molinero, S.; Rodriguez, C.; Chikh, K.; Vanier, M.T. Niemann-Pick C Disease: Use of Denaturing High Performance Liquid Chromatography for the Detection of NPC1 and NPC2 Genetic Variations and Impact on Management of Patients and Families. *Mol. Genet. Metab.* **2005**, *86*, 220–232. [CrossRef]
4. Wassif, C.A.; Cross, J.L.; Iben, J.; Sanchez-Pulido, L.; Cougnoux, A.; Platt, F.M.; Ory, D.S.; Ponting, C.P.; Bailey-Wilson, J.E.; Biesecker, L.G.; et al. High Incidence of Unrecognized Visceral/Neurological Late-Onset Niemann-Pick Disease, Type C1, Predicted by Analysis of Massively Parallel Sequencing Data Sets. *Genet. Med.* **2016**, *18*, 41–48. [CrossRef] [PubMed]
5. Pineda, M.; Mengel, E.; Jahnová, H.; Héron, B.; Imrie, J.; Lourenço, C.M.; van der Linden, V.; Karimzadeh, P.; Valayannopoulos, V.; Jesina, P.; et al. A Suspicion Index to Aid Screening of Early-Onset Niemann-Pick Disease Type C (NP-C). *BMC Pediatr.* **2016**, *16*, 107. [CrossRef]
6. Wijburg, F.A.; Sedel, F.; Pineda, M.; Hendriksz, C.J.; Fahey, M.; Walterfang, M.; Patterson, M.C.; Wraith, J.E.; Kolb, S.A. Development of a Suspicion Index to Aid Diagnosis of Niemann-Pick Disease Type C. *Neurology* **2012**, *78*, 1560–1567. [CrossRef] [PubMed]
7. Kruth, H.S.; Cupp, J.E.; Khan, M.A. Method for Detection and Isolation of Cholesteryl Ester-containing "Foam" Cells Using Flow Cytometry. *Cytometry* **1987**, *8*, 146–152. [CrossRef]
8. Boernig, H.; Geyer, G. Staining of Cholesterol with the Fluorescent Antibiotic "Filipin". *Acta Histochem.* **1974**, *50*, 110–115.
9. Vanier, M.T.; Latour, P. Laboratory Diagnosis of Niemann-Pick Disease Type C: The Filipin Staining Test. *Methods Cell Biol.* **2015**, *126*, 357–375. [CrossRef] [PubMed]
10. Probert, F.; Ruiz-Rodado, V.; Te Vruchte, D.; Nicoli, E.R.; Claridge, T.D.W.; Wassif, C.A.; Farhat, N.; Porter, F.D.; Platt, F.M.; Grootveld, M. NMR Analysis Reveals Significant Differences in the Plasma Metabolic Profiles of Niemann Pick C1 Patients, Heterozygous Carriers, and Healthy Controls. *Sci. Rep.* **2017**, *7*, 6320. [CrossRef]
11. Jiang, X.; Sidhu, R.; Porter, F.D.; Yanjanin, N.M.; Speak, A.O.; Te Vruchte, D.T.; Platt, F.M.; Fujiwara, H.; Scherrer, D.E.; Zhang, J.; et al. A Sensitive and Specific LC-MS/MS Method for Rapid Diagnosis of Niemann-Pick C1 Disease from Human Plasma. *J. Lipid Res.* **2011**, *52*, 1435–1445. [CrossRef]
12. Reunert, J.; Fobker, M.; Kannenberg, F.; Du Chesne, I.; Plate, M.; Wellhausen, J.; Rust, S.; Marquardt, T. Rapid Diagnosis of 83 Patients with Niemann Pick Type C Disease and Related Cholesterol Transport Disorders by Cholestantriol Screening. *EBioMedicine* **2015**, *4*, 170–175. [CrossRef]
13. Boenzi, S.; Deodato, F.; Taurisano, R.; Martinelli, D.; Verrigni, D.; Carrozzo, R.; Bertini, E.; Pastore, A.; Dionisi-Vici, C.; Johnson, D.W. A New Simple and Rapid LC-ESI-MS/MS Method for Quantification of Plasma Oxysterols as Dimethylaminobutyrate Esters. Its Successful Use for the Diagnosis of Niemann-Pick Type C Disease. *Clin. Chim. Acta* **2014**, *437*, 93–100. [CrossRef]
14. Giese, A.K.; Mascher, H.; Grittner, U.; Eichler, S.; Kramp, G.; Lukas, J.; Te Vruchte, D.; Al Eisa, N.; Cortina-Borja, M.; Porter, F.D.; et al. A Novel, Highly Sensitive and Specific Biomarker for Niemann-Pick Type C1 Disease. *Orphanet J. Rare Dis.* **2015**, *10*, 78. [CrossRef] [PubMed]
15. Welford, R.W.D.; Garzotti, M.; Lourenço, C.M.; Mengel, E.; Marquardt, T.; Reunert, J.; Amraoui, Y.; Kolb, S.A.; Morand, O.; Groenen, P. Plasma Lysosphingomyelin Demonstrates Great Potential as a Diagnostic Biomarker for Niemann-Pick Disease Type C in a Retrospective Study. *PLoS ONE* **2014**, *9*, e114669. [CrossRef]
16. Jiang, X.; Sidhu, R.; Mydock-McGrane, L.; Hsu, F.F.; Covey, D.F.; Scherrer, D.E.; Earley, B.; Gale, S.E.; Farhat, N.Y.; Porter, F.D.; et al. Development of a Bile Acid-Based Newborn Screen for Niemann-Pick Disease Type C. *Sci. Transl. Med.* **2016**, *8*, 337ra63. [CrossRef]
17. Mazzacuva, F.; Mills, P.B.; Mills, K.; Platt, F.; Maekawa, M.; Porter, F.D.; Clayton, P.T. Identification of New Biomarkers Suitable for an Early Diagnosis of Niemann-Pick C1. *Mol. Genet. Metab.* **2016**, *117*, S78. [CrossRef]
18. Patterson, M.C.; Clayton, P.; Gissen, P.; Anheim, M.; Bauer, P.; Bonnot, O.; Dardis, A.; Dionisi-Vici, C.; Klünemann, H.H.; Latour, P.; et al. Recommendations for the Detection and Diagnosis of Niemann-Pick Disease Type C: An Update. *Neurol. Clin. Pract.* **2017**, *7*, 499–511. [CrossRef] [PubMed]
19. Maekawa, M.; Jinnoh, I.; Matsumoto, Y.; Narita, A.; Mashima, R.; Takahashi, H.; Iwahori, A.; Saigusa, D.; Fujii, K.; Abe, A.; et al. Structural Determination of Lysosphingomyelin-509 and Discovery of Novel Class Lipids from Patients with Niemann-Pick Disease Type C. *Int. J. Mol. Sci.* **2019**, *20*, 5018. [CrossRef] [PubMed]
20. Sidhu, R.; Mondjinou, Y.; Qian, M.; Song, H.; Kumar, A.B.; Hong, X.; Hsu, F.-F.; Dietzen, D.J.; Yanjanin, N.M.; Porter, F.D.; et al. N-Acyl-O-Phosphocholineserines: Structures of a Novel Class of Lipids That Are Biomarkers for Niemann-Pick C1 Disease. *J. Lipid Res.* **2019**, *60*, 1410–1424. [CrossRef]
21. Patterson, M.C.; Hendriksz, C.J.; Walterfang, M.; Sedel, F.; Vanier, M.T.; Wijburg, F. Recommendations for the Diagnosis and Management of Niemann-Pick Disease Type C: An Update. *Mol. Genet. Metab.* **2012**, *106*, 330–344. [CrossRef]
22. Geberhiwot, T.; Moro, A.; Dardis, A.; Ramaswami, U.; Sirrs, S.; Marfa, M.P.; Vanier, M.T.; Walterfang, M.; Bolton, S.; Dawson, C.; et al. Consensus Clinical Management Guidelines for Niemann-Pick Disease Type C. *Orphanet J. Rare Dis.* **2018**, *13*, 50. [CrossRef]

23. Shammas, H.; Kuech, E.M.; Rizk, S.; Das, A.M.; Naim, H.Y. Different Niemann-Pick C1 Genotypes Generate Protein Phenotypes That Vary in Their Intracellular Processing, Trafficking and Localization. *Sci. Rep.* **2019**, *9*, 5292. [CrossRef]
24. Vanier, M.T. Niemann-Pick Disease Type C. *Orphanet J. Rare Dis.* **2010**, *5*, 16. [CrossRef]
25. Millat, G.; Marçais, C.; Tomasetto, C.; Chikh, K.; Fensom, A.H.; Harzer, K.; Wenger, D.A.; Ohno, K.; Vanier, M.T. Niemann-Pick C1 Disease: Correlations between NPC1 Mutations, Levels of NPC1 Protein, and Phenotypes Emphasize the Functional Significance of the Putative Sterol-Sensing Domain and of the Cysteine-Rich Luminal Loop. *Am. J. Hum. Genet.* **2001**, *68*, 1373–1385. [CrossRef]
26. Ribeiro, I.; Marcão, A.; Amaral, O.; Sá Miranda, M.C.; Vanier, M.T.; Millat, G. Niemann-Pick Type C Disease: NPC1 Mutations Associated with Severe and Mild Cellular Cholesterol Trafficking Alterations. *Hum. Genet.* **2001**, *109*, 24–32. [CrossRef]
27. Guatibonza Moreno, P.; Pardo, L.M.; Pereira, C.; Schroeder, S.; Vagiri, D.; Almeida, L.S.; Juaristi, C.; Hosny, H.; Loh, C.C.Y.; Leubauer, A.; et al. At a Glance: The Largest Niemann-Pick Type C1 Cohort with 602 Patients Diagnosed over 15 Years. *Eur. J. Hum. Genet.* **2023**, *31*, 1108–1116. [CrossRef] [PubMed]
28. Park, W.D.; O'Brien, J.F.; Lundquist, P.A.; Kraft, D.L.; Vockley, C.W.; Karnes, P.S.; Patterson, M.C.; Snow, K. Identification of 58 Novel Mutations in Niemann-Pick Disease Type C: Correlation with Biochemical Phenotype and Importance of PTC1-like Domains in NPC1. *Hum. Mutat.* **2003**, *22*, 313–325. [CrossRef] [PubMed]
29. Gieselmann, V. Cellular Pathophysiology of Lysosomal Storage Diseases. In *Fabry Disease: Perspectives from 5 Years of FOS*; Oxford PharmaGenesis: Oxford, UK, 2006; ISBN 190353903X.
30. Polten, A.; Fluharty, A.L.; Fluharty, C.B.; Kappler, J.; von Figura, K.; Gieselmann, V. Molecular Basis of Different Forms of Metachromatic Leukodystrophy. *N. Engl. J. Med.* **1991**, *324*, 18–22. [CrossRef] [PubMed]
31. McInnes, B.; Potier, M.; Wakamatsu, N.; Melancon, S.B.; Klavins, M.H.; Tsuji, S.; Mahuran, D.J. An Unusual Splicing Mutation in the HEXB Gene Is Associated with Dramatically Different Phenotypes in Patients from Different Racial Backgrounds. *J. Clin. Investig.* **1992**, *90*, 306–314. [CrossRef] [PubMed]
32. Paron, F.; Dardis, A.; Buratti, E. Pre-MRNA Splicing Defects and RNA Binding Protein Involvement in Niemann Pick Type C Disease. *J. Biotechnol.* **2020**, *318*, 20–30. [CrossRef]
33. Millat, G.; Chikh, K.; Naureckiene, S.; Sleat, D.E.; Fensom, A.H.; Higaki, K.; Elleder, M.; Lobel, P.; Vanier, M.T. Niemann-Pick Disease Type C: Spectrum of HE1 Mutations and Genotype/Phenotype Correlations in the NPC2 Group. *Am. J. Hum. Genet.* **2001**, *69*, 1013–1021. [CrossRef] [PubMed]
34. Tarugi, P.; Ballarini, G.; Bembi, B.; Battisti, C.; Palmeri, S.; Panzani, F.; Di Leo, E.; Martini, C.; Federico, A.; Calandra, S. Niemann-Pick Type C Disease: Mutations of NPC1 Gene and Evidence of Abnormal Expression of Some Mutant Alleles in Fibroblasts. *J. Lipid Res.* **2002**, *43*, 1908–1919. [CrossRef]
35. Macías-Vidal, J.; Gort, L.; Lluch, M.; Pineda, M.; Coll, M.J. Nonsense-Mediated MRNA Decay Process in Nine Alleles of Niemann-Pick Type C Patients from Spain. *Mol. Genet. Metab.* **2009**, *97*, 60–64. [CrossRef]
36. Yamamoto, T.; Nanba, E.; Ninomiya, H.; Higaki, K.; Taniguchi, M.; Zhang, H.; Akaboshi, S.; Watanabe, Y.; Takeshima, T.; Inui, K.; et al. NPC1 Gene Mutations in Japanese Patients with Niemann-Pick Disease Type C. *Hum. Genet.* **1999**, *105*, 10–16. [CrossRef]
37. Encarnação, M.; Coutinho, M.F.; Cho, S.M.; Cardoso, M.T.; Ribeiro, I.; Chaves, P.; Santos, J.I.; Quelhas, D.; Lacerda, L.; Leão Teles, E.; et al. NPC1 Silent Variant Induces Skipping of Exon 11 (p.V562V) and Unfolded Protein Response Was Found in a Specific Niemann-Pick Type C Patient. *Mol. Genet. Genom. Med.* **2020**, *8*, e1451. [CrossRef]
38. Fernandez-Valero, E.M.; Ballart, A.; Iturriaga, C.; Lluch, M.; Macias, J.; Vanier, M.T.; Pineda, M.; Coll, M.J. Identification of 25 New Mutations in 40 Unrelated Spanish Niemann-Pick Type C Patients: Genotype-Phenotype Correlations. *Clin. Genet.* **2005**, *68*, 245–254. [CrossRef] [PubMed]
39. Zhang, X.H.F.; Chasin, L.A. Computational Definition of Sequence Motifs Governing Constitutive Exon Splicing. *Genes Dev.* **2004**, *18*, 1241–1250. [CrossRef] [PubMed]
40. Goren, A.; Ram, O.; Amit, M.; Keren, H.; Lev-Maor, G.; Vig, I.; Pupko, T.; Ast, G. Comparative Analysis Identifies Exonic Splicing Regulatory Sequences-The Complex Definition of Enhancers and Silencers. *Mol. Cell* **2006**, *22*, 769–781. [CrossRef] [PubMed]
41. Nadjar, Y.; Hütter-Moncada, A.L.; Latour, P.; Ayrignac, X.; Kaphan, E.; Tranchant, C.; Cintas, P.; Degardin, A.; Goizet, C.; Laurencin, C.; et al. Adult Niemann-Pick Disease Type C in France: Clinical Phenotypes and Long-Term Miglustat Treatment Effect. *Orphanet J. Rare Dis.* **2018**, *13*, 175. [CrossRef]
42. Anheim, M.; Lagha-Boukbiza, O.; Fleury-Lesaunier, M.C.; Valenti-Hirsch, M.P.; Hirsch, E.; Gervais-Bernard, H.; Broussolle, E.; Thobois, S.; Vanier, M.T.; Latour, P.; et al. Heterogeneity and Frequency of Movement Disorders in Juvenile and Adult-Onset Niemann-Pick C Disease. *J. Neurol.* **2014**, *261*, 174–179. [CrossRef] [PubMed]
43. Ohno, K.; Suzuki, K. Multiple Abnormal Beta-Hexosaminidase Alpha Chain MRNAs in a Compound-Heterozygous Ashkenazi Jewish Patient with Tay-Sachs Disease. *J. Biol. Chem.* **1988**, *263*, 18563–18567. [CrossRef] [PubMed]
44. Pineda, M.; Juríčková, K.; Karimzadeh, P.; Kolniková, M.; Malinová, V.; Torres, J.; Kolb, S.A. Evaluation of Different Suspicion Indices in Identifying Patients with Niemann-Pick Disease Type C in Clinical Practice: A Post Hoc Analysis of a Retrospective Chart Review. *Orphanet J. Rare Dis.* **2019**, *14*, 161. [CrossRef]
45. Jang, W.; Park, J.; Chae, H.; Kim, M. Comparison of In Silico Tools for Splice-Altering Variant Prediction Using Established Spliceogenic Variants: An End-User's Point of View. *Int. J. Genom.* **2022**, *2022*, 5265686. [CrossRef] [PubMed]
46. Walker, L.C.; Hoya, M.d.l.; Wiggins, G.A.R.; Lindy, A.; Vincent, L.M.; Parsons, M.T.; Canson, D.M.; Bis-Brewer, D.; Cass, A.; Tchourbanov, A.; et al. Using the ACMG/AMP Framework to Capture Evidence Related to Predicted and Observed Impact on Splicing: Recommendations from the ClinGen SVI Splicing Subgroup. *Am. J. Hum. Genet.* **2023**, *110*, 1046–1067. [CrossRef]

47. Li, X.; Wang, J.; Coutavas, E.; Shi, H.; Hao, Q.; Blobel, G. Structure of Human Niemann-Pick C1 Protein. *Proc. Natl. Acad. Sci. USA* **2016**, *113*, 8212–8217. [CrossRef]
48. Gong, X.; Qian, H.; Zhou, X.; Wu, J.; Wan, T.; Cao, P.; Huang, W.; Zhao, X.; Wang, X.; Wang, P.; et al. Structural Insights into the Niemann-Pick C1 (NPC1)-Mediated Cholesterol Transfer and Ebola Infection. *Cell* **2016**, *165*, 1467–1478. [CrossRef]
49. Caminsky, N.; Mucaki, E.J.; Rogan, P.K. Interpretation of MRNA Splicing Mutations in Genetic Disease: Review of the Literature and Guidelines for Information-Theoretical Analysis. *F1000Research* **2014**, *3*, 282. [CrossRef]
50. Anna, A.; Monika, G. Splicing Mutations in Human Genetic Disorders: Examples, Detection, and Confirmation. *J. Appl. Genet.* **2018**, *59*, 253–268. [CrossRef]
51. Sarkar, A.; Panati, K.; Narala, V.R. Code inside the Codon: The Role of Synonymous Mutations in Regulating Splicing Machinery and Its Impact on Disease. *Mutat. Res. Rev. Mutat. Res.* **2022**, *790*, 108444. [CrossRef]
52. Macías-Vidal, J.; Rodríguez-Pascau, L.; Sánchez-Ollé, G.; Lluch, M.; Vilageliu, L.; Grinberg, D.; Coll, M.J. Molecular Analysis of 30 Niemann-Pick Type C Patients from Spain. *Clin. Genet.* **2011**, *80*, 39–49. [CrossRef]
53. Marelli, C.; Guissart, C.; Hubsch, C.; Renaud, M.; Villemin, J.-P.; Larrieu, L.; Charles, P.; Ayrignac, X.; Sacconi, S.; Collignon, P.; et al. Mini-Exome Coupled to Read-Depth Based Copy Number Variation Analysis in Patients with Inherited Ataxias. *Hum. Mutat.* **2016**, *37*, 1340–1353. [CrossRef] [PubMed]
54. Dardis, A.; Zampieri, S.; Gellera, C.; Carrozzo, R.; Cattarossi, S.; Peruzzo, P.; Dariol, R.; Sechi, A.; Deodato, F.; Caccia, C.; et al. Molecular Genetics of Niemann–Pick Type C Disease in Italy: An Update on 105 Patients and Description of 18 NPC1 Novel Variants. *J. Clin. Med.* **2020**, *9*, 679. [CrossRef]
55. Terada, C.; Mirarchi, F.; Marino, R.; Eiroa, H.; Berensztein, E. Molecular and Functional Study of Pediatric Patients with Niemann-Pick C in Argentina. *Medicina* **2022**, *82*, 308–312.
56. Fancello, T.; Dardis, A.; Rosano, C.; Tarugi, P.; Tappino, B.; Zampieri, S.; Pinotti, E.; Corsolini, F.; Fecarotta, S.; D'Amico, A.; et al. Molecular Analysis of NPC1 and NPC2 Gene in 34 Niemann-Pick C Italian Patients: Identification and Structural Modeling of Novel Mutations. *Neurogenetics* **2009**, *10*, 229–239. [CrossRef]
57. Imrie, J.; Heptinstall, L.; Knight, S.; Strong, K. Observational Cohort Study of the Natural History of Niemann-Pick Disease Type C in the UK: A 5-Year Update from the UK Clinical Database. *BMC Neurol.* **2015**, *15*, 257. [CrossRef]
58. Di Leo, E.; Panico, F.; Tarugi, P.; Battisti, C.; Federico, A.; Calandra, S. A Point Mutation in the Lariat Branch Point of Intron 6 of NPC1 as the Cause of Abnormal Pre-MRNA Splicing in Niemann-Pick Type C Disease. *Hum. Mutat.* **2004**, *24*, 440. [CrossRef]
59. Zhan, X.; Lin, N.; Zhang, H.W.; Gao, X.L.; Qiu, W.J.; Han, L.S.; Ye, J.; Gu, X.F. Blood 7-ketocholesterol level, clinical features and gene mutation analysis of 18 children with Niemann-Pick disease type C. *Zhonghua Er Ke Za Zhi Chin. J. Pediatr.* **2016**, *54*, 419–423. [CrossRef]
60. Tängemo, C.; Weber, D.; Theiss, S.; Mengel, E.; Runz, H. Niemann-Pick Type C Disease: Characterizing Lipid Levels in Patients with Variant Lysosomal Cholesterol Storage. *J. Lipid Res.* **2011**, *52*, 813–825. [CrossRef] [PubMed]
61. Rodríguez-Pascau, L.; Coll, M.J.; Vilageliu, L.; Grinberg, D. Antisense Oligonucleotide Treatment for a Pseudoexon-Generating Mutation in the NPC1 Gene Causing Niemann-Pick Type C Disease. *Hum. Mutat.* **2009**, *30*, E993–E1001. [CrossRef]
62. Sun, X.; Marks, D.L.; Park, W.D.; Wheatley, C.L.; Puri, V.; O'Brien, J.F.; Kraft, D.L.; Lundquist, P.A.; Patterson, M.C.; Pagano, R.E.; et al. Niemann-Pick C Variant Detection by Altered Sphingolipid Trafficking and Correlation with Mutations within a Specific Domain of NPC1. *Am. J. Hum. Genet.* **2001**, *68*, 1361–1372. [CrossRef]
63. Kılıç Yıldırım, G.; Yarar, C.; Şeker Yılmaz, B.; Ceylaner, S. Niemann-Pick Type C Disease with a Novel Intronic Mutation: Three Turkish Cases from the Same Family. *J. Pediatr. Endocrinol. Metab.* **2022**, *35*, 535–541. [CrossRef]
64. Almeida, L.S.; Pereira, C.; Aanicai, R.; Schröder, S.; Bochinski, T.; Kaune, A.; Urzi, A.; Spohr, T.C.L.S.; Viceconte, N.; Oppermann, S.; et al. An Integrated Multiomic Approach as an Excellent Tool for the Diagnosis of Metabolic Diseases: Our First 3720 Patients. *Eur. J. Hum. Genet.* **2022**, *30*, 1029–1035. [CrossRef] [PubMed]
65. Ren, S.C.; Tian, Z.X.; Deng, Y.X.; Wang, Y.J.; Wu, X.J.; Zhang, Y.Z.; Gao, B.Q. Clinical features and gene mutation analysis of patients with Niemann-Pick disease type C. *Zhonghua Yi Xue Za Zhi* **2018**, *98*, 284–288. [CrossRef] [PubMed]
66. Salman, A.; Cougnoux, A.; Farhat, N.; Wassif, C.A.; Porter, F.D. Association of NPC1 Variant p.P237S with a Pathogenic Splice Variant in Two Niemann-Pick Disease Type C1 Patients. *Am. J. Med. Genet. Part A* **2017**, *173*, 1038–1040. [CrossRef] [PubMed]
67. Alfadhel, M.; Benmeakel, M.; Hossain, M.A.; Al Mutairi, F.; Al Othaim, A.; Alfares, A.A.; Al Balwi, M.; Alzaben, A.; Eyaid, W. Thirteen Year Retrospective Review of the Spectrum of Inborn Errors of Metabolism Presenting in a Tertiary Center in Saudi Arabia. *Orphanet J. Rare Dis.* **2016**, *11*, 126. [CrossRef]
68. Héron, B.; Valayannopoulos, V.; Baruteau, J.; Chabrol, B.; Ogier, H.; Latour, P.; Dobbelaere, D.; Eyer, D.; Labarthe, F.; Maurey, H.; et al. Miglustat Therapy in the French Cohort of Paediatric Patients with Niemann-Pick Disease Type C. *Orphanet J. Rare Dis.* **2012**, *7*, 36. [CrossRef]
69. Stranneheim, H.; Lagerstedt-Robinson, K.; Magnusson, M.; Kvarnung, M.; Nilsson, D.; Lesko, N.; Engvall, M.; Anderlid, B.-M.; Arnell, H.; Johansson, C.B.; et al. Integration of Whole Genome Sequencing into a Healthcare Setting: High Diagnostic Rates across Multiple Clinical Entities in 3219 Rare Disease Patients. *Genome Med.* **2021**, *13*, 40. [CrossRef]
70. Ganapathy, A.; Mishra, A.; Soni, M.R.; Kumar, P.; Sadagopan, M.; Kanthi, A.V.; Patric, I.R.P.; George, S.; Sridharan, A.; Thyagarajan, T.C.; et al. Multi-Gene Testing in Neurological Disorders Showed an Improved Diagnostic Yield: Data from over 1000 Indian Patients. *J. Neurol.* **2019**, *266*, 1919–1926. [CrossRef]

71. Kaur, P.; do Rosario, M.C.; Hebbar, M.; Sharma, S.; Kausthubham, N.; Nair, K.; Shrikiran, A.; Ramesh Bhat, Y.; Lewis, L.E.S.; Nampoothiri, S.; et al. Clinical and Genetic Spectrum of 104 Indian Families with Central Nervous System White Matter Abnormalities. *Clin. Genet.* **2021**, *100*, 542–550. [CrossRef]
72. Zampieri, S.; Bembi, B.; Rosso, N.; Filocamo, M.; Dardis, A. Treatment of Human Fibroblasts Carrying NPC1 Missense Mutations with MG132 Leads to an Improvement of Intracellular Cholesterol Trafficking. *JIMD Rep.* **2012**, *2*, 59–69. [CrossRef] [PubMed]
73. Carnicer-Cáceres, C.; Villena-Ortiz, Y.; Castillo-Ribelles, L.; Barquín-Del-Pino, R.; Camprodon-Gomez, M.; Felipe-Rucián, A.; Moreno-Martínez, D.; Lucas-Del-Pozo, S.; Hernández-Vara, J.; García-Serra, A.; et al. Influence of Initial Clinical Suspicion on the Diagnostic Yield of Laboratory Enzymatic Testing in Lysosomal Storage Disorders. Experience from a Multispecialty Hospital. *Blood Cells Mol. Dis.* **2023**, *98*, 102704. [CrossRef]
74. Kresojević, N.; Dobričić, V.; Lukić, M.J.; Tomić, A.; Petrović, I.; Dragašević, N.; Perović, I.; Marjanović, A.; Branković, M.; Janković, M.; et al. Genetic and Phenotypic Variability in Adult Patients with Niemann Pick Type C from Serbia: Single-Center Experience. *J. Neurol.* **2022**, *269*, 3167–3174. [CrossRef]
75. Zhang, H.; Wang, Y.; Lin, N.; Yang, R.; Qiu, W.; Han, L.; Ye, J.; Gu, X. Diagnosis of Niemann-Pick Disease Type C with 7-Ketocholesterol Screening Followed by NPC1/NPC2 Gene Mutation Confirmation in Chinese Patients. *Orphanet J. Rare Dis.* **2014**, *9*, 82. [CrossRef] [PubMed]
76. Kluenemann, H.H.; Nutt, J.G.; Davis, M.Y.; Bird, T.D. Parkinsonism Syndrome in Heterozygotes for Niemann-Pick C1. *J. Neurol. Sci.* **2013**, *335*, 219–220. [CrossRef] [PubMed]
77. Synofzik, M.; Harmuth, F.; Stampfer, M.; Müller Vom Hagen, J.; Schöls, L.; Bauer, P. NPC1 Is Enriched in Unexplained Early Onset Ataxia: A Targeted High-Throughput Screening. *J. Neurol.* **2015**, *262*, 2557–2563. [CrossRef] [PubMed]
78. van der Sluijs, P.J.; Aten, E.; Barge-Schaapveld, D.Q.C.M.; Bijlsma, E.K.; Bökenkamp-Gramann, R.; Donker Kaat, L.; van Doorn, R.; van de Putte, D.F.; van Haeringen, A.; ten Harkel, A.D.J.; et al. Putting Genome-Wide Sequencing in Neonates into Perspective. *Genet. Med.* **2019**, *21*, 1074–1082. [CrossRef]

Disclaimer/Publisher's Note: The statements, opinions and data contained in all publications are solely those of the individual author(s) and contributor(s) and not of MDPI and/or the editor(s). MDPI and/or the editor(s) disclaim responsibility for any injury to people or property resulting from any ideas, methods, instructions or products referred to in the content.

Attachment 3

Lost (and found) in Translation: the Potential of microRNAs

Hugo David, Isaura Ribeiro, Luís Vieira, Catarina Carneiro Silva, Maria Francisca Coutinho, Juliana Inês Santos, Esmeralda Martins, Anthony H. Futerman, Dulce Quelhas, Sandra Alves & Marisa Encarnação

Oral Communication at the *VI CECA Meeting*, **2023**

Lost (and found) in Translation: the Potential of microRNAs

Hugo David [1,2,3,4], Isaura Ribeiro [5,6], Luís Vieira [7], Catarina Carneiro Silva [7], Maria Francisca Coutinho [1,2,3], Juliana Inês Santos [1,2,3], Esmeralda Martins [5,6], Anthony H. Futerman [8], Dulce Quelhas [5,6], Sandra Alves [1,2,3], Marisa Encarnação [1,2,3]

[1] Research and Development Unit, Department of Human Genetics, National Institute of Health Doutor Ricardo Jorge, Porto, Portugal
[2] Center for the Study of Animal Sciences (CECA), ICETA, University of Porto, Porto, Portugal
[3] Associate Laboratory for Animal and Veterinary Sciences (AL4AnimalS), Porto, Portugal
[4] Department of Biology, Faculty of Sciences, University of Porto, Porto, Portugal
[5] Unidade de Bioquímica Genética, Centro de Genética Médica Dr. Jacinto Magalhães, Centro de Referência em Doenças Hereditárias do Metabolismo, Centro Hospitalar e Universitário de Santo António, Porto, Portugal
[6] Unit for Multudisciplinary Research in Biomedicine, ICBAS, University of Porto, Porto, Portugal
[7] Technology and Innovation Unit, Department of Human Genetics, National Institute of Health Doutor Ricardo Jorge, Lisbon, Portugal
[8] Department of Biomolecular Sciences, Weizmann Institute of Science, Rehovot, Israel

Abstract:

Niemann-Pick Type C (NPC, MIM #257220) is a rare, neurodegenerative lysosomal storage disorder caused by pathogenic variants in either the *NPC1* or *NPC2* genes, which encode proteins responsible for the lysosomal export of unesterified cholesterol, that gets accumulated in lysosomes, triggering a cascade of other molecular events, ultimately resulting in the severe neuro-visceral symptomatology associated with this disorder. [1]. NPC1 protein has also been identified as the cellular entrypoint of the Ebola and Marburg viruses [2], further highlighting the importance of studying NPC.

Its nonspecific presentations alongside the rarity of this disorder make it so that several patients go through many appointments and various medical specialties before obtaining a correct diagnosis, which can take decades [1]. Even patients with identical genotypes may present different manifestations, indicating other factors – namely epigenetics – might play a significant role in NPC progression.

microRNAs (miRNAs) are 20-22 nucleotide strands of non-coding RNA that act as templates for the RNA-induced silencing complex (RISC) to recognize a complementary region in target mRNA molecules and repress their translation [3]. Despite their small size, miRNAs play an immense role in cellular development, differentiation and homeostasis, and their dysregulation is associated with the progress of numerous neurological diseases [4].

These miRNA molecules are exported as a means of intercellular communication and they can be detected and reliably quantified in circulation within various bodily fluids, including blood serum, where they have proved quite stable [5] – posing them as ideal candidates for novel disease biomarkers.

Our goal with this project is to evaluate the potential of circulating microRNAs as diagnostic and/or prognostic biomarkers for Niemann-Pick Type C disease, by using RNA-Sequencing (RNA-Seq) technologies to detect differentially expressed miRNAs in patients' and controls' skin fibroblasts, and employing quantitative real-time polymerase chain reaction (qRT-PCR) to validate these RNA-Seq hits on skin cells and sera. In addition, we also intend to use a plethora of cellular and molecular methodologies to further unveil the mechanisms underlying NPC1 function in healthy and affected individuals.

Preliminary results indicate there are some differentially expressed miRNAs in NPC patients when compared to controls, but additional analysis and hit validation are still due.

References:

[1] Patterson M. *GeneReviews*. 2020.
[2] Carette J, et al. *Nature*. 2011; 477(7364): 340-3.
[3] Bartel D, et al. *Cell*. 2004; 116(2): 281-97.
[4] Esteller M. *Nature Reviews Genetics*. 2011; 12(12): 861-74.
[5] Chen X, et al. *Cell Research*. 2008; 18(10): 997-1006.

Acknowledgements:

This work received financial support from the Foundation for Science and Technology (EXPL/BTM-TEC/1477/2021), the Center for the Study of Animal Science (UIDB/00211/2020) and the Associate Laboratory for Animal and Veterinary Sciences (LA/P/0059/2020).

Attachment 4

No Place Like the Lysosome: a Study on NPC1 Protein Trafficking

Hugo David, Isaura Ribeiro, Sofia Carvalho, Maria Francisca Coutinho, Dulce Quelhas, Sandra Alves & Marisa Encarnação

Oral Communication at the *2nd Meeting of the AL4AnimalS*, **2023**

No Place Like the Lysosome: a Study on NPC1 Protein Trafficking

David H [1,2,3,4,*], Ribeiro I [5,6], Carvalho S [1,2,3], Coutinho MF [1,2,3], Quelhas D [5,6], Alves S [1,2,3], Encarnação M [1,2,3]

[1] Research and Development Unit, Department of Human Genetics, National Institute of Health Doutor Ricardo Jorge, Porto, Portugal
[2] Centre for the Study of Animal Sciences (CECA), ICETA, University of Porto, Porto, Portugal
[3] Associate Laboratory for Animal and Veterinary Sciences (AL4AnimalS), Portugal
[4] Department of Biology, Faculty of Sciences, University of Porto, Porto, Portugal
[5] Unidade de Bioquímica Genética, Centro de Genética Médica Dr. Jacinto Magalhães, Centro de Referência em Doenças Hereditárias do Metabolismo, Centro Hospitalar e Universitário de Santo António, Porto, Portugal
[6] Unit for Multidisciplinary Research in Biomedicine, University of Porto, Porto, Portugal

* hugo.david@insa.min-saude.pt

Keywords: NPC1, protein trafficking, deglycosylation, immunofluorescence, disease models.

Niemann-Pick Type C (NPC) is a rare, neurodegenerative lysosomal storage disorder caused by pathogenic variants in either the *NPC1* or *NPC2* genes, which encode proteins responsible for the lysosomal export of unesterified cholesterol. This lipid gets accumulated in lysosomes, triggering a cascade of other cellular events, ultimately resulting in the severe neurovisceral symptomatology associated with this disease.

The NPC1 protein is co-translationally *N*-glycosylated and folded in the endoplasmic reticulum, before being transported to the Golgi apparatus where it undergoes processing to a mature complex glycosylated protein, which ultimately localizes to the lysosomes. Most of the disease-causing variants in the *NPC1* gene lead to conformational changes that result in disruption of NPC1 trafficking, but these mechanisms still remain somewhat obscure for some of these pathogenic mutations.

Our objective is to survey and study the trafficking of NPC1 protein in patients and controls, through deglycosylation studies for the endogenous protein and through immunofluorescence assays following the production of tagged recombinant proteins. This study will feature and compare the most widely studied disease causing variant worldwide (p.I1061T), as well as the most prevalent in Portugal (p.A1035V).

In the future, we plan on extending this study to other, more trustworthy, disease models, such as stem cell-derived neuronal cells and $NPC^{-/-}$ cellular models that mimic the NPC pathological phenotype.

***Acknowledgments*:** This work received financial support from the Foundation for Science and Technology (EXPL/BTM-TEC/1477/2021), the Centre for the Study of Animal Science (UIDB/00211/2020) and the Associate Laboratory for Animal and Veterinary Sciences (LA/P/0059/2020).

Attachment 5

Exosomal microRNAs as Possible Biomarkers for a Rare Disease affecting Lipids

Marisa Encarnação, Hugo David, Isaura Ribeiro, Luís Vieira, Catarina Carneiro Silva, Esmeralda Martins, Maria Teresa Cardoso, Anthony H. Futerman, Dulce Quelhas, Sandra Alves & Marisa Encarnação

Poster Presentation at the *2nd Meeting of the Portuguese Network on Extracellular Vesicles*, **2023**

Exosomal microRNAs as Possible Biomarkers for a Rare Disease Affecting Lipids

Marisa Encarnação[1,2,3] Hugo David[1,2,3,4], Isaura Ribeiro[5,6], Luís Vieira[7], Catarina Carneiro Silva[7], Esmeralda Martins[8], Maria Teresa Cardoso[9], Anthony H. Futerman[10], Dulce Quelhas[4,5], and Sandra Alves[1,2,3]

[1] Research and Development Unit, Department of Human Genetics, National Institute of Health Doutor Ricardo Jorge, Porto, Portugal
[2] Center for the Study of Animal Sciences (CECA), ICETA, University of Porto, Porto, Portugal
[3] Associate Laboratory for Animal and Veterinary Sciences (AL4AnimalS), Porto, Portugal
[4] Department of Biology, Faculty of Sciences, University of Porto, Porto, Portugal
[5] Unidade de Bioquímica Genética, Centro de Genética Médica Dr. Jacinto Magalhães, Centro de Referência em Doenças Hereditárias do Metabolismo, Centro Hospitalar e Universitário de Santo António, Porto (CHUdSA), Portugal
[6] Unit for Multidisciplinary Research in Biomedicine, ICBAS, University of Porto, Porto, Portugal
[7] Technology and Innovation Unit, Department of Human Genetics, National Institute of Health Doutor Ricardo Jorge, Lisbon, Portugal
[8] Centro de Referência em Doenças Hereditárias do Metabolismo, CHUdSA, Portugal
[9] Centro de Referência de Doenças Metabólicas, Centro Hospitalar Universitário de São João (CHUSJ), Porto, Portugal
[10] Department of Biomolecular Sciences, Weizmann Institute of Science, Rehovot, Israel

Exosomes mediate the communication between cells and the characterization of their content can provide important insights into health and disease. Their cargo includes proteins, lipids and nucleic acids (including microRNAs (miRNAs)). miRNAs regulate many cellular processes, including metabolism. The lysosomal storage disorder Niemann-Pick type C (NPC, MIM#257220) alters the availability of cholesterol and other lipids affecting cellular mechanisms leading to progressive neurodegeneration. However, disease progression is difficult to predict even for siblings with the same pathogenic variant, which, among other factors, can be due to epigenetics, namely miRNAs. We have used high-throughput sequencing approaches to obtain the miRNA profiling of NPC patients in order to identify novel therapeutic targets for RNA-based drugs and biomarkers through the characterization of serum miRNAs. miRNA profiling also holds great promises for understanding the wide range of clinical presentation of NPC patients and we have found some differentially expressed miRNA in patients compared to controls.

Funding: This work received financial support from PT national funds (FCT/MCTES, Fundação para a Ciência e Tecnologia and Ministério da Ciência, Tecnologia e Ensino Superior) through the project with the reference EXPL/BTM-TEC/1477/2021. We also thank the project with the reference UIDB/00211/2020.

Attachment 6

Tangled: a tale about NPC1 Protein Trafficking

Hugo David, Isaura Ribeiro, Maria Teresa Cardoso, Paulo Castro Chaves, Mariana Pintalhão, Esmeralda Martins, Luís Vieira, Catarina Carneiro Silva, Dulce Quelhas, Frances M. Platt, Andrea Ballabio, Sandra Alves & Marisa Encarnação

Oral Communication at the *AL4AnimalS.biotech Meeting*, **2023**

X Oral Communication __ Poster

Tangled: a tale about NPC1 Protein Trafficking

H. David [1,2,3,4]; I. Ribeiro [5,6,7]; M. T. Cardoso [8], P. Castro Chaves [8], M. Pintalhão [8], E. Martins [6], L. Vieira [9], C. Carneiro Silva [9], D. Quelhas [5,6,7], F. M. Platt [10], A. Ballabio [11], S. Alves [1,2,3], M. Encarnação [1,2,3*]

[1] Research and Development Unit, Department of Human Genetics, National Institute of Health Doutor Ricardo Jorge, Porto, Portugal

[2] Center for the Study of Animal Sciences (CECA), ICETA, University of Porto, Porto, Portugal

[3] Associate Laboratory for Animal and Veterinary Sciences (AL4AnimalS), Portugal

[4] Department of Biology, Faculty of Sciences, University of Porto, Porto, Portugal

[5] Unidade de Bioquímica Genética, Centro de Genética Médica Doutor Jacinto Magalhães, Centro Hospitalar e Universitário de Santo António (CHUdSA), Porto, Portugal

[6] Clinical and Experimental Human Genomics (CHEG) Group, Unit for Multidisciplinary Research in Biomedicine (UMIB), ICBAS, University of Porto, Porto, Portugal

[7] European Reference Network for Rare Hereditary Metabolic Disorders (MetabERN), Reference Center for Diagnosis and Treatment, CHUdSA, Porto, Portugal

[8] Reference Center for Diagnosis and Treatment, Centro Hospitalar Universitário de São João (CHUSJ), Porto, Portugal

[9] Technology and Innovation Unit, Department of Human Genetics, National Institute of Health Doutor Ricardo Jorge, Lisbon, Portugal

[10] Department of Pharmacology, University of Oxford, Oxford, United Kingdom

[11] Telethon Institute of Genetics and Medicine (TIGEM), Naples, Italy

* Marisa Encarnação, marisa.encarnacao@insa.min-saude.pt

Keywords: Niemann-Pick type C disease, pathogenic variants, disease models, microRNAs, biomarkers.

Introduction:

Despite the surplus of publications regarding Niemann-Pick type C (NPC), no demonstrably effective therapy has been found for patients carrying this disease, and many of its features remain enigmatic (Patterson, 2020). NPC presents with vast phenotypic variability, with clinical manifestations ranging from a swiftly progressing neonatal form to an adult-onset chronic condition, which is often mistaken for other psychiatric disorders (Las Heras *et al.*, 2023). In the large majority of cases, NPC disease is due to missense variants on the *NPC1* gene, some of which have already been demonstrated to be functional, if they could bypass the endoplasmic reticulum's quality control machinery (Gelsthorpe *et al.*, 2008). Such a finding opens the door for therapeutic approaches based on proteostasis modulators, whose assessment relies on the usage of suitable disease models.

Materials and Methods:

Seeing as animal- and induced pluripotent stem cell (iPSC)-based models did not prove appropriate to study the intracellular trafficking of the affected protein (Schultz *et al.*, 2022), we created variant-specific *in vitro* models of NPC disease, by stably transducing *NPC1*$^{-/-}$ ARPE-19 cell lines with several constructs encoding different fluorescently-tagged variants of NPC1. Using these newly established cell lines, alongside patient-derived primary skin fibroblasts, we set out to investigate the lysosomal positioning, trafficking routes and

degradation pathways elicited by two of the most common *NPC1* variants (p.Ile1061Thr and p.Ala1035Val). We also tried to shed some light on the underlying mechanisms conferring the disease its extreme variability, by tracing the microRNA (miRNA) profile of NPC patients using next-generation small RNA sequencing. Lastly, we selected some of the differentially expressed miRNA hits for qRT-PCR validation in patients' sera.

Results:
The trafficking and degradation studies on the two models of NPC disease evidenced altered lysosomal biogenesis and positioning – with decreased organelle turnover and perinuclear clustering – and revealed p.Ile1061Thr- and p.Ala1035Val-NPC1's likely retention in the endoplasmic reticulum and targeting for degradation by both the proteasome and the lysosome. We found a number of dysregulated miRNAs in patient cell samples, and we validated two significantly upregulated species in patient serum (miR-143-3p and miR-199a-3p), which might be useful both as new minimally-intrusive, specific, time- and cost-effective diagnostic biomarkers of NPC and as indicators of disease progression and response to therapy.

Conclusions:
Overall, these comprehensive molecular and functional studies contributed to the continuous effort in unveiling the pathological mechanisms which underly NPC disease. Moreover, we generated a new *in vitro* model to study the effect of *NPC1* variants on protein trafficking and degradation, which could even be used in large-scale drug screenings for pre-approved proteostasis modulator-based therapeutic approaches; we retraced the miRNA expression profile of NPC patients; and we proposed two serum miRNAs as new putative biomarkers of this disease.

References:

Gelsthorpe, M. E., Baumann, N., Millard, E., Gale, S. E., Langmade, S. J., Schaffer, J. E., & Ory, D. S. (**2008**). Niemann-Pick Type C1 I1061T Mutant Encodes a Functional Protein That Is Selected for Endoplasmic Reticulum-associated Degradation Due to Protein Misfolding. *The Journal of Biological Chemistry*, *283*(13), 8229. https://doi.org/10.1074/JBC.M708735200

Las Heras, M., Szenfeld, B., Ballout, R. A., Buratti, E., Zanlungo, S., Dardis, A., & Klein, A. D. (**2023**). Understanding the phenotypic variability in Niemann-Pick disease type C (NPC): a need for precision medicine. *NPJ Genomic Medicine*, *8*(1). https://doi.org/10.1038/S41525-023-00365-W

Patterson, M. (**2020**). Niemann-Pick Disease Type C. *GeneReviews®*. https://www.ncbi.nlm.nih.gov/books/NBK1296/

Schultz, M. L., Schache, K. J., Azaria, R. D., Kuiper, E. Q., Erwood, S., Ivakine, E. A., Farhat, N. Y., Porter, F. D., Pathmasiri, K. C., Cologna, S. M., Uhler, M. D., & Lieberman, A. P. (**2022**). Species-specific differences in NPC1 protein trafficking govern therapeutic response in Niemann-Pick type C disease. *JCI Insight*, *7*(23). https://doi.org/10.1172/JCI.INSIGHT.160308

Acknowledgments and funding - This work received financial support from the Foundation for Science and Technology (EXPL/BTM-TEC/1477/2021), the Centre for the Study of Animal Science (UIDB/00211/2020) and the Associate Laboratory for Animal and Veterinary Sciences (LA/P/0059/2020).

Conflict of interests – The authors declare no conflict of interest.

Attachment 7

RNARARE Project Flyer

Hugo David, Sandra Alves & Marisa Encarnação

Flyer to divulge the *RNARARE Project*, **2023**

Projeto RNARARE

Como podem contribuir?

Neste momento, precisamos de amostras de sangue de doentes com diagnóstico clínico e molecular de NPC.

Para isso, basta contactar-nos por e-mail e nós faremos chegar as instruções de colheita.

Para além do consentimento informado dos doentes, seria importante termos também informação sobre:

- a variante patogénica do gene *NPC1* ou *NPC2*;
- a idade de diagnóstico e os primeiros sintomas;
- a terapia em curso (caso aplicável).



Marisa Encarnação
marisa.encarnacao@insa.min-saude.pt

Sandra Alves
sandra.alves@insa.min-saude.pt

fct Fundação para a Ciência e a Tecnologia

EXPL/BTM-TEC/1477/2021

Instituto_Nacional de Saúde Doutor Ricardo Jorge

Projeto RNARARE

Quem somos?

Fazemos parte de um grupo de Investigação e Desenvolvimento em Doenças Lisossomais de Sobrecarga (DLSs), sediado no Instituto Nacional de Saúde Doutor Ricardo Jorge, no Porto.

Temos mais de uma década de experiência no estudo de várias DLSs, entre elas a doença de Niemann-Pick tipo C (NPC).

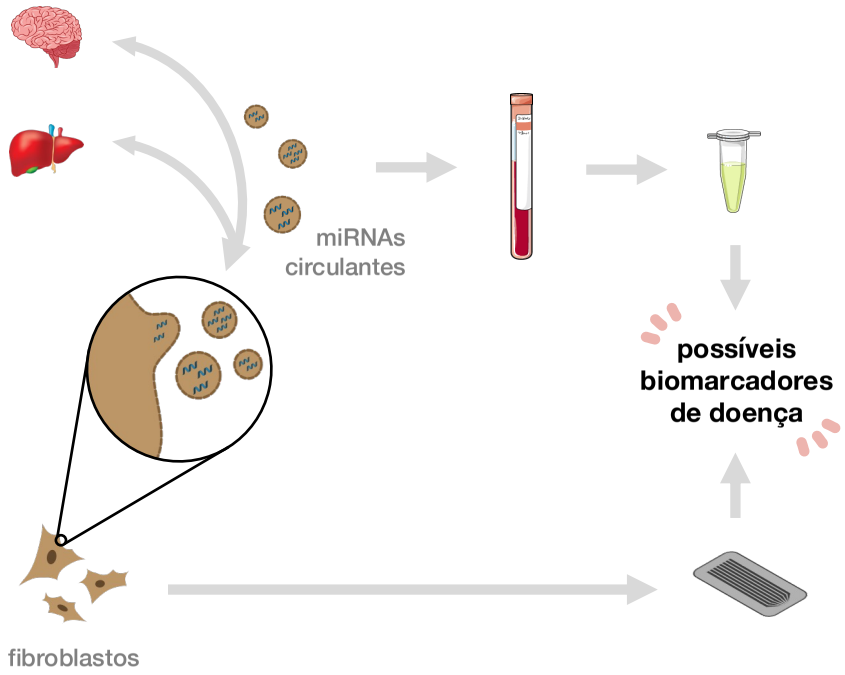
Através de colaborações nacionais e internacionais, temos realizado estudos de sequenciação em larga escala, tanto a nível do genoma como do transcriptoma, com o objetivo de desvendar os mecanismos de doença, encontrar biomarcadores e definir potenciais alvos terapeuticos.

Grupo de Doenças Lisossomais de Sobrecarga
Departamento de Genética Humana
Instituto Nacional de Saúde Doutor Ricardo Jorge

Projeto RNARARE

Qual é o nosso objetivo?

Com este projeto, pretendemos estudar o perfil de RNAs não codificantes em doentes com Niemann-Pick tipo C, quer em células, quer em circulação no sangue, numa tentativa de encontrar biomarcadores de doença e de melhor compreender de que forma a epigenética poderá afetar doenças monogénicas como a NPC.



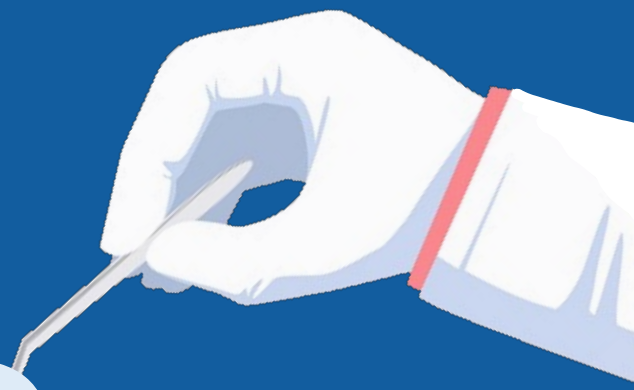
Attachment 8

CRISPR: Applications to Study Human Genetic Diseases

Marisa Encarnação, Hugo David & Rodrigo Leite de Oliveira

Flyer to divulge the *CRISPR: Application to Study Human Genetic Diseases* casual seminar, **2022**

CASUAL SEMINARS



CRISPR

Applications to Study Human Genetic Diseases

Rodrigo Leite de Oliveira, PhD

Assistant Professor, CRISPR Expertise Center
Amsterdam University Medical Centers

22/12

11h00

INSA Porto

Instituto_Nacional de Saúde Doutor Ricardo Jorge

Amsterdam UMC Universitair Medische Centra

Attachment 9

Autonomous Informed Consent Forms for the RNARARE Project

DECLARAÇÃO DE CONSENTIMENTO INFORMADO E ESCLARECIDO [1] [2]

Esta declaração enquadra-se num projeto cuja população alvo inclui crianças. Desta forma, sempre que este consentimento informado se aplicar a menores com discernimento, todas as eventuais dúvidas por eles colocadas serão esclarecidas, pelo médico referenciado utilizando linguagem adequada, e obtido o respetivo assentimento.

RNARARE Estudos de RNA na identificação de novos biomarcadores em doenças metabólicas neurodegenerativas

Designação do Estudo/Projecto (em português):

Eu, abaixo-assinado,

(nome completo do participante no projeto)

compreendi a explicação escrita e verbal que me foi dada pelo médico referenciado, acerca deste projeto de investigação, tomando conhecimento dos objetivos, métodos, benefícios previsíveis e riscos potenciais, bem como das garantias de confidencialidade previstas para os dados que disponibilizo. Foi-me dado tempo de reflexão e oportunidade de fazer as perguntas que julguei necessárias, obtendo respostas satisfatórias.

Sei que tenho o direito de recusar, a qualquer momento, a minha participação no projeto através do contacto com o investigador responsável abaixo identificado, sem que isso possa ter como efeito qualquer prejuízo na assistência que me é prestada. Sei também que não terei quaisquer despesas adicionais decorrentes da participação, uma vez que a colheita de sangue será realizada aquando da deslocação à consulta regular.

Pretendo ser informado, através de médico referenciado, de resultados da investigação que possam vir a demonstrar-se de utilidade clínica para a sua doença

☐ SIM ☐NÃO

Se terminado este projeto ainda existir alguma das amostras biológicas facultadas, autorizo que sejam conservadas para utilização em estudos futuros, devidamente aprovados pela Comissão de Ética para a Saúde do INSA?

☐ SIM ☐NÃO

Se SIM, pretendo que as amostras sejam tornadas anónimas de forma definitiva

☐ SIM ☐NÃO

Autorizo a utilização dos resultados obtidos, devidamente anonimizados, para publicações científicas?

☐ SIM ☐NÃO

Estas são as condições em que decido livremente aceitar que participe no estudo/investigação

Data: ____ / _____ / 20____

Assinatura do participante

Assinatura do investigador responsável

Investigador responsável pelo projeto

Nome
Contactos

Assinatura do médico que prestou esclarecimentos

Médico que prestou os esclarecimentos devidos e apresentou o consentimento

Nome
Contactos

Encarregado de Proteção de Dados no INSA, IP

Nome
Contactos

1 Considerando a "Declaração de Helsínquia" da Associação Médica Mundial (Brasília 2013)

2 Feito e assinado em duplicado sendo entregue um exemplar ao responsável, juntamente com o documento informativo.

Attachment 10

Non-autonomous Informed Consent Forms for the RNARARE Project

DECLARAÇÃO DE CONSENTIMENTO INFORMADO E ESCLARECIDO PARA PARTICIPANTES PRIVADOS DO EXERCÍCIO DE AUTONOMIA [1] [2]

Para participantes privados do exercício de autonomia

RNARARE Estudos de RNA na identificação de novos biomarcadores em doenças metabólicas neurodegenerativas

Designação do Estudo/Projecto (em português):

Eu, abaixo-assinado,

(nome completo do representante do participante)

Em representação de

(nome completo do participante privado do exercício de autonomia)

compreendi a explicação escrita e verbal que me foi dada pelo médico referenciado, acerca deste projeto de investigação, tomando conhecimento dos objetivos, métodos, benefícios previsíveis e riscos potenciais, bem como das garantias de confidencialidade previstas para os dados que disponibilizo. Foi-me dado tempo de reflexão e oportunidade de fazer as perguntas que julguei necessárias, obtendo respostas satisfatórias.

Sei que tenho o direito de recusar, a qualquer momento, a minha participação no projeto através do contacto com o investigador responsável abaixo identificado, sem que isso possa ter como efeito qualquer prejuízo na assistência que me é prestada. Sei também que não terei quaisquer despesas adicionais decorrentes da participação, uma vez que a colheita de sangue será realizada aquando da deslocação à consulta regular.

Pretendo ser informado, através de médico referenciado, de resultados da investigação que possam vir a demonstrar-se de utilidade clínica para a sua doença

☐ SIM ☐NÃO

Se terminado este projeto ainda existir alguma das amostras biológicas facultadas, autorizo que sejam conservadas para utilização em estudos futuros, devidamente aprovados pela Comissão de Ética para a Saúde do INSA?

☐ SIM ☐NÃO

Se SIM, pretendo que as amostras sejam tornadas anónimas de forma definitiva

☐ SIM ☐NÃO

Autorizo a utilização dos resultados obtidos, devidamente anonimizados, para publicações científicas?

☐ SIM ☐NÃO

Estas são as condições em que decido livremente aceitar que participe no estudo/investigação

Data: ____ / _____ / 20____

Assinatura do participante

Assinatura do investigador responsável

Investigador responsável pelo projeto

Nome
Contactos

Assinatura do médico que prestou esclarecimentos

Médico que prestou os esclarecimentos devidos e apresentou o consentimento

Nome
Contactos

Encarregado de Proteção de Dados no INSA, IP

Nome
Contactos

1 Considerando a "Declaração de Helsínquia" da Associação Médica Mundial (Brasília 2013)

2 Feito e assinado em duplicado sendo entregue um exemplar ao responsável, juntamente com o documento informativo.